THE REGULATORY ROLE AND ENVIRONMENTAL SENSITIVITY OF DNA METHYLATION IN NEURODEVELOPMENT

Marisol Resendiz

Submitted to the faculty of the University Graduate School
in partial fulfillment of the requirements
for the degree
Doctor of Philosophy
in the Program of Medical Neuroscience,
Indiana University
August 2017

Accepted by the Graduate Faculty, Indiana University, in partial fulfillment of the requirements for the degree of Doctor of Philosophy.

Doctoral Committee

June 1, 2017

_____

Feng C. Zhou, Ph.D, Chair

_____

Xiaoming Jin, Ph.D

_____

Debomoy K. Lahiri, Ph.D

_____

Charles R. Goodlett, Ph.D

_____

Richard Day, Ph.D

DEDICATION

I dedicate this dissertation to my father, who challenged me to live a life of impact and conquer the limits of my own expectations. Your dedication and relentless pursuit of truth have been my guiding light and I am forever grateful.

ACKNOWLEDGEMENTS

I wish to thank my advisor Dr. Feng Zhou for his patience and guidance during my doctoral training. I thank him for allowing me the opportunity to hone my strengths and for consistently pushing me to improve technically and analytically. I also wish to thank the other members of my research committee, Dr. Xiaoming Jin, Dr. Charles Goodlett, Dr. Richard Day, and Dr. Debomoy Lahiri. I sincerely appreciate their time, support, and constructive critique of my research throughout my training.

I thank all the people who contributed to my scientific work, particularly Sherry Lo, Yuanyuan Chen, Nailcan Ozturk, Darryl Watkins, and Darren Chang. I thank Sherry for her assistance with methyl-sensitive restriction enzyme assays and for her guidance and assistance with genomic analysis, pyrosequencing, and early embryonic assays. I thank Yuanyuan Chen for her assistance with immunohistochemistry and confocal microscopy. I thank Nailcan Ozturk for his training in the FASD animal model and his assistance in immunohistochemistry, morphometric analysis, and Western Blotting. I thank Darryl Watkins for his assistance with the animal model. Finally, I thank Darren Chang for his assistance with global methylation assays and quantitative PCR. I would also like to thank Feng Yang, Lijun Ni, and Dr. Charles Anthony for their technical instruction during the early portion of my training.

I also wish to acknowledge our collaborators Dr. Jill Reiter, Kerry Sanders, and Ron Unkel and I thank Dr. Chrisine Czackowski for her hard work in procuring the NIAAA training grant 2T32AA007462-31, which financially supported my training for four years. I wish to thank the administrative staff of the Department of Anatomy and

Cell Biology and the Stark Neuroscience Research Institute, especially Kate McMillan, Marthe Cadet-Lorgeat and Nastassia Belton. I also thank Latasha Gilson and Mary Harden for their assistance with my training grant.

I am grateful to all the people that provided moral support and professional guidance over the course of my study. I thank my mentors Dr. Graciela Unguez, Dr. Mozella Garcia, Dr. Sherry Greene, Dr. James Williams, and Dr. Paul Ardafyio. I am also indebted to my colleagues Rena Meadows, Grace Santa-Cruz Chavez, Kristin Hollister, Karl Koehler, Tina Wang, Carlos Rodriguez and Angelina Hernandez. Finally, I thank my family and friends for their unwavering support and encouragement throughout this journey.

PREFACE

In 1809 Jean-Baptiste Lamarck described a theory once held by Hippocrates and Aristotle which ascribed evolutionary adaptation as a process that occurred directly from one generation to the next- that physiological adaptations acquired during an organism's lifetime in response to environmental pressures were passed immediately to offspring. Short lived, the notion was widely discredited in part by experiments executed by August Weismann which asserted that germ cells alone could account for inheritance of traits and were incapable of being affected by somatic cells and thus, environmental pressure. Charles Darwin's theories of evolution and natural selection, along with Gregor Mendel's work on inheritance effectively replaced Lamarckism by the early 20th century and have endured as the principle mechanisms for evolutionary adaptation and inheritance of traits.

The emergence of epigenetics, or the study of stably heritable phenotypes resulting from chromosomal changes without alterations to the DNA sequence, has prompted a re-examination of Lamarckian theory and challenged the long-held belief that genetics bear the sole weight of organismal physiology, functionality, and adaptation. Though the heritability of epigenetic modifications remains a subject of contention among experts and limits the evolutionary scope of the mechanism, decades of past and emerging research have illuminated very clear and biologically relevant roles for epigenetics which rival, or, more accurately, complement the principles of genetics in guiding organismal physiology.

Marisol Resendiz

THE REGULATORY ROLE AND ENVIRONMENTAL SENSITIVITY OF DNA METHYLATION IN NEURODEVELOPMENT

The emerging field of epigenetics is expanding our understanding of how biological diversity is generated in the face of genetic limitations. One epigenetic mechanism in particular, DNA methylation, has demonstrated a dynamic range during neural development. Here, we provide evidence that DNA methylation occurs as a cell-unique program aiding in the regulation of neurodevelopmental gene expression. DNA methylation has demonstrated sensitivity to external inputs ranging from stress to chemical exposure and dietary factors. To explore DNA methylation as a means of communicating early-life stress to the brain, we utilized a mouse model of fetal alcohol spectrum disorders (FASD). FASD presents a range of neurodevelopmental deficits and is a leading cause of neurodevelopmental disabilities in the United States. Predicated on the knowledge of alcohol's teratogenic role in brain development, we describe that the normal pattern of cortical DNA methylation and epigenetic correlates is similarly impacted by prenatal alcohol exposure. Due to the biochemical interaction of alcohol metabolism and the pathways regulating DNA methylation synthesis, we further investigated whether dietary manipulation could normalize the cortical DNA methylation program and aid in the protection of FASD characteristics. We found that the alcohol-sensitive DNA methylation landscape is dually capable of registering dietary intervention, demonstrating normalization of disease-related patterns in the cortex and

improved neurodevelopmental gene expression and morphology. Finally, we investigated the DNA methylation landscape in a crucial corticodevelopmental gene to more accurately define the breadth and scope of the environmental impacts at the nucleotide level. We found that alcohol and dietary supplementation are selective for regions associated with transcriptional control. Collectively, the evidence supports that DNA methylation plays a regulatory role in development and that its sensitivity to external inputs is dynamic and detectable at the smallest genomic level. Importantly, DNA methylation landscapes are adaptable and thus bear diagnostic and therapeutic potential.

Feng C. Zhou, Ph.D., Chair

TABLE OF CONTENTS

LIST OF TABLES xiv

LIST OF FIGURES xv

LIST OF ABBREVIATIONS xviii

DISSERTATION OUTLINE 1

CHAPTER 1: CELL-UNIQUE DNA METHYLATION DYNAMICS IN THE NORMALLY-DEVELOPING BRAIN 3

1.1 INTRODUCTION 3

1.1.1 Structural Regulation Conveys Biological Heterogeneity 3

1.1.2 Epigenetic Modifications 3

1.1.3 DNA Methylation 4

1.1.4 DNA Methylation Dynamics 7

1.1.5 Role of DNA Methylation in Neural Development 10

1.1.6 Developmental DNA Methylation Programs in the Brain 14

1.1.7 Research Aims 16

1.2 MATERIALS AND METHODS 18

1.2.1 Animals 18

1.2.2 Immunohistochemistry 18

1.2.3 Confocal Microscopy 22

1.2.4 Quantification of 5mC and 5hmC using molecular enzymatic assays 22

1.2.5 Quantitative Gene Specific DNA methylation analysis 23

1.2.6 qPCR for gene expression 24

1.2.7 Statistical analysis 25

1.3 RESULTS 25
1.3.1 Purkinje Cell DNA Methylation Reprogramming 25
1.3.2 Granule Neuron DNA Methylation Reprogramming 28
1.3.3 Epigenetic Correlates of Post-Mitotic DNA Methylation Reprogramming 30
1.3.4 Functional Impact of the DNA Methylation Program 41
1.3.5 DNA Methylation Program in the Embryonic Cortex 46
1.4 DISCUSSION 53
1.4.1 Post-Mitotic DNA Methylation Reprogramming: Evidence from the PC.....53
1.4.2 DNA Methylation Programs in Complimentary Cell Types 55
1.4.3 DNA Methylation Reprogramming as a Functional Mechanism 57
1.4.4 Summary and Conclusions 58
CHAPTER 2: DYSREGULATION OF NEURODEVELOPMENT AND DNA METHYLATIONBY ALCOHOL.....64
2.1 INTRODUCTION 64
2.1.1 Environmental Sensitivity and Heritability of DNA Methylation.....64
2.1.2 Alcohol and Methyl and Acetyl Metabolism.....66
2.1.3 Fetal Alcohol Spectrum Disorders (FASD) 70
2.1.4 Developmental Alcohol Exposure and DNA Methylation 71
2.1.5 Cortical Impact of FASD 73
2.1.6 Research Aims 74
2.2 MATERIALS AND METHODS.....76
2.2.1 Overview of experimental prenatal alcohol exposure 76
2.2.2 Animals and treatments.....77
2.2.3 Embryo isolation and tissue preparation.....78
2.2.4 Immunocytochemistry analysis 78
2.2.5 Densitometry analysis (H score) and cortical thickness assessment 81

2.2.6 Cell Counting and Morphometric Analyses 82
2.2.7 Western blot of the methylation-binding protein MeCP2.....83
2.2.8 Global DNA methylation analysis 84
2.2.9 Statistical Analysis.....85
2.3 RESULTS 87
2.3.1 Alcohol-Induced Cortical Thinning in the Embryonic Cortex 87
2.3.2 Molecular Correlates of Alcohol-Induced Cortical Thinning.....87
2.3.3 The DNA Methylation Program is Modified by Fetal Alcohol Exposure.....89
2.3.4 Global versus Cell-Specific Characterization of DNA Methylation in the FASD Cortex 90
2.4 DISCUSSION.....99
2.4.1 Cortical Dysmorphology in FASD 99
2.4.2 Epigenetic Correlates of the Molecular Drivers of Cortical Dysmorphology.....101
2.4.3 Reconciling Cell and Tissue-Wide Epigenetic Analysis in FASD Studies.....105
2.4.4 Summary and Conclusions 110
CHAPTER 3: THE NORMALIZING CAPACITY OF
S-ADENOSYLMETHIONINE SUPPLEMENTATION IN A MOUSE MODEL
OF FASD 115
3.1 INTRODUCTION 115
3.1.1 Methyl Metabolism in Neural Development 115
3.1.2 Nutritional Deficiency and Developmental Epigenetics.....116
3.1.3 Alcohol Disruption of Methyl Metabolism During Pregnancy 119
3.1.4 Nutritional Intervention Strategies in FASD 121
3.1.5 Neural Targets for Intervention in the FASD Cortex 123
3.1.6 Research Aims 125
3.2 MATERIALS AND METHODS.....127
3.2.1 Overview of Experimental Treatments.....127
3.2.2 Animals and Treatments 128

3.2.3 Embryo Isolation and Tissue Preparation 130

3.2.4 Immunohistochemistry Analysis 130

3.2.5 Densitometry Analysis (H score), Cell Counting, and Cortical Thickness Assessment.....133

3.2.6 Cell Counting and Morphometric Analyses 134

3.2.7 Global DNA Methylation Analysis 135

3.2.8 Gene Expression Analysis 136

3.2.9 Methyl-CpG Pyrosequencing.....137

3.2.10 Statistical Analysis.....138

3.3 RESULTS 140

3.3.1 Gestation and Fetal Characteristics.....140

3.3.2 Role of S-AMe supplementation as a Cortical Neuroprotector 142

3.3.3 Effect of Alcohol and S-AMe Supplementation on Genetic Targets of Cortico-Development 156

3.3.4 Cortex-wide and Gene Specific Alcohol-induced Epigenetic Alteration and S-AMe normalization.....160

3.4 DISCUSSION 177

3.4.1 Neuroprotective Role of S-AMe in Alcohol-induced Cortical Deficits 177

3.4.2 Genomic Normalization of FASD targets via S-AMe supplementation 180

3.4.3 Identification of a Novel, Functional DMR in the Cortical Specification Gene *Fezf2*.....187

3.4.4 Summary and Conclusions 189

COMPREHENSIVE DISCUSSION.. 192

FUTURE DIRECTIONS. 197

APPENDIX A: SUPPLEMENTAL FIGURES 201

APPENDIX B: SUPPLEMENTAL TABLES.....203

REFERENCES 215

CURRICULUM VITAE

LIST OF TABLES

Table 1. Antibodies used for neurodevelopmental assessment of DNA methylation…. ..21

Table 2. Differentially methylated regions of cerebellar gene targets for DNA methylation analysis by restriction enzyme digestion and qPCR…….....42

Table 3. Antibodies used for neurodevelopmental and DNA methylation assessment in the alcohol-exposed E17 cortex…….....80

Table 4**.** Summary of cortico-structural alterations induced by alcohol in animal models…….....113

Table 5. Antibodies used for neurodevelopmental and DNA methylation assessment in the S-AMe supplemented E17 cortex…… 132

LIST OF FIGURES

Figure 1. Two distinct forms of DNA methylation....9

Figure 2. Global epigenetic trends in neural stem cell differentiation....12

Figure 3. Purkinje cell DNA de-methylation and re-methylation in the postnatal cerebellum....32

Figure 4. Persistent immunoreactivity of calbindin D-28k in Purkinje cells of the developing cerebellum....34

Figure 5. Pre-absorption confirms the specificity of the anti-5hmC antibody....35

Figure 6. Quantitative detection of cell-specific DNA methylation confirms Purkinje cell de-methylation and granule cell methylation....36

Figure 7. Developmental chromatin remodeling of Purkinje cells is apparent by intranuclear localization of 5mC and 5hmC during postnatal....37

Figure 8. De-methylation and re-methylation are synchronized with the turnover of DNMT1 and Tet1 throughout the maturation of Purkinje cells....38

Figure 9. Postnatal de-methylation is supported by the diminished immunoreactivity of the methyl binding proteins MeCP2 and MBD1....39

Figure 10. Postnatal loss of 5hmC is synchronized with the loss of downstream derivatives 5fC and 5caC in Purkinje cells....40

Figure 11. Purkinje cell-preferring genes undergo simultaneous de-methylation and transcriptional upregulation during peak synaptogenesis....44

Figure 12: Comparative phenotypic and DNA methylation dynamics in the embryonic cortex....52

Figure 13. Independent DNA methylation program of Purkinje, granular and basket cells during development....61

Figure 14: The DNA methylation program of the embryonic cortex....62

Figure 15. Effect of alcohol metabolism on acetylation and methylation of histones and DNA....69

Figure 16. Epigenetically-modified neurodevelopmental gene targets of alcohol....75

Figure 17: Summary of experimental procedures.....86

Figure 18: Alcohol reduces cortical thickness and Tbr2-im expression in the E17 frontal cortex.....92

Figure 19: Alcohol reduces ventricular proliferation and neuronal maturation in the E17 frontal cortex 93

Figure 20: Alcohol inhibits 5mC and cellular maturity in the E17 cortical plate.....94

Figure 21: 5-hmC-im is reduced in the lower cortex but upregulated in the E17 cortical plate 95

Figure 22: Alcohol-induced MeCP2 up-regulation in the E17 cortex.....96

Figure 23. Quantitative DNA methylation (5-mC and 5-hmC) reveals tissue-wide alcohol-related de-methylation in the E17 cortex.....97

Figure 24. Cortical plate density is unchanged by alcohol but nuclear morphology is negatively impacted 98

Figure 25. Epigenetic mechanisms and potential manifestations of fetal alcohol spectrum disorders 114

Figure 26. Experimental paradigm for fetal alcohol and S-adenosylmethionine supplementation.....139

Figure 27. Alcohol does not impact gestational characteristics of experimental dams.....147

Figure 28. Alcohol transiently inhibits fetal body weight at E17 but does not impact brain weight.....148

Figure 29. Alcohol reversibly decreases liver but not brain *Mat2a* and liver and cortex-wide 5mC.....149

Figure 30. Alcohol- induced cortical thinning is persistently ameliorated by S-AMe supplementation 150

Figure 31. Alcohol reversibly reduces nuclear area in the E17 cortical plate 151

Figure 32. Alcohol decreases the number of proliferating cells at the cortical neuroepithelium 152

Figure 33. Alcohol-induced Tbr2 reduction is ameliorated by S-AMe supplementation in the intermediate zone.....153

Figure 34. Alcohol-induced NeuN (im) decrease is ameliorated by S-AMe supplementation……154

Figure 35. Alcohol increases Vglut1 expression in the cortical plate……..155

Figure 36. Alcohol does not impact early pro-neural gene expression in the E17 cortex…….167

Figure 37. S-AMe supplementation partially normalizes alcohol-induced dysregulation of cortical specification genes.....168

Figure 38. Alcohol- induced upregulation of the epigenetic genes Tet3 and Ehmt2 is mitigated by S-AMe supplementation.....170

Figure 39. Alcohol-induced laminar 5mC upregulation is normalized by S-AMe supplementation.....172

Figure 40. Laminar 5hmC is unaffected by alcohol or S-AMe in the E17 cortex.....173

Figure 41. *Fezf2* gene, regulatory regions, and predicted transcription factor binding sites.....174

Figure 42. Fezf2 promoter and enhancer 434 are hypermethylated by alcohol treatment and partially normalized by S-AMe supplementation.....175

Figure 43. Environmental signal integration is mediated by methyl metabolism and epigenetic regulation of the genome.....200

LIST OF ABBREVIATIONS

5'UTR 5'	Untranslated region
5caC	5-carboxylcytosine
5fC	5-formylcytosine
5hmC	5-hydroxymethylcytosine
5mC	5-methylcytosine
5MTHF	5-methyltetrahydrofolate
ADH	Alcohol dehydrogenases
ALDH	Aldehyde dehydrogenases
BER	Base excision repair
BHMT	Betaine homocysteine S-methyltransferase
BEC	Blood ethanol concentration
CP	Cortical plate
DAB	Diaminobenzidine
DMR	Differentially methylated region
Ns-DMR	Nutrient-sensitive differentially methylated region
DMP	DNA methylation program
DNMTs	DNA methyltransferase
EGLi	External granule layer (inner)
EGLo	External granule layer (outer)
E	Embryonic day
FAS	Fetal alcohol syndrome
FASD	Fetal alcohol spectrum disorder
GC	Granule cell
HDAC	Histone deacetylase
HMTs	Histone methyltransferase
IHC	Immunohistochemistry
IGL	Inner granule layer
IPC	Intermediate progenitor cells
IZ	Intermediate Zone
LV	Lateral ventricle
MZ	Marginal Zone
MAT	Methyl adenosyltransferase
MBD1-4	Methyl-binding domain protein 1-4
MeCp2	Methyl-binding protein 2
MS	Methionine synthase
MSRE	Methyl-sensitive restriction enzyme
ML	Molecular layer
NE	Neuroepithelium
NPCs	Neural progenitor cells
NSCs	Neural stem cells
PcG	Polycomb group complex
PF	Pair-fed
PGCs	Primordial germ cells

P	Postnatal day
PC	Purkinje cell
PCL	Purkinje cell layer
RCGs	Radial glial cells
ROS	Reactive oxygen species
S-AH	S-adenosylhomocysteine
S-AMe	S-adenosylmethionine
SP	Subplate
SVZ	Subventricular zone
TDG	Thymine-DNA glycosylase
TET1-3	Ten eleven translocase enzyme 1-3
TSSs	Transcriptional start sites
VZ	Ventricular zone

DISSERTATION OUTLINE

Chapter 1: Cell-unique DNA methylation dynamics in the normally-developing brain

- Goal: characterize DNA methylation dynamics during normal, cellular development
- Rationale: DNA methylation has been implicated in gene regulation and cellular specification, though an in-depth characterization of cell-specific epigenetic landscapes has not been performed
- Hypothesis: DNA methylation is unique and dynamic during neural specification, guiding developmental cues through transcriptional regulation
- Approach: Examination of DNA methylation in two major cell types of the developing cerebellum (CB) and the neocortex

Chapter 2: Dysregulation of neurodevelopment and DNA methylation by alcohol

- Goal: Investigate alcohol-mediated cortico-deficits and alteration of developmental DNA methylation patterns
- Rationale: Evidence suggests that alcohol disrupts normal epigenetic landscapes and manifests neurodevelopmental dysregulation
- Hypothesis: DNA methylation is a window by which alcohol exposure may disrupt critical transcriptional profiles, leading to neurodevelopmental obstruction
- Approach: Investigate parallel DNA methylation correlates of cortical laminar formation in a mouse model of fetal alcohol spectrum disorder (FASD)

Chapter 3: The normalizing capacity of S-adenosylmethionine supplementation in a mouse model of FASD

- Goal: Investigate the role of S-adenosylmethionine supplementation in the mitigation of alcohol-induced DNA methylation and developmental disruption
- Rationale: Alcohol has demonstrated inhibitory capacity on methyl-metabolism, closely associated with DNA methylation biosynthesis
- Hypothesis: S-AMe supplementation will ameliorate the epigenetic and phenotypic dysregulation of alcohol in FASD
- Approach: Supplement liquid alcohol diet with S-AMe to evaluate its normalizing potential in FASD

CHAPTER 1: CELL-UNIQUE DNA METHYLATION DYNAMICS IN THE NORMALLY-DEVELOPING BRAIN

1.1 INTRODUCTION

1.1.1 Structural Regulation Conveys Biological Heterogeneity

The genetic code, which instructs the production of all organismal proteins, is limited in its intrinsic diversity to account for changes in biological heterogeneity. While some endogenous mechanisms exist at the pre-transcriptional level (i.e. alternative splicing, genetic variants, DNA transposons, etc.), other post-translational modifications have been identified as contributors of proteomic diversity. In essence, due to the interdependent nature of the genetic code, intermediary transcripts, and the translated protein product, structural influences (at every level) presumably bear significant impact on end point production and as such, are important contributors to biological heterogeneity. In the past few decades, a sophisticated understanding of an array of modifications that influence gene expression without altering the underlying sequence. Broadly termed "epigenetic modifications", these alterations bear important structural implications; and while the examination of all is beyond the scope of this Dissertation, much attention will be given to one particular class.

1.1.2 Epigenetic Modifications

Epigenetic mechanisms are largely classified by their ability to alter genetic outputs via the impact on the structural characteristics of chromatin, consequently regulating the accessibility of transcriptional elements. One well-studied class is known as histone modifications, referring to factors influencing the chemical (structural) bonds between DNA and histone proteins. Due to the negative charge of the DNA phosphate

backbone relative to the positively-charged histone octamers of the nucleosome, factors such as post-translational chemical modifications of histones (i.e. methylation, acetylation, phosphorylation, ubiquitination, sumoylation) may collectively impact the electro-dynamics of the DNA-protein bonds. Another class of epigenetic modifications which may influence chromatin or impact gene expression is known as non-coding RNA. These include a variety of mRNA or genomic-targeting sequences, typically accompanied by chromatin modifying enzymes or translation-inhibiting enzymes. Finally, in a vein similar to histone modifications, DNA methylation refers to covalent chemical modifications occurring on cytosine bases of the genome which can alter the electrodynamics of DNA-DNA or DNA-protein bonds underlying the three dimensional structure of chromatin.

While the highly likely scenario is that a multitude of epigenetic marks converge on critical loci to affect meaningful structural change, more often than not, these alterations are investigated independently. Although several lines of evidence suggest that cross-talk indeed exists between epigenetic modifications (i.e., DNA methylation recruitment of histone modification enzymes, etc.), fundamental epigenetic study, in order to form a more complete and in-depth characterization, continues to be examined in singularity. Ultimately, as a clearer understanding emerges, investigators can begin to shift attention to inter-epigenetic relationships.

1.1.3 DNA Methylation

The focus of this study centered on DNA methylation, the oldest and most well-studied epigenetic modification class. DNA methylation was originally defined by the addition of a methyl group to the 5’ carbon of a cytosine base (termed 5-methylcytosine

and hereto denoted as “5mC”), though, as described below, has in recent years expanded to include a handful of derivations. This chemical reaction is performed by the enzyme family of DNA methyltransferases (DNMTs). It is commonly accepted that DNMT1 and DNMT2 are involved in methyl transfer during DNA replication and repair to maintain a previously methylated cytosine state. This notion is partially supported by the increased affinity of DNMT1 for hemi-methylated DNA (Bestor 1992). On the other hand, the DNMT3a and DNMT3b isoforms are believed to play a role in *de novo* methyl transfer, with DNMT3a proposed to play a slightly larger neurogenic role (Wu, Coskun et al. 2010). Coincidentally, DNMTs have displayed differential expression across developmental stages, with loss of function experiments demonstrating a relatively larger role for DNMT3a and 3b during the early developmental stages (Okano, Bell et al. 1999).

Other than the reported predilection of DNMT1 for hemi-methylated DNA, the particulars of DNMT recruitment remain the subject of active research. In cancer cells, for example, high-throughput screening has allowed the identification of methylation-prone and methylation-resistant loci (Feltus, Lee et al. 2006), with results supporting a previously held notion that CG-rich loci display selective association with DNMT1 (Robert, Morin et al. 2003). More broadly, these findings suggest that DNMTs may be recruited by intrinsic sequence features. Other reported recruitment factors include phosphorylation of RelA/p65 in mouse embryonic fibroblasts and the stem-cell associated transcription factor SALL4 (Liu, Mayo et al. 2012, Yang, Corsello et al. 2012). Interestingly, one 2006 study demonstrated the direct recruitment of DNMTs by the Polycomb group (PcG) protein EZH2 to EZH2-targeting sequences (Vire, Brenner et

al. 2006), presenting evidence of a link between genomic sequence and DNMT-recruiting proteins.

DNA methylation may influence transcription in two ways. First, due to the electrostatic interaction of positively charged histone octamers (which form the basis of the nucleosome protein cores) and negatively charged DNA (maintaining the DNA-protein bond), the cumulative effect of even subtle DNA methylation changes may influence the electrostatic dynamics and alter the structural profile of DNA-protein bonds. In turn, the strength or weakness of those bonds dictates the level of chromatin compactness, defining the accessibility of the DNA to transcriptional machinery such as RNA polymerases and transcription factors. Importantly, just as methylation of cytosines may strengthen the DNA-protein bond and condense the chromatin, other modifications (i.e. histone acetylation) may weaken the DNA-protein bond, decreasing chromatin compaction and increasing accessibility of transcriptional elements. Second, a variety of methyl-DNA binding proteins exist which demonstrate an affinity toward methylated DNA. These proteins are recruited to methylated DNA sites and often bind repressive, chromatin remodeling complexes, among other proteins. For example, methyl-binding domain 2 (MBD2) has been shown to play a role in cancer (Detich, Theberge et al. 2002) while MBD3 has been implicated in stem cell differentiation (Kaji, Nichols et al. 2007). Additionally emerging evidence has identified some methyl-binding proteins with unique features (such as MBD1, MBD4) which are capable of binding unmethylated DNA (Jorgensen, Ben-Porath et al. 2004) and which demonstrate endonuclease activity (Bellacosa, Cicchillitti et al. 1999). These and other proteins have been reviewed in mammalian tissues by Lan et al. (Lan, Hua et al. 2010).

Previously, it was believed that DNA methylation was a transient modification, though years of research has revealed that DNA methylation can be lasting, in some cases reported to be transmissible to subsequent generations through the germline (Sharma 2013). Importantly, in 2009 a group of researchers confirmed the mammalian existence of 5-hydroxymethylcytosine (hereto referred as "5hmC"), a derivative of 5mC catalyzed by the Ten-eleven translocation protein family (TET1-3) (Kriaucionis and Heintz 2009, Tahiliani, Koh et al. 2009). TET enzymes can further convert 5hmC to 5-formylcytosine (5fC) and subsequently 5-carboxycytosine (5caC) in a step-wise manner, though these are found at very low levels (Ito, Shen et al. 2011). Because 5hmC is a substrate for TET enzymes, it is considered as an intermediary of DNA demethylation. Due to the incompatibility of 5hmC with DNMT enzymes, the presence of 5hmC may indicate a mechanism of passive demethylation. The discovery of 5hmC is particularly meaningful in the absence of confirmed active demethylation pathway elements (Schiesser, Hackner et al. 2012).

1.1.4 DNA Methylation Dynamics

Previous understanding held that DNA methylation was a purely repressive mark, acting to silence the expression of DNA. Today, a clearer picture has emerged revealing that DNA methylation is dynamic, acting in both activating and repressive capacity (Jones and Takai 2001, Ball, Li et al. 2009) likely influenced by genomic positioning (i.e. promoter or intragenic, Figure 1). Complimentary to 5mC, 5hmC offers a similar diversity that appears to be rooted in genomic positioning (Pastor, Pape et al. 2011, Wu, D'Alessio et al. 2011). Various reports have identified 5hmC in regions complimentary to 5mC and highly enriched in activated regions of the genome (Song, Szulwach et al. 2011,

Szulwach, Li et al. 2011, Serandour, Avner et al. 2012). 5hmC, though less abundant than 5mC, is highly enriched in the brain and in maturing neuronal cells and tissues, making the marker of particular relevance in neurological research (Munzel, Globisch et al. 2010). Further, emerging study has identified the diverse binding capacity of the two major methyl marks, further suggesting their diverse roles in biological function (Chen, Damayanti et al. 2014). As commercial scientific technology advances the capability for differentiation of 5mC and 5hmC, overlapping and distinct profiles of the two will become even clearer.

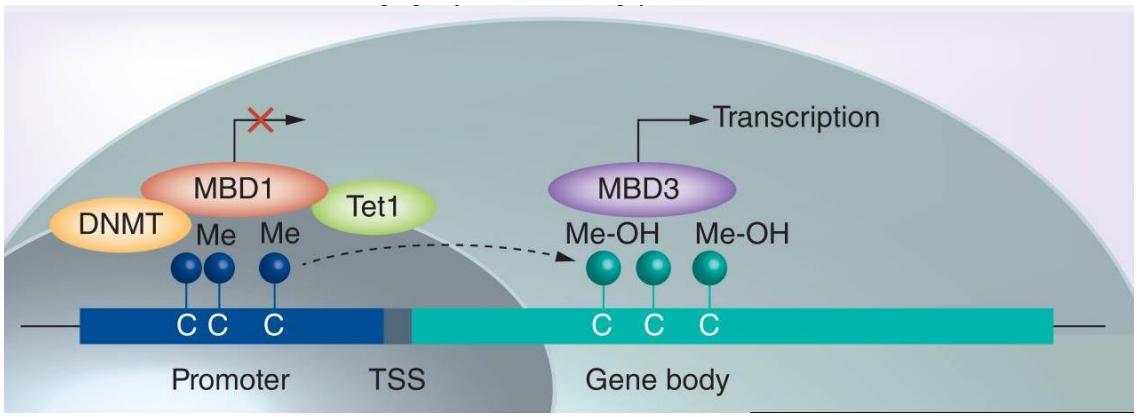

Figure 1. Two distinct forms of DNA methylation
DNMT transfers a methyl group to cytosine bases to form 5-methylcytosine (5mC). 5mC is found at CpG rich islands in the promoter regions of the gene. Canonically, CpG methylation is associated with silenced gene activation (represented by the 'X'), often through methyl CpG-binding proteins (i.e., MBD1), which recognize 5mC sites and recruit negative transcriptional regulatory proteins. The Tet family enzymes can further bind 5mC and hydroxylate the methyl group into 5-hydroxylmethylcytosine (5hmC). A shift of 5hmC from promoter to the gene-body regions is genomically observed. 5hmC have shown preference for differential methyl CpG-binding proteins (e.g., MBD3) and increasingly found to link to transcriptionally activating complexes. The complementary distribution and differential role of 5mC and 5hmC provide a new dynamic for epigenetic regulation of the complex development.C: Cytosine; DNMT: DNA methyl transferase; Me: Methylation; TSS: Transcription start site.

1.1.5 Role of DNA Methylation in Neural Development

The capacity of DNA methylation to influence three dimensional chromatin structure endows the important biological function of steering the progression of cell and tissue development. Alternatively, DNA methylation status may ensure the stability and maintenance of a cell-specific program. The advancement of high-throughput DNA methylation analyses has provided furthered insight into the modification's role in cellular and organismal development, maintenance and plasticity. Contrary to pre-existing beliefs, DNA methylation is earning a new reputation as a dynamic and programmable epigenetic marker, consequently allowing for a greater role in development and plasticity. The dire consequences of deletions and mutations of epigenetic genes such as DNMT and MeCP2, embryonic lethality (Li, Bestor et al. 1992, Okano, Bell et al. 1999) and detrimental nervous system development (Amir, Van den Veyver et al. 1999, Guy, Hendrich et al. 2001) respectively, have confirmed the developmental importance of DNA methylation. Further, the relevance of 5hmC in neural development (and in the brain during adulthood) appears to be supported by its relatively high abundance in neural tissues (Munzel, Globisch et al. 2010).

At the level of the neural stem cell, 5mC has been shown to be upregulated during neuroepithelial (NE) commitment, followed by a rapid drop during NE specification into mature neuronal populations (Chen, Damayanti et al. 2014). Alternatively, 5hmC appears to be enriched at sites of active maturation compared to neuroprogenitor sites (Stroud, Feng et al. 2011, Wu, D'Alessio et al. 2011, Kubiura, Okano et al. 2012). At the gene-level, 5mC appears to play a dynamic role in various genes required for differentiation, implicating 5mC hyper and hypomethylation as necessary strategies for neural

conversion of stem cells (Singh, Shiue et al. 2009, Cortese, Lewin et al. 2011, Hirabayashi, Shiota et al. 2013). Moreover, it has been proposed that while 5hmC may not be directly responsible for mediating gene activation, its enrichment at neural gene clusters during early neural progenitor specification suggests a role for 5hmC as a "primer" for eventual demethylation (and consequent expression) of those genes (Tan, Xiong et al. 2013).

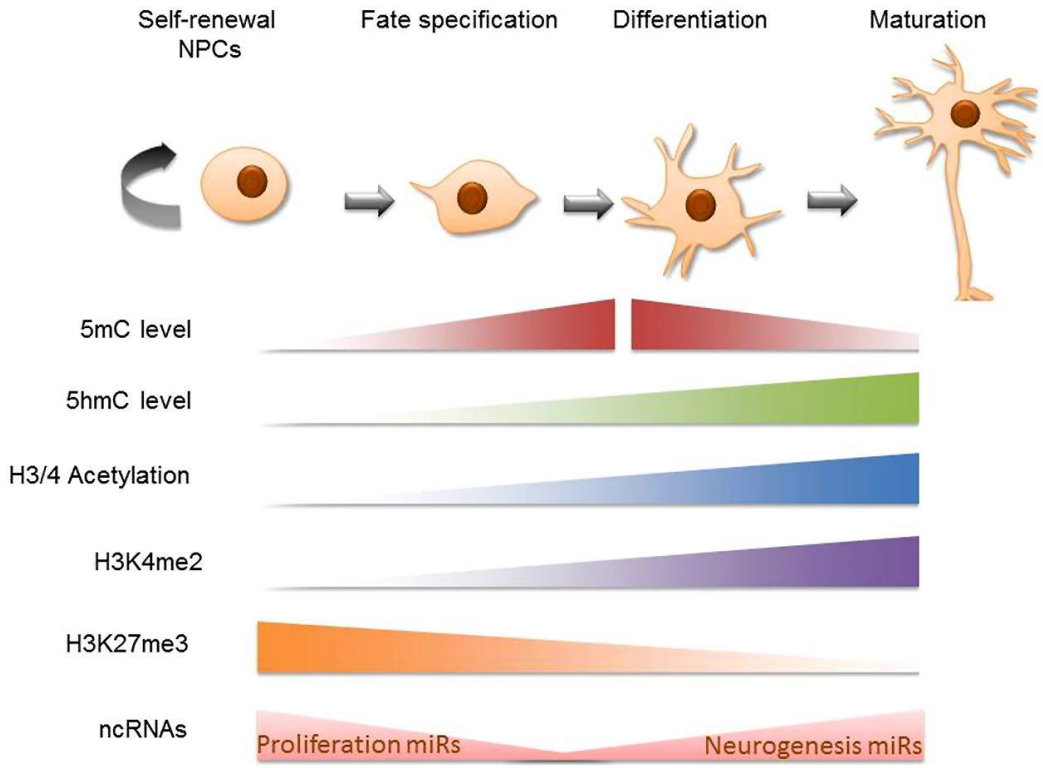

Figure 2. Global epigenetic trends in neural stem cell differentiation
Schematic diagram of cellular epigenetic program during neurogenesis. The top panel shows cell states during neurogenesis, from self-renewing neural progenitor cells (NPCs) to fate-determined neuroblasts, to differentiating and maturating neurons. The epigenetic programing is mapped in the bottom panel accordingly: cells gain 5 mC at the beginning of cell specification and sequentially gain 5 hmC at the beginning of cell differentiation; both 5 mC and 5 hmC accumulate during neuronal differentiation and maturation while at later stages of neuronal maturation, 5 mC levels decrease (Chen, Ozturk et al. 2013). Global trends in H3 and H4 acetylation have been traced *in vivo* to find that mature cells such as those in the mouse cortical plate are richer for these markers than the neural progenitor cells that preceed them (Cho, Kim et al. 2011). Histone 3 lysine 4 dimethylation (H3K4me2) is primarily acquired in the neural progenitor cell stage and becomes pronounced in the matured brain cell stage (Zhang, Parvin et al. 2012). H3K27me3 has been shown to be negatively correlated with 5 hmC on intergenic regions during NPC differentiation (Hahn, Qiu et al. 2013). Finally, MicroRNAs that support proliferative gene expression are diminished as self-renewable NPCs become specified neural precursors while pro-neurogenesis non coding RNA are upregulated during neural stem cell (NSC) conversion to mature neuronal states (Meza-Sosa, Pedraza-Alva et al. 2014).

Epigenetic modifications have been identified throughout various stages of neural differentiation including at the level of cell cycle regulation, neuronal and glial fate specification, all the way to late-stage feature specification and plasticity (Resendiz, Mason et al. 2014). For example, the pluipotency-maintaining genes *Oct4*, *Nanog*, and *Sox2* have been identified as targets of DNA methylation reprogramming during development, with *Nanog* trading enhancer 5hmC methylation for promoter 5mC methylation during silencing (Kim, Park et al. 2014). NSC differentiation analysis has also identified the differential methylation of *Notch1*, *Hes5*, and a number of downstream Notch1 targets. These are particularly relevant due to the prominent role that Notch1 signaling plays in directing astroglial and opposing pro-neural fates (Hisahara, Chiba et al. 2008, Das, Choi et al. 2013). Finally, large scale DNA methylation modifications have been shown to be critical for memory consolidation and synaptic plasticity in the hippocampus during adulthood (Vecsey, Hawk et al. 2007, Miller, Campbell et al. 2008), expanding the relevance of DNA methylation in neuronal systems beyond the developmental stage.

Importantly, while DNA methylation landscapes are changed throughout the course of neural specification (Figure 2), it is critical to acknowledge that these modifications do not occur independently of other epigenetic modifications. In fact, several lines of evidence exist for inter-epigenetic crosstalk (Jobe, McQuate et al. 2012). For example, acquisition of intragenic 5hmC during neural differentiation has been linked to loss of H3K27me3 and concomitant loss of promoter Polycomb repressor marks (Hahn, Qiu et al. 2013). As such, though evidence of DNA methylation as a guidingdevelopmental program is presented, the future of epigenetic investigation most

certainly requires the consideration of parallel histone modifications and non-coding RNA.

From a rational perspective, the reprogrammability of the chromatin landscape during cell specification makes sense in order to accommodate the fluctuating transcriptional profiles which are necessary to guide cellular change. Indeed, studies using DNMT-inhibiting agents such as 5-azacitadine and histone de-acetylases (HDACs) confirm the importance of normally occurring epigenetic landscapes for the proper and timely transition of the transcriptional profiles which dictate cellular specificity in the brain (Singh, Shiue et al. 2009).

1.1.6 Developmental DNA Methylation Programs in the Brain

Similar to the observed pattern of DNA methylation in neural stem cell progression, DNA methylation changes are highly orchestrated during mouse embryonic development. From the pronuclear stage of an embryo, paternal and maternal genomes are asynchronously altered by a wave of cell-wide demethylation through the blastocyte stage. This demethylation occurs passively and is predominantly mediated by loss of DNMT1 and DNMT3 and subsequent replication-dependent loss of 5mC and 5hmC (Mayer, Niveleau et al. 2000, Inoue and Zhang 2011). A second wave of demethylation is observed in primordial germ cells (PGCs) as they migrate to the gonadal ridge by embryonic (E) day 8.5-12.5 (Hajkova, Erhardt et al. 2002, Yamazaki, Mann et al. 2003, Maatouk, Kellam et al. 2006). This de-methylation, however, is not fully penetrant as many elements escape de-methylation including some CG rich regions (also termed CpG islands) of both the female and male PGCs, imprinting control elements, X-inactivated genes, and DNA transposons (Lane, Dean et al. 2003, Popp, Dean et al. 2010). Early

DNA methylation reprogramming is completed by a third wave of DNMT3-mediated *de novo* methylation during gametogenesis (Hajkova, Erhardt et al. 2002).

Pre-implantation embryos further undergo *de novo* methylation after implantation (Monk, Boubelik et al. 1987, Kafri, Ariel et al. 1992), establishing the first embryonic somatic methylation program which, when disrupted, can lead to the development of neural tube deficits (Dunlevy, Burren et al. 2006). Though this process is not fully understood, DNA re-methylation has been shown to occur bimodally between housekeeping genes and tissue-specific genes, consequently conferring specificity of some cells and heterogeneity of the early tissues (Lange and Schneider 2010). Post-implantation, during early neurulation, a specific profile of the DNA methylation landscape becomes clearer. Present in a gradient from ventral (high) to dorsal (low), 5mC apparently coincides with the pattern of neural specification. This pattern is also observed along the neural axis, with 5mC peaking at the mid/hindbrain and diffusing rostrally and caudally toward the forebrain and caudal neural tube, respectively (Zhou, Chen et al. 2011). These patterns argue that DNA methylation is spatially and temporally coincidental with neural tube development during early gestation. Further, the Zhou study reported an intranuclear shift from 5mC presentation in the form of aggregated punctates toward a more homogenous distribution, likely indicating a transition from genomic hypermethylation to a "relaxation" of genomic clusters required for embryonic progression.

Progressively, throughout brain development DNA methylation landscapes and dynamics have been proposed to play critical roles. An examination of the hippocampus identified a 5mC to 5hmC transition was correlated with neural differentiation in the

region (Chen, Ozturk et al. 2013). Interestingly, this study revealed that distinct cell types of the hippocampus expressed unique DNA methylation patterns. At E15, 5mC is abundant in hippocampal precursors though, by E17, neuroepithelial (NE) precursors undergo extensive loss of 5hmC and to a lesser degree, 5mC. As NE cells initiate radial migration through the intermediate zone, migrating neurons re-acquire 5mC and 5hmC, peaking as neurons reach their mature state in the Cornus Ammonis (CA). These findings suggested that 5mC and 5hmC are required for neural migration and specification of pyramidal neurons in the CA region. Additional analysis in the dentate gyrus confirmed that 5hmC is co-localized with NeuN, a marker of neuronal maturity. 5mC on the other hand demonstrated a more complex distribution and co-localization with Sox2 positive progenitors. Overall, this model allowed the visualization of unique DNA methylation signatures specific to cellular states within the developing hippocampus. This profile beckoned the characterization of DNA methylation landscapes in parallel neural systems, where the roles of DNA methylation markers could be compared and contrasted.

1.1.7 Research Aims

In light of the mounting evidence positioning DNA methylation as a regulatory mechanism in neural development, some questions remain. For example, though across various studies it has been observed that DNA methylation is a feature unique to the maturation state, it remains unclear whether all neurons observe similar DNA methylation programs or whether unique cell types exhibit distinguishing epigenetic features throughout their developmental course. Another critical aim was the examination of DNA methylation at the gene level. If, as hypothesized, DNA methylation and other epigenetic modifications function to aid in the regulation of critical developmental genes

during cellular specification, relevant gene networks should reveal differential epigenetic signatures at the onset of their expression/quiescence. As commercial technology improves, investigative tools such as methyl-sensitive sequencing and high-throughput automation will ensure that the future of epigenetics includes a thorough profiling of the developmental genome.

Another major unanswered question revolves around the extent of DNA methylation reprogramming. Traditionally, due to the replicative quiescence of neurons and the belief that methylation can only be lost through replication-dependent demethylation, it is thought that post-mitotic DNA methylation is very stable (Irwin, Pentieva et al. 2016). Thus, post-mitotic epigenetic reprogramming has not been thoroughly evaluated as a mechanism of cellular plasticity beyond mitosis. Though an active demethylase has not been demonstrated in the brain, demethylation has indeed been observed in the post-mitotic hippocampal neurons. Believed to play a role in the modulation of synaptic plasticity and memory consolidation, DNA methylation has been shown to be dynamically regulated in a post-mitotic, replication-independent context (Miller, Gavin et al. 2010, Guo, Su et al. 2011).Whether this form of DNA methylation reprogramming is utilized in other post-mitotic neurons remains to be examined.

The primary aim of this thesis revolved around the characterization of DNA methylation dynamics during normal, cellular development in two independent neural regions. Though DNA methylation has been implicated in gene regulation and cellular specification, an in-depth characterization and evaluation of cell-specific epigenetic landscapes had not been previously performed in the postnatal cerebellum or the embryonic cortex. We hypothesized that DNA methylation is a unique and dynamic

element guiding developmental cues through transcriptional regulation, exhibiting precise spatial and temporal patterns relevant to the developing system. To examine these at length, we first characterized DNA methylation patterns in the two major and complimentary cell types of the postnatal cerebellum at various time points. Further, the strata of the embryonic cortex, encompassing multiple cell types in various states of development, were profiled.

1.2 MATERIALS AND METHODS

1.2.1 Animals

C57BL/6J mice from Jackson Laboratory were used in accordance with Indiana University Animal Care and Use Committee protocols. A two-hour mating paradigm was used to obtain embryonic tissues and pups. Pregnancies could thus be tracked to the nearest two-hour interval of conception. Conception was denoted as embryonic (E) day 0. The day of birth was denoted as postnatal day (P) 0. After deep CO_2 euthanasia, embryos were harvested from dams at E17 by removal from the embryonic sack. Each embryo was either immersion-fixed in 20 mL of fixative prepared from 4% paraformaldehyde (PFA) for immunohistochemistry. Five independent litters are represented in the E17 cortex analysis. For cerebellar analysis, six P7, four P14, six P21, four P28, and four P45 mice were selected from at least four different litters, anesthetized by CO2 inhalation, and transcardially perfused with saline, followed by 4% paraformaldehyde fixation. Pup brains were dissected and post-fixed for a minimum of 48 hours.

1.2.2 Immunohistochemistry

Brains were subsequently embedded in 10% gelatin blocks and sectioned by free-floating vibratome (Leica VIT100S) at 40µm, coronally. Prior to immunohistochemical

detection, sections were cleared of endogenous peroxidases using 10% H_2O_2 in phosphate-buffered saline (PBS) for 10 min and permeabilized with 1% TritonX-100 in PBS for 30 min. A secondary permeabilization step involved the incubation of sections in 2N HCl for 15-30 minutes. Next, incubation with a primary antibody diluted in species-appropriate normal serum (1.5% serum, 0.1% TritonX-100 in PBS) was performed for 18 h at room temperature.

Antibodies used in this study are summarized in Table 1. To address issues including antibody penetration and inherent reduction of Purkinje cell (PC) immunoreactivity, we performed an immunostain using the Purkinje cell marker calbindin-D28K. Additionally, to establish the specificity of the 5hmC antibody, a preabsorption assay was performed for the anti-5hmC antibody (1:1000, rabbit polyclonal IgG, Active Motif) using 5hmC synthesized DNA (Methylated DNA Standard Kit, #55008, Active Motif, 50 ng/μ l, at a working dilution of 1:20 molar ratio) overnight at 4°C.

Biotinylated secondary antibodies (Jackson ImmunoResearch, West Grove, PA) were used at 1:500 for 90 minutes after primary antibody incubation, followed by 90 minutes of incubation in biotin-streptavidin conjugated tertiary antibodies (1:500). Optical detection of immunoreactivity was accomplished by 3,3'-Diaminobenzidine (DAB) (Sigma-Aldrich, St. Louis, MO) at 0.05% followed by activation with 0.003% H_2O_2 over an average of 3–8 min. Sections were subsequently counterstained with methyl green (Nissl stain). All stainings were examined under light microscopy for cellular analysis (Leitz Orthoplan 2 microscope; Ernst Leitz GMBH, Wetzlar, Germany).

and photographed with a Spot RT color camera (Diagnostic Instruments, Inc., Sterling Heights, MI).

For immunofluorescence detection, sections were incubated for 90 minutes in species-appropriate Alexa Fluor 488 and 546 conjugated IgG secondary antibodies (Thermo Fisher Scientific, Waltham MA). After PBS wash, sections were mounted on SuperFrost slides (Thermo Fisher Scientific, Waltham MA) and coated with DAPI Pro-long Gold antifade mountant (Thermo Fisher Scientific, Waltham MA).

Table 1. Antibodies used for neurodevelopmental assessment of DNA methylation

Primary Antibodies	**Company**	**Catalog #**	**dilution**	**predicted wt.**
5-methylcytosine	Eurogentec	BI-MECY-0100	1:2000	N/A
5-methylcytosine	Active Motif	AM61255	1:2000	N/A
5-hydroxymethylcytosine	Active Motif	AM39769	1:3000	N/A
calbindin/D28k	Bioss, USA	bs-3758R	1:1000	28 kDa
DNMT1	Abcam	ab87654	1:1000	~183 kDa
TET1	GeneTex	GTX124207	1:500	~220 kDa
MBD1	Santa Cruz Biotech.	sc-10221	1:200	~89 kDa
MeCP2	Cell Signaling Tech.	D4F3XP-R	1:1000	75 kDa
5-formylcytosine	Active Motif	AM61224	1:2000	N/A
5-carboxycytosine	Active Motif	AM61226	1:2000	N/A
Ki67	Novus Biologicals	NB110-89717	1:500	324 kDa
Tbr2	Millipore	AB2283	1:500	58 kDa
NeuN	Cell Signaling Tech.	D3S3I	1:500	46-55 kDa
P2Y1	Millipore	AB9263	1:1000	~42 kDa
Secondary Antibodies				
AlexaFlour 488	ThermoFisher Scientific	ab150077	1:500	~150 kDa
AlexaFlour 546	ThermoFisher Scientific	A-11003	1:500	~150 kDa
Goat anti Rabbit biotinylated	Jackson ImmunoResearch	111-065-003	1:500	~160 kDa
Horse anti Mouse biotinylated	Vector Laboratories	BA-2000	1:500	~152-165 kDa
Donkey anti Guinea Pig biotinylated	Vector Laboratories	BA-7000	1:500	~152-165 kDa

1.2.3 Confocal Microscopy

Confocal fluorescent images were obtained with an Olympus FV1000-MPE Confocal Microscope mounted on an Olympus IX81 inverted microscope stand with a 60x water-immersed objective. Sequential excitation at 488 nm and 559 nm was provided by argon and diode lasers, respectively. Emission was collected by spectral detectors in channels one and two with user-specified min and max wavelengths. Z-stack images were collected over a thickness of 4.5 μm in 0.3 μm step intervals. After sequential excitation, green and red fluorescent images of the same cell were saved and analyzed by Olympus Fluoview FV10-ASW software. The term co-localization refers to the overlap of green and red fluorescence in an image pair, as measured by confocal microscopy.

1.2.4 Quantification of 5mC and 5hmC using immunoabsorbance assays

To independently assess quantitative cellular methylation, 25μm coronal sections were obtained from flash-frozen cerebellum at ages P8 (N=8) and P29 (N=8) using a Leica Cryostat CM1900. Sections were mounted onto 2μm thick PEN membrane slides (Microdissect Gmbh, Herborn, Germany) and stained with 4X Thionin solutions. Slides were further dehydrated in series 50%, 75%, 90%, and 100% ethanol. Sections were viewed under 10X magnification using a Leica laser microdissection microscope (Leica CTR6500). The cerebellar layers were morphologically discernible by Thionin stain and dissected by laser into a flat cap 0.65mL Eppendorf tube containing 65μL of DNA extraction buffer (Arcturus Picopure DNA Extraction kit, Applied Biosciences). DNA was next purified using DNA Clean and Concentrator (Zymo, Irving, CA) according to manufacturer's instructions.

100ng and 200ng of purified cellular gDNA was used for MethylFlash™ Methylated DNA Quantification Kit and MethylFlash™ Hydroxymethylated DNA Quantification Kit respectively, according to manufacturer's instruction (Epigentek, Farmingdale, NY). Absolute quantification was performed using a five-point standard curve and further transformed to represent the ratio of methylated DNA (5mC or 5hmC) to total DNA. For presentation purposes, these were further transformed to denote expression of the methyl mark in relation to the control group totals (normalized).

1.2.5 Quantitative Gene Specific DNA methylation analysis

Genomic DNA (2µg) was extracted from cerebellum samples and digested. There were four treatment groups for each sample: uncut, methyl-sensitive enzyme (MSRE; *Hha* I or *Hpa* II; New England Biolabs, Ipswich, MA), methyl-dependent enzyme (*Mcr*BC; New England Biolabs, Ipswich, MA), and double digest with a methyl-sensitive and a methyl-dependent enzyme. Each digest was conducted with 10 U enzyme and incubated for 12 hours at 37°C. In the double digest sample, the first digest was performed using the methyl-sensitive enzyme, and the enzyme was heat inactivated by incubating at 65°C for 20 minutes. Prior to the second digestion, we purified the singly-digested DNA by phenol: chloroform extraction, and then precipitated the samples with 0.2 volumes of 1.5 M ammonium acetate and 2 volumes of 100% ethanol and re-suspended them in 1 X $T_{10}E_1$ buffer. Prior to amplification, all DNA was purified by phenol: chloroform extraction followed by ethanol precipitation and quantified by Nanodrop ND-1000 Spectrophotometer (NanoDrop Products, Wilmington, DE). We used 40ng of DNA from each digestion for quantitative PCR reaction with iTaq Universal SYBR Green mix (BioRad, Hercules, CA) and locus-specific primers (Table B-2,

Appendix B) using an iCycler PCR machine (BioRad, Hercules, CA). We used the default setting to obtain the cycle threshold (Ct) values, and normalized the digested samples to the uncut samples to calculate the delta Ct value. DNA methylation levels were determined by the average MSRE delta Ct value based on the calculation of $100 \times 2^{-\Delta Ct}$. Three or four biological replicates for both P7 and P29 animals were used for this analysis.

1.2.6 qPCR for gene expression

We added 10 volumes of RNA Stat-60 (Tel-Test, Inc., Friendwood, TX) to the snap-frozen P7 or P29 cerebellum, and homogenized and incubated the sample at room temperature for 5 minutes. To purify the RNA, we extracted the samples for 5 minutes with 0.2 ml chloroform/ ml RNA Stat, and centrifuged the samples for 15 minutes at 12,000 RPM (max) at 4°C. We transferred the aqueous layer to a new tube and precipitated the RNA for 10 minutes at room temperature with 0.5 ml isopropanol/ ml RNA Stat and then centrifuged the sample for 10 minutes at 12,000 RPM (max) at 4°C. The pellet was washed with 75% ethanol, vortexed, and centrifuged for 5 minutes at maximum speed at 4°C. We dried the pellet and dissolved it in 300 µl DEPC H_2O. RNA concentration was measured by NanoDrop ND-1000 Spectrophotometer (NanoDrop Products, Wilmington, DE). We performed DNase treatment using the TURBO DNA-free kit (Life Technologies, Grand Island, NY) to one µg of total RNA extracted from each sample by following the manufacture's instruction. DNase treated RNA was then converted into cDNA using iScript cDNA synthesis kit (Bio-Rad, Hercules, CA). Quantitative RT-PCR was performed using 50 ng of cDNA as a template for qRT-PCR in combination with TaqMan® Gene Expression Master Mix (Life Technologies, Grand

Island, NY) and TaqMan Gene-specific probes (Table B-1, Appendix B; Life Technologies, Grand Island, NY) on a StepOnePlus™ Real-Time PCR System (Life Technologies, Grand Island, NY). We assayed four biological replicates for P7 and P29. Cycling reactions were performed in duplicate. The relative expression of each gene was calculated based on the ΔΔCt value, where the results were normalized to the average Ct value of *Gapdh*.

1.2.7 Statistical analysis

A randomized design with a one–way arrangement of the treatments, "Age (P7 & P29)" data, was analyzed through the Generalized Linear Model procedure on SAS and comparisons between treatments were done through the Least Square Means procedure. All quantitative data were represented as the mean and standard error of the mean (SEM). Statistical analysis was performed between P7 and P29 DNA using a one tailed student t-test assuming unequal variance (GraphPad, Prism 6.0). The threshold for statistical significance was $p<0.05$.

1.3 RESULTS

1.3.1 Purkinje Cell DNA Methylation Reprogramming

Purkinje cell (PC) analysis is facilitated in part by the prominent and distinct morphological characteristics of its development. Purkinje cells originating from the ventricular zone of the cerebellar primordium begin to migrate and arrange a monolayer at a target region known as the Purkinje Cell Layer (PCL) ~E14.5-16.5 in mice. Purkinje cells contribute the primary GABAergic output to deep cerebellar nuclei which aid in control of movement and gait (Jayabal, Ljungberg et al. 2015, Vinueza Veloz, Zhou et al. 2015). During early migration and PCL formation, 5mC and 5hmC appear abundantly in

the nucleus of PCs, with 5mC particularly displayed as aggregate punctates and 5hmC expressing a more euchromatin distribution (Figure 3A and 3D, red crossed arrows). A distinguishing feature of PCs begins to occur after the first postnatal week, wherein PCs embark on a morphological transformation including the formation of apical dendrites followed by robust outgrowth of the extensive PC dendritic arbors and parallel fiber synaptogenesis (McKay and Turner 2005, Paul, Cai et al. 2012). Between the first and second postnatal weeks of development, the Purkinje cell dendritic area grows to as much as 10,000 μm^2 (Altman 1969) and a cell-unique upregulation of synaptic genes is observed (Rong, Wang et al. 2004, Sotelo 2004, Kirsch, Liscovitch et al. 2012, Paul, Cai et al. 2012). Interestingly, that period of cellular transformation was observably accompanied by the dramatic loss of 5mC, 5hmC, and DNA methylation correlates (Figure 3B, 3E, red dashed circles indicate the borders of the PC perikarya). By postnatal day 45, when peak PC synaptogenesis has subsided (Paul, Cai et al. 2012, Arancillo, White et al. 2015), PCs exhibit a partial remethylation of 5mC and 5hmC which is in agreement with the intranuclear distribution of mature-state 5mC (i.e. heterogeneous rather than aggregate or punctate distribution) (Zhou, Chen et al. 2011). Moreover, demethylation of PCs was observed to occur in a gradient overlapping the known maturation gradient of the cerebellum from the deep fissures to the superficial folia (Morris, Beech et al. 1985, Goodlett, Hamre et al. 1990). These phenomena were observed consistently throughout the rostro-caudal axis of the cerebellum.

To address concerns of incomplete penetrance of the DNA methyl markers in the mature PCs as a potential confounding factor, we performed stage matched immunohistochemical detection of the PC-specific marker calbindin D28-k. The calcium-

binding protein is a reliable and abundant marker unique to Purkinje cells in the cerebellum (Whitney, Kemper et al. 2008). As shown in Figure 4, it is consistently expressed in PCs throughout maturation, indicating that diminished immunoreactivity of the cell is not a likely confound for the observed demethylation. Moreover, the distinct intranuclear distribution of the DNA methylation markers at P7 combined with antibody pre-absorption assays (Figure 5) provided evidence of a distinct and reliable DNA methylation marker immunoreactivity in the cerebellum.

To confirm the immunohistochemical profiles of 5mC and 5hmC, a secondary strategy was initiated whereby the molecular profile of 5mC and 5hmC content was independently assessed. First, laser capture microdissection was used to isolate populations of Purkinje cells and extract their genomic DNA. While PC microdissection (due to the presence of adjacent basket interneurons and overlapping Bergman glia bodies) could not totally purify the PC population, the unique DNA methylation program of the PCs relative to these cell types (described below) was such that we could confidently assume was representative of the assay results. Next, quantitative detection of 5mC and 5hmC was carried out using the MethylFlash^{TM} Methylated DNA Quantification (Epigentek, Carlsbad CA) assays. As presented in Figure 6, semi-pure PC populations underwent a nearly ten-fold decline in genomic 5mC (Figure 6A, $p<0.01$), and an 8-fold drop in 5hmC from P7 to P29 (Figure 6B, $p<0.0001$). These results are consistent with the PC immunostaining patterns observed in Figure 3 and confirmed DNA methylation reprogramming in the post-mitotic PCs.

As mentioned previously, a dynamic 5mC and 5hmC intranuclear distribution was observed in the P7 PC nuclei. 5mC presented as punctate aggregates while 5hmC

displayed a euchromatin distribution (Figure 7), the two of which are not overlapping. As PC nuclei mature, however, 5mC adopts a more homogenous distribution similar to what we have previously observed in the embryonic neural tube (Zhou, Chen et al. 2011). This dynamic DNA methylation expression harkens back to the reported genomic complementarity of 5mC and 5hmC and likely relates to a functional diversity (Chen, Damayanti et al. 2014). Further, this stage-dependent distribution of 5mC in PCs provides further support for the early role of 5mC as a repressor of genomic "clusters" compared to a more relaxed and diffuse function in mature cells. Importantly, the chromatin remodeling of 5mC does not appear to be a cell-unique feature, displaying similar chromatin re- arrangement in granule neurons.

1.3.2 Granule Neuron DNA Methylation Reprogramming

While various DNA methylation landscape analyses have by now demonstrated or alluded to a maturation-dependent DNA methylation program, the cerebellar profile allowed the cross-examination of complementary cell types, complete with unique temporospatial developmental patterns. The most obvious was apparent in the granule neuron, the primary glutamatergic neuron of the cerebellum. Derived from the dorsal-most rhombic lip of the primordial cerebellar ventricular zone, granule cells adopt a DNA methylation program that is distinct from the reprogramming characterized in the Purkinje cell.

At P7, at the cerebellar superfice, mitotic granule precursors residing in the outer limits of the external granular layer (EGL^{o}) are largely un-methylated. As the granule precursors exit the cell cycle and migrate into the inner EGL (EGL^{i}) (also distinguishable by their elongated somata (Hatten 1990)), they undergo *de novo* 5mC and 5hmC

methylation. This phenomena is clearly distinguishable by the brown coloring of the EGL^i relative to the EGL^o (Figure 3A and 3D, blue crossed arrows), which demarcates the commitment of precursors to a granule fate and the initial stages of radial migration. Further, as the granule cells migrate inward from the EGL^i toward their target position at the Inner Granule Layer (IGL), 5mC and 5hmC levels continually increase in accordance with the maturation stage of the cell, peaking as they settle at their final destination. Granule neurons in contrast to PCs, appear to maintain the acquired 5mC and 5hmC marks throughout adulthood (Figure 3C, 3F; blue crossed arrows).

Laser capture microdissection and subsequent quantitative analysis of molecular 5mC further supported the stage-dependent acquisition of granule neuron methylation. Proliferating granule cells of the EGL were compared with post-mitotic granule cells of the IGL at P7. Between the period of cell-cycle arrest and radial migration to the IGL, granule neurons nearly doubled their 5mC expression (Figure 6C, $p<0.02$). Further, even after granule cells reach the IGL, they gradually continued to acquire 5mC from P7 to P29 (Figure 6D, $p<0.007$), a time-frame overlapping with granule cell parallel fiber synapse formation (P14-P28) (Paul, Cai et al. 2012).

The developmental timeline of granule cells, like PCs, is coincidental with the DNA methylation reprogramming of the cell. The major DNA methylation reprogramming of the granule neuron is observed during P7-P14, coincident with peak migration of the cells (Komuro, Yacubova et al. 2001) and bifurcation of parallel fibers. Though seemingly straightforward, the developmental progression of granule neurons, which deliver excitatory glutamatergic drive to PCs and modulate its excitability, are

crucial to the proper formation and function of the cerebellar architecture (Volpe and Adams 1972, Hatten 1999).

Granule and Purkinje neurons are not the only cells that demonstrate a temporospatial DNA methylation program in the cerebellum. Stellate interneurons of the Molecular Layer (ML), Golgi interneurons in the IGL, and basket cells (Figure 3**,** purple dots) surrounding PCs in the PCL similarly undergo epigenetic reprogramming unique to their developmental course. Interestingly, these interneurons are born from the same ventricular region as PCs (Zhang and Goldman 1996), yet exhibit an epigenetic course more closely resembling granule neurons than PCs. Stellate and basket interneurons, for example, acquire DNA methylation as they complete their migratory paths around the second postnatal week (Stroud, Feng et al. 2011) and retain their methylation even after their maturation has been completed (approximately the fourth and fifth postnatal weeks).

1.3.3 Epigenetic Correlates of Post-Mitotic DNA Methylation Reprogramming

To further scrutinize the cellular DNA methylation programs of the postnatal cerebellum, we profiled DNA methylation-conferring enzymes and methyl-DNA binding proteins. At P7, DNMT1 displayed a distribution similar to 5mC, as characterized by an intranuclear punctate distribution (Figure 8A). TET1 expression, on the other hand, mirrored 5hmC, as denoted by a euchromatin intranuclear distribution (Figure 8D). By the third postnatal week, PC loss of both DNMT1 and TET1 were clearly observable (Figure 8B and 8E), re-emerging again at P45 to confer the subsequent wave of PC remethylation (Figure 8C and 8F). This observation supports the expression patterns of the enzyme products detailed previously.

Further support for DNA methylation reprogramming was obtained from methyl-DNA binding protein profiles. MeCP2 was present in P7 PCs in punctate distribution confirmation (Figure 9A) reminiscent of 5mC, an observation which is in agreement with previous reports of 5mC-MeCP2 binding complementarity. Additional evidence of a 5mC-MeCP2 relationship was provided by the parallel remodeling of MeCP2 from P7 to P21 in PCs. Notably, MeCP2 does not undergo complete loss in maturing PCs, though a significant reduction is observed during synaptogenesis and axonal-dendritic outgrowth (Figure 9B). MBD1 also showed a loss of expression at P21, though some PCs appear to retain this methyl binding protein (Figure 9D). Collectively, the presentation of the epigenetic correlates of 5mC and 5hmC support the PC DNA methylation program. Finally, incomplete loss of the methyl-CpG binding proteins (MBDs) may be rooted in the proclivity of the MBDs to interact with histone methylation modifications which were not examined in this study (Schmitz, Albert et al. 2011, Chittka, Nitarska et al. 2012, Wang, Yue et al. 2014).

As a final assessment of cerebellar DNA methylation reprogramming, we examined downstream intermediates of the passive demethylation pathway including 5fC and 5caC. We observed that the presentation of the markers was highly coordinated with 5mC and 5hmC (Figure 10). The 5caC and 5fC were detected in abundance in PCs at P7, but were no longer detectable at P21-P28, in line with 5mC and 5hmC loss. The concordant loss of 5mC and downstream intermediates sheds some interesting light on the replication-independent mechanisms likely guiding post-mitotic DNA methylation reprogramming.

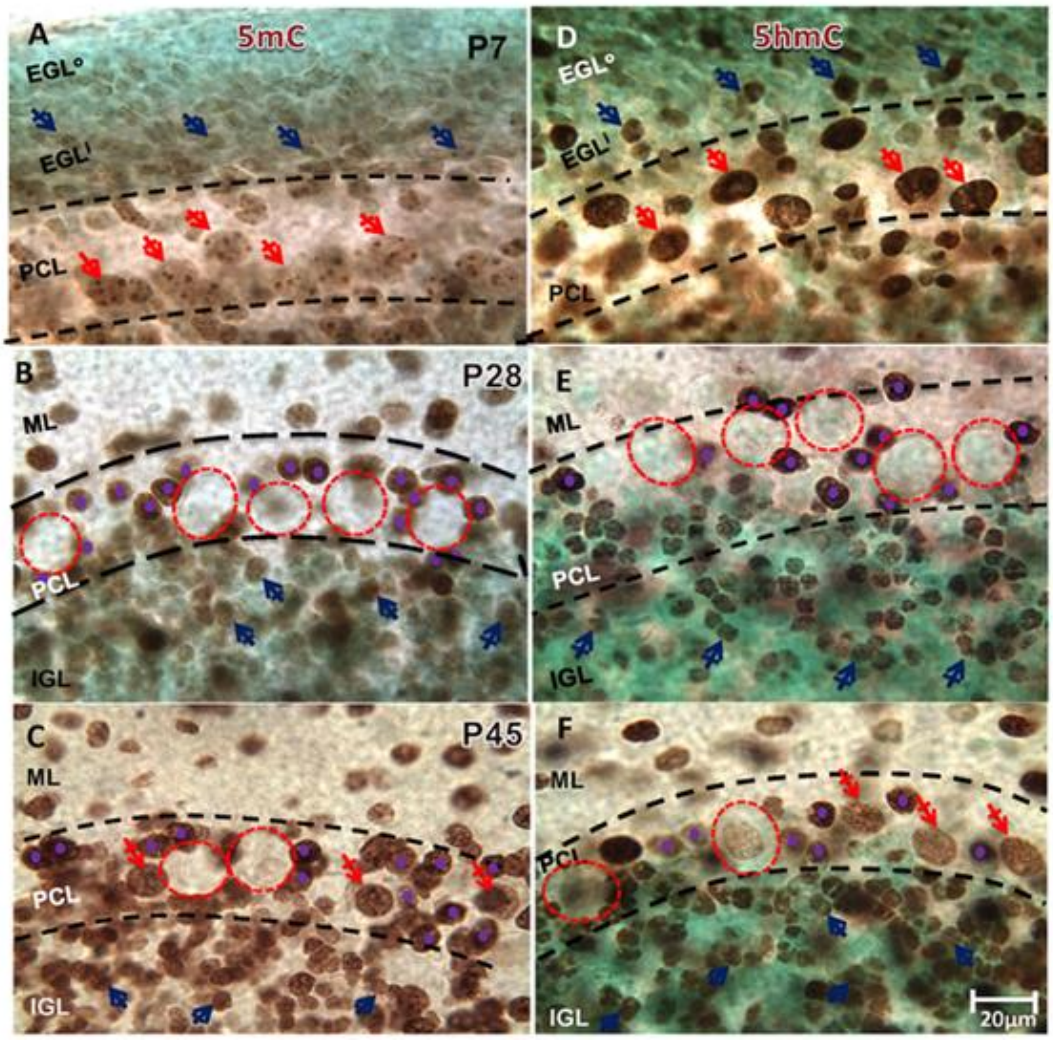

Figure 3. Purkinje cell DNA de-methylation and re-methylation in the postnatal cerebellum

(A) 5mC-immunostaining (im) is intensively present in the nucleus (size >12µm) of postmitotic Purkinje Cells (PC) at P7 (red, crossed arrows) at PC layer (PCL). 5mC is also distinctively present only in the non-dividing granule cells of the inner portion of the External Granule Layer (EGLi, blue crossed arrows) but not outer portion of EGL (EGLo). (B) By P28, the waning of 5mC-im was evident in PCs (red, dashed circles; ~20µm diameter). Basket cells surrounding the PCs (purple dots, <8µm) were intensively immunostained by 5mC (as well as all other interneurons). Mature granule cells inhabiting the Inner Granule Layer (IGL) retained the acquired 5mC-im throughout the remainder of the time-course. (C) By P45 re-methylation of PCs occurred as the 5mC-im returned to some but not to all de-methylated PCs (red, crossed arrows denote re-methylated PCs). (D) At P7, 5hmC immunostaining (im) is intensively present in PCs (red, crossed arrows), though distributed distinctly from 5mC. Some granule cells of the inner EGL express 5hmC-im though not at the upper surface of the EGL, where granule cell progenitors reside. (E) At P28, a clear de-methylation of 5hmC occurs in the PCs (red, dashed circles) as occurs with 5mC. Granule cells which have migrated to the IGL

continue to acquire 5hmC (blue, crossed arrows) as do the emerging basket interneurons surrounding the perimeter of PCs (purple dots). (F) At P45, re-methylation of 5hmC occurs in line with 5mC re-methylation at PCs (red, crossed arrows denote re-methylated PCs). Interneurons and granule cells appear to refrain from de-methylation throughout their developmental time-course. Scale bars: A-F=20μm; Methyl Green Nissl counterstain. Dashed red circles depict the approximate boundaries of the PC cell body. Dashed black lines depict approximate boundaries of the PCL.

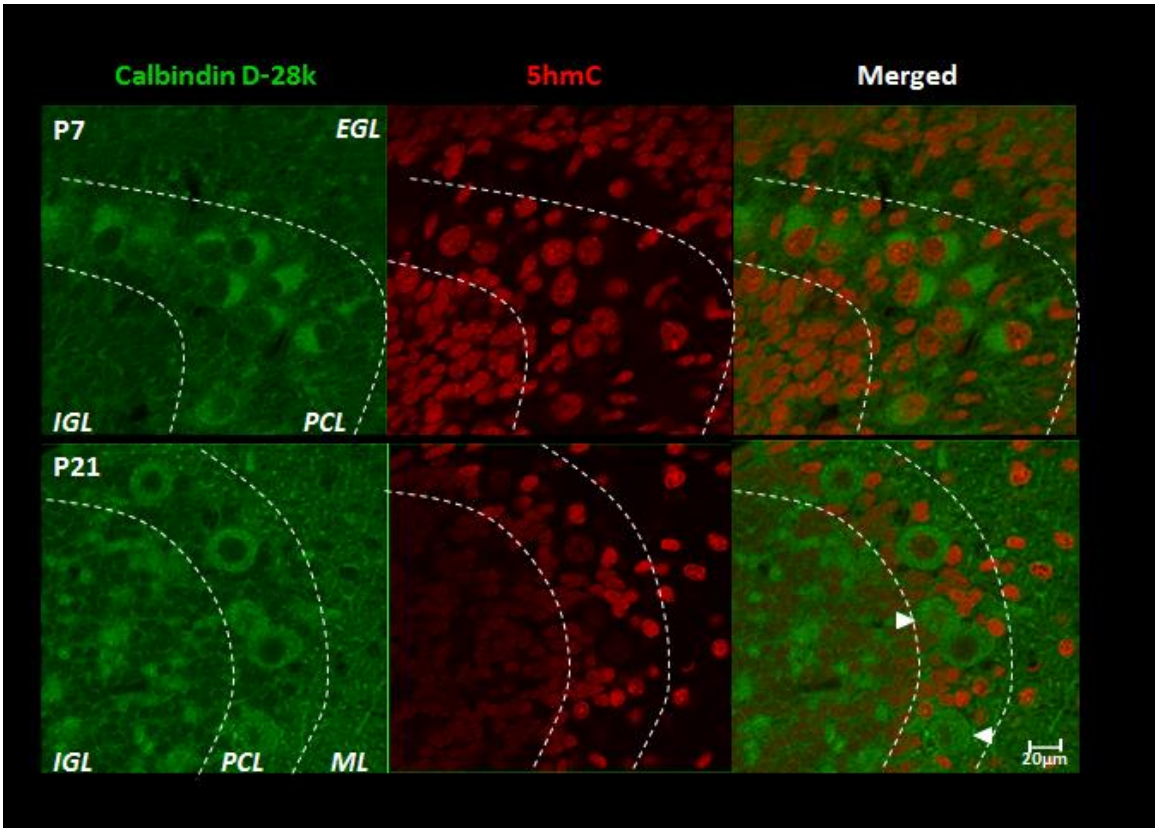

Figure 4. Persistent immunoreactivity of calbindin D-28k in Purkinje cells of the developing cerebellum

The calcium-binding protein Calbindin D-28k (green) is a characteristic Purkinje cell protein and appears markedly immunoreactive at P7 in the PCL. At P7, 5hmC (red) is also abundant in PC nuclei and granule cells of the inner EGL and IGL. At P21, even while an abundance of DNA methylation markers undergo dramatic loss of immunoreactivity, Purkinje cells retain calbindin expression. In contrast, interneurons emerging in the ML (as well as basket cells surrounding the large Purkinje bodies) abundantly express 5hmC at P21. EGL: external granule layer, IGL: internal granule cell layer, PCL: Purkinje cell layer, ML: molecular layer. Dashed borders represent the approximate cytological borders of the PCL.

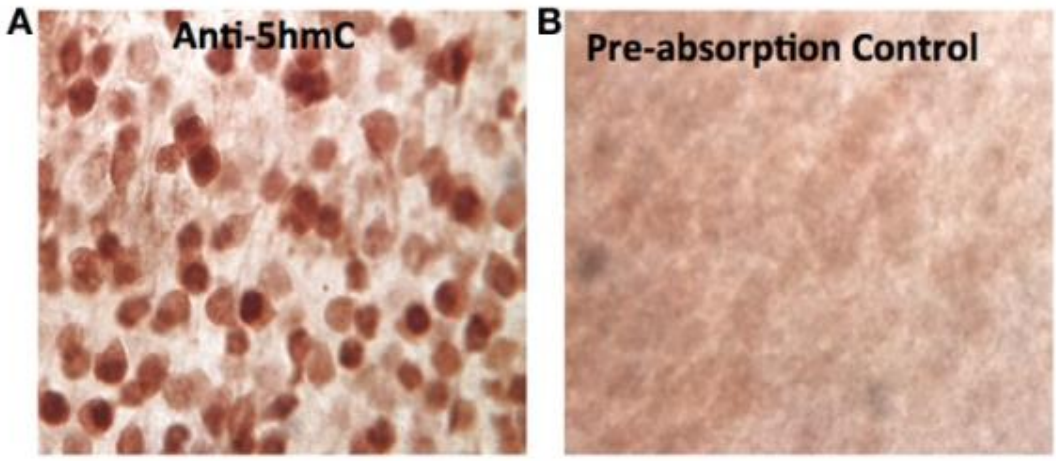

Figure 5. Pre-absorption confirms the specificity of the anti-5hmC antibody
The specificity of the crucial anti-5hmC antibody against 5hmC was characterized by pre-absorption of anti-5hmC antibody (1:1000, rabbit polyclonal IgG, Active Motif) with 5hmC synthesized DNA (Methylated DNA Standard Kit, #55008, Active Motif, 50 ng/μ l, at a working dilution of 1:20 molar ratio) overnight at 4°C. (A) Before absorption, the anti-5hmC immunostaining in the cortex shows distinct 5hmC staining pattern, (B) while the staining pattern was abolished or drastically reduced after 5hmC-preabsorption.

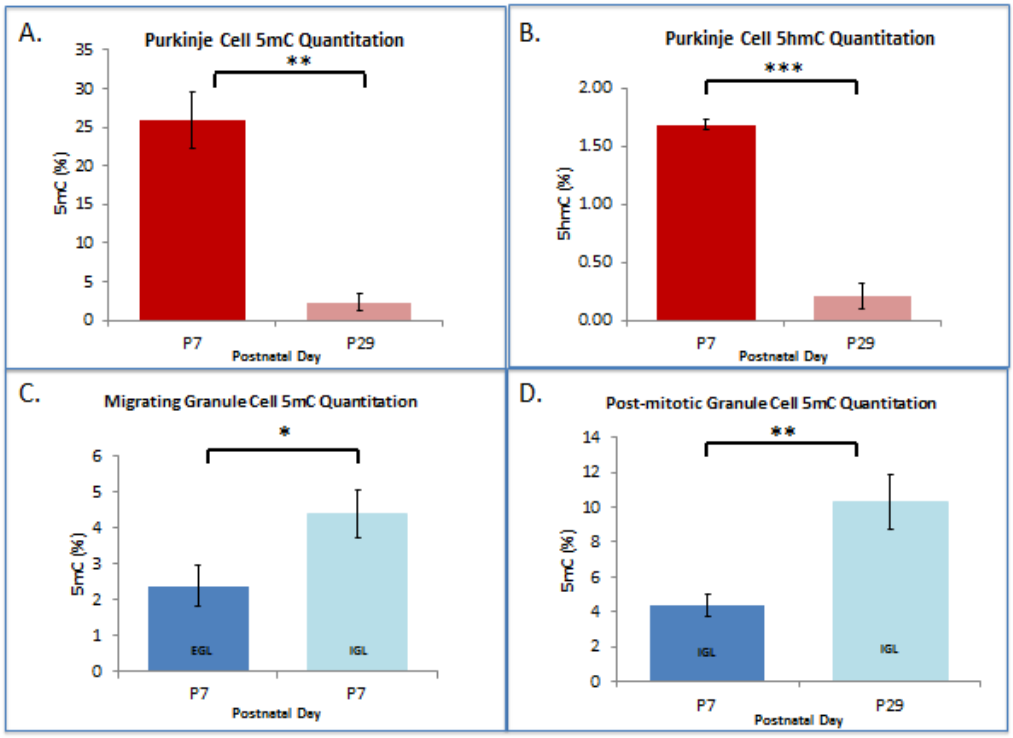

Figure 6. Quantitative detection of cell-specific DNA methylation confirms Purkinje cell de-methylation and granule cell methylation

Purified gDNA obtained from laser micro-dissected Purkinje and Granule cells was quantitatively analyzed for 5-methylcytosine and 5-hydroxymethylcytosine content (%) via antibody-based colorimetric assay. (A-B) Purkinje cells undergo remarkable loss of both 5mC and 5hmC between the first and fourth post-natal weeks, coincident with the Purkinje cell morphological and transcriptional transformation. (C-D) Granule cells of the external granule surface, as they undergo radial migration into the internal granule layer and become post-mitotic, acquire 5mC as indicated by earlier immunohistochemical analysis (Figure 3). Further, granule cells of the internal granule layer (IGL) continue to acquire methylation between the first and fourth postnatal week as granule cells settle into their mature state. (A.) **P-value=0.0078; (B.) ***P-value=0.0001; N=4 per age. (C.) *P-value=0.0186; (D.)** P-value=0.0036; N=8 per age.

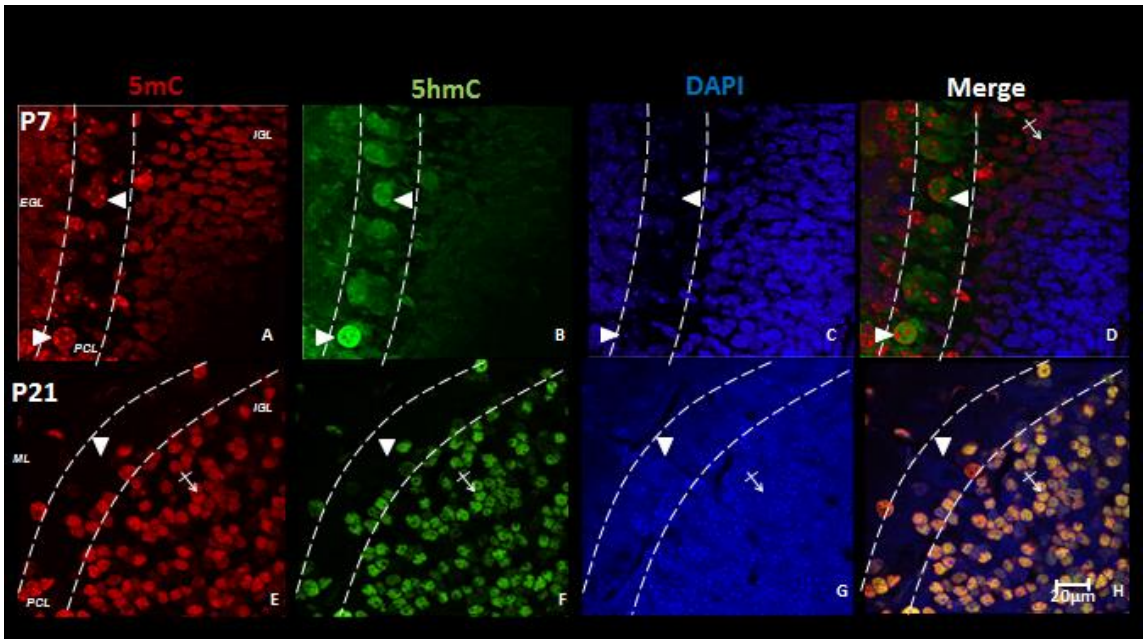

Figure 7. Developmental chromatin remodeling of Purkinje cells is apparent by intranuclear localization of 5mC and 5hmC during postnatal development
While distributed throughout the nucleus at the embryonic stage (not shown), at P7, major 5mC-immunostaining (im) (red) is packed into large punctates in the DAPI dense (blue), heterochromatin regions of the PCs located in the Purkinje Cell Layer (PCL) (A, white arrows). (B) 5hmC (green) was detected primarily in the euchromatin DAPI sparse regions (B, white arrows). At P7, as the granule cells in the external granular layer (EGL) migrate into the internal granular layer (IGL), 5mC appears to precede 5hmC expression, as no overlap was observed at P7 (D, crossed arrows). De-methylation of 5mC and 5hmC in PCs progresses through P14 and peaks between P21 and P28. Notice the loss of 5mC and 5hmC in most of the PCs in the PCL (E, F white arrows). In contrast, DNA methylation in granule cells is independent of the PC program. At P21, when migration from the EGL has ceased and cells have permanently settled in the IGL, there is significant overlap between 5mC and 5hmC as denoted by yellow fluorescence (H, crossed arrows). Furthermore, by P21 the characteristic punctate staining of 5mC observed during the first postnatal week has been replaced by a more homogenous distribution in the matured, rounded nuclei of the granule cells. ML: molecular layer. Scale bar: A-H=20µm.

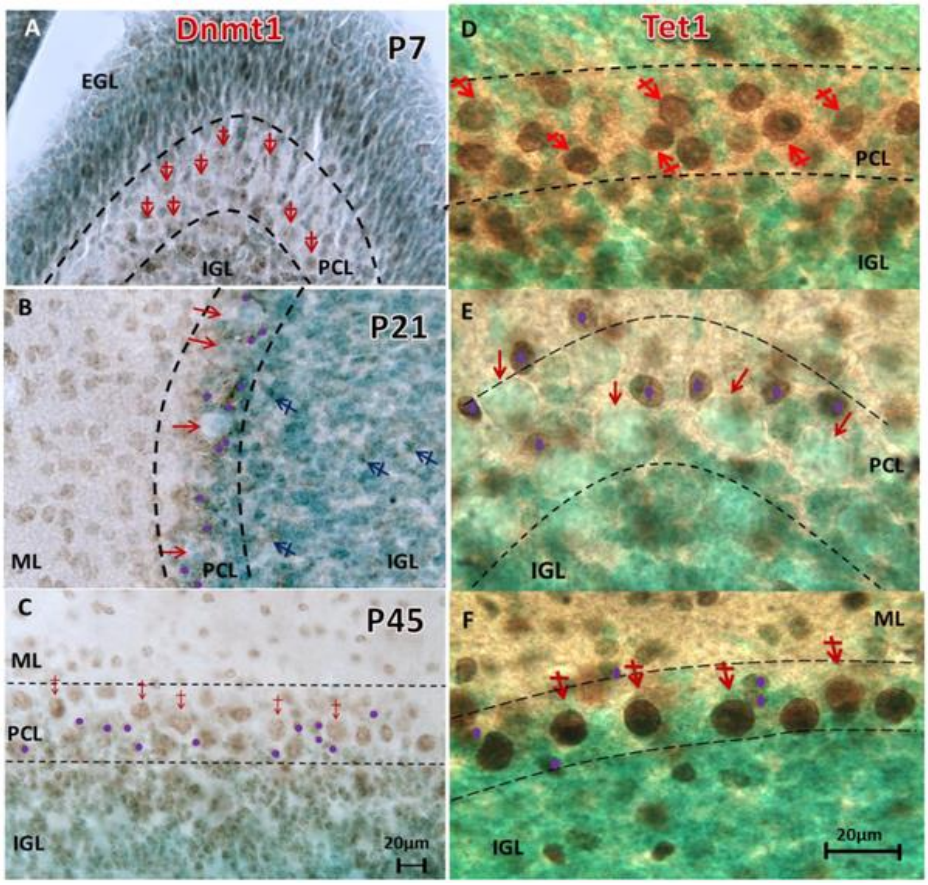

Figure 8. De-methylation and re-methylation are synchronized with the turnover of DNMT1 and Tet1 throughout the maturation of Purkinje cells

The peak heterochromatin appearance of 5mC-im (Figure 1) occurs at the same time as peak Dnmt1-im (A, red crossed arrows). Similarly, the peak euchromatin staining of 5hmC-im (Figure 1) occurs at the same time as peak Tet1-im (D, red crossed-arrows) in PCs at P7. De-methylation follows progressively, as by P21 many PCs lacked DNMT1 (B, red arrows), and subsequently were devoid of Tet1 (E, red arrows). The methyl green counterstaining reveals 5hmC negative and Tet1-negative PC cell bodies (red arrows). Meanwhile, surrounding basket cells (and other interneurons) acquire Tet1 (E, purple dots). By P45, as re-methylation of 5mC is occurring, DNMT1-im is notably returned to the PC nuclei (C, red crossed-arrows). Similarly, Tet1 is observed parallel with the resumed observation of DNMT1-im expression (F, red crossed arrows) in PCs. PCL: Purkinje layer; EGL: external granule layer; IGL: internal granule layer. Scale bars: A-C=20µm; D-F=20µm.

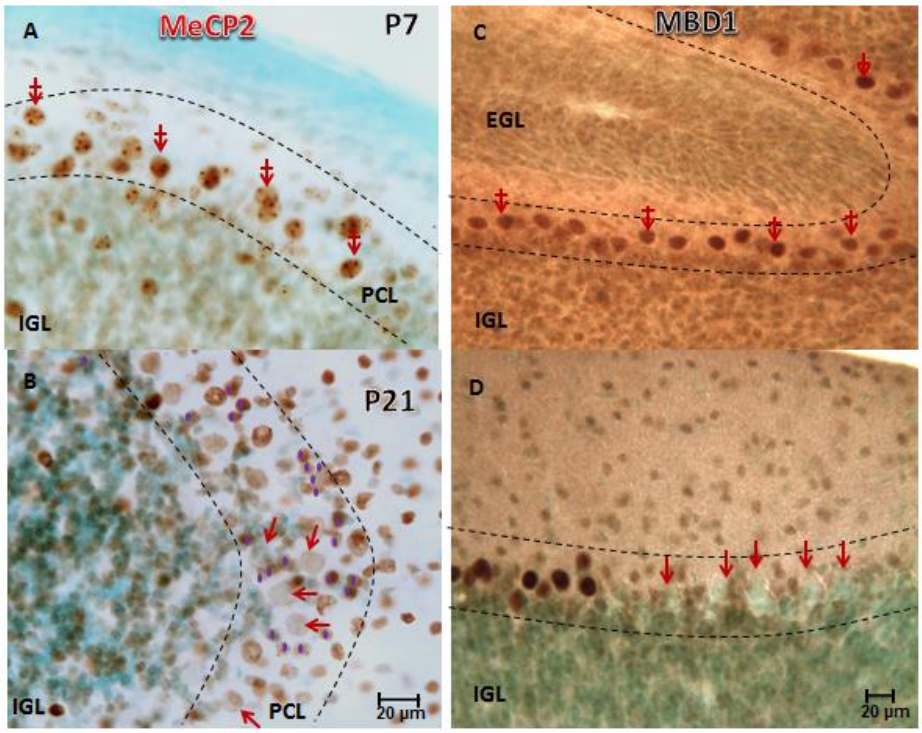

Figure 9. Postnatal de-methylation is supported by the diminished immunoreactivity of the methyl binding proteins MeCP2 and MBD1
(A)Marked MeCP2 was found in the nuclei of PCs at P7 (red, crossed arrows) where its granular distribution within the nuclei is co-localized at this time point with 5mC (Figure 1). A noticeable waning of MeCP2-immunostainning in the PCs is observed by P21 (B, red arrows), though not to the extent observed in 5mC at the S-AMe time point. Basket interneurons (purple dots), on the other hand, acquire MeCP2 as they for a perimeter around the PCs. A similar de-methylation phenomenon is observed with MBD1-im at P21 in some but not all PCs observed (D, red arrows). PCs aligned in the deeper regions of the cerebellar foliae were more susceptible to this loss. IGL: internal granule cell layer, PCL: Purkinje cell layer, ML: molecular layer, Counterstaining: Nissl green. Scale bar: A-D= 20 µm.

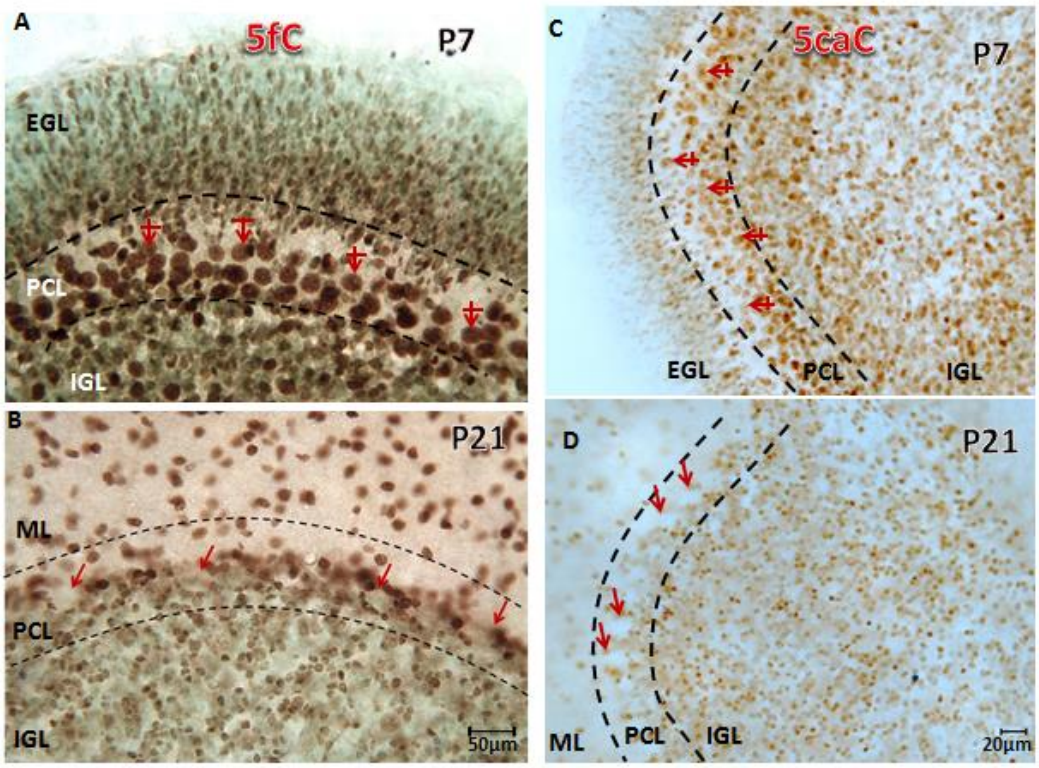

Figure 10. Postnatal loss of 5hmC is synchronized with the loss of downstream derivatives 5fC and 5caC in Purkinje cells
(A)5fC and 5caC are downstream metabolites of 5hmC (catalyzed by Tet enzymes) and prevail throughout cerebellar neurons including PCs (red, crossed arrow) and post-mitotic granule cells at P7 (A,C). As 5hmC is de-methylated at P21 (Figure 3), 5fC and 5caC are also greatly reduced (B, D, red arrows). On the other hand, as PCs undergo de-methylation of the 5fC and 5caC derivatives, surrounding basket cells acquire immunoreactivity. IGL: internal granule cell layer, PCL: Purkinje cell layer, ML: molecular layer, Nissl counterstaining: methyl green. Scale bar: A-B= 50µm, C-D=20µm.

1.3.4 Functional Impact of the DNA Methylation Program

Though the correlation between DNA methylation reprogramming and cellular and neural development has been widely documented, its presupposed role in transcriptional regulation and the particular transcriptional targets have not been clearly outlined. To determine whether these cell-specific, cell-wide demethylation events were reflected at the gene level in PCs, we investigated the cerebellar DNA methylation status of *Grid2, Cacna1g, Itpr1, Ppp1r17, Syt2* and *Rgs8*, which undergo PC specific turnover between P7 and P29. These genes were selected based on their predominant expression in PCs during the robust synaptogenesis period according to the Cerebellar Development Transcriptome Database (CTD-DB) (http://www.cdtdb.neuroinf.jp/CDT/Top.jsp) (Table B-2, Appendix B). Briefly, *Grid2* encodes the glutamate ionotropic receptor delta type subunit 2, *Cacna1g* encodes the calcium voltage-gated channel subunit alpha 1g, the *Itpr1* gene encodes the inositol 1,4,5-triphosphate receptor type 1, and *Ppp1r17* encodes the regulatory subunit 17 of the protein phosphatase 1. The gene *Syt2* encodes the synaptic vesicle membrane protein, which is thought to function as a calcium sensor and exocytosis. Finally, the gene *Rgs8* encodes the regulator of G-protein signaling 8, a regulatory and structural component of G protein-coupled receptor complexes. Particularly, these selected genes were cross-referenced against a previous high-throughput analysis identifying differentially hydroxymethylated genomic regions of cerebellar DNA between P7 and P42 (Table 2) (Szulwach, Li et al. 2011). The above genes met both criteria and were further pursued for methylation-specific restriction enzyme (MSRE) digestion qPCR.

		Genomic Position				% DNA methylation		
Symbol	Chr	GRCm38/mm10 Dec 2011	NCBI37/mm9 July 2007	Szulwach et al., 2011*	Gene Region	P7	P29	p value
Cacna1g	11	94475570–94475919	94336884–94337233	94336856–94337487	Promoter to Intron 1	72%	10%	0.0003
	11	94433798–94434145	94295112–94295459	94294907–94295732	Exon 17	3%	6%	0.18
	11	94428990–94429289	94290304–94290603	94290388–94290643	Intron 21 to Intron 22	9%	78%	0.0018
	11	94425603–94425939	94286917–94287253	94286602–94287380	Exon 25 to Intron 25	50%	83%	0.2
Grid2	6	64015530–64015858	63965524–63965852	63965601–63965939	Intron 4	112%	42%	0.0037
Ppp1r17	6	56011797–56012089	55961791–55962083	N/A	Promoter	95%	102%	0.7
	6	56026217–56026531	55976211–55976525	N/A	Exon 3 to Exon 4	118%	127%	0.86
Itpr1	6	108212871–108213125	108162865–108163119	N/A	Promoter to Exon 1	0.07%	0.11%	0.78
	6	108456741–108456940	108406735–108406934	108406713–108407010	Intron 44	0.62%	0.38%	0.23
	6	108550320–108552689	108501381–108501617	108501267–108501528	Downstream	109%	113%	0.11
Rgs8	1	153659694–155506824	155506824–155507042	155506651–155507232	Intron 1	23%	46%	0.0026
	1	153671065–153671346	155518195–155518476	155517949–155518550	Intron 4	100%	84%	0.78
Syt2	1	134707086–134707325	136603663–136603902	136603350–136604406	Intron 2	95%	38%	0.045

Table 2. Differentially methylated regions of cerebellar gene targets for DNA methylation analysis by restriction enzyme digestion and qPCR

* Szulwach, K. E., Li, X., Li, Y., Song, C. X., Wu, H., Dai, Q., Irier, H., Upadhyay, A. K., Gearing, M., Levey, A. I. et al. (2011). 5-hmC-mediated epigenetic dynamics during postnatal neurodevelopment and aging. Nature neuroscience 14, 1607-1616.

MSRE qPCR allowed for the quantitative assessment of methylated cerebellar DNA across different time points. The PC-preference of the investigated genes further allowed a cell-specific examination of PCs in lieu of purified PC DNA. This strategy could be used to investigate whether the immunohistochemical distribution of 5mC and 5hmC could be traced onto functional PC genes during the developmental time course. Results demonstrated that DNA methylation reprogramming was not fully unilateral, demonstrating both up and downregulation at different loci. For example *Grid2* and *Syt2*, which are detected at the synapse, underwent demethylation within the gene body by P29, diminishing by 42% ($p=0.0037$; Figure 11B). Similarly, *Syt2* demonstrated a marked demethylation in the gene body (95% to 38%; $p=0.045$) between P7 and P29 (Figure 11D). However, an examination of independent sites on the *Cacna1g* gene, encoding a low voltage calcium channel that is widely detected in neurons, revealed concomitant loss of promoter methylation (72% at P7 to 10% at P29; $p=0.0003$) and acquisition of gene body methylation (9% to 78%; $p=0.0018$) between the two developmental stages (Figure 11F). Although two other sites within the gene body of *Cacna1g* showed an increase in DNA methylation at P29, they were not statistically significant. Additionally, the G-protein signaling regulator gene *Rgs8* demonstrated a 23% increase in gene body DNA methylation between P7 (23%) and P29 (46%) ($p=0.0026$). Various other investigated genes demonstrated that not all examined loci undergo epigenetic reprogramming. The promoter and gene body of *Ppp1r17* (a regulatory subunit of protein phosphatase 1), for example, remained completely methylated through P7 and P29, while the promoter and gene body of the *Itpr2* gene (an inositol triphosphate receptor) remained relatively unmethylated throughout these two stages.

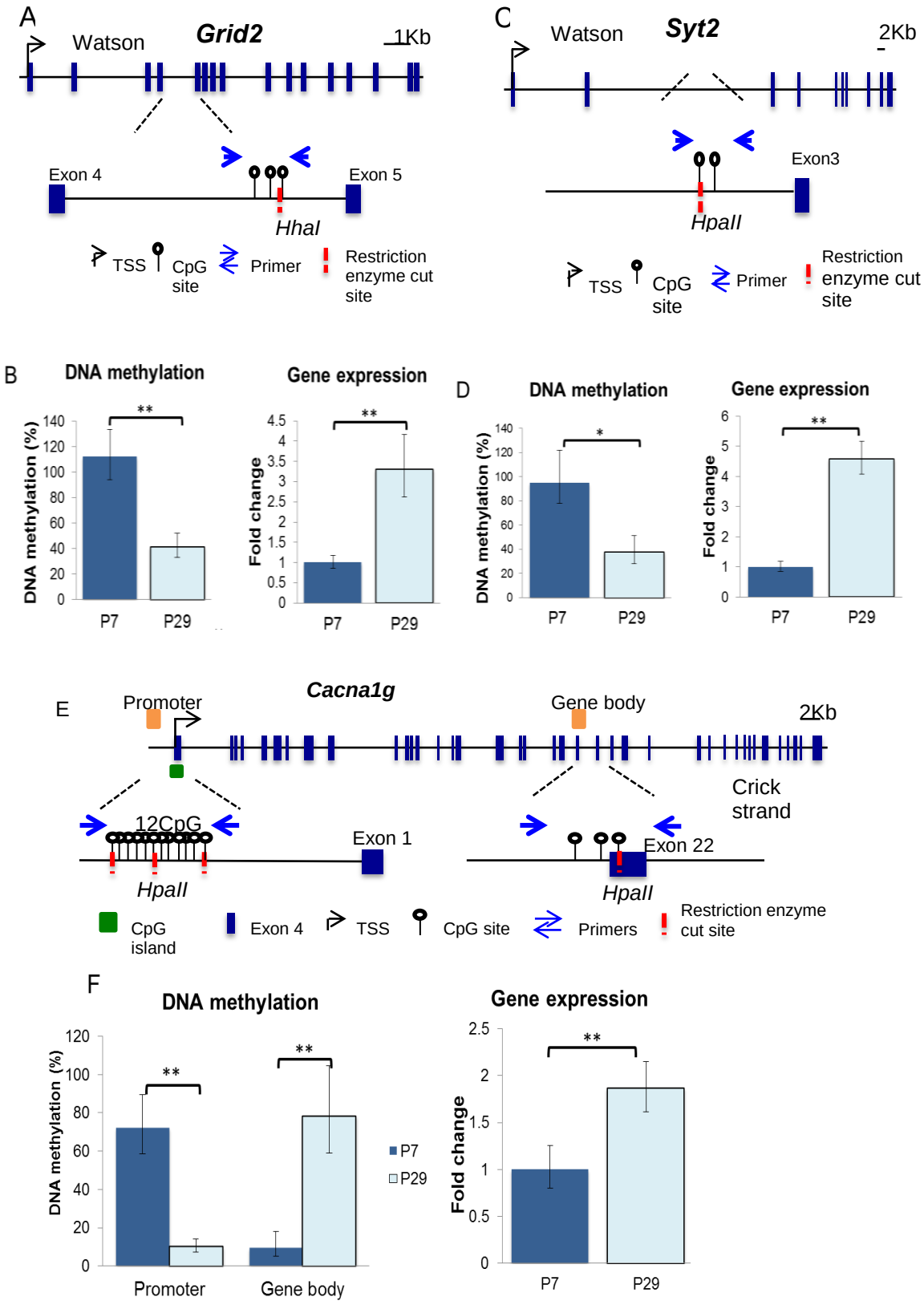
A
Watson
Grid2
1Kb
Exon 4
Exon 5
HhaI
TSS
CpG site
Primer
Restriction enzyme cut site
C
Watson
Syt2
2Kb
Exon3
HpaII
TSS
CpG site
Primer
Restriction enzyme cut site
B
DNA methylation
DNA methylation (%)
P7
P29
Gene expression
Fold change
P7
P29
D
DNA methylation
DNA methylation (%)
P7
P29
Gene expression
Fold change
P7
P29
E
Cacna1g
Promoter
Gene body
2Kb
Crick strand
12CpG
Exon 1
HpaII
Exon 22
HpaII
CpG island
Exon 4
TSS
CpG site
Primers
Restriction enzyme cut site
F
DNA methylation
DNA methylation (%)
Promoter
Gene body
P7
P29
Gene expression
Fold change
P7
P29

Figure 11. Purkinje cell-preferring genes undergo simultaneous de-methylation and transcriptional upregulation during peak synaptogenesis

(A) Diagram of Grid2 gene structure. Transcription start site (TSS): black bent arrow; exons: black boxes. Grid2 is transcribed from the Watson strand. A region in the intron 4 was analyzed. The lower half of the panel is a magnification of the target region. Three CpG dinucleotides and one HhaI cleavage site are located in the target region (Chr6:64,015,530-64,015,858). Displaying primer (blue, straight arrow), CpG dinucleotides (white "lollipops"), and restriction enzyme cleavage sites (red, dashed lines). (B) Analysis of Grid2: This Figure represents DNA methylation changes between P7 and P29 following digestion with HhaI. The P7 cerebellum is highly methylated, while the P29 cerebellum shows about a 60% reduction in DNA methylation. P-value=0.0037. Gene expression of Grid2: Quantitative RT-PCR of P7 and P29. Grid2 is expressed 3.3 fold higher in P29 than in P7 cerebellum. P-value = 0.0006. (C) Analysis of Syt2. We amplified the following genomic region for Syt2: Chr1: 136603663+136603902. (D) This Figure represents DNA methylation changes between P7 and P29 following digestion with HpaII. The P7 cerebellum is almost completely methylated, while P29 cerebellum shows about a 60% reduction in DNA methylation. P-value=0.045. From P7 to P29, *Syt2* mRNA expression is increased 4.6 –fold. (E) *Analysis of Cacna1g.* We amplified the following genomic region for *Cacn1g*: Chr11: 94336884 - 94337233. (F) This Figure represents DNA methylation changes between P7 and P29 following digestion with *Hpa* II. The P7 cerebellum is ~ 72% methylated, while P29 cerebellum shows only 10% methylation. P-value=0.0003. Gene body methylation analysis reveals a reciprocal relationship across ages, where P7 methylation begins around 10% and spikes to about 80% by P29. Overall gene expression was increased 2-fold across this time. *$p<0.05$, **$p<0.005$

These results showed that DNA methylation reprogramming affecting cerebellar (particularly PC) development may occur through various genomic regions beyond the regulatory promoter. Additionally, as described earlier, DNA methylation changes during development are dynamic. Some genes experience accumulation of DNA methylation while others observe diminished DNA methylation, indicating that the apparent near-totality of immunohistological demethylation in PCs requires a closer examination. Finally, the functional contribution of DNA methylation reprogramming was confirmed by gene expression analysis. Among *Grid2*, *Cacna1g*, *Syt2* and *Rgs8,* all genes were upregulated by P29 with fold changes of 3.3 (p=0.0006), 1.9 (p=0.0037), 4.6 (p=0.0001) and 10.6 (p=0.0001), respectively. *Itpr1* and *Ppp1r17* transcripts have similarly been reportedly upregulated in cerebellar DNA by P42 in a previous study (Szulwach, Li et al. 2011). Taken together, these results corroborate the early immunological profile of PC DNA methylation reprogramming and provide support for the mechanism as a regulatory element in cellular and cerebellar progression.

1.3.5 DNA Methylation Program in the Embryonic Cortex

To examine whether cell-unique DNA methylation occurs during the development of neurons in other developing brain regions, we investigated the DNA methylation profile of the embryonic cortex. At embryonic day 17, the cerebral cortex exhibits a unique stratified architecture containing multiple neuronal populations in various states of maturity. After neural tube closure, neuroepithelial cells begin to transform into radial glial cells (RGCs) coincidental with the onset of cortical neurogenesis (Kriegstein and Gotz 2003). From the lateral ventricular formation, a proliferative ventricular zone is formed, populated by replicative RGCs. This region

undergoes asymmetrical cell division, giving rise to RGC clones (cortical neuron precursors) and simultaneously producing an intermediate progenitor cell (IPC) which migrates outward to become an inhabitant of the adjacent subventricular zone (SVZ). In the SVZ, intermediate progenitors undergo 1-3 rounds of symmetrical cell division (Noctor, Martinez-Cerdeno et al. 2004). IPCs, distinguishable by their distinct morphology and protein expression patterns (i.e. Tbr2 (Englund, Fink et al. 2005)) produce cortical neurons, particularly of the upper cortical layer (Tarabykin, Stoykova et al. 2001), and olfactory bulb neurons (Lois and Alvarez-Buylla 1993). Moreover, this two-tiered replicative mechanism is believed to be a unique feature of mammalian neurogenesis which contributes to the formation of a rather large cortical surface (Cheung, Kondo et al. 2010).

The intermediate zone (IZ) is largely populated by the radial glial processes that serve as scaffolds for migrating cortical neurons, which subsequently traverse the IZ and settle in an inside out fashion (with newly arriving cells migrating and settling past the existing neurons) in the cortical plate (CP). Interestingly, the IZ has also been found to be heavily populated by cortical interneurons originated from the ganglionic eminence (Nadarajah, Alifragis et al. 2003). Due to the zonal splitting of the primordial plexiform cortical layer by the emerging CP, the oldest and most mature cortical neurons are located in the superficial marginal zone (MZ) and the deeper subplate (SP) layers. Like the proliferating zones and the intermediate layer, the SP is developmentally transient and is believed to play an important role in the functional capacity of subcerebral projection neurons (Ghosh, Antonini et al. 1990) and the maturation of layer IV and visual cortex elements (Kanold, Kara et al. 2003). The MZ, on the other hand, is made up of

glutamatergic Cajal-Retzius (CR) cells and GABAergic interneurons. The secretion of the glycoprotein reelin from CR cells has been particularly implicated in the proper formation of the cortical plate layers and cortical circuitry (Costa, Davis et al. 2001).

During normal development, we observed that DNA methylation progresses in an orderly and predictable manner in differentiating cortical precursors, parallel to previous observations in early neurulation (Zhou, Chen et al. 2011, Zhou 2012). By E17 the VZ (Figure.12A–C), the neurogenic layer of the developing neocortex, exhibited strong proliferative activity as demonstrated by Ki67 immunoreactivity (Figure.12D) and dense Tbr2 positive cells (indicative of intermediate progenitors (IPs)) detaching from the ventricular surface and migrating into the upper cortical layers along radial glia fibers (Figure.12E). During this time we observed a robust expression of 5mC followed by the muted emergence of 5hmC (Figure.12A-B). At the subventricular zone (SVZ), the secondary proliferative compartment of the developing cortex, Ki67 positive cells were less apparent (Figure.12D), but contained dense Tbr2-im fibers extending from the VZ (Figure.12E). Similar 5mC and 5hmC distribution was observed in the SVZ compared to the VZ, with only a slight reduction of 5mC (Figure.12A-B) observed. Notably, the methyl-CpG binding protein MeCP2 was absent in both ventricular regions (Figure.12C).

At E17, the IZ was highly populated by Tbr2-expressing IPCs and their vertical projections which were originated in the VZ and SVZ (Figure 12E). In this zone, proliferation was drastically reduced as marked by the absence of Ki67 immunoreactivity. 5mC in the IZ resumed levels observed in the VZ while 5hmC appeared unchanged (consistently less abundant compared to 5mC) (Figure.12A-B). The subplate (SP) featured the first appearance of round-shaped, mature neurons (as

characterized by their expression of NeuN) (Figure 12G). The rounded nuclear appearance was in sharp contrast to the ellipsoidal shaped nuclei typical of the NeuN-absent ventricular regions. The SP also contained the Tbr2 and P2Y1-expressing fibers of the migratory IPCs (Figure 12F-G). An interesting divergence of 5mC and 5hmC was observed in the SP, where 5mC was present in both round and ellipsoidal-shaped nuclei (Figure.12A) while 5hmC was reserved distinctly for the mature, round-shaped nuclei (Figure 12B). Further, 5hmC-positive neurons in this region were highly correlated with the NeuN-positive cells (Figure.12G) and, next to the MZ, the SP observed the most abundant expression of 5hmC. In contrast to 5mC and 5hmC, MeCP2 was minimally apparent in the SP (Figure 12C).

Finally, at E17 the CP contains maturing neurons which will make up the future cortical layers. Proliferation was absent in the CP while Tbr2-expressing fibers were tapered compared to the IZ and lower layers (Figure 12E). NeuN-expressing neurons appeared to be variable within the layer, distributed into three apparently distinct sublayers within the CP (Figure 12G). The appearance of these observed borders within the layer are likely affected by variable cellular densities and interspersal of migrating neurons. Concordant with the three CP sublayers, 5mC immunoreactivity also appeared distributed in the three sublayers with an immuno-intensity gradient inversely proportional to that of NeuN (middle < top and bottom) (Figure 12A). The distribution of 5hmC was, in contrast, well-aligned with the NeuN-im pattern (middle > top and bottom) (Figure 12B). Similar to the SP layer, 5hmC appeared to only occupy the mature, round-shaped nuclei, whereas 5mC was more ubiquitously expressed. MeCP2 in the CP remained relatively weak (Figure 12C), concentrated at the lower-most CP region.

Temporal and spatial cues tightly regulate the transcriptional profiles of emerging cells of the cortex. From the emergence of RGCs to the reelin signaling emanating from Cajal-Retzius cells in the MZ, the precise expression of scheduled genes may have critical implications for cortical development and subsequently cortical function (Costa, Davis et al. 2001). As such, elucidating the regulatory mechanisms underlying cellular ontogeny may be critically important in developmental disease. Here, we observed that DNA methylation patterns of the cortical laminae were aligned with cellular differentiation processes in agreement with the epigenetic narrative presented earlier in neurulation, hippocampus and cerebellar development. The onset of 5mC at neuroepithelial zones has been previously hypothesized to prepare the cell for the downregulation of pluripotency genes in the wake of specification (Kim, Park et al. 2014, Resendiz, Mason et al. 2014). At the cortical ventricular zones, 5mC was abundant, diminishing slightly as progenitors exited the cell-cycle and initiated upward radial migration. Subsequently, 5mC was upregulated secondarily as migrating neurons settled in their target cortical zones and initiated morphological and functional modifications. This cyclical presentation of 5mC is reminiscent of the PC DNA methylation program in the cerebellum and supports the notion that cells may undergo various waves of DNA methylation reprogramming. Another feature of 5mC expression included indiscriminate expression across various cell types within a cortical layer as distinguished by cellular morphology. 5hmC, a bivalent epigenetic mark, observed a more straightforward progression in the embryonic cortex. Predictably upregulated in the zones which housed the most mature cortical neurons, 5hmC also was distinctively present in the rounded, mature cortical cells. These findings echo the presentation of the marker in parallel

hippocampal systems (Chen, Ozturk et al. 2013) and align with the presupposed role of 5hmC in priming cells for activation of genes required for cellular specification.

The restricted emergence of the methyl-binding protein MeCP2 in the mature zones of the embryonic cortex are consistent with previous findings (Kishi and Macklis 2004, Mullaney, Johnston et al. 2004) and support the dual binding of MeCP2 with both 5mC and 5hmC (Chahrour, Jung et al. 2008, Mellen, Ayata et al. 2012, Chen, Damayanti et al. 2014). This finding challenges the strictly repressive role of the methyl-binding protein and implicates the protein in more dynamic transcriptional regulation. Ultimately, the epigenetic characterization of the embryonic cortex strengthens the cell-unique and stage-dependent DNA methylation program that has been building since the emergence of early studies in neural stem cells. This study, across various neural systems and cell types, has demonstrated a systematic orchestration of DNA methylation and DNA methylation correlates operating in tandem with cellular progression.

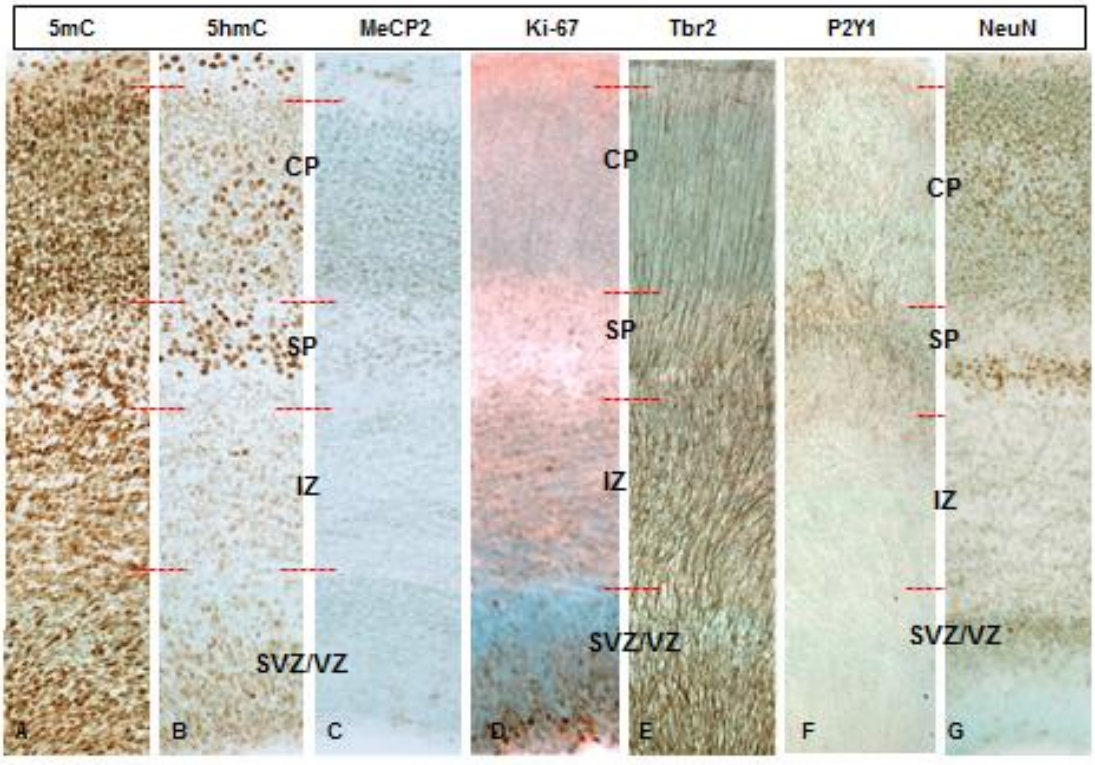

Figure 12: Comparative phenotypic and DNA methylation dynamics in the embryonic cortex
(A-C) Representative cortical columns from the Chow E17 frontal neocortex immunostained with DMP markers (5mC, 5hmC, MeCP2) and (D-G) phenotypic neural markers (Ki-67, Tbr2, P2Y1 and NeuN) are presented for comparison of the DMP dynamics along the radially progressing corticogenesis of the E17 brain. SVZ/VZ (Subventricular Zone/Ventricular Zone); IZ (Intermediate Zone); SP (Subplate; and CP (Cortical plate).

1.4 DISCUSSION

1.4.1 Post-Mitotic DNA Methylation Reprogramming: Evidence from the PC

Evidence from adult hippocampal synaptic plasticity modeling first illuminated the capacity of acute DNA methylation remodeling in the adult brain (Levenson, Roth et al. 2006). These findings led the proposition that DNA methylation (as well as other epigenetic modifications) may be a mechanism underlying post-mitotic neural plasticity. This notion is a meaningful one given that, to-date, the bulk of neural epigenetic investigation has focused on early cell commitment (i.e. stem cell to neural progenitor). Moreover, the absence of concrete evidence of active (replication-independent) DNA demethylases has led many to believe that post-mitotic DNA methylation reprogramming was not a serious contender in the realm of plasticity-conferring mechanisms.

Here, our study yielded pronounced evidence of post-mitotic DNA methylation reprogramming, including a wave of DNA methylation erasure followed by *de novo* methylation. Like the findings revealed in the adult hippocampus, evidence of DNA methylation reprogramming were observed acutely, along regulatory and intragenic regions of functionally relevant transcripts. Unlike the work of Levenson et al., immunological detection suggests that the extent of DNA methylation reprogramming is far wider-reaching than the predictable scope of late-onset neural plasticity, at least in the cerebellar Purkinje cell.

In the absence of cell-replication (passive) DNA demethylation, Purkinje cell reprogramming is likely mediated by active mechanisms. Currently, there are two proposed pathways by which active DNA demethylation may occur. The first centers around the idea of direct 5mC removal via deamination and subsequent base excision

repair (BER) or nucleotide excision repair mechanisms (Grin and Ishchenko 2016). The second proposes DNA demethylation occurs through the step-wise modification of the methylated cytosine base. For example, oxidation of 5mC could produce 5hmC which may be deaminated and subsequently excised by the AID (activation-induced deaminase)/APOBEC (apolipoprotein B mRNA editing enzyme complex) (Guo, Su et al. 2011). Alternatively, 5hmC could persistently be oxidized by TET enzymes to produce 5-fC and 5-caC. Subsequently, base-excision repair enyzmes such as Thymine DNA Glycosylase (TDG) could mediate demethylation of the derivatives, though this strategy is likely to be detrimental to the DNA on a large scale (Maiti and Drohat 2011). Alternatives to base-excision mediated demethylation are limited to the existence of enzymatic removal, which, though observed in some pathways, has yet to be supported in the brain (Wu and Zhang 2010). Whatever mechanisms are ultimately revealed, post-mitotic DNA methylation reprogramming may play a large role in the synaptic morphological plasticity that underlies enduring long term depression/potentiation in the brain.

The evidence observed in this study supports a mechanism by which 5mC demethylation concurrently affects all known hydroxylated intermediates, as their expression was highly dependent on 5mC. However, the fact remains that there is still much to learn regarding post-mitotic DNA methylation reprogramming, particularly where large-scale demethylation is concerned. Thus far, only one mechanism has been supported in the plasticity of the adult brain, that is, TET1-induced oxidation and subsequent deamination by the AID/APOBEC mechanism which was observed to occur in an activity-dependent manner (Guo, Su et al. 2011). Though attractive, *in vitro* this

mechanism was found to be 5hmC-specific and sequence selective, suggesting that perhaps this mechanism works cooperatively with other un-specified deaminases in the post-mitotic brain.

1.4.2 DNA Methylation Programs in Complementary Cell Types

The cell-wide DNA demethylation and remethylation of the Purkinje cells was unique to that cell type within the observed time course. Cerebellar granule neurons in contrast exhibited a more simplified DNA methylation program, acquiring stable 5mC and 5hmC only after their exit from the cell cycle (which coincided with the onset of radial migration from the EGL to the IGL) (Figure 13). The cell-wide acquisition of DNA methylation markers may signal the onset of cell cycle exit/neuronal specification. This is supported by the DNA methylation program of later-born cerebellar interneurons, which follow the neurogenic pattern from the emergence of granule layer interneurons (i.e. Golgi) to the later-arriving molecular layer interneurons (i.e. stellate, basket).

While intrinsic temporal features may play a role in cell-unique DNA methylation patterns, it should be noted that even within similarly patterned cells (i.e. granule and interneurons), various nuances exist which complicate the extrapolation of generalities such as cell-cycle exit- associated DNA methylation acquisition. For example, though the two cell categories display similar, protracted acquisition of DNA methylation markers during cell cycle exit, it has been reported that cerebellar interneurons may actually retain some intermediate state (not ever fully entering G_0 phase) (Leto, Bartolini et al. 2009). This allows cerebellar interneurons the plasticity to be “re-shaped” by the manipulation of extrinsic cues which would otherwise not be possible in a fully committed state. In this way, two cell types with apparently similar intrinsic transcriptional and epigenetic

courses deviate and call into question how much of the DNA methylation program, if any, is mediated by external cues. Interneuron characteristics also challenge the notion that cellular milestones such as cell cycle exit are entirely accountable for cell-wide DNA methylation reprogramming.

Another observed developmental phenomenon which shed some contrasting light on the DNA methylation program of the PCs was the embryonic cortical landscape. Like the post-mitotic DNA methylation "waves" which characterized postnatal PCs, cortical progenitors observed comparatively mild DNA methylation reprogramming throughout their developmental course, as detectable through immunological evaluation (Figure 14). The defining feature of DNA methylation reprogramming in the cortex was not cell-wide erasure and *de novo* methylation rather, a complementarity of 5mC and 5hmC across the cortical strata. For example, in the SVZ/VZ, 5mC was pronounced, subsiding in favor of 5hmC at the SP, where the earliest born (most mature) cortical neurons reside. Two more waves of shifting abundance occur within the complex CP layer. The observed "redistribution" of 5mC and 5hmC are reminiscent of the intranuclear positioning of the two markers which takes place in the cerebellum from P7 to P21. Recall that during the early stage, PCs and granule neurons exhibit a mutually exclusive distribution within the nucleus, co-localizing in a more "relaxed" euchromatin distribution only during later stages (Figure 7). That DNA methylation patterning additionally coincided with the genomic re-distribution of gene-specific DNA methylation from the promoter (P7) to the gene body (P29) (Figure 11F). Only gene-specific methylation analysis in the cortex will decipher whether the same genomic redistributions are in play and mediating immunological observations. Certainly, the developmental cortex demonstrates that the

cellular DNA methylation program is not always a case of absolute acquisition or erasure, but in some cases a more subtle conversion which remains to be substantiated in functional cortical gene networks. The cortical pattern does, however, reiterate the plasticity of the DNA methylation program in pre-and post-mitotic neurons, supporting the observations of Levenson et al in the adult hippocampus and our characterization in the cerebellum.

1.4.3 DNA Methylation Reprogramming as a Functional Mechanism

Beyond the need to corroborate cell-wide DNA methylation programs within functional gene networks, it remains important to understand how and why some genes apparently escape reprogramming. For example, though transcriptomes have been well characterized across cellular development, fluctuations in gene expression are not always attributable to DNA methylation changes (i.e. *Ppp1r17*, *Itpr2* in the cerebellum). The obvious answer is that perhaps some functionally relevant genes are regulated by other epigenetic mechanisms or even non-epigenetic mechanisms, which begs the deeper question, what determines the regulatory mechanisms of a gene? Yet another possibility may be the sub-optimality of the available genomic DNA methylation assays. For example, in our cerebellar study, MSRE qPCR was not able to distinguish 5mC and 5hmC methylation. Further, the examination of genomic regions was based on previously identified differentially methylated sites and not absolute coverage of the entire gene. Due to the relevance of 5mC and 5hmC genomic transitions and the likelihood that DNA methylation may be functionally important beyond the promoter, future studies will need to adopt more inclusive, unbiased approaches.

Finally, there is a need, just as in primordial germ cell reprogramming to better understand how if any genomic elements are protected from DNA methylation erasure post- mitotically. Equally important is a better understanding of the elements which recruit *de novo* DNA methylation. One report has proposed that TET-mediated hydroxylation may serve as an inhibitory mechanism for aberrant DNA hypermethylation (Wiehle, Raddatz et al. 2015). Others have proposed that activity-dependent intercellular signaling may underlie the recruitment of DNMT3A in the adult brain (required for *de novo* methylation) (Levenson, Roth et al. 2006). Surely we are still in the nascent stages of the exploration of epigenetic mechanisms and the future promises many milestones in our understanding of the mediators of the DNA methylation program and its fluidity.

1.4.4 Summary and Conclusions

The observations made in the postnatal cerebellum and the embryonic cortex greatly expand the epigenetic profile of the developing central nervous system. This cellular view paves the way for high-throughput genomic methyl-sequencing of cellular transcriptomes and strengthens the case for DNA methylation programming as a guiding element of neural progression. The distinct morphology and well-documented developmental course of the postnatal cerebellum allowed for a cell-specific assessment between the first and sixth postnatal weeks. While DNA methylation turnover has been documented previously during pre-implantation and during early neural tube formation, the cerebellar assessment revealed a post-mitotic population undergoing a large-scale demethylation and remethylation not previously reported. Moreover, the reprogramming of the cells was corroborated by epigenetic correlates and quantitative molecular assessment. Collectively, our observations showcased the cell-unique nature of DNA

methylation landscapes, illustrating that DNA methylation reprogramming, though detectable on a global scale, is highly dependent on cellular context. This was exemplified further across the cortical layers, where DNA methylation status was predictably correlated to proliferative, migratory, or synaptogenic status.

Across all examined systems, recurring motifs included cell cycle exit, migration, and cellular maturation as developmental correlates of DNA methylation reprogramming. Additionally, 5hmC was consistently observed in mature-state cellular specification, which corroborates various reports of 5hmC as an activating marker during cellular differentiation (Stroud, Feng et al. 2011, Wu, D'Alessio et al. 2011). Why some cells like cerebellar granule neurons and interneurons apparently undergo unilateral reprogramming while others like cortical progenitors and PCs are subjugated to multiple waves of DNA methylation reprogramming is a subject requiring further study. This may perhaps be rooted in some cellular complexity requiring large-scale transcriptional fluctuations to accommodate functional or structural demands. On the other hand, in light of the findings of PC gene targets (some of which were not subject to DNA methylation reprogramming), it may be entirely possible that other non-DNA methylation factors are collaboratively at work mediating transcriptional regulation. As such, it is with caution that investigators should attempt to extrapolate gene level to cell-level methylation and vice versa. Fortunately, as better epigenetic technologies emerge, complementary methods of investigation will become increasingly accessible to fill the gaps between cell-wide immunological trends and the precise cellular methylome.

While elucidating the cellular specificity and spatial and temporal profiles of DNA methylation across developing neural systems is a momentous step forward, much

remains to be answered regarding the mechanistic features and consequential outcomes of DNA methylation reprogramming. For example, what factors are at work in the recruitment of DNA methylating enzymes and their dynamics during reprogramming across cells are not known. Similarly, though labeling of MeCP2 and MBD1 was performed, a direct-binding analysis of 5mC and 5hmC methyl-binding proteins in the future will be needed to fully confirm methylated DNA and methyl-binding protein dynamics. By a similar token, teasing out the precise genomic distribution of 5mC versus 5hmC may reveal important details about the regulatory DNA methylation program. Here, MSRE qPCR was indiscriminant toward 5mC versus 5hmC but new methyl-sequencing strategies will allow deeper and precise examination of the two markers going forward.

Finally, as previously mentioned, DNA methylation reprogramming as a means for structural and transcriptional regulation is likely only partially explanatory. As documented in the literature, epigenetic modifications of chromatin often beget others. As such, a complete and comprehensive picture of epigenetic reprogramming in the developing brain will require an examination of multiple epigenetic modifications in tandem. Ultimately, only a complete and accurate account of epigenetic marks, recruitment elements, and transcriptional regulators will help to elucidate one of the most important questions of reprogramming as a regulatory mechanism, that is, is epigenetic modification an obligatory precedent of developmental outcomes or do intrinsic/extracellular developmental cues shape epigenetic landscapes associated with development?

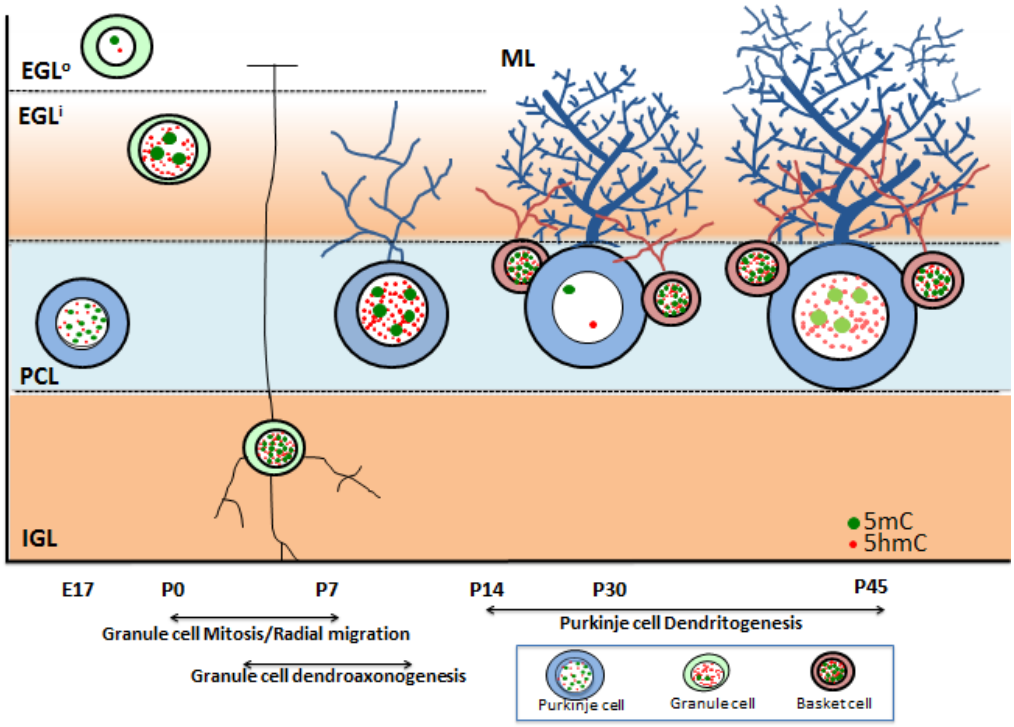

Figure 13. Independent DNA methylation program of Purkinje, granular and basket cells during development

This scheme illustrates the cell-specific epigenetic distribution of the DNA methylation marks 5mC (green dots) and 5hmC (red dots) in the nuclei of neurons during development of the cerebellum. As cerebellar granule cells (light green) occupy the outer external granule layer (EGL^o), they are still mitotic and devoid of 5mC and 5hmC. Immediately after completing mitosis, these granule cells exit the cell cycle and begin radial migration through the inner EGL, PCL, and finally into the internal granule layer (IGL). As soon as granule cells break through the EGL^o, they strongly acquire 5mC and 5hmC, though these two methylation marks are independently distributed in the nuclei of granule cells. From P7 forward, mature granule cells of the IGL maintain their methylation, though these become homogenously distributed in contrast to pre-migration distribution. Independently, Purkinje cells (PC) of the cerebellum exhibit a unique epigenetic program. Post-mitotic Purkinje cells generated in the dorsal rhomboid lip at E14 and arrived at the Purkinje cell layer (PCL) at E17 and already express 5mC quite prominently (and to a lesser extent 5hmC). As the PC grow in size, it becomes clear that 5mC are distributed in a granular fashion in heterochromatin, while 5hmC are distributed as fine particles in euchromatin. Remarkably, just prior to PC's undergoing characteristic dendritogenesis and synaptogenesis (P14-30), a dramatic loss of 5mC and 5hmC occurs in their nuclei. As Purkinje cells settle into synaptic maturity, 5mC and 5hmC reappear in the nuclei though diminished from peak levels observed at P7. In contrast, the basket interneurons closely associated with PCs appear to have acquired a rich expression of 5mC and 5hmC while PCs undergo de-methylation and re-methylation.

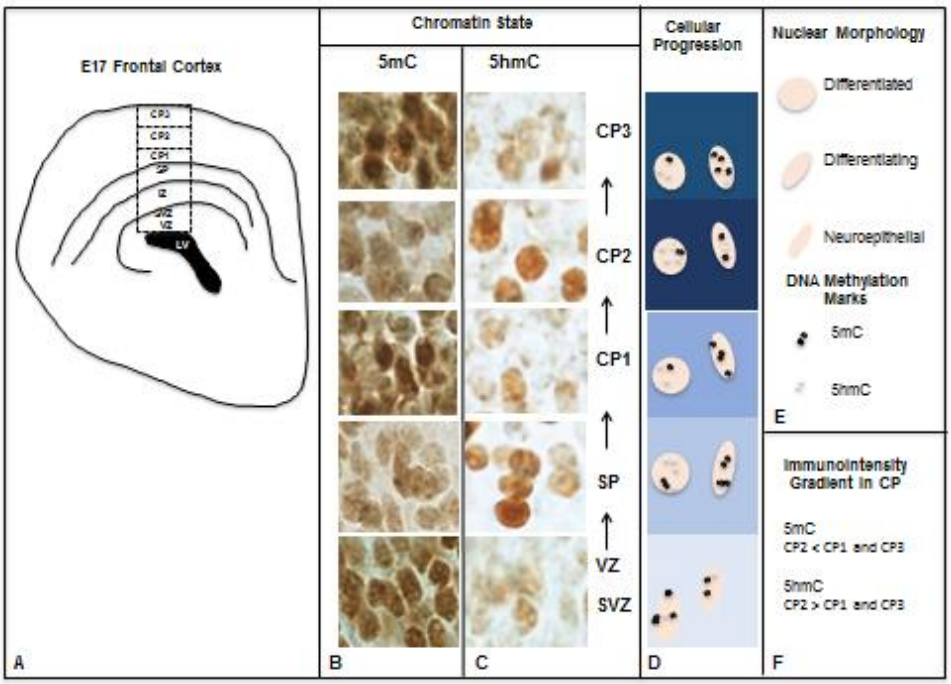

Figure 14: The DNA methylation program of the embryonic cortex
(A)At E17, the embryonic cortex develops in distinct layers progressing from the roof of the lateral ventricle (LV). Neuroepithelial (NE) cells sequentially migrate through the proliferative ventricular zone (VZ) to the uppermost cortical superficies. (B,C) During this developmental progression, cells of the layers are diverse in their maturity state and simultaneously unique in their chromatin distribution of DNA methylation markers. Specifically, NE cells of the proliferative VZ exhibits strong 5mC (B) followed by a weaker 5hmC signal (C). (B-D) As these cells undergo differentiation and radial migration into the subplate layer (SP), cellular morphology changes from ellipsoidal to larger, rounded nuclei. During this transition, a characteristic rise in 5hmC is observed, in contrasts to a weakening of 5mC. € Nuclear morphology and DNA methylation mark legend. (B-D,F) As cells reach their target layers within the cortical plate (CP), the distribution (immunointensity gradient) of 5mC/5hmC shows opposite trend within 3 sublayers of the CP (CP1/2/3). SVZ (Subventricular Zone)

In conclusion, DNA methylation (and associated epigenetic marks) appear and disappear in accordance with the spatial and temporal developmental patterns that are unique to individual cell types. This presentation demonstrates an association with cell-unique gene regulation and markers of cellular specification and provides novel evidence of a post-mitotic, reprogrammable DNA methylation developmental program. These findings also demonstrate that DNA methylation landscapes do not change "globally", but rather fluctuate as unique signatures of evolving cellular states according to the temporal transcriptional requirements rendering the appropriate morphological and functional capacity of the cell.

If the DNA methylation program is a major component of transcriptional regulation during development and epigenetic mechanisms are sensitive to external cues (see Chapter 2), could the program confer environmental input at the cellular level? The answer is likely to impact our understanding of a host of developmental abnormalities. If so, DNA methylation landscapes may open a world of diagnostic and therapeutic possibilities.

CHAPTER 2: DYSREGULATION OF NEURODEVELOPMENT AND DNA METHYLATION BY ALCOHOL

2.1 INTRODUCTION

2.1.1 Environmental Sensitivity and Heritability of DNA Methylation

The environmental sensitivity of epigenetic mechanisms has been extensively documented. Factors such as nutritional disparity, early-life stress, pollution, substances of abuse, and maternal care are just some of the many proposed environmental contributors of epigenetic modification (Heijmans, Tobi et al. 2008, Madrigano, Baccarelli et al. 2011, Suderman, McGowan et al. 2012). Further, studies performed in monozygotic twins have provided valuable evidence for the environmental contributions of differential epigenetic profiles (Segal, Montoya et al. 2017). Interestingly, early findings demonstrated that epigenetic variability of monozygotic twins can actually begin prior to birth, suggesting environmental influencers of the epigenetic code can function as early as the prenatal environment (Ollikainen, Smith et al. 2010, Gordon, Joo et al. 2012). Since then, a host of prenatal and perinatal investigations have identified factors such as folate consumption, predatory stress, and chemical exposures such as alcohol and lead (Gonseth, Roy et al. 2015, Sen, Heredia et al. 2015, St-Cyr and McGowan 2015, Boschen, McKeown et al. 2016) as DNA methylation-altering environmental factors during neural development.

Importantly, these factors and the subsequent epigenetic modifications have been characterized for their persistence in later life (Vineis, Chatziioannou et al. 2017), suggesting that environmentally-mediated epigenetic modifications may act as a molecular recording mechanisms for environmental information. Moreover, the

implications of stable and lasting epigenetic modifications include their evolution and adaptability over time, perhaps driving forward or reversing pathological courses already in play due to genetic or other factors. Of course, that argument would require a more comprehensive understanding of the functional "thresholds" which would render the chromatin structure vulnerable to differential transcription, the likes of which are rudimentary at this time. Additional considerations would require unraveling whether cell types, cell states, and accompanying genomic information experience differential sensitivity to environmental impacts. In other words, whether cellular chromatin are more vulnerable during a particular organismal phase or perhaps more responsive to specific outward influences over others remains largely unknown. Finally, epigenetic dynamics must be further defined in the context of genetic interaction.

The notion of epigenetic memory has in recent years become increasingly important due to reports of transgenerational heritability. Occurring through the transmission of epigenetic signatures in gametes, environmental factors such as pre-reproductive stress in females (Zidan, Rezk et al. 2015) and fetal alcohol exposure in males (Govorko, Bekdash et al. 2012), among others, have empirically demonstrated the heritability of acquired epigenetic change. Though unsubstantiated in human studies to date, several lines of epidemiological evidence suggest transgenerational epigenetic mechanisms at work in human beings as well (Veenendaal, Painter et al. 2013, Yehuda, Daskalakis et al. 2014). Given the known epigenetic erasure which occurs in the germline during transmission, it is likely, though not certain, that the mechanisms at work protecting the demethylation of elements like the imprinting of certain parental genes (Guibert, Zhao et al. 2012, Hackett, Sengupta et al. 2013) may also play a role in the

preservation of transgenerational epigenetic signatures. Despite the growing body of knowledge, and the ever-expanding implications for epigenetic landscapes, how environmental influences are mechanistically transduced into the epigenetic code remains poorly understood. At least one environmental element is molecularly poised to offer insight into how environmental influences impact epigenetic profiles during development.

2.1.2 Alcohol and Methyl and Acetyl Metabolism

Alcohol metabolism begins by oxidation into acetaldehyde, a known teratogen. Simultaneously, the breakdown of alcohol into acetaldehyde includes the production of reactive oxygen species (ROS). The metabolism of alcohol during acute exposure is mediated by the enzyme alcohol dehydrogenase (ADH) while chronic alcohol exposure is believed to increase metabolism by recruitment of hepatic cytochrome P450 isoform 2E1 (CYP2E1). Secondarily, an enzyme known as aldehyde dehydrogenase (ALDH) is responsible for the irreversible conversion of acetaldehyde into acetate, mainly in the liver. The metabolism of alcohol is thought to proceed rather quickly to avoid the elevation of acetaldehyde levels. In healthy males, about 77% of ingested alcohol is converted to acetate (Siler, Neese et al. 1999), prompting the notion that acetate is alcohol's primary metabolite and complementing reports of low levels of acetaldehyde accumulation in the blood after alcohol consumption (Umulis, Gurmen et al. 2005). Acetate may bind coenzyme A through the enzyme acetyl-coenzyme A synthetase (AceCS1). Acetyl CoA is a major substrate of the cellular energy cycle but may also donate an acetyl group to histone proteins through the histone acetyltransferase (HAT) family of enzymes. Acetylation of histones is generally thought to facilitate gene

activation by altering the binding of DNA to core histone proteins (Zakhari 2013). Additionally, acetate is a direct inhibitor of class I histone deacetylases (HDACs) in hepatic cells and neurons (Soliman, Smith et al. 2012). Accordingly, the metabolism of alcohol has a direct biochemical route toward the alteration of the chromatin structure. Furthermore, alcohol variability such as frequency of consumption and age of the consumer have been shown to alter the enzymatic activities of ALDH in response to alcohol, influencing the accumulation of alcohol metabolites and increasing the production of ROS', which themselves may interfere with histone acetylation (Chrostek, Tomaszewski et al. 2005, Mello, Ceni et al. 2008, Brooks and Zakhari 2014).

Beyond acetyl metabolism and histone modification, alcohol metabolically accesses a second biochemical pathway that is closely intertwined with epigenetic mechanisms. The sole methyl donor for DNA and histone methylation, S-adenosylmethionine (S-AMe) (produced through the metabolism of dietary folate, betaine, and methionine) is impacted at various metabolic stages by alcohol and alcohol-derived ROS'. For example, alcohol has been shown to decrease serum folate levels, the folate intermediate metabolite 5-methyltetrahydrofolate (5-MTHF), as well as the 5-MTHF conferring enzyme (Eichner and Hillman 1973, McGuffin, Goff et al. 1975, Berlin, Cameron et al. 2010). Downstream, the intermediate 5-MTHF is converted to methionine by the enzyme methionine synthase (MS) which is decreased by up to 50% in models of alcoholism (Finkelstein, Cello et al. 1974, Barak, Beckenhauer et al. 2002).

A secondary dietary methyl source is also biochemically impacted by alcohol. Choline, upon oxidative conversion to betaine, is enzymatically converted to methionine by betaine-homocysteine methyltransferase (BHMT). Like ALDH, the BHMT enzyme

appears to exhibit a context-dependent response to alcohol exposure, elevated by acute exposures but diminished chronically (Barak, Beckenhauer et al. 1996). Alcohol additionally has been correlated with decreased levels of methyl metabolism co-factors including B6, B12, and riboflavin (Lumeng 1978, Kanazawa and Herbert 1985, Subramanian, Subramanya et al. 2013), which may contribute to the observed alcohol-related inhibition of methyl metabolism enzymes. Finally, past methionine biogenesis, alcohol has been observed to impact role players involved in the production of the "active" methyl donor substrate S-AMe. Predominantly, alcohol-induced oxidative stress has been shown to decrease both the expression and activity of methyl adenosyltransferase (MAT) and the hepatic production of S-AMe and DNA methylation (Chawla, Watson et al. 1996, Avila, Carretero et al. 1998, Lu, Huang et al. 2000), though the modality of alcohol in S-AMe production and DNA methylation may be more complex in other tissues.

Folate, choline, and methionine metabolism have each been independently shown to regulate normal neural development in some capacity (Serrano, Garcia-Silva et al. 2010, Wu, Dyer et al. 2012). Aside from altering methyl and acetyl metabolism, alcohol has also been shown to hinder the transfer of folic acid from mother to offspring, though earlier studies reported that transfer is actually elevated by alcohol exposure (Lin 1991, Hutson, Stade et al. 2012). This, taken together with the known interaction of alcohol and alcohol metabolites in methyl metabolism suggest a practical pathway for alcohol to impact neural development. In that vein, it is unsurprising that folate deficiency during developmental periods mirror some of the phenotypes of fetal alcohol exposure (Molloy, Kirke et al. 2008).

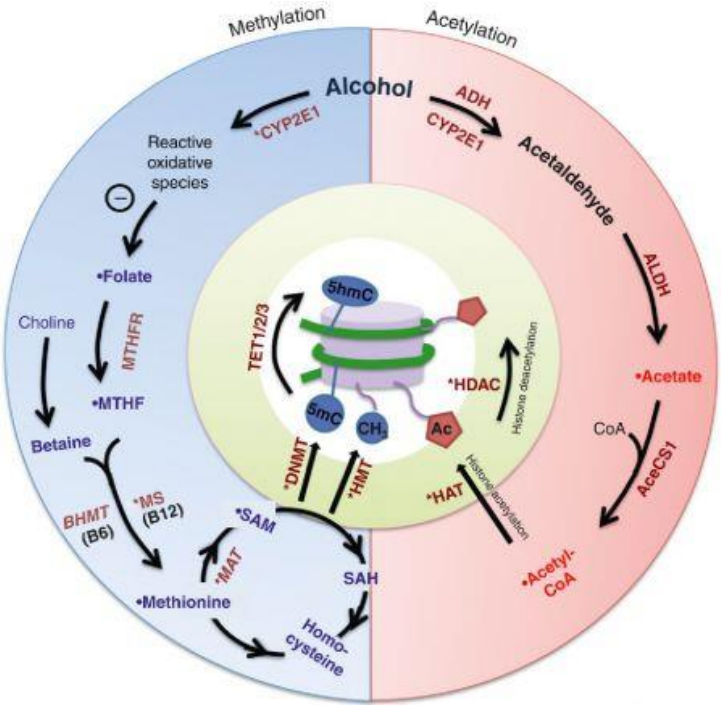

Figure 15. Effect of alcohol metabolism on acetylation and methylation of histones and DNA

On the acetylation side (red hemisphere), alcohol is metabolized by ADH and CYP2E1 into acetaldehyde. This process produces many reactive oxygen species that pour over to affect folate metabolism. Acetaldehyde is further metabolized to acetate by ALDH enzymes. Acetate is then converted to acetyl-CoA, the acetyl donor for histone acetylation enzymes acting on the amino acids of variable histone proteins (center). Once established, histone deacetylases can remove the acetyl group. On the methylation side (blue hemisphere), dietary folate is metabolized by MTHFR to methyl tetrahydrofolate (MTHF). Meanwhile, dietary choline is converted to betaine. Betaine and MTHF both serve as the methyl donor for homocysteine conversion to methionine by the enzyme methionine synthase (MS). Methionine next becomes “activated” by methyl adenosyltransferase enzymes into the fi nal methyl donor form, known as S-adenosylmethionine (S-AMe). S-AMe is utilized by both DNA methyltransferases and histone methyl transferases to the 5’ carbon of cytosine bases or histone tail residues, respectively (center). Solid dots: substrate; Stars: enzymes, which are known to be affected by alcohol.

2.1.3 Fetal Alcohol Spectrum Disorders (FASD)

Alcohol exposure during gestation may lead to a host of developmental deficits manifested across a range of severities. These include but are not limited to craniofacial dysmorphologies, delayed growth, microcephaly, intellectual disabilities, and impaired psychosocial skills. Classically, children manifesting growth deficiency, facial characteristics, and central nervous system damage are diagnosed under the classification known as Fetal Alcohol Syndrome (FAS), affecting 2 out of 1000 live births with treatment costs estimated around $5.8 billion in the US alone. FAS is a leading cause of non-genetic intellectual disability in the Western world; though today, a broader classification is used to cover five diagnostic categories linked to alcohol-related developmental deficits. Known as Fetal Alcohol Spectrum Disorders (FASD), this category (though not itself a diagnostic term) includes affected patients from categories including FAS, partial FAS, alcohol related neurodevelopmental disorder (ARND) and alcohol related birth defects (ARBD). Under this umbrella, covering the more mild and subtle manifestations of alcohol-related disorders, an estimated ten times more patients have been identified compared to classical FAS statistics.

Despite the range of severities existing within FASD, it is believed that many more affected individuals escape the diagnostic criteria and progress through life unevaluated and untreated (de Sanctis, Memo et al. 2011). It has been proposed that these patients who do not present distinct phenotypes in early-life may go on to experience manifestations of the exposure in later life, typically involving impaired cognitive plasticity and/or maladaptive behaviors (Famy, Streissguth et al. 1998, O'Connor, Shah et al. 2002, Burd, Klug et al. 2003). Due to the extensive evaluation of fetal alcohol

exposure as a teratogen and the observation that even minimal exposures during gestation can affect the developing brain(Zucca and Valenzuela 2010, Valenzuela, Morton et al. 2012), there is no acknowledged tolerable level of gestational drinking. While largely preventable, it is important to consider that almost half of all women of childbearing age are drinkers (CDC 2002). Further, considering that nearly half of all pregnancies are unplanned (Harper, Rocca et al. 2015) and that pregnancy detection in these cases can surpass four weeks, it becomes increasingly clear that there is a subset of the population at perpetual risk for acute exposure.

Finally, recent findings have uncovered evidence revealing that alcohol-mediated effects may actually be transmitted even in the absence of direct fetal exposure, presumably through the germ line. Interestingly, offspring of alcohol-exposed parents included differential expression of critical neurodevelopmental genes as well as genes involved in chromatin remodeling and transcriptional regulation (Przybycien-Szymanska, Rao et al. 2014). These findings not only greatly expand the window of offspring vulnerability to alcohol but also shed important light on paternal contributions of alcohol-related developmental dysregulation. Indeed, several studies have reported that paternal alcohol consumption is associated with low birth weight, reduced cognitive ability, and early pregnancy loss (Hegedus, Alterman et al. 1984, Little and Sing 1987, Henriksen, Hjollund et al. 2004). Moreover, the gametic preservation of differential DNA methylation of the H19 imprinting region in response to paternal preconception drinking has been previously observed (Ouko, Shantikumar et al. 2009) and is hypothesized to be maintained in some loci through multiple generations (Sarkar 2016).

2.1.4 Developmental Alcohol Exposure and DNA Methylation

The alteration of intrinsic DNA methylation by alcohol during development was perhaps best observed by a study utilizing the agouti viable yellow (A^{vy}) mouse mutant allele. This allele contains a methylation-sensitive region within the A^{vy} locus which is responsible for coat color ranging from yellow (unmethylated) to pseudoagouti (highly methylated) (Kaminen-Ahola, Ahola et al. 2010). In this study the agouti locus was hypermethylated by prenatal alcohol exposure, though, as referenced previously, the nature of alcohol on DNA methylation is bilateral, demonstrating hyper and hypomethylation across various models. For example, DNA methylation is decreased by alcohol at the H19 imprinting control site of sperm, placenta, and the critical NMDA receptor gene *Nr2b* in cortical neurons (Marutha Ravindran and Ticku 2004, Haycock and Ramsay 2009, Ouko, Shantikumar et al. 2009).

Various other tissues and developmental gene targets of alcohol have been previously reviewed (Resendiz, Chen et al. 2013) and a screen of methylation profiles in alcohol-exposed neural stem cells and embryos have revealed the alteration of over 1000 genes including various neurodevelopmental genes (Liu, Balaraman et al. 2009, Zhou, Zhao et al. 2011). In late gestation models of alcohol exposure, global DNA methylation alterations in the hippocampus and prefrontal cortex have been observed (Otero, Thomas et al. 2012, Marjonen, Sierra et al. 2015). The functional implications of alcohol-altered DNA methylation signatures is substantiated by the findings that developing neural systems exposed to DNMT inhibitors present phenotypic aberrations strikingly similar to FASD (Zhou, Chen et al. 2011). Notwithstanding, alcohol has demonstrated histone modification capacity including bidirectional dysregulation of histone 3 (H3) acetylation and H3 methylation in neural tissues (Guo, Su et al. 2011, D'Addario, Caputi et al. 2013).

Similarly, alcohol has been shown to alter the expression of miRNA profiles in neural stem cells (Wang, Zhang et al. 2009), with similar studies suggesting that miRNA sensitivity varies according to cell type and differentiation state (Miranda 2012). Collectively, evidence of alcohol-sensitive epigenetic mechanisms has mounted across gene systems involved in cell-cycle regulation, cell survival, early pro-neuron commitment, along with a host of genes implicated in developmental syndromes (Figure 16).

2.1.5 Cortical Impact of FASD

One of the hallmark manifestations of alcohol-related developmental disease is cognitive impairment of varying degrees (Green 2007, Jones, Hoyme et al. 2010, Jacobson, Jacobson et al. 2011, Lebel, Mattson et al. 2012). The underlying factors of protracted neurological deficits of FASD include reduced brain volume, corpus callosum volume, and grey matter (Nardelli, Lebel et al. 2011, Yang, Phillips et al. 2012). Imaging studies in human FASD patients have confirmed cortical abnormalities compared to healthy controls (Sowell, Mattson et al. 2008, Yang, Roussotte et al. 2012, Robertson, Narr et al. 2016), although whether alcohol increases or decreases cortical areas is unclear. It is likely that a variety of variables across studies may contribute to the range of observations. As such, and particularly because of the serious implications of cortical dysmorphology to the cognitive and adaptive capacity of the offspring, there remains a need to continue to evaluate the effect of fetal alcohol exposure on cortical abnormalities.

Further study demonstrated that the fundamental aberrations of the forebrain may have a basis in cortical apoptosis, neurotrophic factors, migration, and/or morphological determination (Aronne, Guadagnoli et al. 2011, Chikhladze, Ramishvili et al. 2011,

Lawrence, Otero et al. 2012, Riar, Narasimhan et al. 2016, Lebedeva, Zakharov et al. 2017). Despite what is known or suspected about the molecular underpinnings of alcohol-related cortical disruption, the corresponding transcriptional targets have not been well-studied. Additional questions remain including, what are the exposure thresholds of these molecular events (i.e. alcohol dosage, time and length of exposure) and what are the mechanisms translating the environmental insult to the genome?

2.1.6 Research Aims

The action of alcohol on methyl metabolism and DNA methylation biogenesis positions aberrant DNA methylation as a potential mechanism for the neuroteratogenicity of alcohol. The previous discussion of normal DNA methylation progression during cortical development offers a point of reference by which to evaluate alcohol-related dysregulation of the program. We hypothesized that the DNA methylation program is predictably responsive to fetal alcohol exposure and may be a mechanism informing the neurodevelopmental transcriptome of the teratogenicity of exposure. The investigative approach included evaluating parallel DNA methylation makers and methylation correlates alongside multiple cues of cortical laminar formation in a mouse model of FASD. We found that fetal alcohol exposure drives cortical abnormalities in the wake of DNA methylation dysregulation. These findings shed important light on how fetal insults may establish, maintain, and manifest cognitive and behavioral deficits.

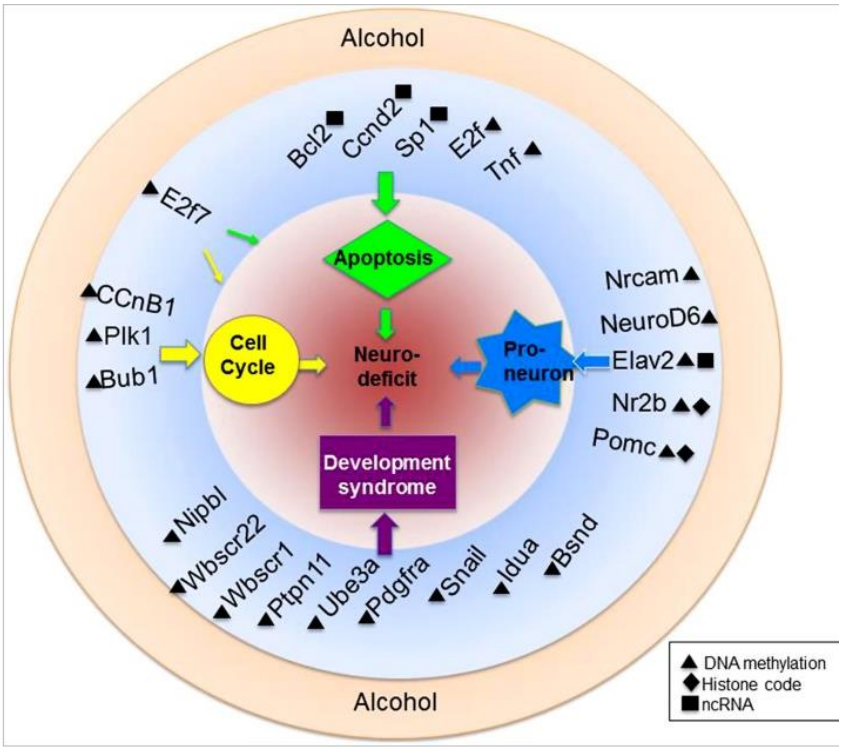

Figure 16. Epigenetically-modified neurodevelopmental gene targets of alcohol
Alcohol is a teratogen with known capabilities to alter the epigenome. Highlighted here are just a fraction of genes within various biological pathways of known vulnerability to ethanol-mediated epigenetic alteration. Also depicted are genes associated with known developmental syndromes and their epigenetic alteration. Genes are more specifically discussed and referenced in the text.

2.2 MATERIALS AND METHODS

2.2.1 Overview of experimental prenatal alcohol exposure

In this study, alcohol was administered via liquid diet according to the paradigm illustrated in Figure 17A. The time course and types of analysis are summarized in Figure 17B. Mice were conditioned to receive the liquid diet prior to mating. After conception, the liquid diet was re-introduced and alcohol was administered from E7–E16 (corresponding to brain development in the late first and second human trimester equivalent). The 4% alcohol liquid diet (v/v) administered in this paradigm has been reported in previous and parallel studies to produce a range of blood ethanol concentrations (BEC) of 100–200 mg/dL (Anthony, Vinci-Booher et al. 2010, Chen, Ozturk et al. 2013). Briefly, six non-pregnant females receiving 4% v/v alcohol were used for BEC analysis. Blood samples were harvested through the tail vein 2 h or 6 h after introducing the fresh alcohol-PMI diet at 10:00 AM during the dark cycle, on days 2, 4 and 6 during treatment. Adequate volume of blood (15 µL) was collected in heparinized tubes, and plasma was isolated through centrifugation and stored at −80 °C prior to analysis with a gas chromatograph (GC, Agilent Technologies; model 6890). Each sample was analyzed in duplicate.

Under these treatments, no significant difference in dam body weight was observed from the start of treatment (E7) to E14, though PF and Alcohol groups did exhibit lower gestational weights during E15 and E16 (Chen, Ozturk et al. 2013). While our previous studies were aimed at the early neural tube (E10) and early brain primodium (E15), the current study focused on the stage prior to birth, at the peak of rodent cortical layer formation (E17).

2.2.2 Animals and treatments

All mice were used in accordance with National Institute of Health and Indiana University Animal Care and Use (IACUC) guidelines. The protocol was approved by the Laboratory Animal Resource Center (LARC) animal ethics committee of Indiana University. C57BL/6 (B6) (10–14 weeks old, ~20 g body weight) nulliparous female mice (Harlan, Inc., Indianapolis, IN) were used in the study. Mouse breeders were individually housed upon arrival and acclimated for at least one week before mating. The mice were maintained on a 12-h reverse light-dark cycle (lights on: 10:00 PM–10:00 AM) and were provided laboratory chow and water *ad libitum*. Mice were then randomly assigned to three treatment groups: Chow (N = 7), Pair-Fed (PF, N = 5), and Alcohol (Alc, N = 7). Each litter was considered N = 1; the littermates of each dam were distributed for the analyses described in the following sections. The PF and Alc groups were pre-treated with liquid diet (see below) for 7 days before mating. Females were bred with male breeders for a 2-h period (10:00 AM to 12:00 noon). All animals were mated daily over a period of no more than 3 weeks, during which time all animals were on *ad libitum* chow and water diets. The presence of a vaginal plug at the end of the 2-h mating session was considered as indicative of conceptus, and that hour was designated as hour 0 and embryonic day (E) 0. A liquid-diet paradigm was carried out as previously detailed (Chen, Ozturk et al. 2013). Briefly, all alcohol treatment groups received 4% alcohol v/v in liquid diet (Purina Micro-Stabilized Diet [PMI], Purina Mills Inc., Richmond, Indiana) as instructed by supplier with 4% w/v sucrose added, and administered using a 35-mL drinking tube (Dyets Inc., NY). The PF group was given the PMI diet mixture with the addition of maltose dextran (MD) (to substitute alcohol

calories). The volume of the PF diet was restricted to that of a matched dam from the alcohol group throughout the course of treatment. The Chow group was maintained on a standard chow diet and water *ad libitum* throughout gestation. On E5, pregnant dams in PF and Alc groups were placed on an unrestricted PF liquid diet for acclimation. Either 4% v/v alcohol (Alc group) or restricted volume isocaloric liquid diet (PF group) was initiated on E7 through the end of E16, after which all liquid diets resumed standard lab chow diet. On E17, dams from all three groups were euthanized for embryo harvest. In addition, E16 embryos from Chow groups (N = 4) were specifically harvested for developmental stage comparison (Figure 17).

2.2.3 Embryo isolation and tissue preparation

After deep CO_2 euthanasia, embryos were harvested from dams at E17 by removal from the embryonic sack. Each embryo was either immersion-fixed in 20 mL of fixative prepared from 4% paraformaldehyde (PFA) for immunohistochemistry or immediately dissected for brain tissue and snap-frozen and stored in a −80 °C freezer until Western blot or global methylation analysis. Fixed embryos were subsequently weighed, dissected for brains, gelatin-blocked, and post-fixed for at least 24 h at 4 °C before sectioning was performed for immunocytochemistry (average N: Chow = 5, Alc N = 5, and PF N = 4; animal number for each staining is shown in Results).

2.2.4 Immunohistochemistry

One Alc and either one PF or Chow brain were embedded in a single 10% gelatin block with careful rostrocaudal and dorsoventral alignments. Gelatin blocks were fixed with 4% PFA and sectioned in 40-µm thick coronal sections on a floating vibratome (Leica Microsystems; Buffalo Grove, IL). The section pairs (Alc-PF or Alc-Chow) were

processed equally in all immunohistochemical procedures. The section pairs were then cleared of endogenous peroxidases using 10% H_2O_2 in phosphate-buffered saline (PBS) for 10 min and permeabilized with 1% TritonX-100 in PBS for 30 min before incubation with a primary antibody diluted in goat kit (1.5% goat serum, 0.1% TritonX-100 in PBS) for 18 h at room temperature. Epigenetic antibodies used in this study are summarized in Table 3 below. The section pairs were then incubated for 90 min in goat anti-rabbit IgG or goat anti-mouse secondary antibodies conjugated with biotin (Jackson ImmunoResearch, West Grove, PA) followed by Streptavidin-AP (1:500, Jackson ImmunoResearch, West Grove, PA) for 90 min. The immunostaining was visualized by incubation in 0.05% 3,3′-diaminobenzidine (DAB) and 0.003% H_2O_2 over an average of 3–8 min, followed by counterstaining with methyl green. All stainings were photographed under light microscopy for cellular analysis (Leitz Orthoplan 2 microscope; Ernst Leitz GMBH, Wetzlar, Germany).

Table 3. Antibodies used for DNA methylation assessment in the E17 cortex

Primary Antibodies	**Company**	**Catalog #**	**dilution**	**predicted wt.**
5-methylcytosine	Eurogentec	BI-MECY-0100	1:2000	N/A
5-methylcytosine	Active Motif	AM61255	1:2000	N/A
5-hydroxymethylcytosine	Active Motif	AM39769	1:3000	N/A
MBD1	Santa Cruz Biotech.	sc-10221	1:200	~89 kDa
MeCP2	Cell Signaling Tech.	D4F3XP-R	1:1000	75 kDa
Ki67	Novus Biologicals	NB110-89717	1:500	324 kDa
Tbr2	Millipore	AB2283	1:500	58 kDa
P2Y1	Millipore	AB9263	1:1000	~42 kDa
NeuN	Cell Signaling Tech.	D3S3I	1:500	46-55 kDa
ß Tubulin	Abcam	ab15568	1:2000	55 kDa
GAPDH	Abcam	ab8245	1:2000	37 kDa
Secondary Antibodies				
Goat anti Rabbit biotinylated	Jackson ImmunoResearch	111-065-003	1:500	~160 kDa
Horse anti Mouse biotinylated	Vector Laboratories	BA-2000	1:500	~152-165 kDa
Donkey anti Guinea Pig biotinylated	Vector Laboratories	BA-7000	1:500	~152-165 kDa

2.2.5 Densitometry analysis (H score) and cortical thickness assessment

Upon observing epigenetic immunostainings under a light microscope, the immunoreactive nuclei (based on evidence of the brown-color DAB reactions) exhibited a differential staining profile within different subcortical regions. In order to reflect this differential expression, we employed H scoring for nuclear densitometry analysis (Singh, Shiue et al. 2009, Chen, Ozturk et al. 2013) of each cell nucleus within each individual selected subcortical region (VZ+SVZ, SP, and CP).

For the analysis, all immunostained pictures were taken using a Leitz Orthoplan 2 microscope with a Spot RT color camera (Diagnostic Instruments, Inc., Sterling Heights, MI). Bright-field images were taken with consistent setup and exposure time for each antibody staining. Immunostained images were converted to the 16-bit color format, and staining intensity was measured using Image J (National Institutes of Health, Bethesda, MD). To measure the subcortical regions of prefrontal neocortex, a rectangular box of equal dimensions (150 μm in width) was selected at the same rostro-caudal level of E17 coronal brain sections. Lateral ventricle and corpus callosum were considered as landmarks of the prefrontal cortex. The staining intensities of marks were defined based on the optical density (OP) values of the nuclei in each subregion of neocortex as follows: Absent – 0 – (OD = 90–120); Weak – 1 – (OD = 120–150); Moderate – 2 – (OD = 150–180); and High – 3 – (OD = 180–210). An equivalent number of cells were evaluated across each section so that cell number would not play a role in the H score percentages. Overall, the immunohistochemical H score of each subcortical region was obtained by the following formula:

3 × percentage of highly stained nuclei + 2 × percentage of moderately stained nuclei + percentage of weakly stained nuclei, giving a range of 0–400.

Cortical thickness was assessed using two independent immunostainings: NeuN and 5mC. Anterior sections of the frontal cortex were rostro-caudally matched between groups and selected for cortical measurements. ImageJ software was used to assess cortical thickness (measured from the base of the SVZ to the edge of the MZ). Subsequently, individual cortical layers were measured (layers were clearly demarcated by cortical cytoarchitecture).

2.2.6 Cell Counting and Morphometric Analyses

Automated cell counts were used to detect cells positive for Ki67 due to the presentation of the immunosignal being punctate and homogenous. In this experiment, sections stained for Ki67 were processed using Image J software according to the following protocol: color deconvolution plugin was used to isolate the brown DAB signal, images were inverted to 8-bit, automated thresholding was performed, and automated particle analysis was performed on the SVZ/VZ region with the selection parameters set to 0.25-1.0 circularity (where 1.0 equals a perfect circle) and size inclusion being 50-600 (pixel^2). Results were presented as number of particles (cells) detected per sample ±SEM.

To assess cell density, cortical sections from 5mC staining procedures were counterstained by Methyl-Green dye (Nissl) which allowed for the visualization of 5mC positive as well as 5mC negative nuclei. After Brightfield imaging under a light microscope (see “Densitometry analysis and cortical thickness assessment”), a select region targeting the mid cortical plate was binned ($0.025mm^2$) across all brain sections at

a high magnification. Nuclei were counted using the multi-point counting tool on ImageJ software (NIH, Bethesda MA). At least two sections taken from the anterior cortex of each subject were averaged for total nuclei/area. Additionally, at least two subjects from each litter were represented in the assessment (where *n*=litter).

A similar procedure was used to analyze nuclear morphology. Due to the non-circularity of some cortical cells, the major and minor axes of each nuclei were measured across the anterior CP. In some cases, where nuclei were quite circular, the nuclei length and diameter were arbitrarily selected and interchangeable. In cases of non-circular morphology, the major (longest) and minor (perpendicular to major) axis were clearly distinct and thus represented independently. A straight line tool was used in all cases to measure the major and minor axes of the nuclei. Finally, nuclear area was calculated based on the following equations: circular area=πr^2 (where r=minor axis/2) and ellipse area=πab (where a=minor axis/2, b=major axis/2). Distinction between circular and non-circular nuclei was made if major axis was ≥1.5 times the minor axis. At least 100 nuclei from the selected region were measured per cortical section and at least two sections per subject were represented in the average. Each N represents one litter in these assessments. To help minimize experimenter bias, images were randomly examined, meaning, experimental groups were not evaluated as continuous cohorts throughout the imaging session.

2.2.7 Western blot of the methylation-binding protein MeCP2

Western blotting was carried out to confirm MeCP2 protein expression differences at E17 between groups, which were initially observed in MeCP2 immunostainings. From the preliminary MeCP2 staining, we noticed that MeCP2 was

unilaterally upregulated by alcohol across all cortical layers and in various other brain regions, such as the hippocampus and cerebellum. As such, Western blots of the entire E17 fetal brain were used (N = 4 each) following a standard protocol (Zhou, Patel et al. 1999, Anthony, Zhou et al. 2008, Mason, Anthony et al. 2012). Nuclear protein was isolated from tissue lysates using NE-PER nuclear and cytoplasmic reagents (Thermo Fischer Scientific, Waltham, MA), and sample concentrations were evaluated against a BSA standard curve at OD_{595}. All samples were run in triplicate on two independent gels for each protein examined. Immunoreactive blots were detected using ECL Western Blotting Detection Kit (Thermo Fisher Scientific, Rockford, IL, USA; RPN2108) and exposed to a biomolecular imaging system (ImageQuant, LAS 4000). Densitometric comparisons were made with Image J software. GAPDH density measurements were used as loading controls. All changes in protein expression were reported as a percentage change compared to Chow and PF groups, with a minimum of four samples/treatment group. Statistical analysis was performed by one-way ANOVA on MedCalc software.

2.2.8 Global DNA methylation analysis

Fetal brains were isolated and microdissected under a dissection microscope (Leica MZ6, Leica Microsystems). Neocortical brain tissues were separated from subcortical brain tissue using the borders of the nascent internal capsule as a visual guide. DNA extraction and purification were subsequently performed using silica-based spin-column purification (DNeasy Blood and Tissue kit, Qiagen) according to manufacturer's instructions. Purified DNA was quantified by spectrophotometric absorption at 230, 260, and 280 nm, and the quality and concentration were calculated as the A_{260}/A_{230} and A_{260}/A_{280} ratio (Nanodrop 2000, Thermo Scientific). An average of 100–200 ng of

genomic DNA was used for DNA global methylation analysis performed with the MethylFlash Methylated DNA Quantification Kit and MethylFlash Hydroxymethylated DNA Quantification Kit (Colorimetric; Epigentek Group) according to the manufacturer's instructions. OD values were determined using a PHERAstar FSX microplate reader and MARS Data Analysis Software (BMG Labtech, Cary, NC). Methylation levels were estimated using a standard curve of methylated DNA standards according to the manufacturer's instructions. Presented values reflect the ratio of methylation relative to the control group (normalized).

2.2.9 Statistical Analysis

A Kruskal-Wallis test was used for non-parametric statistical analysis to address differences between the three groups while Conover post-hoc testing was used to identify differences between each of the groups. Statistical analysis was performed using MedCalc software. All data are presented as Mean±Standard Error of the Mean (SEM) and sample sizes reflect litter number represented.

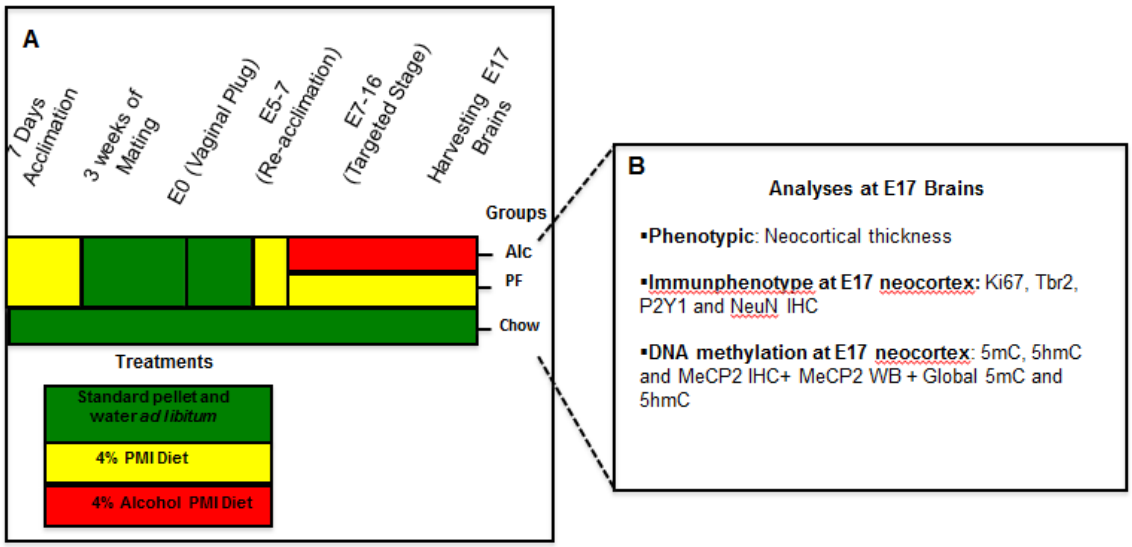

Figure 17: Summary of experimental procedures
(A) C57BL/6J females were conditioned to receive the liquid diet devoid of alcohol for a period of seven days preceding mating. After conception, the liquid diet was re-introduced at E5 and either alcohol or an isocaloric pairfed diet was administered from E7-E16 (equivalent to the late first and second human trimesters). Each color in the schema represents a specific treatment: green (standard pellet and water *ad libitum*), yellow (alcohol-free PMI liquid diet), or red (4% v/v alcohol PMI liquid diet *ad libitum*). (B) At E17, brains from each litter across the three groups were processed for either immunophenotypic or molecular assessments. Alc (alcohol); IHC (immunohistochemistry) and PF (pair-fed)

2.3 RESULTS

2.3.1 Alcohol-Induced Cortical Thinning in the Embryonic Cortex

A mouse model of FASD was used in this study to evaluate aberrant DNA methylation during cortical laminar formation. We observed that alcohol-induced aberrations of phenotypic and epigenetic features are associated in the embryonic cortex, providing evidence that the disruption of the intrinsic DNA methylation program may be a mechanism for the establishment of cortical dysfunction.

One of the most prominent phenotypes observed in this experimental animal model was the occurrence of reduced neocortical thickness, which was consistent with previous observations at E15 (Zhou, Sari et al. 2003, Zhou, Sari et al. 2005). A closer layer-by-layer analysis revealed a reduction in cortical plate (CP) size (Figure 18J, $P<0.005$) as well as an increase in the VZ and SVZ in proportion to the total cortical length (Figure 18K, $P<0.005$). Further evidence of neocortical thinning was demonstrated by the abnormal expansion of lateral ventricles in the Alc group compared to the Chow and PF control groups (Figure.18A–C). To examine the molecular contributors of cortical thinning in the alcohol-affected cortex, several phenotypic markers were examined across the cortical strata.

2.3.2 Molecular Correlates of Alcohol-Induced Cortical Thinning

Aberrations of the ventricular zone during corticogenesis may significantly impact long-term and phenotypic and anatomical outcomes. The source of radial glia proliferation and intermediate progenitor specification, the ventricular regions of the cortex are crucial for radial migration of cortical progenitors and early cortical specification. Genetic studies have demonstrated that intrinsic and morphogenic signals

at the VZ and SVZ precisely govern the emergence of RGCs and IPCs through the sequential expression of gene networks. For example, the onset of cortical neurogenesis requires the suppression of cell adhesion elements such that neuroepithelial cells may adopt the elongated morphology of an RGC. These transitions are thought to be regulated at least in part by the expression of key factors such as Pax6 and vimentin, among others (Taverna, Gotz et al. 2014). Similarly, a distinguishing feature of SVZ versus VZ abiding progenitors appears to be the expression of the transcription factor Tbr2 (Englund, Fink et al. 2005). Tbr2 expression during corticogenesis has been linked to cortical folding, social behaviors in adults, and early lineage specification of cortical glutamatergic neurons (Vasistha, Garcia-Moreno et al. 2015, Belinson, Nakatani et al. 2016, Toda, Shinmyo et al. 2016).

First, we examined the proliferative capacity of cells at the ventricular regions using the maker Ki67, a nuclear cell proliferation marker. In the VZ/SVZ, a significant reduction of Ki67 (+) cells (Figure.19A-C, $P < 0.05$) was observed compared to Chow and PF controls. This finding echoes the inhibitory effects of alcohol on neurogenesis in the hippocampus observed across various models of exposure (Broadwater, Liu et al. 2014, Gil-Mohapel, Titterness et al. 2014, Golub, Zhou et al. 2015, Xu, Yang et al. 2015). And while loss of cortical neurons has been previously reported in developmental alcohol models (Ikonomidou, Bittigau et al. 2000, Coleman, Oguz et al. 2012), diminished proliferation of cortical progenitors as an underlying factor has not been previously substantiated *in vivo*. One study of E18 Tbr2-expressing neuroblasts did reveal, however, that though alcohol did not increase apoptosis, cortical basal progenitors were arrested in G1 phase (Riar, Narasimhan et al. 2016).

Next, we evaluated the expression of NeuN, a nuclear marker of neuronal maturity which is observed in post-mitotic neurons. While NeuN was absent in the proliferating zones, a significant reduction was observed in the E17 Alc group compared to the Chow and PF groups in the cortical subplate (SP)(Figure.19D–F, $P < 0.05$). In the cortical plate (CP), a similar reduction of NeuN expressing cells was detected (Figure 20H, $P < 0.05$). Morphological examination of CP cells further demonstrated that alcohol hinders the progression of immature progenitors toward mature cortical neurons, as denoted by the increased presentation of ellipsoidal shapes in the place of more rounded nuclei (Figure 20D-F).

Further, a notable reduction of Tbr2 immunoreactivity was evident in the E17 Alc group compared to E17 Chow and PF control groups (Figure.18A–C). When further compared to E16 Chow stage controls, the E17 alcohol group was anatomically and phenotypically reminiscent of E16 Chow controls (Figure.18C–D), indicating a cortical developmental delay of around one gestational day. These observations agree with the findings of Rair et al in E15-E18 embryonic cerebral cortex (Riar, Narasimhan et al. 2016).

2.3.3 The DNA Methylation Program is Modified by Fetal Alcohol Exposure

Parallel epigenetic assessment was performed alongside phenotypic markers of cortical development. DNA methylation in the form of 5mC was elevated in the alcohol group ventricular zones, SP, and CP, though statistical significance was only observed in the CP (Figure 20G, $P<0.05$). A secondary feature observed in the 5mC assessment was the heterochromatin, punctate expression within the nuclei of alcohol animals. Comparatively, control cortices exhibited round nuclei with a euchromatin distribution of

5mC within the CP (Figure 20D-F). This feature has been observed in embryonic neural tube and hippocampal examinations of previous FASD models (Zhou, Chen et al. 2011, Chen, Ozturk et al. 2013) and perpetuates the notion that the intranuclear re-distribution of DNA methylation marks like 5mC may be essential intrinsic components of cellular development.

The 5hmC marker demonstrated a similar alcohol-induced hypermethylation in the CP, though unchanged in the SP and diminished by alcohol in the SVZ/VZ (Figure 21D, $P<0.05$). 5hmC-positive nuclei in the alcohol group did not apparently undergo intranuclear re-organization during development. Finally, the methyl-binding protein MeCP2 demonstrated a marked alcohol-induced increase (Figure 22F, $P<0.05$) which was concurrent with DNA hypermethylation. Assessed region wide by Western Blot, a global increase was concurrently observed (Figure 22E, $P<0.005$).

2.3.4 Global versus Cell-Specific Characterization of DNA Methylation in the FASD Cortex

A common representation in previous epigenetic investigations has included the "global" assessment of epigenetic change. From previous work, we and others have found that DNA methylation (and likely various other epigenetic modifications) are context-specific and thus cell-unique. Because of this, global assessments may be limited in their ability to accurately portray epigenetic patterns. In order to compare our study with previous DNA methylation assessments and to offer a contrasting tissue-wide view, we performed an independent molecular 5mC and 5hmC analysis in the E17 neocortex. 5mC analysis demonstrated that alcohol induced a global reduction in DNA methylation

compared to Chow and PF animals (Figure 23A, $P < 0.01$). Additionally, molecular 5hmC levels were overall reduced compared to Chow controls (Figure 23B, $P < 0.05$).

These observations present a different perspective compared to the patterns observed with 5mC and 5hmC in the cortical plate. The inclusion of cortical interneurons and non-neuronal cells in the genomic DNA of the cortical tissue or perhaps the mixing of cells with differential DNA methylation levels is likely responsible for this contrasting pattern. Despite that, alcohol-effects were persistently detectable, even on a global scale and speak to the potent nature of the teratogen on the cortical tissue at large.

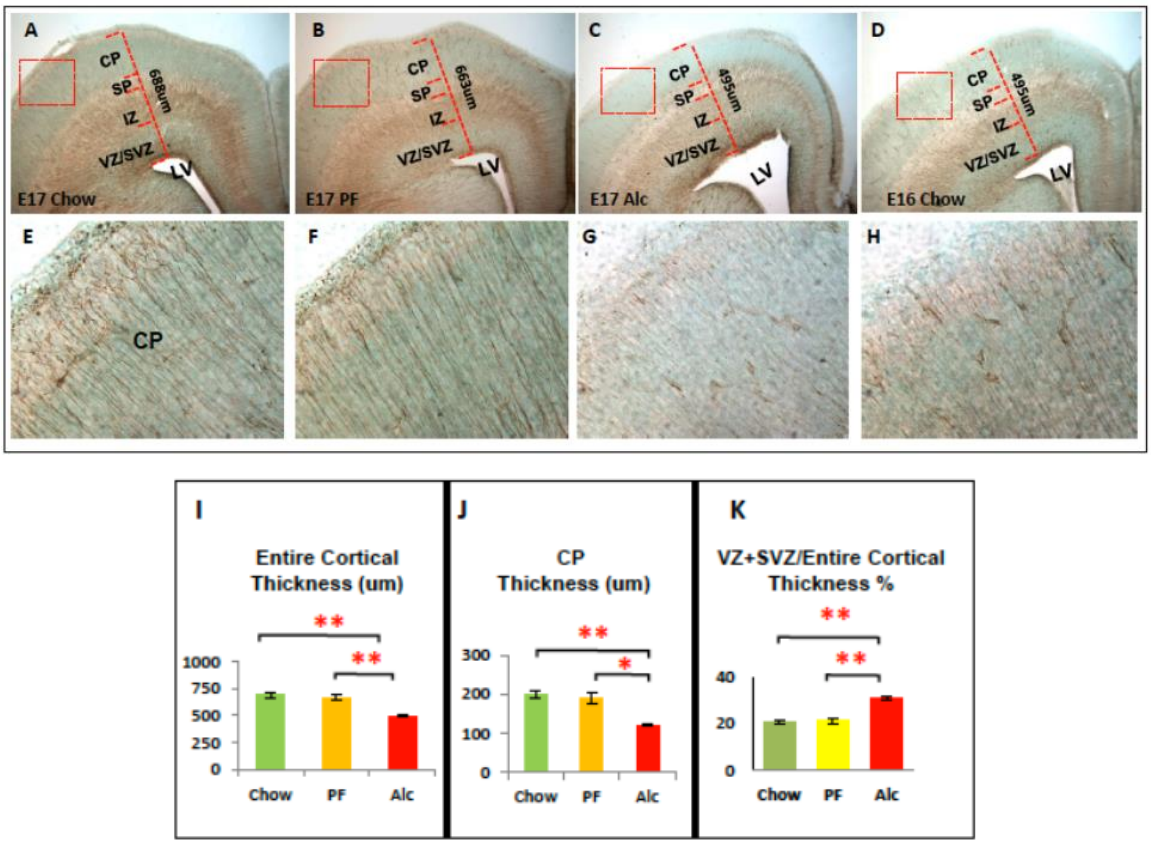

Figure 18: Alcohol reduces cortical thickness and Tbr2-im expression in the E17 frontal cortex

Structural abnormalities were observed during phenotypic investigation. Notably, the thickness of cortical plate (J) as well as the entire thickness of frontal cortex (I) were reduced in alcohol group frontal cortex as compared to their Chow and PF control cortices (A-C). Fetal alcohol exposure also increased the proportion of SVZ+VZ/entire cortical thickness (K) as compared to controls. Lateral Ventricle (LV) expansion was also observed in E17 Alcohol cortices (A-C). (G) Finally, Tbr2-im (a marker for neural progenitor migration) was normally observed as a radially extending fiber ascending from the base of the lateral ventricle up to the pial surface. Alcohol noticeably reduced Tbr2 immunoreactivity in the CP. E16 Chow brains were used as developmental stage controls and more closely resembled the E17 Alcohol developmental state than E17 Chow (C-D,G-H). Quantitative measurements among the 3 groups were analyzed by One-way ANOVA and the difference between paired groups were compared by student t-test. *P<0.05, **P<0.005. N (structural analysis) = Chow (5), PF (5), Alc (5). N (Tbr2-im analysis)=Chow (3) , PF (3), Alc (3), E16 Chow (3). SVZ/VZ (Subventricular Zone/Ventricular Zone); IZ (Intermediate Zone); SP (Subplate) and CP (Cortical plate).

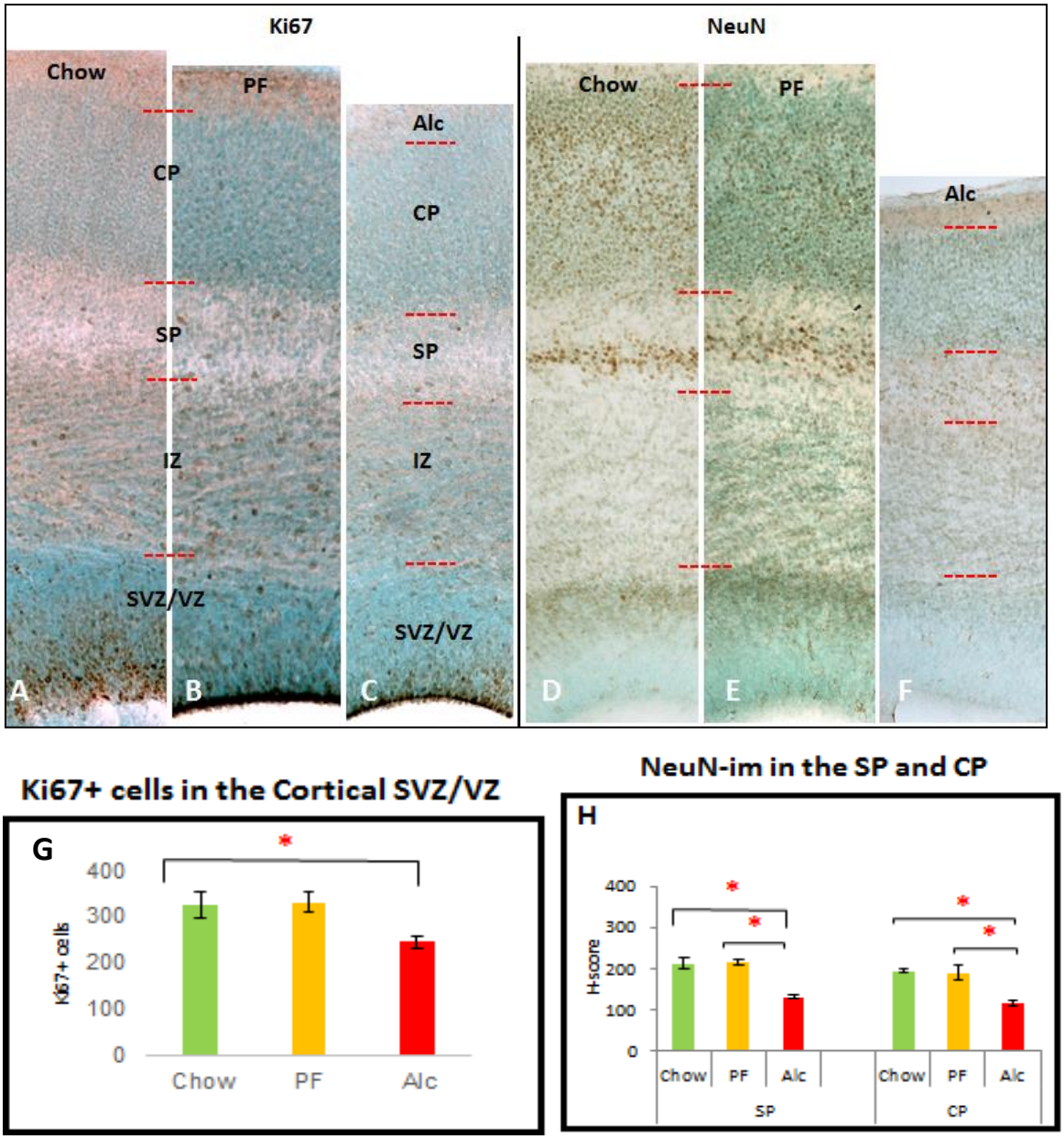

Figure 19: Alcohol reduces ventricular proliferation and neuronal maturation in the E17 frontal cortex

Representative cortical column of E17 Chow (A,D), PF (B,E), and (C,F) Alc group coronal sections for Ki67 and NeuN immunostaining. Fetal alcohol-induced reduction of Ki67 immunoreactivity was observed mainly in the SVZ/VZ zone, the neuroepithelial cellular zones. Quantitative assessment of Ki67+ cells further confirmed an alcohol-related reduction in the SVZ/VZ zone (G); N=Chow (5), PF (4), Alc (7). Alcohol reduced NeuN-im throughout cortical SP and CP layers (F) compared to Chow (D) and PF (C). No significant change was observed between Chow and PF groups. Quantitative assessment of NeuN-im was further quantified by single-cell density analysis (H-Scoring) across the three groups (H). *$p < 0.05$. SVZ/VZ (Subventricular Zone/Ventricular Zone); IZ (Intermediate Zone); SP (Subplate) and CP (Cortical plate)

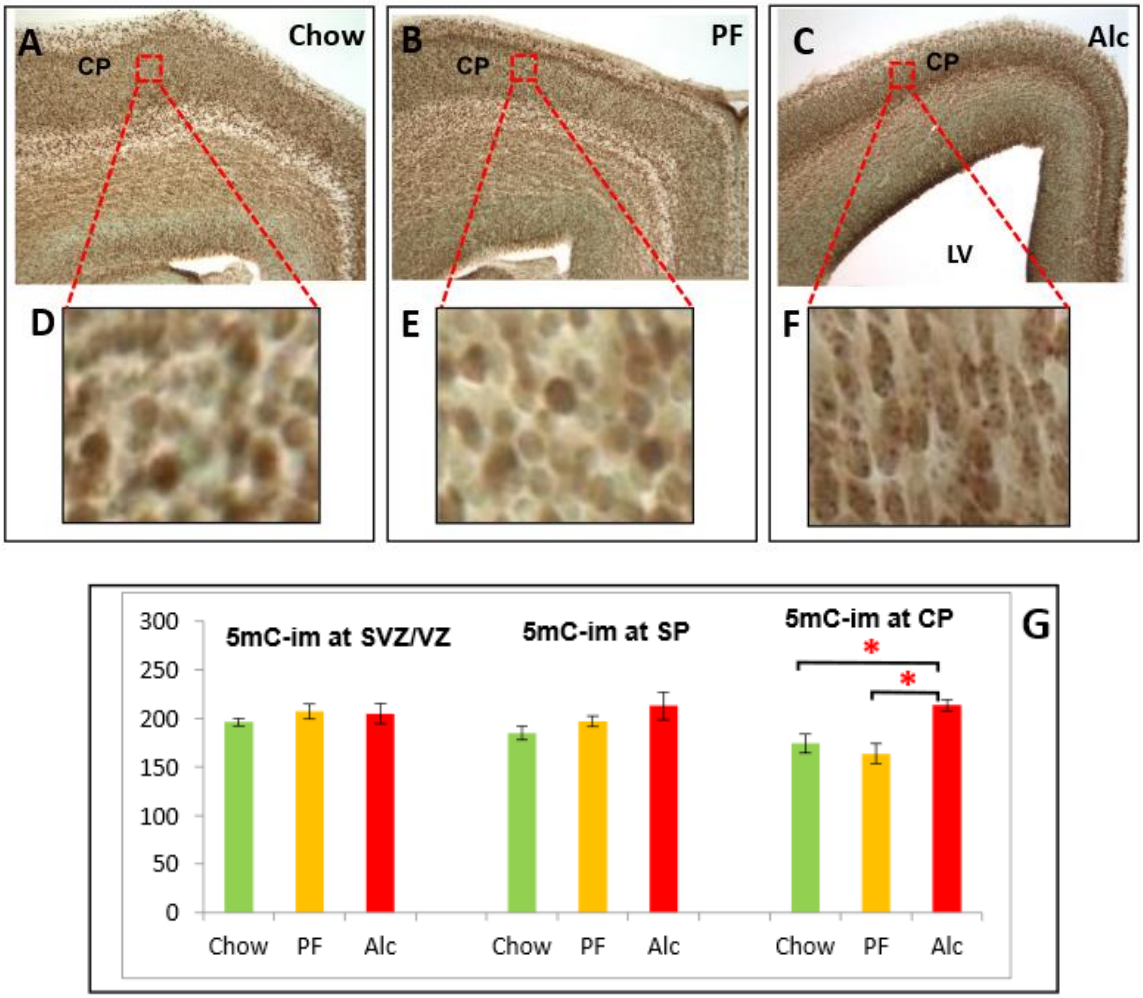

Figure 20: Alcohol inhibits 5mC and cellular maturity in the E17 cortical plate
(A-C) E17 frontal cortex across three groups (Chow, PF, and Alc). Red boxed areas in CP (A-C) was enlarged in all D-F. While no change in 5mC-im was detected across the groups in the SVZ/VZ or SP, 5mC was significantly increased in the Alcohol group CP (G). Enlarged CP areas further demonstrated that alcohol induced a morphological delay of CP neurons (as observed by their ellipsoidal shape and granular intranuclear 5mC-im distribution) compared to the mature, roundedness of Chow and PF CP neurons (D-F). *P<0.05. N=Chow (5) , PF (4), Alc (5). LV (Lateral Ventricle); SVZ/VZ (Subventricular Zone/Ventricular Zone); IZ (Intermediate Zone); SP (Subplate), CP (Cortical plate) and MZ (Marginal Zone).

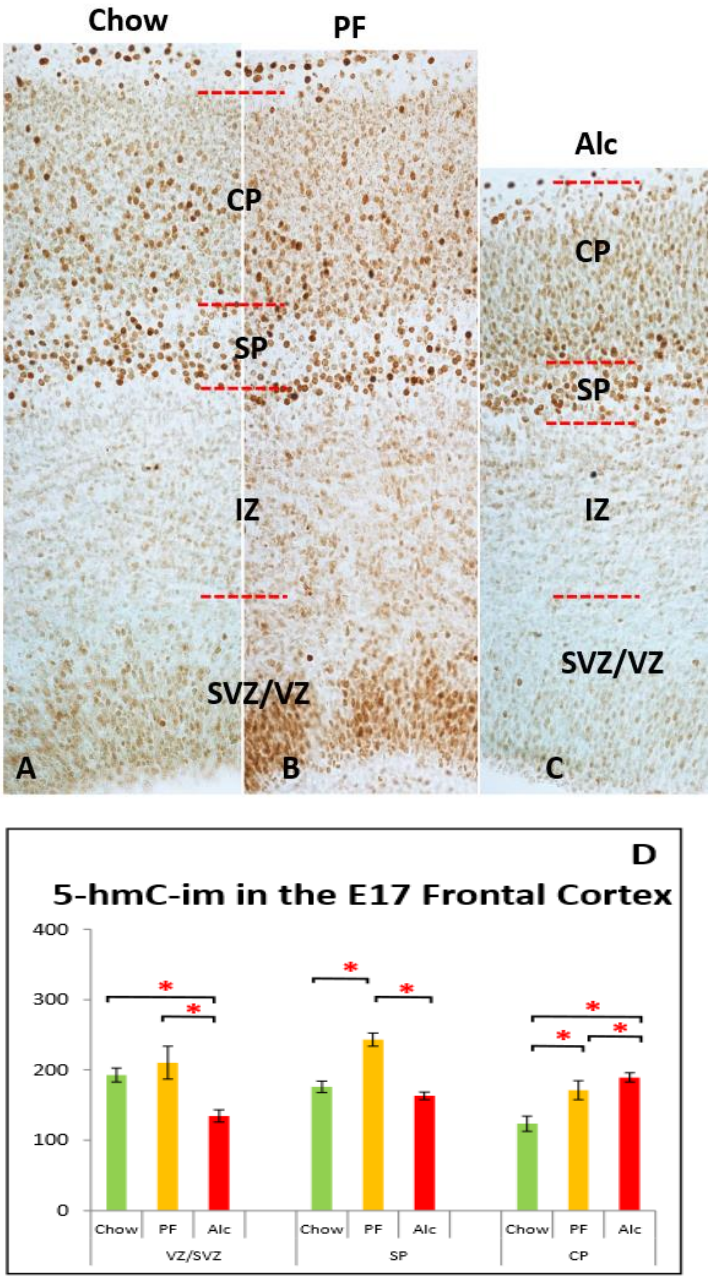

Figure 21: 5-hmC-im is reduced in the lower cortex but upregulated in the E17 cortical plate

(A) Alcohol reduced 5hmC-im at the cortical SVZ/VZ layers compared to Chow and PF controls (B), while no significant change was observed between controls (D). At the SP cortical layer, only significant alternation is detected as an increase in PF group as compared to both Chow and Alc groups. (A-D) A marked increase of 5hmC-im was observed at the CP region in both the PF and Alc groups as compared to Chow group, while a significant increment was also evident at the Alc group CP as compared to PF group . * $P<0.05$. N=Chow (5), PF (4), Alc (5). CP (cortical plate); MZ (marginal zone); SP (subplate); SVZ (subventricular zone) and VZ (Ventricular zone).

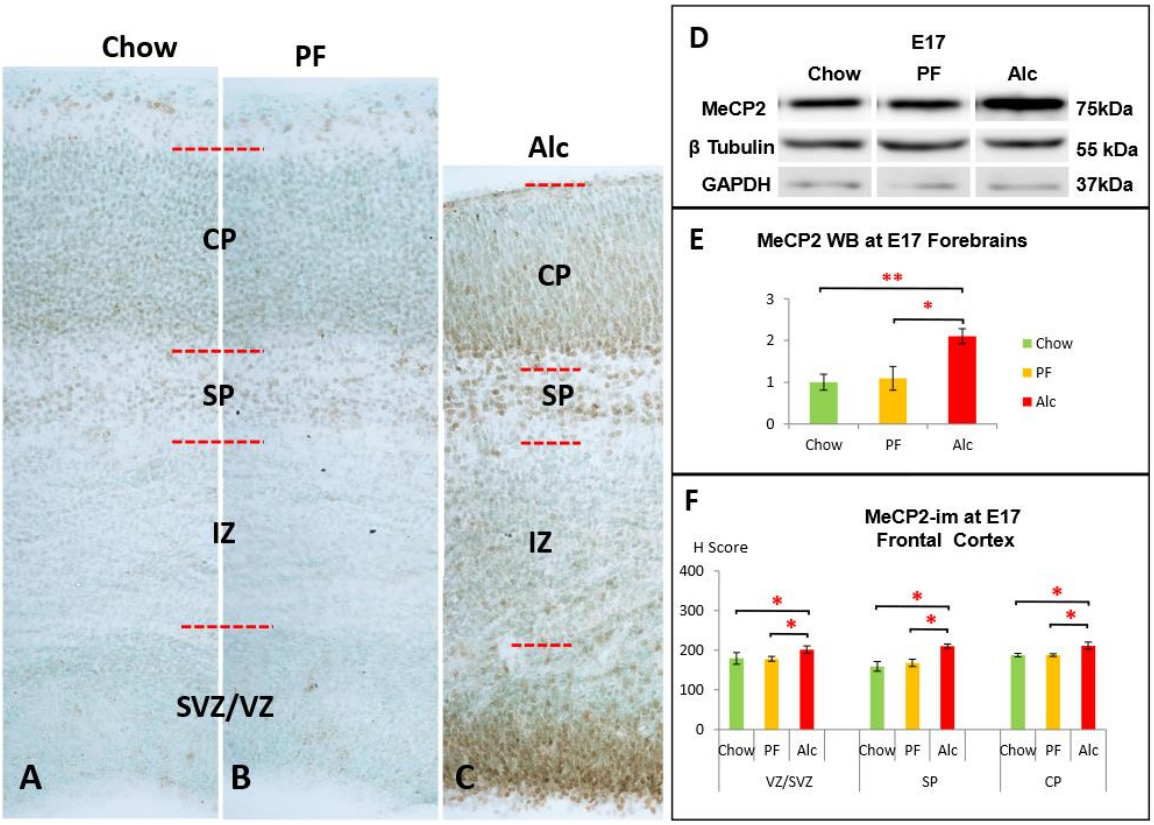

Figure 22: Alcohol-induced MeCP2 up-regulation in the E17 cortex
(A-C) Representative columns from the frontal of E17 cortex across the three groups. (C,F) Alcohol increased MeCP2-im throughout cortical SVZ/VZ, SP and CP layers compared to controls. No significant change was observed between Chow and PF groups. * P<0.05. N=Chow (5), PF (4), Alc (5). (D-E) Densitometry of MeCP2 whole-brain western blot (WB) showed a significant increase of MeCP2 expression at E17 in the Alc group compared to its counterparts. (One-way ANOVA: F=6.95, P<0.05). Post-hoc analysis showed no significant difference between PF and Chow groups. Western Blot band intensity was normalized to GAPDH as an internal control. N=4 (Chow), PF (3), Alc (4). * P<0.05 **P<0.005. WB (Western Blot); blots are presented as cropped segments.

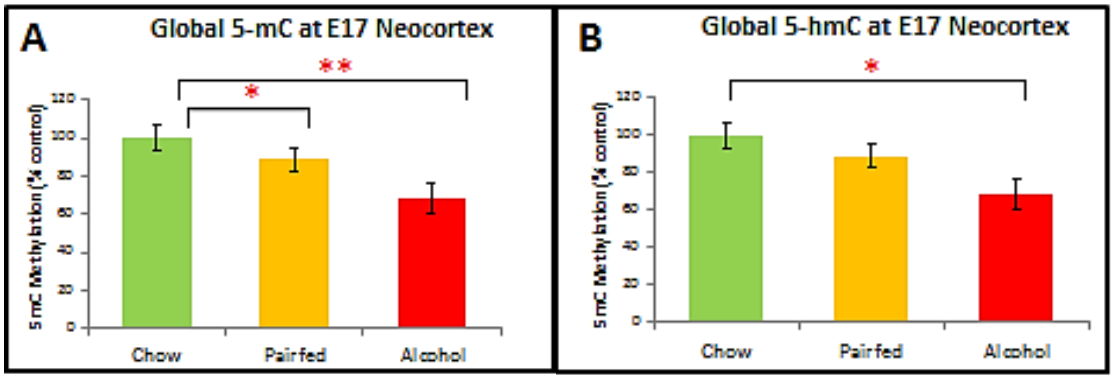

Figure 23. Quantitative DNA methylation (5-mC and 5-hmC) reveals tissue-wide alcohol-related de-methylation in the E17 cortex
Global DNA methylation (5mC) was significantly decreased in the neocortex at E17 (A). Global DNA methylation (5hmC) was also significantly decreased in the neocortex in response to fetal alcohol exposure (B). Means of the three groups were compared by non-parametric Kruskal-Wallis test followed by conover post-hoc test for multiple comparisons. *$p < 0.05$. **$p < 0.01$. Chow (n=6), Pair-fed (n=6), Alcohol (n=6).

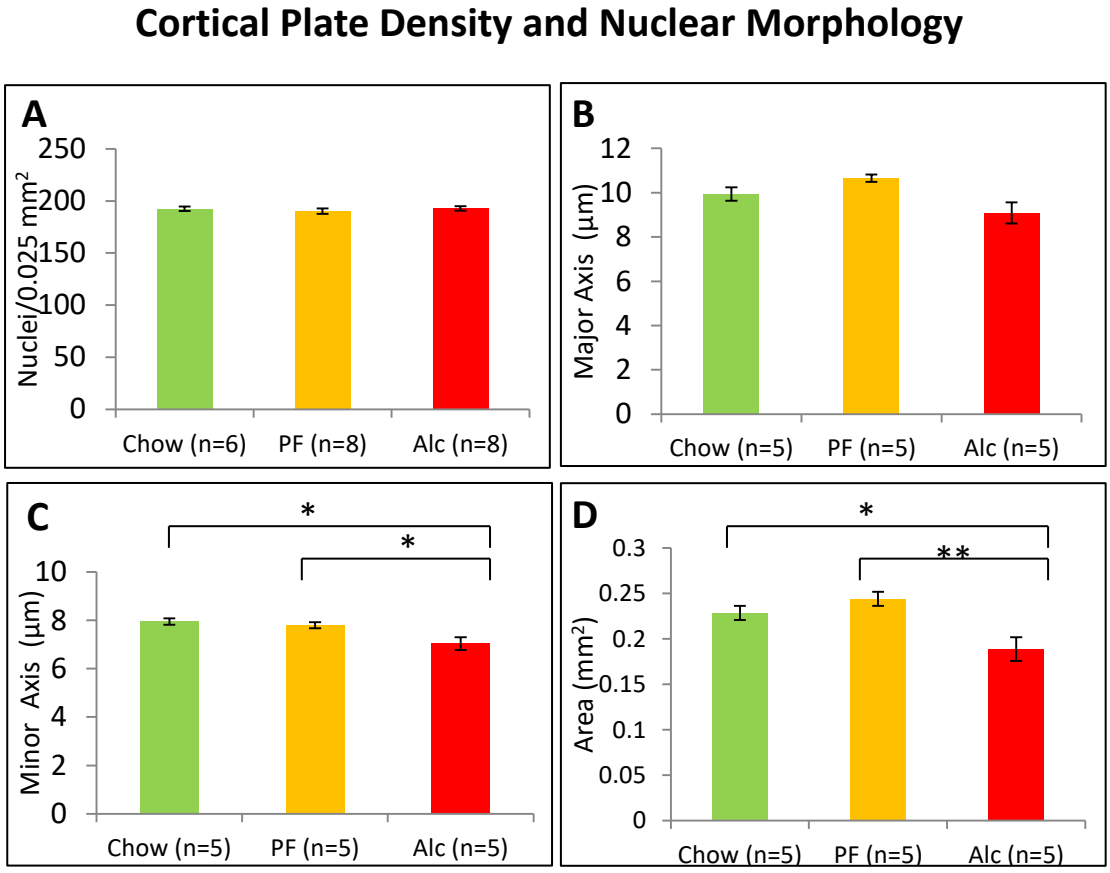

Figure 24. Cortical plate density is unchanged by alcohol but nuclear morphology is negatively impacted

Cortical plate nuclear density was unchanged by experimental treatment (p=0.848)(A). Nuclear length was decreased by alcohol treatment (B) and nuclear diameter was similarly decreased (C). Nuclear area of circular and ellipsoidal neurons was extrapolated from major and minor axes. Alcohol nuclear area was significantly decreased compared to both Chow and PF control groups (D). Means of the three groups were compared by non-parametric Kruskal-Wallis test followed by Conover post-hoc test for multiple comparisons. *$p < 0.05$, **$p < 0.005$.

2.4 DISCUSSION

2.4.1 Cortical Dysmorphology in FASD

Head circumference has been commonly used in the assessment of brain developmental disorders including some subsets of FASD. A recent study confirmed a significant positive correlation between head circumference, brain volume and IQ scores in patients (age 5-19) prenatally exposed to alcohol (Treit, Zhou et al. 2016). Moreover, the study demonstrated that the relationship was predictable from early to late adulthood, indicating that structural deficits persist for a sizable length of time after exposure. These findings confirm previous work concluding that gestational alcohol exposure (of varying degrees) may lead to developmental growth abnormalities across the brain, manifesting most notably in reduced brain volume and corpus callosum malformations (Lebel, Mattson et al. 2012). More importantly, these structural abnormalities may be underlying factors for the cognitive impairment reported in FASD. For example, callosal dysmorphologies have been linked to verbal learning, motor ability, and executive function while hippocampal volume has been linked to verbal ability and recall as reviewed by Lebel et al (Lebel, Mattson et al. 2012). Interestingly, verbal learning has also been associated with structural deficits in the cerebellum and the dorsal frontal cortex (O'Hare, Kan et al. 2005, Sowell, Mattson et al. 2008). Though seemingly straightforward, the structural-functional impact of alcohol is probably more complex in the developing cortex as evidenced by previous studies that have found either no significant correlation or alcohol-mediated increases in cortical thickness.

In reviewing cortical size particularly, as a precedent to the work performed herein, the complexity of alcohol on the cortical structure was continually revealed.

Disruption of neocortical thickness as a consequence of developmental alcohol exposure has been documented in animal studies, including various time courses and doses of alcohol (Table 4). Cortical thinning is apparently a continuous effect occurring from mid-gestation (Zhou, Sari et al. 2004, Aronne, Evrard et al. 2008) to young adulthood in rodent models. Alcohol-induced cortical abnormalities, however, are not unilateral and vary across different cortical regions postnatally (Abbott, Kozanian et al. 2016). In a similar vein, human studies have rarely agreed with the structural effects observed in alcohol rodent models. Longitudinal neuroimaging studies of FASD human patients have reported that while cortical thinning appears to be a normal feature of both FASD adolescents and healthy controls, FASD patients are distinctly affected in the left middle frontal, bilateral precentral, bilateral precuneus and paracingulate, left inferior and bilateral fusiform gyri (Zhou, Lebel et al. 2011). On the other hand, cross-sectional neuroimaging studies have demonstrated that heavy prenatal exposure to alcohol could result in cortical thickening up to 1.2 mm in the bilateral temporal, bilateral inferior parietal and right lateral frontal cortex (Sowell, Mattson et al. 2008). Another FASD adolescent, multi-site study similarly showed thicker frontal, temporal and parietal cortices (Yang, Roussotte et al. 2012).

The diversity of cortical phenotypes may be rooted in variable factors such as patient age range, co-morbidities (e.g. ADHD) and exposures (e.g. acute, chronic, combinatorial with tobacco, etc.), and other unforeseeable factors rendering them incompatible with more controlled rodent studies. A recent analysis by Robertson et al compared regional cortical thickness across continuous measures of prenatal exposure and found that region-specific cortical thinning was inversely related to dose and

frequency of prenatal exposure (Robertson, Narr et al. 2016). Another important distinction between human and animal models is the reported effect of alcohol on cortical folding (De Guio, Mangin et al. 2014), which may limit the ability to cross reference the two types of studies. All things considered, there are many factors to weigh in comparing cortical phenotypes across studies. For the purpose of this study, we attempted to reconcile our results with cortical phenotypes observed in rodent models of prenatal alcohol exposure with comparable Blood Alcohol Concentration (BEC) levels (Table 4). Our study demonstrated distinct cortical thinning, which was subsequently examined at the cellular level using phenotypic and epigenetic markers.

2.4.2 Epigenetic Correlates of the Molecular Drivers of Cortical Dysmorphology

At the base of the cortical column, the neuroepithelial zones demonstrated a reduced expression of the proliferation marker Ki67 in our study. Though alcohol-related reduction of proliferation in neurogenic zones has been previously observed in the hippocampus and thalamus (Leasure and Nixon 2010, Mooney and Miller 2011, Broadwater, Liu et al. 2014), few examples have been documented in the cortex (Huang, He et al. 2015). In several cases, alcohol-diminished neurogenesis was concomitant with regional volume reduction (Kashyap, Frey et al. 2011, Coleman, Oguz et al. 2012) and cognitive and behavioral outcomes (Ehlers, Liu et al. 2013, Golub, Zhou et al. 2015). Some of the neurogenic gene networks proposed to be altered by gestational alcohol include *Adora2a*, *Cxxl1, Dlg4, Hes1*, *Nptx1, Vegfa*, *Fgf13, Ndn*, and *Sox3*. Interestingly, the study also identified decreased *Dnmt* expression, suggesting that alcohol may dysregulate DNA methylation profiles during proliferation (Tyler and Allan 2014). Indeed, our findings relating to the neurogenic zones of the embryonic cortex revealed

that 5hmC (though not 5mC) were diminished by fetal alcohol exposure. Similarly, in the dentate gyrus, a previous study employing our alcohol model demonstrated reduced 5hmC in the alcohol group (Chen, Ozturk et al. 2013). The observation that the more abundant 5mC was unchanged by treatment in the SVZ/VZ may perhaps be rooted in its dual nature in both neurogenesis (mitosis) and the (post-mitotic) production of intermediate progenitors, two prominent features of the neurogenic zone. It is possible that while 5hmC plays a more linear role in proliferation, 5mC may exhibit opposing patterns in mitotic versus post-mitotic events in the region, resulting in an overall unchanged signal.

Despite reduction in proliferation, our laminar assessment demonstrated that the neurogenic SVZ/VZ was actually increased in size (relative to the total cortical length) in the alcohol experimental group. One possible explanation may be that while alcohol reduces proliferation (presumably diminishing cell number in the region), it also hinders the progression of basal progenitors, prolonging their occupancy in the SVZ/VZ and delaying their migration into the IZ and upper layers. During corticogenesis, intermediate progenitors are proposed to account for most of the production of mature cortical neurons (Englund, Fink et al. 2005), suggesting that their timely development may bear significant functional consequences. Evidence for the delayed progression of intermediate progenitors in the SVZ/VZ is provided by the observed reduction of the transcription factor Tbr2 both here and in a previous developmental alcohol study (Riar, Narasimhan et al. 2016). Tbr2 is thought to be a unique indicator of neuron-fated progenitors and has been demonstrated in various studies to be critical for conferring neuronal subtype identity. Interestingly, conditional knockout of Tbr2 during corticogenesis produces

concomitant reduction of cortical surface (though not cortical thickness) (Mihalas, Elsen et al. 2016). Other roles for Tbr2 in neuronal differentiation include cellular migration, including subpalial migration of GABAergic neurons to the cortical SVZ (Sessa, Mao et al. 2010). In the olfactory bulb, a similar expansion of the subventricular zone-rostral migratory stream was observed in response to diminished Tbr2 (Kahoud, Elsen et al. 2014).

Additional evidence for the alcohol-delayed progression of neuron-fated progenitors in the neurogenic zones was provided by the observed reduction of the neuronal marker NeuN in the subplate and cortical plate. NeuN is a DNA/RNA-binding protein that is almost exclusively found in post-mitotic neuronal nuclei. Often used as a biomarker of neuronal maturity, in previous studies of chronic, developmental alcohol exposure, NeuN was decreased in the posterior medial barrel subfield and the motor cortex (Powrozek and Zhou 2005, Teixeira, Santana et al. 2014). The results of this and other studies corroborate the proposed delayed progression of intermediate progenitors in the SVZ/VZ as a consequence of developmental alcohol exposure. In contrast to the DNA hypomethylation (5hmC) associated with alcohol in the SVZ/VZ, the DNA methylation profile of alcohol in the upper cortical layers was generally hypermethylation.

In the SP, the site of the oldest post-mitotic neurons, 5mC remains unchanged though 5hmC demonstrates a reduction compared to nutritional controls (but not Chow controls). This decrease parallels the diminished NeuN immunoreactivity observed in the SP and echoes various reports of a positive correlation between neuronal maturity and 5hmC (Song, Szulwach et al. 2011, Szulwach, Li et al. 2011). Interestingly, though 5hmC

was reduced with alcohol treatment, the methyl-binding protein MeCP2 was significantly increased. Though there is significant co-localization of 5hmC-DNA and MeCP2 in the developing cortex (Chen, Damayanti et al. 2014), the inverse 5hmC/MeCP2 response here warrants further examination. Additionally, while a recent report found that NSCs upregulate and subsequently downregulate protein and mRNA MeCP2 levels following alcohol exposure and withdrawal, respectively (Liyanage, Zachariah et al. 2015), the dynamics of 5mC/5hmC/MeCP2 remain to be elucidated. While MeCP2 has demonstrated a regulatory role in a variety of developmental and disease processes, much less is understood to-date about the mechanisms that regulate the methyl-binding protein. A few studies have tackled this problem, for example, a MeCP2-targeting microRNA has been identified as a regulator of MeCP2 expression and conserved cis-regulatory motifs such as G-quadruplexes have been isolated as potential regulators of MeCP2 pre-mRNA (Bagga and D'Antonio 2013, Han, Gennarino et al. 2013). While insightful, much remains to be elucidated about the regulation of methyl-binding proteins and their intersection with methylated DNA.

In the cortical plate, concordant with decreased NeuN, Tbr2, and decreased CP thickness, all three DNA methylation marks (5mC, 5hmC, and MeCP2) were increased in the Alc group relative to controls. This was in contrast to the 5hmC profiles observed in the SVZ/VZ and SP as well as cortex-wide in global DNA methylation analyses. The discrepancy between DNA hypermethylation in the CP and hypomethylation in the SP and neurogenic layers may lie in the composition of diverse cell types of the CP. Unlike the SVZ/VZ (composed of neuron and glial progenitors) and SP (composed of mature neurons and migrating CP neurons), cells represented in the CP include migrating

neurons, inhibitory interneurons (deep CP), glial cells, and mature cortical neurons of varying specifications (subcerebral projecting, callosal, etc.). The transcriptional requirements of differentiating neurons in the CP may respond differently to alcohol than premitotic and intermediate cells of the lower layers, which we have previously reported demonstrate bivalent action during differentiation (Zhou, Zhao et al. 2011). Evidence that neurons in mature states respond differently to alcohol may be taken from adult models of alcohol seeking and post-dependent rats, where DNA hypermethylation has been observed (Warnault, Darcq et al. 2013, Barbier, Tapocik et al. 2015).

2.4.3 Reconciling Cell and Tissue-Wide Epigenetic Analysis in FASD Studies

Of the few DNA methylation profiles that have been examined in the cortex, all have agreed with reported reductions in DNA methylation in primordial and postnatal cortical regions in response to fetal alcohol (Garro, McBeth et al. 1991, Otero, Thomas et al. 2012). However, all of these studies share the feature of presenting DNA methylation as a cumulative cortical product, indiscriminant of diverse cell types. When considered as such, these findings agree with our global analyses of DNA hypomethylation in the alcohol-exposed cortex (Figure 23). But as unique DNA methylation programs of the postnatal cerebellum and normally developed embryonic cortex demonstrated (see Chapter 1), analysis of "global" or region-wide homogenates may oversimplify the complexity of the epigenetic alcohol response that is observed layer-by-layer.

A second possibility for the divergent presentation of DNA methylation trends in the CP compared to lower layers may relate to differences in cellular density. One report observed that prenatal alcohol was associated with an increase in the number of MGE-derived interneurons in the medial prefrontal cortex (PFC) (Skorput, Gupta et al. 2015),

supporting the likely increased cellular density of the alcohol CP. Finally, as shown in Figure 20(D–F), differential cellular morphology and intranuclear 5mC distribution in the alcohol CP may factor into alcohol-induced hypermethylation in the CP. To examine whether cell density or morphology factored into perhaps an overrepresentation of DNA methylation in the CP, we performed an analysis across the three groups. We report that cell number (as detected by nuclear number/area) was unchanged across all groups (Figure 24A). This finding is in line with a previous alcohol study where BrdU incorporation revealed no changes in the number of corticothalamic neurons (White, Weber et al. 2015). While these findings increase our confidence in the observed DNA methylation profile of the alcohol-affected CP, cell density in a restricted area measurement may not truly reflect the cell density of the total CP, particularly in light of observed decreases in CP thickness.

Morphometric analysis of cellular nuclei in the cortical plate revealed that while cell number was unchanged, nuclear area was significantly compromised by alcohol (Figure 24B, $P < 0.005$). Here, our observations echo the historic findings of alcohol-impaired PC maturation in the cerebellum, where cell number is unaffected, but nuclei are significantly smaller (Volk, Maletz et al. 1981). However, one previous analysis in the medial PFC demonstrated that alcohol was actually associated with increased soma size (Lawrence, Otero et al. 2012). Contrasting observations may be attributable to a wealth of variations in the experimental paradigm (for example, the mPFC observation was performed during an adolescent stage in a perinatal model of alcohol exposure and limited to Layer II/III pyramidal neurons). Interestingly, even in the cerebellar analysis, it was noted that the impact of alcohol on nuclear size was not persistent in advanced ages.

Ultimately, our observed alcohol-mediated developmental deficits may begin to offer an explanation for cumulative cortical thinning. It should be noted however, that a few important contributors were omitted in this study which require future consideration.

Apoptosis is a common cellular phenotype of developmental alcohol exposure (Farber, Creeley et al. (2010), Lebedeva, Zakharov et al. (2017)). Affecting glial and neuronal populations, likely through the suppression of neuronal activity (Lebedeva, Zakharov et al. 2017), dose-dependent, alcohol-induced apoptosis has been demonstrated to peak during the first postnatal week in the neonatal rodent cortex (Ikonomidou, Bittigau et al. 2000). As such, assessment of alcohol-related apoptosis was not featured in our E17 cortical model though its contributions during prenatal periods might be significant. There is a particular need in future studies to consider apoptosis during late corticogenesis as intraneocortical circuitry (and consequent neuronal activity) has been demonstrably altered around this time point in previous FASD rodent models (El Shawa, Abbott et al. 2013). Cell loss due to apoptosis, though not reflected in cell density analysis, may be an important contributor of alcohol-related cortical thinning.

Another limitation of this study was the exclusive use of neuronal migration and maturation markers to characterize the developmental background of target CP populations that include non-neural cells. In a similar vein, the many inhibitory interneurons which inhabit the CP demonstrate a completely different origin site and migratory path than the neurogenic SVZ/VZ-radial migration examined here. Aberrant tangential migration of medial ganglionic eminence-derived cortical interneurons is observed in gestational alcohol models and results in the increased occupancy of GABAergic interneurons in the cortex that persists into young adulthood (Skorput, Gupta

et al. 2015). Similarly, abnormal radial glial migration and the differentiation of astrocytes in the rodent cortex have all been previously reported in response to prenatal alcohol exposure (Miller and Robertson 1993, Valles, Sancho-Tello et al. 1996, Aronne, Guadagnoli et al. 2011). To date, very few studies have profiled the epigenetic characteristics of cortical interneurons and non-neurons independently. One recent study reported that cortical GABAergic interneurons demonstrate a distinct DNA methylation program compared to glutamatergic projection neurons, including decreased 5hmC and increased CpG 5mC hypermethylation (Kozlenkov, Wang et al. 2016). Another study utilized cell sorting techniques to examine the global DNA methylation landscapes of neuronal and non-neuronal cells in the cortex. They determined that neurons showed a tendency toward general hypomethylation and hypermethylation of astrocytic gene networks while non-neuronal nuclei demonstrated hypermethylation of synaptic transmission gene networks, likely reflecting the repressive role of global methylation. Importantly, this study described the increased variation of neuronal DNA methylation as an indicator of increased epigenetic plasticity in neurons. Finally, the authors of this study suggested that global cortical DNA methylation patterns largely reflect non-neuronal cells, and this may not accurately portray the unique DNA methylation program of neurons (Iwamoto, Bundo et al. 2011). Collectively these reports offer new insights and expand support for the idea of cell-unique DNA methylation dynamics which have been described here. Performed under normal conditions in the adult cortex, the expansion of a developmental profile and the evaluation of aberrant (disease) state DNA methylation reprogramming in purified cortical populations is needed in the future.

Some technical considerations should also be addressed at this time. Here, for example, the administration of alcohol via a liquid-diet paradigm required the inclusion of an isocaloric liquid-diet control group (PF), which mirrored the Chow brain anatomically, phenotypically, and epigenetically. The isocaloric pairfed is calorie-matched to account for any existing nutritional deficiency in the liquid diet model not attributable to alcohol itself. While the PF group has been successfully used in various alcohol liquid diet models, some epigenetic sensitivity of the liquid-diet (PF compared to Chow) was detectable here, particularly in 5hmC analyses. Even though the liquid-diet alcohol paradigm allows for control over the alcohol dose and caloric equilibrium in a relatively non-invasive method, some epigenetic differences may arise due to inherent variations between the Chow and PF diet, such as micronutrition, fat content, and stress induced by the yoking of liquid-diet volume to equilibrate caloric content of the alcohol and nutritional control group. Though these variables did not perturb normal development, they cannot be entirely ruled out as environmental contributors of the DNA methylation program.

Finally, due to the observation of many grades of immunoreactivity across various markers in the cortex, we employed a semi-quantitative immunohistochemcial analysis known as the H-score (see Materials and Methods, 2.5). Using this algorithm, the percentage of cells stained at various intensity levels (arbitrarily defined by the experimenter as absent, weak, moderate, and intense) could more accurately reflect the abundance of the antigen than traditional cell counting techniques. To ensure that the categorical percentages were comparable between groups, cell number was normalized within each examined region ensuring that density of cells was not a factor of perceived

immunoreactivity. Due to the nature of optical densitometry in our software to range from completely black (OD=255) to completely white (OD=0), it was necessary to set thresholds which could include "absent" (methyl-green) nuclei as well as the most intensely-labeled nuclei (dark brown). Using cortical sections stained for methyl-green only, we were able to set these thresholds and subsequently define the OD ranges for each of our four immunoreactivity categories. To assuage inherent experimenter bias, cortical sections from different groups were examined non-sequentially. Additionally, randomized selection of nuclei was performed prior to densitometry analysis. Despite each measure taken to minimize the biases of H-scoring, the fact remains that processing procedures and the use of the human eye introduce certain variability in IHC (Rimm, Giltnane et al. 2007). Moreover, the biophysical properties of diaminobenzidine (DAB) as a chromagen monopolize light absorption and limit its visual dynamic range. These phenomena cannot be disregarded and suggest that H-scoring should be taken as a preliminary analysis to be supplemented by more objective, quantitative methods, such as Western Blotting or immunosorbance assays.

2.4.4 Summary and Conclusions

Here, we show for the first time that the altered neocortical DNA methylation program is concomitant with the aberrant laminar patterning of the neocortex as a consequence of embryonic alcohol insult. While a global investigation of DNA methylation markers revealed a cortex-wide reduction following prenatal alcohol exposure, a more detailed examination of the developing cortical laminae revealed that the sub-structural DNA methylation patterning exhibited a far more complex response to alcohol. These epigenetic aberrations were bilateral and parallel with many critical

corticogenic events including progenitor proliferation, migration, and maturation. As is believed to occur in development, these findings together suggest that the dysregulation of the normal DNA methylation program serves as a mechanism by which fetal alcohol confers abnormal gene expression and consequential deficits associated with cortical function.

Despite the complex DNA methylation distribution of various cell types and developmental markers to alcohol exposure, cumulative cortical measures registered a measureable alcohol-response which bears significant structural-functional implications. Though the precise genomic targets of fetal alcohol insult remain to be elucidated in the embryonic cortex another pressing question remains, that is, does epigenetic reprogramming by alcohol drive the developmental response or does alcohol (though other mechanisms) alter developmental processes which produce aberrant methylation as a secondary function? Emerging epigenetic manipulation techniques and high-throughput RNA screens offer solutions for future investigations. In the meantime, the ongoing characterization of alcohol impacts on developmental epigenetic programs provides ample evidence that DNA methylation and transcriptional correlates play a substantial role as "readers" and "writers" of environmental insult during development.

Fetal alcohol perhaps best models this to-date. Exposure has demonstrated the capacity to impact the epigenetic signature of the nervous system from the neural stem cell stage to the embryonic and the late gestational stages (Figure 25). Impressively, many studies have revealed that epigenetic dysregulation may span beyond the course of direct insult (*in utero*), prompting many authors to suggest that an "epigenetic memory" is at work recording environmental insults occurring in early development. Though

reportedly stable, whether these alterations are cumulative or rectifiable is still unknown. Further, the thresholds for functionally meaningful chromatin remodeling will be crucial to characterize for future clinical application.

While the investigation continues, there is mounting evidence to support epigenetic mechanisms such as DNA methylation as developmental instructors of vulnerability to (among other things) psychosocial deficits, propensity for substance abuse, and cancer (Bilinski, Wojtyla et al. 2012, Gonseth, Roy et al. 2015, McCoy, Jackson et al. 2017). Alternatively, a growing repertoire of studies is proposing the reversible nature of epigenetic memory (Kutanzi, Koturbash et al. 2010, Tompkins, Hall et al. 2012) paving the way for a wealth of intervention strategies. And while the sometimes subtle appearance of the epigenetic program may seem marginal, there are very clear molecular pathways from external stimuli to biochemical action and lasting, sometimes multi-generational encoding. An exemplary model of this mechanism, developmental alcohol is perhaps only the beginning.

Strain	Animal Model	Dose, intake of EtOH (v/v)	Period of Exposure	Age of Cortical Analysis	BEC (mg/dL)	Cortical phenotype	Reference
Wistar Rat	IP	20%, 3.5g/kg /d	E10-18	E18	119-300	Cortical thinning	Aronne et al., 2008
C57 BL6 Mice	SA of EtOH in PMI liquid diet	25%	E7-15	E15	40-120	Cortical thinning	Zhou et al., 2004
CD1 Mice	SA of EtOH in Water	25%, 6.76±0. 25 ml/d	E0.5-19.5	P0	103-138	Reduced cortical length	El Shawa et al., 2013
CD1 Mice	SA of EtOH in Water	25%, 6.55±0. 2 ml/d	E0.5-19.5	P0, P20, P50	100-135	Thickening of the frontal, somatosensory and visual cortex; thinning of prelimbic and auditory cortex (P0)	Abbott et al., 2016
C57 BL6/J Mice	SA of EtOH in PMI liquid diet	4%, 13ml/d	E7-16	E17	120-160	Thinning of the anterior cortex	Current Study

Table 4**.** Summary of cortico-structural alterations induced by alcohol in animal models

Comparison of animal model details and BEC range of different studies examining the prenatal alcohol induced cortical phenotypes. Alc (alcohol); BEC (blood alcohol level); IP (intraperitoneal injection) and SA: self-administered

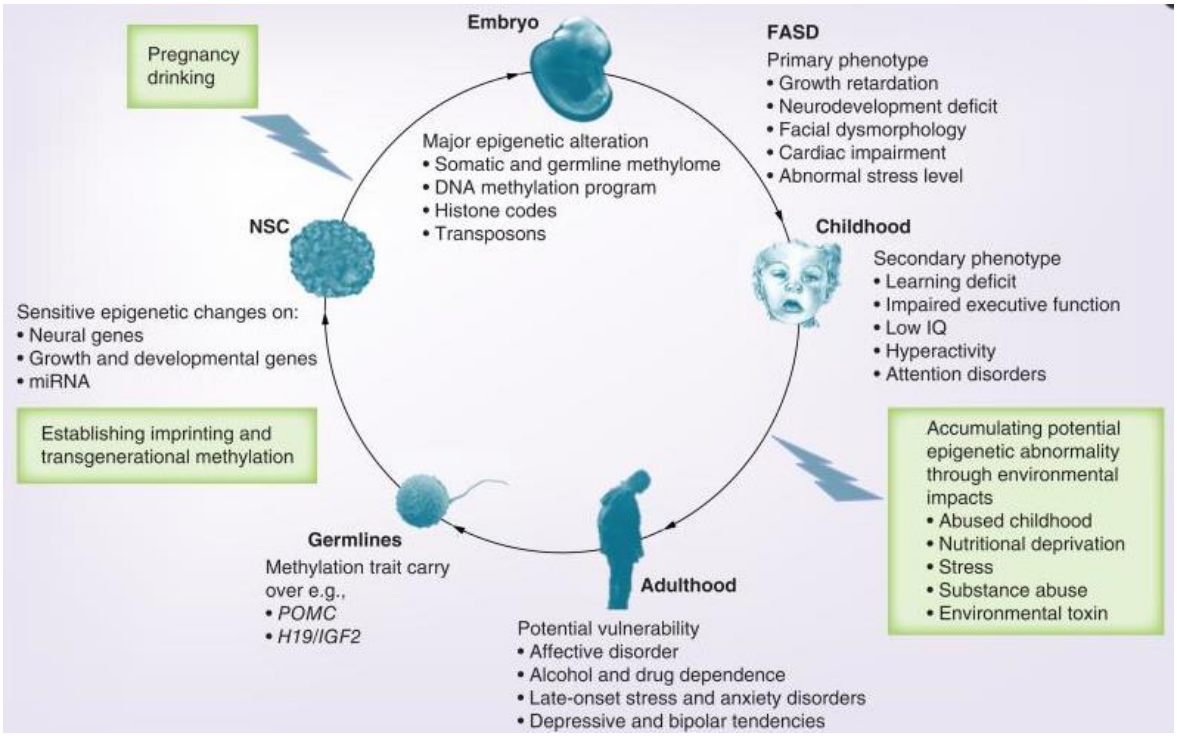

Figure 25. Epigenetic mechanisms and potential manifestations of fetal alcohol spectrum disorders

Maternal alcohol exposure leads to expansive phenotypes of FASD but the mechanisms remain elusive. Besides immediate cellular effects, it is now understood that alcohol extensively alters epigenetics during fetal and NSC development through genomic DNA methylation, cellular DNA methylation programming, histone modification, transposons and miRNA. These epigenetic changes are likely a major upstream disrupter of gene transcription leading to primary phenotypes of FASD (e.g., growth retardation and neurodevelopmental deficit) and collectively compromise brain function and mental faculty as secondary phenotypes in early-life. It is not expected that all epigenetic changes lead to transcriptional and phenotypic changes but increasing evidence suggests that continuous environmental insults may lead to increased epigenetic abnormality. The primary seeding of epigenetic errors and secondary, cumulative epigenetic abnormality via abrasive environment (e.g., childhood abuse and stress) may result in a potential manifestation of FASD beyond the classical diagnosis in adulthood. Moreover, epigenetic errors carried in the germlines may influence the next generations.

CHAPTER 3: THE NORMALIZING CAPACITY OF S-ADENOSYLMETHIONINE SUPPLEMENTATION IN A MOUSE MODEL OF FASD

3.1 INTRODUCTION

3.1.1 Methyl Metabolism in Neural Development

The importance of fetal nutrition has long been acknowledged. Methyl-related nutrition has been particularly scrutinized in neural development. For example, polymorphisms on methionine-metabolism enzymes have been linked with fetal growth impairments (Beaudin, Perry et al. 2012). Additionally, lower serum levels of folate (folic acid) and B12 have been linked with neural tube defects (Kirke, Molloy et al. 1993, Shaw, Schaffer et al. 1995). Recently, Wang et al demonstrated that choline deficiency during gestation led to the reduction of radial glia, intermediate progenitors, and upper layer cortical neurons in the embryonic cortex. This effect persisted up to 4 months in the mouse offspring of choline-deficient dams (Wang, Surzenko et al. 2016). Choline deficiencies can also lead to fetal neuron apoptosis *in vitro* (Yen, Mar et al. 2001) and prenatal choline has demonstrated the ability to alter hippocampal and cortical gene expression (Mellott, Follettie et al. 2007). Unsurprisingly, maternal choline and betaine deficiency have been linked to infantile cognitive impairment (Wu, Dyer et al. 2012). Similar to fetal alcohol exposure and later-life psychosocial disorders, perinatal choline has been correlated with increased risk of schizophrenia in later life (Ross, Hunter et al. 2013). However, the proposition of methyl-metabolism as a unilateral regulator of neural development has been challenged by various studies describing that high levels of dietary methyl precursors can induce hyperhomocysteinemia and negatively impact embryonic

development and cognitive performance (Baydas, Koz et al. 2007, Pickell, Brown et al. 2011, Mikael, Deng et al. 2013).

The mechanisms by which nutritional dysregulation exhibit compound action against neural development are not well known. Previous work has proposed that receptor and transporter deficiency may lie behind nutritionally responsive developmental diseases. Particularly, in neural tube defects, diminished folate transport and disturbance of folate receptors during pregnancy have been associated with increased risk (Cabrera, Shaw et al. 2008, Chen, Yu et al. 2015). Other studies have implicated folate deficiency and increased susceptibility to oxidative stress via ERK activation as mechanisms of neuropathy (Barrera 2012, Kao, Chu et al. 2014). However, due to the parallel phenotypes of methyl insufficiency and surplus, it is likely that the mechanisms governing the methyl metabolism-neural development axis are far more complex.

3.1.2 Nutritional Deficiency and Developmental Epigenetics

Epigenetic mechanisms as mediators of the methyl sensitive-neurodevelopmental pathway have garnered much supporting evidence. Recall that methyl metabolism is a principle component of transmethylation reactions including DNA and histone methylation (Chapter 2, Figure 15). First, genomic studies have revealed variations in susceptibility to methyl insufficiency during development, likely related to genetic variations (Zeisel 2008), which likely impact the epigenome. For example, mutation of the methionine synthase reductase gene (*Mtrr*) has demonstrated transgenerational DNA hypomethylation in liver and uteri, though not in the brain. This differential methylation was positively correlated with phenotype severity (growth restriction, neural tube malformations, etc.) and gene misexpression. Interestingly, in the placenta of wild-type

grandprogeny, differential methylation remained detectable (Padmanabhan, Jia et al. 2013). This study suggests that the sensitivity of a developing system to folate-metabolism is significant and likely mediated in some capacity by epigenetic transmission. Indeed, DNA methylation profiles of nearly 2,000 newborns revealed vast CpG sites that are differentially methylated in response to maternal plasma folate, many of which lie on genes related to birth defects and neurological function (Joubert, den Dekker et al. 2016).

More evidence of epigenetic mechanisms as purveyors of environmental/nutritional impact on the developing neural system comes from deficiency models. For instance, studies of gestational choline deficiency have reported global and gene-specific hypomethylation as well as histone hypomethylation on cell cycle control elements in the fetal hippocampus (Niculescu, Craciunescu et al. 2006, Mehedint, Niculescu et al. 2010). Similarly, a study of neonatal blood from offspring born to mothers of variable folate consumption revealed an inverse correlation between folate and genome-wide DNA methylation, including genes associated with neural crest development and cancer associated genes (Gonseth, Roy et al. 2015). Conversely, a human fetal study of severe neural tube defects in a folic-acid fortified population demonstrated unchanged methylation of genome-wide repetitive elements, indicating that the epigenetic etiology of severe neural dysregulation may be contingent on folate deficiency (Price, Penaherrera et al. 2016).

Just as nutritional deficiency has provided much evidence of epigenetic reprogramming during neural development, supplementation strategies have exhibited an ameliorating potential, reinforcing the contribution of dietary elements like methyl

precursors in regulating the epigenetic landscape during gestation. Substantial evidence exists supporting that daily periconceptional folate supplementation can prevent the incidence of neural tube defects in humans (Tinker, Cogswell et al. 2010, Viswanathan, Treiman et al. 2017). Further, data suggesting that 75% of women of childbearing age in the US do not consume adequate folate have prompted the US Preventative Services Task Force to recommend daily folate supplementation (Viswanathan, Treiman et al. 2017). Maternal supplementation strategies have also manifested ameliorating potential on the epigenetic front. For example, long term folic acid consumption during pregnancy has been associated with increased cord blood DNA methylation (Pauwels, Ghosh et al. 2017). In infants born small for gestational age, umbilical cord blood revealed hypermethylation at six differentially methylated regions in the imprinted H19 gene. However, maternal folic acid supplementation reduced DNA hypermethylation and improved growth outcomes in male offspring (Qian, Huang et al. 2016). Finally, in a rat model of methyl donor deficiency, two micro RNAs and their targets have been previously shown to be upregulated parallel to disrupted brain morphology-outcomes which were reversed by the administration of gestational folic acid supplementation (Geoffroy, Kerek et al. 2016).

It should be noted that dietary elements beyond methyl-contribution have been implicated in epigenetic modulation and neural development. Fetal iron deficiencies, for one, have been linked to chromatin remodeling of the *bdnf* locus in the hippocampus (Tran, Kennedy et al. 2015). Additionally, heat-shock protein induced oxidative damage and associated DNA hypomethylation and histone hyperacetylation in chick embryonic liver was ameliorated in offspring of zinc supplemented mothers (Zhu, Liao et al. 2017).

Equally notable is the evidence that implicates nutritional epigenetics as a mechanism of extra-neural disease etiology, such as cardiovascular disease and cancer (Tobi, Lumey et al. 2009, Loche and Ozanne 2016). Malnutrition or famine in general has also been epigenetically implicated in metabolic syndrome, cardiovascular function and inflammation (Tobi, Lumey et al. 2009, Hernandez-Valero, Rother et al. 2013). Collectively, substantial evidence supports a role for epigenetic mechanisms as regulators of the nutrition-neural developmental axis. While much remains to be understood and clarified about how different methyl donors and other nutritional elements manifest epigenetic modifications, one model of developmental disease etiology offers significant insight.

3.1.3 Alcohol Disruption of Methyl Metabolism During Pregnancy

In Chapter 2, the intersection of alcohol and methyl donor metabolism was introduced. Briefly, alcohol metabolism has been shown to produce reactive oxygen species which inhibit the metabolism of folate, choline, and betaine, dietary methyl donors. Additionally, alcohol and alcohol metabolites have demonstrated inhibitory capacity on various enzymes involved in methyl metabolism (Figure 15). Do the dynamics of alcohol and methyl metabolism persist during pregnancy? Are there unique features during that time? Substantial evidence has elucidated the characteristics of alcohol-induced methyl metabolism dysregulation during gestation. Indeed several studies have reported that plasma methionine concentrations in both dam and fetus are different after gestational alcohol exposure (Hewitt, Knuff et al. 2011, Ngai, Sulistyoningrum et al. 2015). Historically, chronic alcohol consumption has been associated with increased demand for methionine and its subsequent depletion

(Finkelstein, Cello et al. 1974). In a similar vein, methyl metabolism genes in the fetal tissues have also been shown to be sensitive to prenatal alcohol exposure (Ngai, Sulistyoningrum et al. 2015).

In addition to methyl metabolism, alcohol has been shown to interfere with maternal-fetal transmission of methyl metabolic precursors and selectively inhibit the ability of exposed offspring to absorb the nutrients in early life. For example, methionine and folate absorption in the small intestine of the pregnant rat is disrupted by alcohol consumption (Leichter and Lee 1984, Polache, Martin-Algarra et al. 1996, Murillo-Fuentes, Murillo et al. 2003). Maternal-fetal methionine intestinal transport and altered free folate absorption dynamics in the postnatal intestines of alcohol exposed offspring have also been reported (Polache, Martin-Algarra et al. 1996, Tavares, Gomez-Tubio et al. 1999, Hutson, Stade et al. 2012). Finally, folate receptor activity is reportedly decreased by fetal alcohol exposure in offspring rat placenta (Fisher, Inselman et al. 1985).

Recall that both developmental alcohol exposure and nutritional insufficiency have been independently linked to a barrage of neural insults. In light of the various work elucidating the disruptive role of alcohol in methionine metabolism, it is likely that alcohol may work by hijacking maternal-fetal metabolomics, thereby conferring a variety of teratogenic effects. Evidence for this mechanism in neural developmental dysregulation includes parallel alcohol-induced methyl insufficiency and neural deficits. For example, in Xenopus embryos, alcohol exposure compromises neural crest cell migration in tandem with homocysteine accumulation, an indicator of compromised methionine synthesis (Shi, Li et al. 2014). In the postnatal brain of alcohol exposed

offspring, methyl metabolism is observed simultaneously with disrupted mRNA expression of serotonin and glucocorticoid receptors (Ngai, Sulistyoningrum et al. 2015). Fittingly, a recent study identified that deficient choline levels can exacerbate the effects of fetal alcohol on hindlimb coordination, hyperactivity and eye opening (Idrus, Breit et al. 2017). But perhaps the most substantial evidence for the consequential potential of the alcohol-nutrition pathway has come from supplementation studies.

3.1.4 Nutritional Intervention Strategies in FASD

On the premise of alcohol-compromised nutrition, various nutritional supplementation strategies have been attempted to mitigate alcohol phenotypes. Aside from the ameliorating potential of methyl precursor supplementation in alcohol-fed adults (Parlesak, Bode et al. 1998, Barak, Beckenhauer et al. 2003, Kharbanda, Rogers et al. 2005, Bailey, Robinson et al. 2006), various studies have chronicled the developmental impact of supplementation across FASD models, predominantly via methionine, folic acid, betaine, and choline or synthetic variants. Table B-3 (Appendix B) outlines supplementation studies focused on growth anomalies and neurodevelopmental targets. During early gestation, various embryopathic effects, including neurocristopathies, neural tube defects, and embryonic dysmorphologies have been alleviated by developmental supplementation with folic acid (FA), 5-MTHF, and S-AMe, with one study offering that the co-administration of vitamin B12 may further enhance the protective action of the methyl donors (Xu, Li et al. 2006). However, in a few of these acute paradigms, supplementation was unsuccessful as a preventative strategy against neural tube defects and some embryonic growth deficits (Graham and Ferm 1985, Padmanabhan, Ibrahim et al. 2002).

Across supplementation studies performed in chronic alcohol exposure models (predominantly rodent), the protective capacity of methyl-donor supplementation included cortical neuroapoptosis, neurodegeneration, microcephaly, and growth deficits, though in one study, embryopathies were not prevented by methionine+zinc supplementation (Seyoum and Persaud 1997) and in others, gross body/brain weights and other malformations were similarly unaffected (Downing, Johnson et al. 2011, Hewitt, Knuff et al. 2011). Various postnatal and human studies have focused on the behavioral outcomes of methyl supplementation in FASD models. While the literature is rarely unanimous on any given measure, methyl donor supplementation alleviates alcohol-induced deficits in learning, memory, hyperactivity, and balance and coordination. On the other hand, across all examined studies, locomotor and global cognitive measures have consistently lacked a neuroprotective response (Thomas, Garrison et al. 2004, Coles, Kable et al. 2015, Wozniak, Fuglestad et al. 2015, Nguyen, Risbud et al. 2016).

Factors to consider when evaluating previous studies and contrasting outcomes include the dose and time of alcohol exposure, the methyl supplement format and the intervention period. For example, some studies administer methyl donor cocktails (Downing, Johnson et al. 2011, Sogut, Uysal et al. 2017) while others have experimented with methionine, betaine, or 5-MTHF. By far, the majority of animal and human studies have focused on folic acid and choline supplementation. Additionally, some studies pre-treat with methyl supplements, others are delivered simultaneously with alcohol, and a majority of human interventions are delivered mid-gestation or even post-ethanol exposure. Finally, the current body of literature is made up of varying doses of methyl supplements and it is not yet known how this factor impacts experimental outcomes.

3.1.5 Neural Targets for Intervention in the FASD Cortex

Beyond the tissue-wide and functional outcomes that have been continually investigated and observed in FASD models, the field of FASD intervention has, along with technology, advanced toward an era of gene targeting in intervention strategies. The advent of genomic editing tools like CRISPR/Cas9 and transcription activator-like effectors (TALENS) has equipped experimenters with the tools for the precise investigation and manipulation of disease-related targets. As such, now more than ever there is a need to shed light on the specific drivers of alcohol teratogenicity. In the cortex, vulnerability to alcohol has been demonstrated across a multitude of targets.

Compromised cell proliferation in both neurons and glia has been observed in prenatal alcohol models (Chikhladze, Ramishvili et al. 2011, Huang, He et al. 2015) and further study has elucidated possible gene targets involved in cell cycle regulation including cdcs, various cyclins, *Mcm5, Plk1, E2f7* and *Bub1*. Notably, a handful of these targets have shown alcohol-induced hypermethylation at their promoter (Hicks, Lewis et al. 2012). Prenatal alcohol has also demonstrated inhibitory action on the proper specification of radial glial cells, precursors of intermediate progenitors and mature cortical neurons. Investigation of many of the genes conferring these processes has similarly revealed alcohol-sensitivity, including the early glial pathway genes *notch, nestin, wnt,* and *Pax6* in the cerebral cortex (Aronne, Evrard et al. 2008, Hashimoto-Torii, Kawasawa et al. 2011).

The aberrant effects of gestational alcohol on cortical migration have been identified including the tangential migration of GABAergic interneurons and the radial migration of cortical progenitors (Cuzon, Yeh et al. 2008, Aronne, Guadagnoli et al.

2011). Migration-associated gene targets implicated in prenatal alcohol studies include the heat shock factor 2 (HSF2)-binding genes *p35, Dclk1*, and *Dcx* (El Fatimy, Miozzo et al. 2014). *Ex-vivo* models have also identified the TGFß pathway as a target of alcohol during neuronal migration (Siegenthaler and Miller 2004). The inhibitory effects of alcohol on cortical specification may be attributed to the downregulation of genes like *Tbr2*, an important regulator of upper cortical layer specification (Riar, Narasimhan et al. 2016). Interestingly, other independent genomic screens have similarly identified a variety of cortical specification genes, some of which are intricately connected to the Tbr domain. For example, *Satb2, Bhlhb5, Id2, Nr4a3, Foxp1, Pou3f2, Ctip2,* and *Crym* have all been demonstrably downregulated in an FASD model (Hashimoto-Torii, Kawasawa et al. 2011). Finally, the effects of fetal alcohol exposure have been observed in the late-specification of cortical neurons as well, with downregulation of synaptic targets like *Nr2b, GluR1, Cb1r,* and the adenosine A1 receptor (Bellinger, Davidson et al. 2002, Othman, Legare et al. 2002, Toso, Poggi et al. 2005, Subbanna, Shivakumar et al. 2013). Surprisingly, while the majority of reports describe alcohol-related inhibition of synaptic profiles, some synaptic targets of alcohol appear to be upregulated by prenatal alcohol exposure (Marutha Ravindran and Ticku 2004, Toso, Poggi et al. 2005, Kleiber, Diehl et al. 2014). From cell cycle exit to receptor distribution on the pre and post-synaptic terminals of a cortical neuron, various elements are targeted by prenatal alcohol, likely setting the tone for the hallmark cognitive, intellectual, and behavioral maladaptation observed commonly in FASD. A concrete understanding of the alcohol-sensitive gene networks and their dynamics is an important first step to remediation strategies, including nutritional supplementation therapies. Likewise, characterizing genomic regions critical

to cortico-development and function may offer molecular parameters for the evaluation of disease and therapeutic response. Ultimately, the profiling of important alcohol-targets in the developing brain is necessary for gene-targeting strategies such as genetic and epigenetic editing in the future.

3.1.6 Research Aims

A unique feature of methyl supplementation studies in developmental alcohol models is the parallel execution of pre-clinical and clinical investigation. The dietary nature of methyl donors and their high feasibility and tolerability in humans (Wozniak, Fuglestad et al. 2013) allows for the potentially rapid pace of clinical trials and data acquisition. On the other hand, while human trials are offering a wealth of behavioral information on the protective action of methyl donors, a gap in our understanding of the molecular drivers of methyl neuroprotection still exists. This prompts the need for pre-clinical investigation of the underlying mechanisms regulating the developmental output of converging alcohol-nutritive pathways.

Some studies have reported that one way methyl supplementation may counter perinatal alcohol exposure is through the improved intestinal absorption of dietary co-factors like zinc (Tavares, Carreras et al. 2000). And while supplementation does not appear to restore alcohol-restricted absorption of methyl donors, one study found that Selenium+Folic Acid supplementation in a fetal alcohol model enhanced the transporters for their respective substrates in the duodenal mucosa (Nogales, Ojeda et al. 2011). As described in Chapter 2, the biochemical proximity of methyl metabolism to DNA methylation and the previous demonstration of DNA methylation as a developmental regulator beckon the examination of epigenetic mechanisms as mediators of supplemental

neuroprotection. Despite this, to-date, very few alcohol+supplementation studies have characterized epigenetic changes.

What has been reported thus far includes the capacity of choline to remediate region-wide hypermethylation in the hippocampus, though not in the medial prefrontal cortex (Otero, Thomas et al. 2012). Normalization of gene-specific hypermethylation has additionally been reported on the *POMC* gene of adult male offspring (Bekdash, Zhang et al. 2013) and in the *Igf2* gene (Downing, Johnson et al. 2011). Beyond methylation, methyl supplementation has also been shown to normalize repressive histone marks, methyltransferase and methyl binding protein expression, and microRNA expression (Wang, Zhang et al. 2009, Bekdash, Zhang et al. 2013). An important structure for cognition, mobility, and higher order function, the effects of methyl supplementation in the embryonic cortex have not been extensively characterized nor examined through an epigenetic lens. Here, we aimed to establish the dynamics of epigenetic environmental sensitivity through methionine supplementation in a model of fetal alcohol exposure. Using S-adenosylmethionine (S-AMe), which is the active methyl donor for DNA and histone methylation reactions, we hypothesized that supplementation during chronic gestational exposure would exhibit neuroprotective action, possibly conferred through the stabilization of the previously described aberrant cortical DNA methylation program.

3.2 MATERIALS AND METHODS

3.2.1 Overview of Experimental Treatments

In this study, alcohol was administered via liquid diet according to the paradigm illustrated in Figure 26. Mice were acclimated to animal housing conditions one week prior to mating. After conception, the liquid diet was introduced from E5-E6 and experimental treatment was administered from E7-E16 (reflecting the late first and second human trimester equivalent). The 4% alcohol liquid diet (v/v) administered in this paradigm has been previously published in previous and parallel studies to reach a range of blood ethanol concentration (BEC) of 100-200 mg/dL (Anthony, Vinci-Booher et al. 2010, Chen, Ozturk et al. 2013). Briefly, six non-pregnant females receiving 4% v/v alcohol liquid diet were used for BEC analysis. Blood samples were collected via tail vein bleeding method 2 hrs or 6 hrs after the administration of fresh alcohol-PMI diet. Collections were made 2, 4, and 6 days during the course of treatment, alternating between animals so as to provide at least 48 hours between tail bleeds. Adequate volumes of blood (15 µl) were collected in heparinized tubes, and plasma was isolated through centrifugation and stored at -80°C prior to analysis with a Gas Chromatograph (GC, Agilent Technologies; model 6890). Each sample was analyzed in duplicate. A previous fetal alcohol liquid diet study in gestating C57BL/6 mice with identical doses of S-adenosylmethionine administration (10mM) showed that the treatment was well-tolerated by pregnant females and did not interfere with alcohol metabolism or BECs levels (Gauthier, Ping et al. 2010). Similar studies of choline supplementation have echoed that dietary supplementation does not alter peak BEC or interfere with alcohol metabolism (Thomas, Abou et al. 2009).

3.2.2 Animals and Treatments

All mice were used in accordance with National Institute of Health and Indiana University Animal Care and Use (IACUC) guidelines. The protocol was approved by the Laboratory Animal Resource Center (LARC) animal ethics committee of Indiana University. C57BL/6 (B6) (10–14 weeks old, ~20 g body weight) nulliparous female mice (Jackson Labs, Bar Harbor, ME) were used in the study. Mouse breeders were individually housed upon arrival and acclimated for at least one week prior to mating. The mice were maintained on a 12 hr reverse light-dark cycle (lights on: 22:00–10:00) and provided laboratory chow and water *ad libitum*. Mice were then randomly assigned into five treatment groups for E17 study: Chow, Pair-Fed (PF), Alcohol (Alc), Alcohol + S-AMe (Alc+S-AMe), and S-AMe *ad libitum* (S-AMe). Each litter was considered N=1; the littermates of each dam were distributed among the various analyses performed in this study. Chow, PF, Alc, and Alc+S-AMe groups were additionally treated for postnatal day (P) 7 analysis, including N≤5 litters per group. Due to the developmental and epigenetic similarity of the S-AMe control group to the Chow and PF control groups, the group was not included in the P7 analysis.

Females were bred with male breeders for a 2-hr period (10:00 to 12:00). All animals were mated daily over a period of no more than 3 weeks, at which time all animals were on *ad libitum* chow and water diets. The presence of a vaginal plug at the end of the 2-hr mating session was considered as indicative of conceptus and that hour was designated as hour 0, and embryonic day (E) 0. A liquid diet paradigm was modified from a previously detailed study (Chen, Ozturk et al. 2013). Briefly, all alcohol treatment groups received 4% alcohol v/v in liquid diet (Purina Micro-Stabilized Diet (PMI),

Purina Mills Inc., Richmond, Indiana) as instructed by supplier with 4% w/v sucrose added, and administered using 35 ml drinking tube (Dyets Inc., NY). The PF group was given the PMI diet mixture with the addition of maltose dextran (MD) (to substitute alcohol calories). The volume of the PF diet was restricted to that of a dam paired from the alcohol group throughout the course of treatment. The addition of a S-AMe supplemented group (Alc+S-AMe) and S-AMe control was included in this study. The Alc+S-AMe group was administered the 4% alcohol PMI diet as described above, with the daily addition of powdered S-AMe (10mM, Nature Made, Mission Hills CA). A S-AMe control group was also included, administered via daily unrestricted isocaloric PF diet supplemented with 10mM S-AMe. Finally, the Chow group was maintained on a standard chow diet and water *ad libitum* throughout gestation. On E5, pregnant dams in PF, Alc, Alc+SAM, and S-AMe groups were placed on an unrestricted PF liquid diet for a 48 hour acclimation to the liquid diet. Experimental treatment was initiated according to the designated regimen on E7 through the end of E16. After E16, all dams were returned to standard lab chow and water *ad libitum*. For postnatal litters, dams were allowed to give birth, designated postnatal (P) day 0. Approximately six hours after parturition, experimental litters (PF, Alc, and Alc+S-AMe) were switched to be nursed by surrogate Chow-fed dams until harvest on P7. Surrogate dams had previously given birth no more than 48 hours prior to experimental litter births. During surrogacy, litters were randomly culled to six pups/litter in order to decrease possible nutritional deficiencies caused by within-litter competition.

3.2.3 Embryo Isolation and Tissue Preparation

Dams were placed under deep CO2 euthanasia until completely sedated and embryos were harvested from dams at E17 by removal from the embryonic sack. P7 pups were weighed and immediately decapitated. Each embryo/pup was either immersion-fixed in 20 ml of fixative prepared from 4% paraformaldehyde (PFA) for immunohistochemistry, flash frozen in liquid nitrogen, or preserved in RNA later (25mM sodium citrate, 10mM EDTA, 70g ammonium sulfate/100mL solution, pH 5.2).

3.2.4 Immunohistochemistry

Fixed embryos were subsequently weighed, dissected for brain tissue, and assessed for brain weight no more than 48 hours after fixation. Brains taken from each group were embedded in a single 10% gelatin block with careful rostrocaudal and dorsoventral alignments. Gelatin blocks were fixed in 4% PFA for 48 hrs and sectioned in 40 mm thick coronal sections on a floating vibratome (Leica Microsystems; Buffalo Grove, IL). For P7, section-pairs (Chow-PF or Alc-Alc+S-AMe) were processed equally across all immunohistochemical procedures. For all immunohistochemical experiments, sections were cleared of endogenous peroxidases using 3% H_2O_2 in phosphate buffered saline (PBS) for 10 min and permeabilized with 1% TritonX-100 in PBS for 30 min (overnight for Vglut1). For nuclear proteins, an additional 30 min incubation in 2N HCl was performed. Sections were subsequently blocked in species-specific normal serum for 60 min prior to primary antibody incubation. Antibodies used are summarized in Table 5 below. Primary antibodies were diluted in normal serum according to the following dilutions and incubations in primary antibody varied from 18-24 hours at room temperature. Subsequently, sections were incubated for 90 min in biotinylated secondary

antibodies (Jackson ImmunoResearch, West Grove, PA) followed by incubation in Streptavidin-AP (1:500, Jackson ImmunoResearch, West Grove, PA) or Universal Peroxidase ABC HRP Kit (Vector Laboratories, Burlingame, CA) for 90 min. The immunostaining was visualized by incubation in 0.05% 3,3'-diaminobenzidine (DAB) for 15 min, followed by chromagen activation by 0.03% H_2O_2 over a range of of 3-8 minutes. Sections were rinsed and mounted on glass slides followed by counterstaining with methyl green (0.05%, Sigma Aldrich, St. Louis, MO). All stainings were analyzed under light microscopy for cellular analysis using a Leica DM 6000B microscope (Leica Microsystems, Wetzlar, Germany).

Table 5. Antibodies used for neurodevelopmental and DNA methylation assessment in the S-AMe supplemented E17 cortex

Primary Antibodies	**Company**	**Catalog #**	**dilution**	**predicted wt.**
5-methylcytosine	Eurogentec	BI-MECY-0100	1:2000	N/A
5-methylcytosine	Active Motif	AM61255	1:2000	N/A
5-hydroxymethylcytosine	Active Motif	AM39769	1:3000	N/A
Ki67	Novus Biologicals	NB110-89717	1:500	324 kDa
Tbr2	Millipore	AB2283	1:500	58 kDa
NeuN	Cell Signaling Tech.	D3S3I	1:500	46-55 kDa
Vglut1	Millipore	AB5905	1:1000	~62 kDa
Fezf2	ImmunoBiological Labs	18997-S	1:100	~65 kDa
Secondary Antibodies				
Goat anti Rabbit biotinylated	Jackson ImmunoResearch	111-065-003	1:500	~160 kDa
Horse anti Mouse biotinylated	Vector Laboratories	BA-2000	1:500	~152-165 kDa
Donkey anti Guinea Pig biotinylated	Vector Laboratories	BA-7000	1:500	~152-165 kDa

3.2.5 Densitometry analysis (H score) and cortical thickness assessment

Epigenetically immunostained nuclei exhibited a variable staining profile within different cortical layers. In order to reflect this heterogeneity, we employed H scoring as a strategy for nuclear densitometric analysis (Singh, Shiue et al. 2009, Chen, Ozturk et al. 2013) of each cell within the selected cortical subregion (VZ+SVZ, SP, and CP).

Images of immunostained sections were taken using a Leica CTR 6000 camera and Leica Firecam Software Version 1.7.1 (Leica Microsystems, Wetzlar, Germany). Bright-field images were taken with consistent acquisition settings between sections for each antibody analyzed. Images were converted to the 16-bit color format, and staining intensity was assessed using Image J (National Institutes of Health, Bethesda, MD). Calibration was set based on 256 levels of the gray scale. To measure the sub regions of prefrontal neocortex, a rectangular box of equal dimensions (150 μm in width) was selected at the S-AMe rostro-caudal level of E17 coronal brain sections. Lateral ventricle and corpus callosum were used as landmarks to align the prefrontal cortex across all groups. Equal amounts of cells were randomly sampled within the designated dimensions per group. The intensity of the staining in each selected cell was measured on a black-white scale (0-256). These absolute intensity values were subsequently classified based on the optical density (OD) values according to the following guidelines: Absent-0-(OD=256-206), Weak-1-(OD=206-156), Moderate-2-(OD=156-106) and High-3-(OD=106-56). Overall, the immunohistochemical H score of each subcortical region was obtained by the following formula: 3 X percentage of highly stained nuclei + 2 X percentage of moderately stained nuclei + percentage of weekly stained nuclei.

Cortical thickness was assessed using two independent immunostainings: NeuN and 5mC. Anterior sections of the frontal cortex were rostro-caudally matched between groups and selected for cortical measurements. ImageJ software was used to assess cortical thickness (measured from the base of the SVZ to the edge of the MZ). Subsequently, individual cortical layers were measured (layers were clearly demarcated by cortical cytoarchitecture). For P7 analysis, a similar process was used, modified to include multiple cortical subdivisions including: cingulate cortex, primary motor cortex, secondary motor cortex, primary sensorimotor cortex, and forelimb/hindbrain sensorimotor cortex. P7 layer measurements were also taken across layer I, layers II-IV, layer V, and layer VI.

3.2.6 Cell Counting and Morphometric Analyses

Automated cell counts were used to detect cells positive for Ki67 due to the presentation of the immunosignal being punctate and homogenous. In this experiment, sections stained for Ki67 were processed using Image J software according to the following protocol: color deconvolution plugin was used to isolate the brown DAB signal, images were inverted to 8-bit, automated thresholding was performed, and automated particle analysis was performed on the SVZ/VZ region with the selection parameters set to 0.25-1.0 circularity (where 1.0 equals a perfect circle) and size inclusion being 50-600 (pixel^2). Results were presented as number of particles (cells) detected per sample ±SEM.

To assess cell density, cortical sections from 5mC staining procedures were counterstained by Methyl-Green dye (Nissl) which allowed for the visualization of 5mC positive as well as 5mC negative nuclei. After Brightfield imaging under a light

microscope (see "Densitometry analysis and cortical thickness assessment"), a select region targeting the mid cortical plate was binned ($0.025mm^2$) across all brain sections at a high magnification. Nuclei were counted using the multi-point counting tool on ImageJ software (NIH, Bethesda MA). At least two sections taken from the anterior cortex of each subject were averaged for total nuclei/area. Additionally, at least two subjects from each litter were represented in the assessment (where *n*=litter).

A similar procedure was used to analyze nuclear morphology. Due to the non-circularity of some cortical cells, the major and minor axes of each nuclei were measured across the anterior CP. In some cases, where nuclei were quite circular, the nuclei length and diameter were arbitrarily selected and interchangeable. In cases of non-circular morphology, the major (longest) and minor (perpendicular to major) axis were clearly distinct and thus represented independently. A straight line tool was used in all cases to measure the major and minor axes of the nuclei. Finally, nuclear area was calculated based on the following equations: circular area=πr^2 (where r=minor axis/2) and ellipse area=πab (where a=minor axis/2, b=major axis/2). Distinction between circular and non-circular nuclei was made if major axis was ≥1.5 times the minor axis. At least 100 nuclei from the selected region were measured per cortical section and at least two sections per subject were represented in the average. Each N represents one litter in these assessments. To help minimize experimenter bias, images were randomly examined, meaning, experimental groups were not evaluated as continuous cohorts throughout the imaging session.

3.2.7 Global DNA Methylation Analysis

Fetal brains were isolated and microdissected under a Dissection Microscope (Leica MZ6, Leica Microsystems). Neocortical brain tissues were separated from subcortical brain tissue using the borders of the nascent internal capsule as a visual guide. DNA extraction and purification was subsequently performed using silica-based spin-column purification (DNeasy Blood and Tissue kit, Qiagen) according to manufacturer's instructions. Purified DNA was quantified by spectrophotometric absorption at 230, 260, and 280nm and the quality and concentration was calculated as the A_{260}/A_{230} and A_{260}/A_{280} ratio (Nanodrop 2000, Thermo Scientific). An average of 100-200 ng of genomic DNA was used for DNA global methylation analysis performed with the MethylFlash Methylated DNA Quantification Kit and MethylFlash Hydroxymethylated DNA Quantification Kit (Colorimetric; Epigentek Group) according to the manufacturer's instructions. OD values were determined using a PHERAstar FSX microplate reader and MARS Data Analysis Software (BMG Labtech, Cary, NC). Methylation levels were estimated using a standard curve of methylated DNA standards provided by the manufacturer. Relative methylation (percent of total DNA) was calculated according to the following calculations:

5-mC%=(sample OD-neg control OD)/(slope of the standard curve*input DNA (ng))*100%

5-hmC%= ((sample OD-neg control OD)/(slope of standard curve*5))/input DNA (ng)*100%

Global methylation data were presented as percent of control group values.

3.2.8 Gene Expression Analysis

RNA was extracted from cortical tissue by RNA extraction kit (RNeasy Mini Kit, Qiagen Valencia, CA) according to manufacturer's instructions. One microgram of cortical RNA was converted to cDNA using the High Capacity Reverse Transcription Kit (Applied Biosystems, Foster City CA). Next, 100ng of cDNA was loaded per reaction and at least three reactions were examined per gene expression assay per sample. Taqman PCR Master Mix was used with Taqman Probes (Applied Biosystems, Foster City CA) for an array of neurodevelopmental genes (Table B-4, Appendix B). Relative expression was calculated according to the [delta] [delta] Ct method, using the ubiquitous ribosomal gene 18S as an internal control. Reactions were performed on AB Step One Plus Real Time PCR System (Applied Biosystems, Foster City CA).

3.2.9 Methyl-CpG Pyrosequencing

Site-specific methylation analysis was performed using Pyromark Q24 CpG Assay (Qiagen, Valencia, CA). One microgram of gDNA was bisulfite treated using Zymo's EZ DNA Methylation Gold kit (Zymo, Irvine CA). Two microliters of the bisulfite-converted DNA was next used as input for pyro-PCR using custom oligos (IDT, Coralville IA) or commercial Pyromark CpG Assays (Table B-4, Appendix B) using Pyromark PCR Kit (Qiagen, Valencia, CA). Once PCR product was confirmed by gel electrophoresis, 20uL of PCR Product was incubated with CpG Assay reagents and sequenced using Pyromark Q24 Workstation (Qiagen, Valencia, CA). PROMO transcription factor prediction software was used to generate predicted transcription factor binding sites within the analyzed sequence of the gene (Messeguer et al 2002). Control oligo was used as a positive control in all assays. Percent methylation of all CpGs

in the sequence as well as cumulative methylation was presented within each of the differentially methylated regions (DMR) investigated.

3.2.10 Statistical Analysis

IBM SPSS Statistical software (Version 24) was used to perform all statistical analyses. Comparison of group means was performed by one-way ANOVA, with Welch's correction when groups violated the homogeneity of means test (assessed by Levene's Test of equality of variances). Where statistical significance was observed ($P \geq 0.05$), either Tukey's HSD (ANOVA) or Games-Howell (Welch's) post-hoc analysis was carried out. All data are presented as means± standard error of the mean (SEM). All birth data were presented as litter averages to account for litter size effects. Across all experiments, sample size (n) denotes the number of represented litters within each group. A detailed summary of statistics is provided for all quantitative assessments in Table B-5, Appendix B.

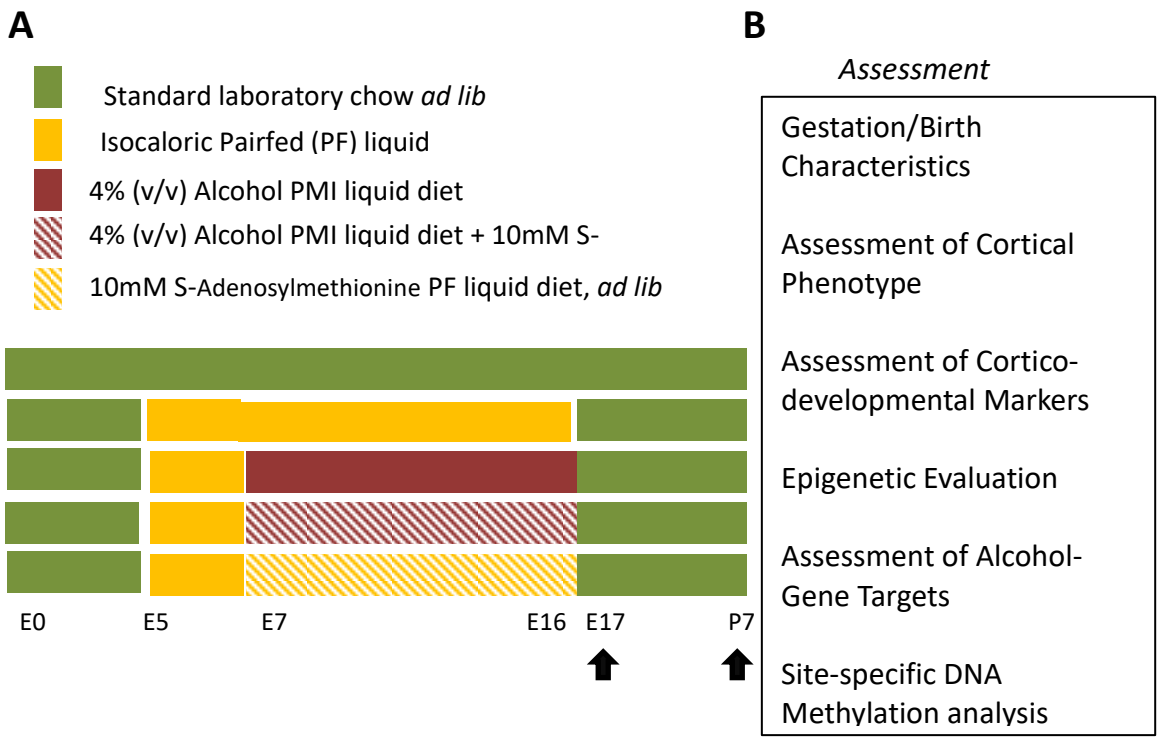

Figure 26. Experimental paradigm for fetal alcohol and S-adenosylmethionine supplementation
(A) Representative scheme of experimental treatment paradigm. Conception was designated as embryonic (E) day 0. Liquid diet acclimation was initiated on E5 and experimental treatments were integrated into liquid diet from E7-E16. Pairfed (PF) groups were calorically matched to Alcohol and Alc+S-AMe groups by volumetric restriction to PF diet (alcohol calories supplemented by maltose dextran). All liquid diet treatments were terminated on E17 and dams were returned to standard lab diet on that day. Harvests were performed on E17 or P7 (arrows). (B) Experimental workflow included analyses performed across each of the listed categories at the E17 stage.

3.3 RESULTS

3.3.1 Gestation and Fetal Characteristics

Maternal weight and alcohol intake was monitored daily throughout the course of this study as alcohol exposure reportedly impacts appetite and feeding behaviors (Kokavec 2008). Due to the use of a liquid diet model, combining alcohol administration with daily nutrition, alcohol-induced loss of appetite could be severely detrimental. However, we report that gestational weight gain was overall unchanged by experimental treatment. Moreover, gestational consumption of the experimental liquid diets was comparative to nutritional control levels, averaging around 13mL/day (Figure 27 B). Finally, because alcohol and alcohol+S-AMe groups were unrestricted in their daily access to the diet, we evaluated whether the two alcohol-administered groups consumed different amounts of diet (alcohol) throughout gestation. There were no observed differences in the consumed liquid diet across the two-alcohol receiving groups on either day throughout gestation (Figure 27C) indicating that both Alc and Alc+S-AMe dams ingested equivalent amounts of alcohol daily. These levels of alcohol consumption have been previously shown in our lab to produce blood ethanol content (BECs) around 120-160 mg/dL (Anthony, Vinci-Booher et al. 2010, Chen, Ozturk et al. 2013). Additionally, several methyl-supplementation studies have determined that the supplementation of an alcohol diet with 10mM S-adenosylmethionine does not alter the BEC of a dam (Gauthier, Ping et al. 2010).

Next we examined the fetal characteristics of the experimental litters across all groups. Alcohol-exposed fetuses demonstrated a significant decrease in body weight at E17 (Figure 28A, $P<0.001$). S-AMe supplemented fetuses also showed a decreased body

weight compared to Chow and S-AMe controls. However, no intergroup differences were found in fetal brain weight. To examine whether deficits in body weight persisted beyond the exposure timeframe, we evaluated pup body weights at postnatal day 7. No group differences were detectable by P7, in either body or brain weight (Figure 28 C-D). These findings are consistent with the notion that body weight impacts are typically observed in high dose alcohol studies rather than low dose studies (such as our own) (Abel 1996). Finally, neither alcohol nor S-AMe treatment affected the average number of pups/litter.

To evaluate the effect of prenatal alcohol on methyl metabolism in our model, we examined the expression of the S-AMe-producing enzyme methionine adenosyltransferase 2A (*Mat2a*) in the liver and brain. In the fetal liver, the *Mat2a* gene expression was significantly decreased by maternal alcohol treatment (Figure 29A, $P<0.0001$), consistent with previous reports (Ngai, Sulistyoningrum et al. 2015). Here we observed that S-AMe supplementation of the alcohol diet normalized liver *Mat2a* to levels comparable to controls. Interestingly, unrestricted S-AMe access (no alcohol) expressed the highest level of the transcript, indicating that methyl supplementation does not diminish the expression of *Mat2a* rather increases it. In the brain, the sensitivity of the gene to alcohol exposure was absent, on the other hand, the sensitivity of the cortical tissue to S-AMe persisted beyond the liver, where a majority of alcohol and methyl metabolism occurs. The findings suggest that at the gene level, fetal alcohol's influence on methyl metabolism may be limited to the fetal liver, unlike S-AMe supplementation, which exhibits a more dynamic range.

To further examine whether alcohol or S-AMe supplementation impacted the DNA methylation products 5mC and 5hmC, whole tissue DNA was quantitatively

assessed using an immuno-absorbance assay. While both the liver and cortex were sensitive to alcohol exposure and exhibited decreased 5mC consistent with diminished S-AMe production (Figure 29C, cort P=0.05; liver P= 0.028), Alc+S-AMe treatment did not produce a significantly different outcome. However, the trend of the S-AMe supplemented alcohol group was such that they were not statistically significant from control groups. Notably, though the unrestricted S-AMe nutritional control exhibited higher than normal *Mat2a* in the liver and brain, expression of 5mC was comparable to Chow and Pairfed controls (Figure 29C). Finally, quantitation of 5hmC revealed no changes across groups in either liver or cortical tissue (Figure 29D). These results confirm the sensitivity of methyl metabolism to fetal alcohol exposure in our paradigm and illuminate the sensitivity of the liver and cortex to S-AMe supplementation. Finally, our results echo previous findings of global DNA methylation patterns (Figure 23) and place the effects of methyl-supplementation into perspective on a tissue-wide scale.

3.3.2 Role of S-AMe supplementation as a Cortical Neuroprotector

To interrogate whether S-AMe supplementation of the fetal alcohol exposure paradigm could abrogate the growth deficits of alcohol on the embryonic cortex, we examined the phenotypic characteristics on a structural, molecular, and genomic level. First and foremost, we evaluated whether methyl-supplementation via the active methyl donor S-AMe could normalize one of the prominent FASD features previously observed in our experimental model-cortical thinning. Recall in Chapter 2 that fetal alcohol exposure dramatically reduced the length of the embryonic cortical column. Here, we used identical metrics and 1) confirmed the cortical thinning phenotype in a second cohort of E17 fetuses, 2) observed the normalizing potential of S-AMe supplementation

(Figure 30A, $P<0.004$), and 3) describe that normalization of the cortical structure is preserved beyond the window of intervention, postnatally at the vulnerable sensorimotor cortex (Figure 30B, $P=0.001$).

As a secondary measure of cellular growth and to examine (as in Chapter 2) whether differing cellular densities were at least partial contributors to our observations of alcohol-induced cortical thinning and neuroprotection by S-AMe supplementation, we quantified all cells present in a representative fraction of the cortical plate and report no differences in total cell number across all groups (Figure 31A). While neither alcohol nor S-AMe impacted cell densities in the E17 cortical plate, nuclear size was found to be significantly decreased by prenatal alcohol exposure, an effect mitigated significantly by S-AMe supplementation (Figure 31B, $P<0.0001$). Our findings echo the observations made in Chapter 2 and expand upon the neuroprotective contributions of S-AMe supplementation toward the preservation of nuclear area which may greatly contribute to cortical plate size.

Layer-specific analysis further revealed that nearly all cortical layers of the E17 cortex were negatively impacted by alcohol exposure. At the P7 stage, the alcohol-sensitivity of the sensorimotor cortex appears relegated to layers II-IV and VI. Similarly, while the normalizing capacity of Alc+S-AMe occurs in the SP and MZ at E17, it is restricted to the VI layer postnatally (Figure A-1, Appendix A). Regardless, total cortical thickness trends are echoed at least one week after birth. These results elucidate the persistent sensitivity of the cortex to gestational alcohol exposure and are the first to describe that S-AMe supplementation can protect against alcohol-induced cortical thinning in a lasting manner.

To corroborate the structural findings of our experimental paradigm at a molecular level, various critical processes of cortical maturation and expansion were investigated. First, cellular proliferation was examined at the neurogenic zones of the cortex, the SVZ/VZ. Immunohistochemical detection of Ki67+ nuclei was performed and an automated cell counting tool was used to determine whether alcohol and/or S-AMe impacted the number of Ki67+ nuclei. We found that alcohol significantly decreased the number of Ki67+ nuclei, indicative of reduced proliferation of cortical progenitors and radial glial in the SVZ/VZ (Figure 32B, P=0.036), though the transcript for Ki67 was not significantly altered by either treatment. S-AMe supplementation did not exhibit significantly higher Ki67+ nuclei compared to the alcohol group however, it did not significantly differ from controls. These findings support our previous observation that alcohol reduces cortical proliferation but suggests that S-AMe supplementation may play a limited role in neurogenic proliferation.

A prominent regulator of intermediate progenitor conversion in the cortex, the transcription factor Tbr2 has been often used as a tool in the identification of cortical projection neuron precursors (Kowalczyk, Pontious et al. 2009). Previously, alcohol exposure has been shown to induce cytostasis of Tbr2+ populations, likely hindering the symmetric division of cortical precursors (Riar, Narasimhan et al. 2016). Interestingly, Tbr2 deletion produces microcephaly-a hallmark feature of FASD (Baala, Briault et al. 2007). Here we examined Tbr2 nuclei and fibers across the SVZ/VZ, IZ, and CP. Using immunohistochemistry we quantitatively assessed the number of Tbr2+ nuclei and found that alcohol exposure significantly decreased the detectable Tbr2+ nuclei in the IZ and CP (Figure 33B, IZ P=0.015; CP P=0.016), though not the SVZ/VZ as a previous fetal

alcohol report has shown (Hashimoto-Torii, Kawasawa et al. 2011). Further, though S-AMe supplementation was not significantly neuroprotective of Tbr2 in the CP, it demonstrated ameliorating potential in the IZ, where migrating intermediate progenitors are most concentrated (Vasistha, Garcia-Moreno et al. 2015). Despite the proteomic observations, an assessment of *Tbr2* mRNA in the cortex did not demonstrate either alcohol or S-AMe sensitivity (Figure 33C).

A frequent marker of neuronal maturity, NeuN is expressed in the nuclei of post-mitotic (committed) neurons. Due to the well-demonstrated growth-inhibitory nature of alcohol on neurons, we investigated alcohol and S-AMe supplementation's effects on the expression of NeuN in the embryonic cortex. As shown in Figure 34, alcohol significantly decreased NeuN in the upper cortical layers (SP, CP), where neuronal maturity is most advanced. This finding corroborates several previous reports (Powrozek and Zhou 2005, Teixeira, Santana et al. 2014). Though the gene encoding NeuN (*Rbfox3*) does not change in reaction to alcohol or S-AMe at E17, we did observe that S-AMe normalized the expression of NeuN protein in the SP and CP (Figure 34C-D, SP $P=0.035$; CP $P= \leq 0.0001$).

Finally, to round out our phenotypic assessment of the molecular drivers of cortical development, we examined the expression of a presynaptic protein which plays an important role in glutamate transport and is expressed in neuron-rich regions. Vesicular glutamate transporter 1 (Vglut1) is a vesicle-bound, sodium-dependent phosphate transporter distributed at presynaptic membranes, where synaptic vesicles reside. Several studies have described the inhibitory action of prenatal alcohol on glutamatergic release (Yunes, Estrella et al. 2015) and glutamate receptors (Savage,

Montano et al. 1991). In contrast, other studies have reported that developmental alcohol exposure may actually increase glutamate release in the fetal cortex (Reynolds, Penning et al. 1995). Because glutamate dynamics can be a potent source of cytotoxicity in the brain, here, we examined the role of prenatal alcohol on the expression of Vglut1 in the cortex. We found prenatal alcohol increased the expression of *Scl17a7* (the gene encoding Vglut1), though S-AMe did not appear to mitigate this upregulation (Figure 35G, P=0.035). Immunohistochemical analysis confirmed the action of alcohol on the Vglut1 protein in the cortical plate. Comparatively, in this analysis, S-AMe demonstrated a protective role (Figure 35F, P <0.0001). Our results ultimately support the findings of Reynolds et al and hint that alcohol may abnormally upregulate glutamate transport and signaling during late gestation. Interestingly, alcohol-induced glutamatergic increase has been linked to increased frequency of excitatory post-synaptic currents in pyramidal neurons and anxiety- like behaviors in a third trimester model of FASD (Baculis, Diaz et al. 2015).

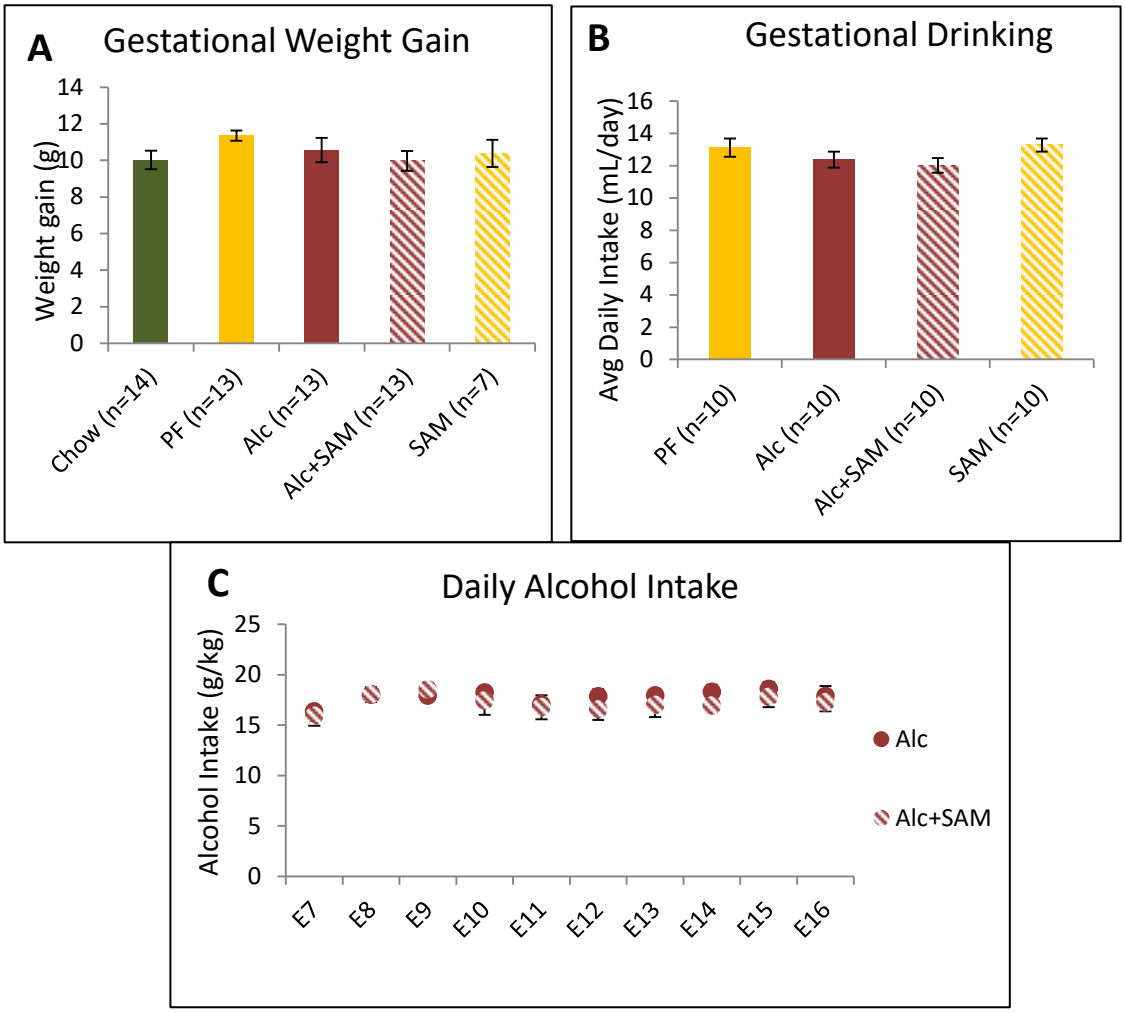

Figure 27. Alcohol does not impact gestational characteristics of experimental dams (A)Average weight gain of group dams from weight at conception to weight at E17 (B) Average daily intake of liquid diet from start of experimental treatment (E7) to end of experimental treatment (E16) (C) Daily Alcohol Intake calculated from average daily total liquid diet drinking of Alc and Alc+S-AMe experimental groups (E7-E16); no group differences in daily liquid diet or alcohol consumption were detected across gestation.

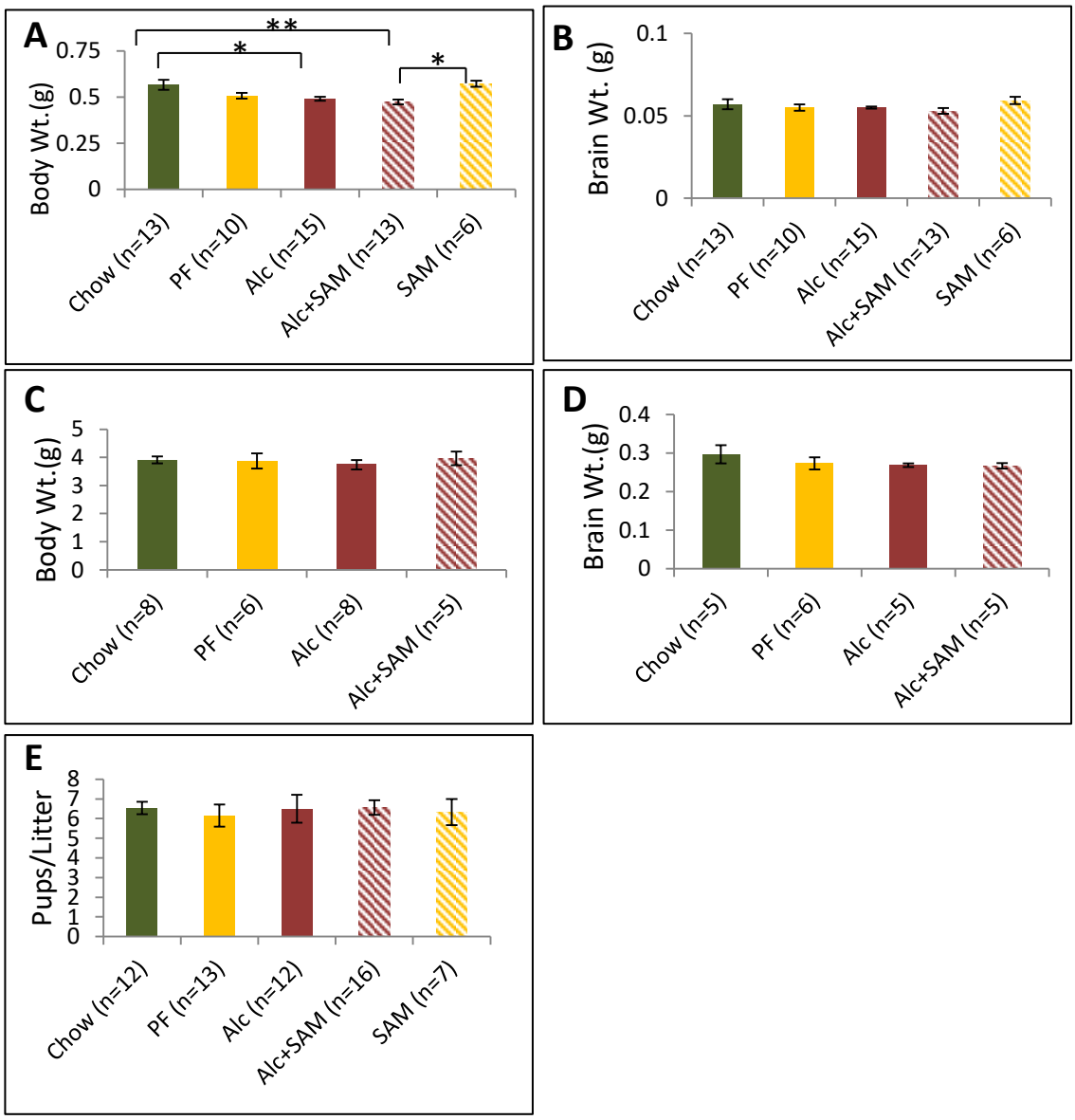

Figure 28. Alcohol transiently inhibits fetal body weight at E17 but does not impact brain weight

(A)Average fetal body weight as determined by average fetal weight/litter at E17; alcohol-receiving groups demonstrated decreased fetal body weight though this effect did not persist postnatally (B) Average fetal brain weight/litter as determined by dissected brain weight at E17 (C) Average body weight of pups/litter as measured at P7 (D) Average brain weight of pups/litter as determined by dissected brain weight at P7 (E) Average number of pups/litter across all experimental groups. *$p \leq 0.05$; **$p \leq 0.005$.

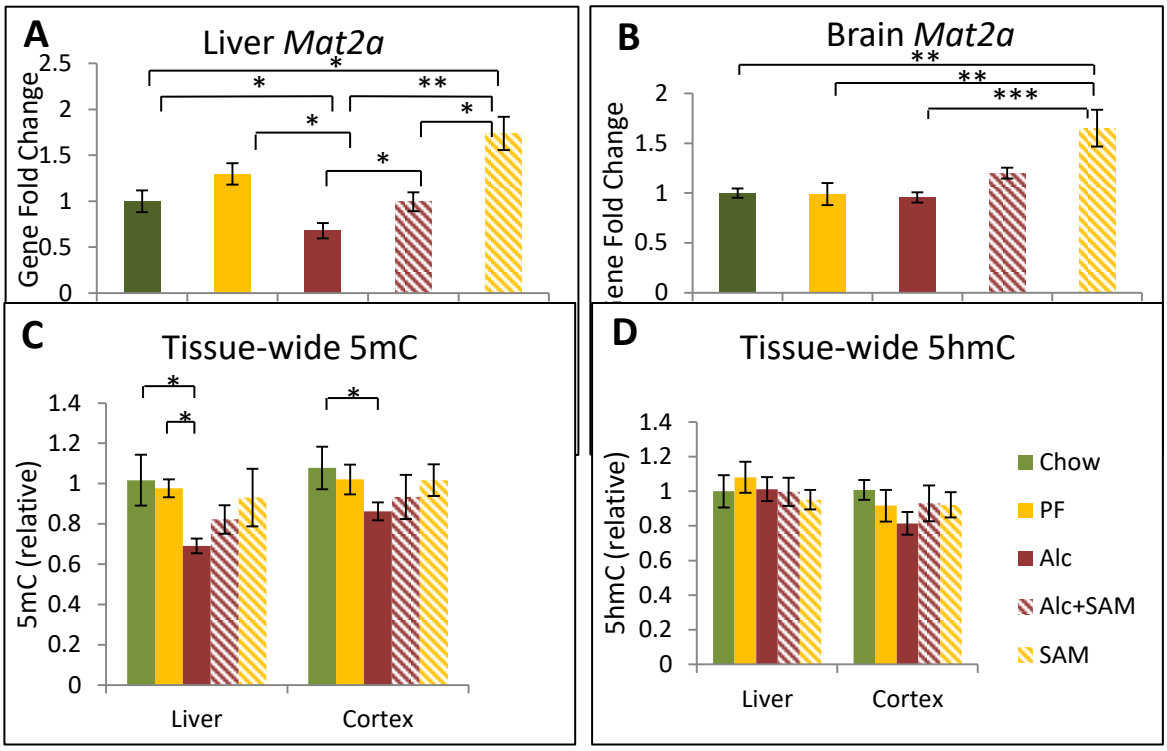

Figure 29. Alcohol reversibly decreases liver but not brain *Mat2a* and liver and cortex-wide 5mC

(A)Liver *Mat2a* expression measured by quantitative PCR revealed that alcohol decreased the expression of the transcript in the fetal liver at E17, an effect normalized by supplementation with S-AMe. Unrestricted S-AMe diet demonstrated the highest expression of *Mat2a.* (B) Brain *Mat2a* expression did not reflect alcohol-related changes, though unrestricted S-AMe access significantly increased the expression of the transcript. (C) Liver and cortex 5mC was reduced tissue-wide by fetal alcohol exposure. S-AMe supplementation was not significantly different from either alcohol or controls. (D) Liver and cortex 5hmC was unchanged across all groups. *p≤0.05; **p≤0.005; ***p≤0.0005.

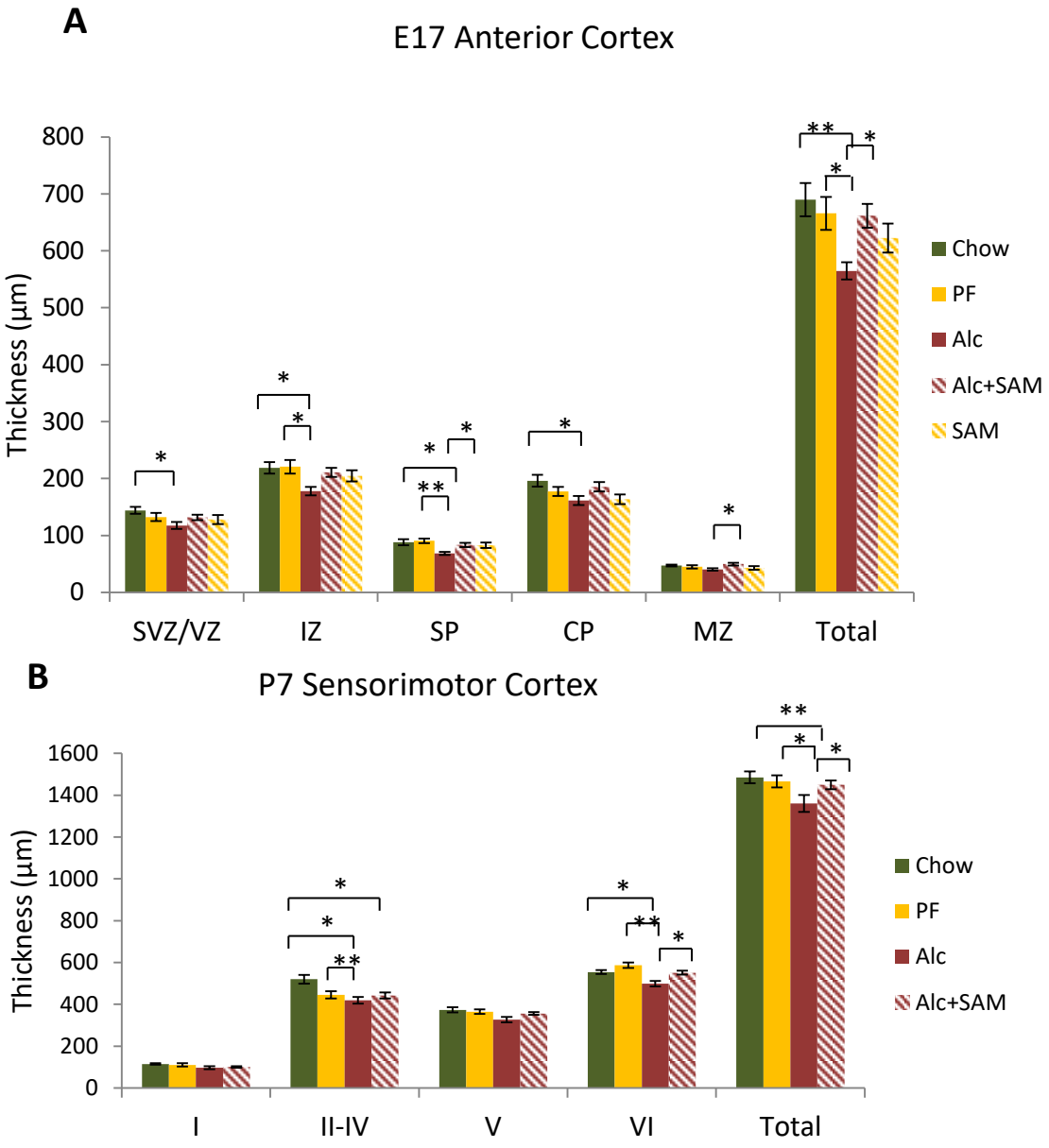

Figure 30. Alcohol- induced cortical thinning is persistently ameliorated by S-AMe supplementation

(A)Cortical length was measured from the base of the SVZ to the roof of the MZ. Alcohol-induced reductions were detected across all zones except the MZ. In the SP and cumulatively, S-AMe supplementation protected the cortical laminae from Alcohol-induced thinning. (B) Alcohol-induced cortical thinning persisted into postnatal (P) day 7 in the sensorimotor region of the anterior cortex, particularly in the II-IV and VI layers of the cortex. S-AMe supplementation continued to provide neurprotection from Alcohol-induced cortical thinning on P7. *p≤0.05, **p≤0.005; SVZ/VZ: subventricular zone/ventricular zone, IZ: intermediate zone, SP: subplate, CP: cortical plate, MZ: marginal zone.

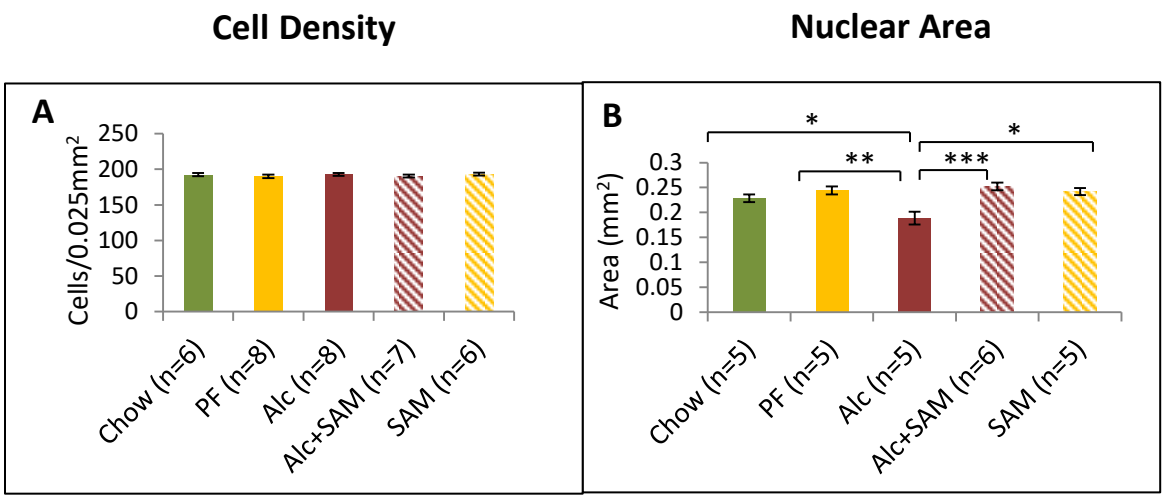

Figure 31. Alcohol reversibly reduces nuclear area in the E17 cortical plate
(A) Cell density was assessed using the Methyl-Green Nissl stain. Cell number was unchanged across groups within a 0.025 mm^2 area selected from the mid cortical plate. (B) Nuclear morphology was evaluated from a random sample of 100 cells within the cortical plate. Alcohol group nuclei were significantly smaller than all other groups and S-AMe supplementation was neuroprotective against this nuclear size reduction. *p≤0.05; **p≤0.005; ***p≤0.0005.

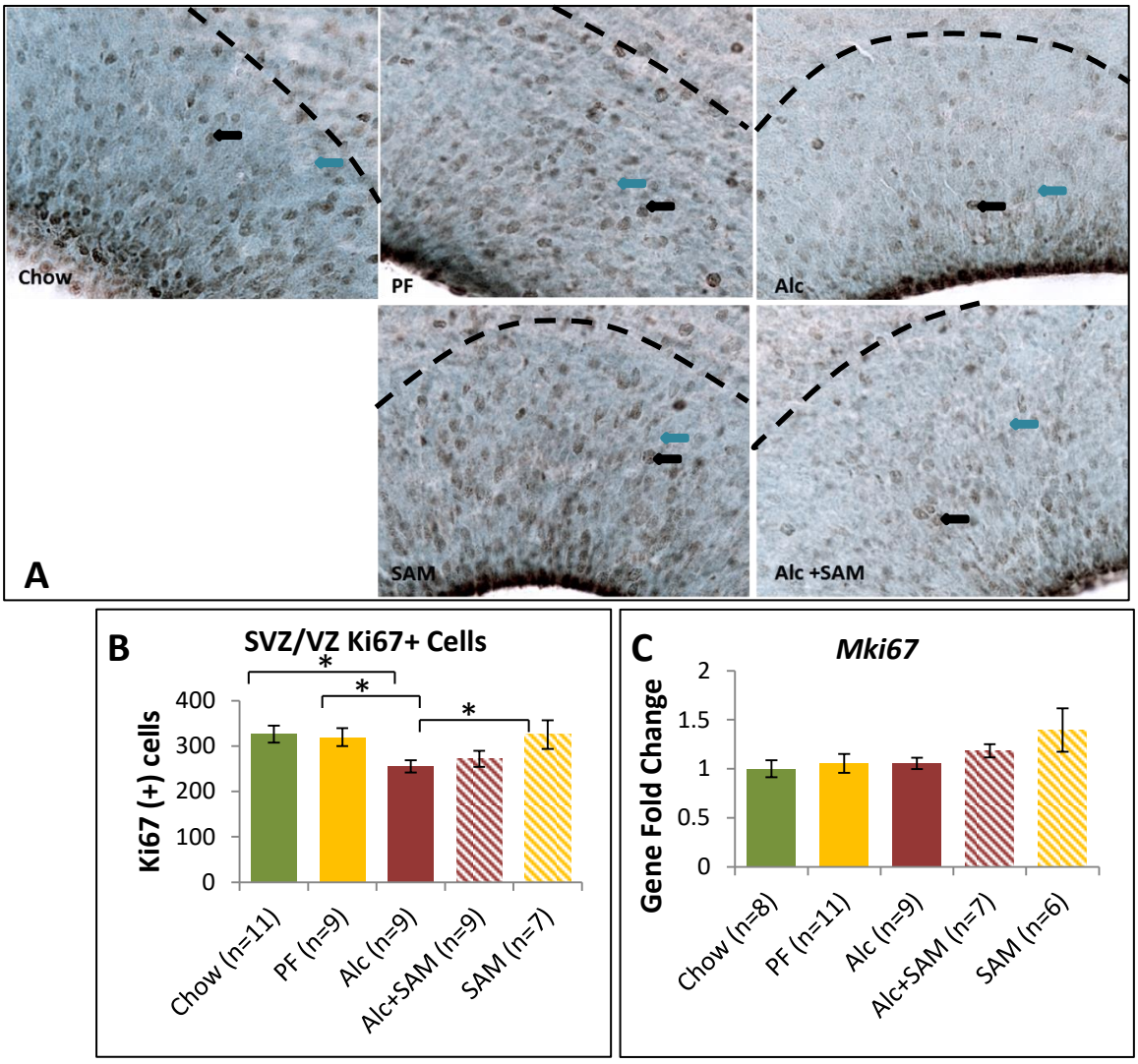

Figure 32. Alcohol decreases the number of proliferating cells at the cortical neuroepithelium

(A) Representative images from the SVZ/VZ stained for the cell proliferation marker Ki67. Area beneath the black dashed line denotes the SVZ/VZ regions. Black arrows demonstrate positively stained nuclei, blue arrows demonstrate Ki67 negative nuclei. (B) Average number of Ki67+ cells detected by automated particle analysis tool using ImageJ showed significant decline in Ki67+ cells in the Alcohol group compared to controls (C) Relative expression of Ki67 mRNA (encoded by the gene *Mik67* across cortical tissue samples at E17 showed no detectable transcript changes. *p≤0.05; SVZ/VZ: subventricular zone/ventricular zone.

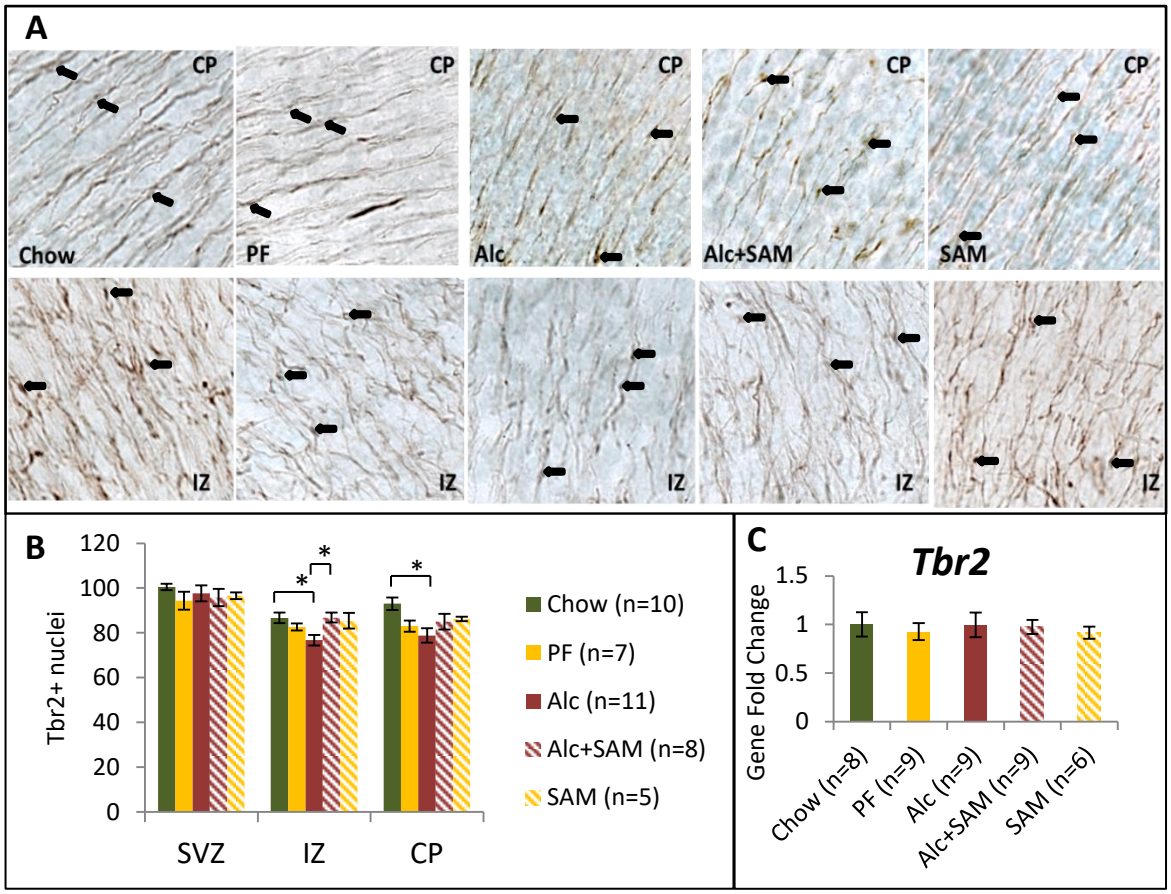

Figure 33. Alcohol-induced Tbr2 reduction is ameliorated by S-AMe supplementation in the intermediate zone

(A) Qualitative representation from the CP and IZ of brain sections immunostained for Tbr2, a marker of intermediate progenitors of the cortex. Top row represent Tbr2+ nuclei and fibers in the CP. Bottom row represent Tbr2+ nuclei and fibers in the IZ. Black arrows indicate some examples of positively stained nuceli. (B) Quantitative examination of Tbr2+ nuclei showed no differences in the SVZ and an alcohol-related decrease in the IZ and CP. In the IZ, where Tbr2 abundance was highest, S-AMe supplementation demonstrated a protective effect. (C) Quantitative expression of the Tbr2 transcript revealed no significant changes across the groups. SVZ/VZ= subventricular zone/ventricular zone; CP=cortical plate; IZ=intermediate zone. *$p \leq 0.05$.

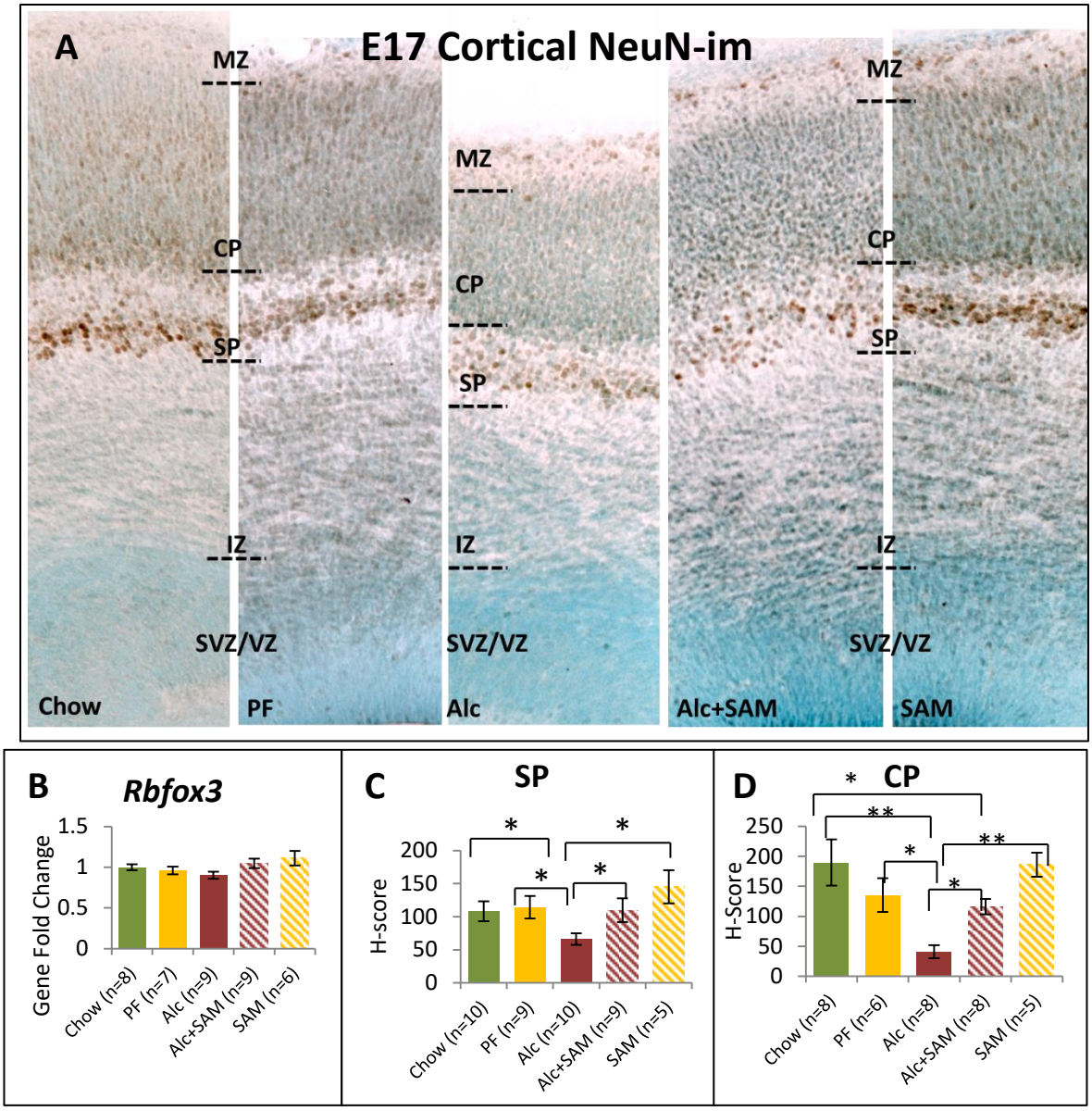

Figure 34. Alcohol-induced NeuN (im) decrease is ameliorated by S-AMe supplementation

(A)Representative cortical sections immunostained for the neural maturation marker NeuN. Dashed lines represent the approximate borders of the cortical sublayers at E17. NeuN is expressed in the upper layers of the cortex, including the SP and CP (B) Relative expression of NeuN mRNA (encoded by the gene *Rbfox3*) across cortical tissue samples at E17 shows no detectable transcript changes (C-D) Measured immunoreactivity of cells as determined by H-scoring show a marked decrease in NeuN-im in the Alcohol group in the SP sublayer and the CP sublayer. *p≤0.05, **p≤0.005, ***p≤0.0005; SVZ/VZ: subventricular zone/ventricular zone, IZ: intermediate zone, SP: subplate, CP: cortical plate, MZ: marginal zone.

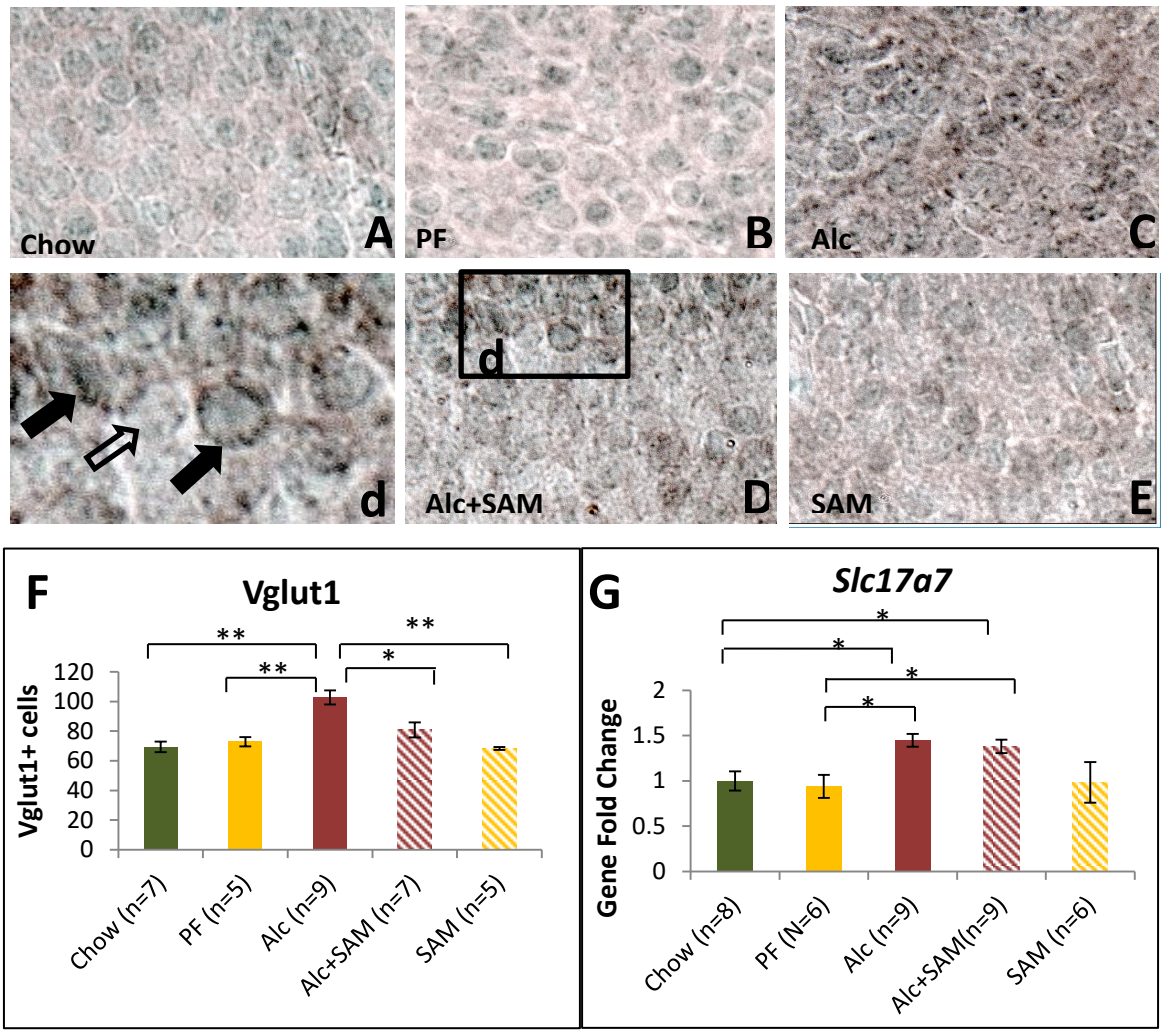

Figure 35. Alcohol increases Vglut1 expression in the cortical plate
Representative immunoreactivity of Vglut1 in the cortical plate of (A) Chow (B) PF (C) Alcohol (D) Alc+SAM and (E) SAM treated offspring. The presynaptic protein mostly accumulated at the cellular membrane and can be observed in dense regions of the cell perimeter (d, black arrows). In comparison, the perikarya of Vglut1-negative cells is observable by methyl-green counterstaining but devoid of presynaptic Vglut1 densities (d, clear arrow). (F) The number of Vglut1+ neurons was significantly increased compared to controls. S-AMe supplementation significantly diminished this effect. (G) Slc17a7 expression (encoding Vglut1) was similarly upregulated by alcohol cortex-wide. Alc+SAM in this assay did not mitigate the alcohol-induced upreguatlion. *$p \leq 0.05$; **$p \leq 0.005$

3.3.3 Effect of Alcohol and S-AMe Supplementation on Genetic Targets of Cortico-Development

Epigenetic studies have perpetually revealed the tissue and cellular specificity of DNA methylation landscapes across development. Similarly, high throughput studies continue to observe that DNA methylation is dynamic across genes, and even within different genetic elements (i.e. promoter, exon, intron, UTR, enhancer, etc.). As such, the future of DNA methylation study is contingent upon narrowing specific cellular populations and genetic contexts. With that in mind, we set out to explore the effects of fetal alcohol exposure and S-AMe supplementation on various genes across the timeline of cortical development in an attempt to narrow the alcohol and methyl-sensitive cortical transcriptome for future epigenetic study.

While several studies have used high-throughput methods like RNA-Seq to identify multitudes of genes and gene pathways altered by prenatal alcohol, to-date methyl-supplementation studies (particularly performed in an alcohol-context) have investigated only a handful of genes and gene networks. Based on the observation that both alcohol and S-AMe supplementation demonstrated significant impact across various molecular markers, it was important to investigate genetic correlates as the corresponding transcripts were not usually accountable in the E17 tissue. The strategy employed for genetic investigation of cortico-developmental genes was coverage spanning the early to late embryogenic pathways previously identified to be critical for cortical development and forebrain size.

One of the earliest pro-neural genes, *Ascl1* is expressed from the most nascent cortical stages to late corticogenesis. The gene in its earliest context works to oppose the

Notch signaling pathway, diverting multipotent cells away from glial fates toward cortical progenitors. It is a positive regulator of Cajal-Retizus (MZ layer) neurons and has been shown to promote reelin and Tbr2 expression (Dixit, Zimmer et al. 2011). Interestingly, postnatally *Ascl1* shifts to play a positive regulatory role on both cortical proliferation and oligodendrocyte specification, particularly in response to demyelinating insults (Nakatani, Martin et al. 2013). Finally, the gene has been identified as an effector and direct target of the RhoA suppressing *Rnd3*, a critical factor for cortical migration within the CP (Pacary, Heng et al. 2011).

A collaborator of *Ascl1*, the pro-neural gene *Ngn2* has demonstrated similar capacity during corticogenesis. Genetic ablation and ectopic expression studies have revealed that *Ascl1* and *Ngn2* play important roles in establishing the ventral and dorsal telencephalon, respectively (Casarosa, Fode et al. 1999, Fode, Ma et al. 2000). Additionally, the two coordinate early neural specification and migration (Bertrand, Castro et al. 2002, Pacary, Heng et al. 2011). During later stages, *Ngn2* works synergistically with the proneural *Ngn1* in the specification of glutamatergic neurons deep layers (V/VI) of the cortex (Fode, Ma et al. 2000, Schuurmans, Armant et al. 2004). All the while, *Ngn1* has the capacity to inhibit gliogenesis via sequestration and inhibition of transcription complexes like CPB-Smad and STATs at pro-glial genes (Sun, Nadal-Vicens et al. 2001).

Together, this network of early pro-neural genes plays a diverse and coordinated role in the early commitment and specification of multipotent progenitors toward neural lineages. *Ascl1* and *Ngn1* have been identified as epigenetic targets during neural development (Cimadamore, Amador-Arjona et al. 2013, Hirabayashi, Shiota et al. 2013)

and *Ascl1* and *Ngn2* have demonstrated sensitivity to prenatal alcohol exposure previously (Kim, Go et al. 2010). Examination of their alcohol and methyl sensitivity at E17 in this study revealed however, that neither of the three pro-neural genes were significantly changed by either alcohol of S-AMe supplementation (Figure 36B-D).

Next, we investigated genes involved in cortical specification, a process proceeding early pro-neural commitment. In the developing cortex, genetic ablation studies and ectopic expression studies have identified several key genes temporally regulated to produce the major subtypes of the cortex, cortico-cortico (i.e. callosal) projecting neurons, corticothalamic, and subcerebral projecting neurons. While *Tbr2* plays an early role in conferring intermediate precursors of cortical neurons, the transcription factor *Tbr1* is highly expressed in early born (post-mitotic) glutamatergic cortical neurons (Hevner, Shi et al. 2001). *Tbr1* is positively regulated by *Satb2* and plays a crucial role in the specification of callosal projecting neurons of layers II-V (Srinivasan, Leone et al. 2012). During early cortical specification *Satb2* (and to a lesser extent *Ctip2*) is enriched in and important for callosal specification (Alcamo, Chirivella et al. 2008). While callosal neurons are specified, both *Tbr1* and *Satb2* cooperatively act to suppress the regulators of the subcortical fate specifiers-*Fezf2* and *Ctip2* (Srinivasan, Leone et al. 2012, Leone, Heavner et al. 2015). Subsequently, direct repression of *Fezf2* by *Tbr1* binding at the 3' region particularly promotes corticothalamic identity in layer VI neurons (Han, Kwan et al. 2011). The expression of *Satb2* and *Tbr1* subsides according to temporal transcriptional cues, giving rise to the expression of *Fezf2* and downstream *Ctip2* in the formation of deep-layer subcerebral projection neurons (Arlotta, Molyneaux et al. 2005, Chen, Wang et al. 2008). Like *Tbr2* and *Satb2*, *Fezf2* and *Ctip2* cooperatively

suppress the callosal fate regulators (*Tbr2* and *Satb2*) to guide cortical neurons toward subcortical fates (Canovas, Berndt et al. 2015). Finally, layer VI differentiation is mediated by the direct binding and inhibition of *Fezf2* by *Sox5* (Kwan, Lam et al. 2008).

Collectively, this regulatory gene network gives rise to the major cortical subtypes and dysregulation, ectopic expression, and mutation of these profiles give rise to severe cortical phenotypes including microcephaly, intellectual deficiency, and propensity for later life diseases such as schizophrenia (Gulsuner, Walsh et al. , Rosenfeld, Ballif et al. 2009, Zhang, Li et al. 2014).The determination of cortical subtypes via this network has been shown to be highly dependent on the timing of repressive elements and the shift to effector roles for several of these genes. Intriguingly, genes like *Fezf2* have been targeted by Polycomb group (PcG) complex proteins, with the level of binding effectively driven by histone methylation at the *Fezf2* promoter (Morimoto-Suzki, Hirabayashi et al. 2014). Moreover, other genes have demonstrated epigenetic regulation during development, including the histone methylation of *Tbr1* (Büttner, Johnsen et al. 2010), the DNA methylation and histone modification of *Ctip2* (Marban, Suzanne et al. 2007, Tan, Nishi et al. 2012), and the interaction of *Satb2* with various chromatin remodeling elements in cortical specification (Gyorgy, Szemes et al. 2008).

In the evaluation of the gene network's sensitivity to prenatal alcohol exposure and the investigation of S-AMe supplementation as a potential neuroprotector, we found that while not all genes were altered by alcohol or S-AMe, the two important subcerebral fate specifiers, *Fezf2* and *Ctip2*, were impacted. Specifically, *Fezf2* was significantly reduced by alcohol and this inhibition was significantly ameliorated by S-AMe supplementation (Figure 37C, P=0.004). These effects were further corroborated by

immunohistochemical evaluation Fezf2 at the cortical plate (Figure A-2, Appendix A, P=0.038). Conversely, the *Ctip2* transcript was significantly upregulated by alcohol, though S-AMe supplementation did not normalize its expression (Figure 37E, P=0.01). These results present a possible genetic route for the phenotypic manifestations of alcohol and S-AMe supplementation observed earlier in the experimental paradigm.

3.3.4 Cortex-wide and Gene Specific Alcohol-induced Epigenetic Alteration and S-AMe normalization

Finally, to investigate whether epigenetic correlates existed parallel to observed phenoyptic and genetic alterations of the experimental model, we performed gene expression analysis of critical epigenetic enzymes, particularly those involved in transmethylation reactions (i.e. DNA and histone methylation). While in Chapter 2 some layer-by-layer DNA methylation examination was performed, here we expanded our approach to determine whether the normalizing potential of S-AMe supplementation could be traced to the epigenome. Due to the highly integrated nature of epigenetic modifications during cortical formation, we hypothesized that both alcohol and methyl-supplementation would impact the cortical epigenome.

Three critical methylation enzyme classes regulate all DNA and histone methylation reactions. The DNMT family regulates both maintenance (DNMT1) and *de novo* methylation, the latter of which is both dynamically performed by DNMT3a and DNMT3b during neural development (Watanabe, Uchiyama et al. 2006). The methylation of DNA is largely contingent upon the availability of the active methyl donor S-AMe, which upon loss of its methyl group to cytosine bases, is transformed to S-adenosylhomocysteine (SAH). Methylated DNA can subsequently be converted to

hydroxymethylated DNA by the TET enzyme family. While all TET isoforms have been shown to play a role in neuronal differentiation, TET3 has been specifically identified as a critical role player in the terminal differentiation of neurons (Li, Yang et al. 2015). As discussed earlier in Chapter 1, TET enzymes may continue the conversion of hydroxymethylated DNA (5hmC) to produce 5fC and subsequently 5caC along a proposed demethylation pathway which could culminate in the deamination and decarboxylation of 5caC by thymidine DNA glycosylase (TDG) or base-excision repair enyzmes. Finally, S-AMe may alternatively donate its methyl group toward histone methylation. This process is conferred by a variety of histone methyltransferases (HMTs) including Ehmt2 (G9a), a conserved repressive histone 3 lysine 9 (H3K9) methylatranferase which has been implicated in dysregulated neuronal transcription, cognition, and environmental adaptation (Schaefer, Sampath et al. 2009). Unlike DNA methylation, histone methyltransfer is a reversible reaction mediated by a class of enzymes known as histone demethylases (HDMs), but little about them in the context of developmental alcohol models (Kyzar, Zhang et al. 2016).

Cortex-wide, we investigated the gene expression patterns of DNMTs, TETs, and *Ehmt2* across our experimental paradigm. We found that while DNMT transcripts are largely unaffected by alcohol or S-AMe at E17, the *TET3* and *Ehmt2* genes were significantly upregulated by alcohol (Figure 38 F-G; TET3 $P=0.033$; Ehmt2 $P<0.0001$). In both cases, S-AMe supplementation markedly prevented the alcohol-induced upregulation. Interestingly, an earlier examination of cortex-wide DNA methylation (Figure 29 C-D) demonstrated that 5mC but not 5hmC was downregulated by alcohol,

and in that instance S-AMe supplementation did not significantly normalize alcohol-induced conditions.

Taking a more cell-specific approach, we examined the distribution of 5mC and 5hmC in the E17 cortex. Guided by our observations in Chapter 2, here we set out to 1) confirm the DNA methylation patterns of alcohol-exposed cortices and 2) evaluate the role of S-AMe supplementation. In the SVZ/VZ, 5mC showed a trend toward alcohol-induced signal reduction, though this trend was not statistically significant (Figure 39B). In the mature upper cortical layers, the SP and CP, 5mC was significantly increased compared to controls (Figure 39C-D; SP P=0.008; CP P=0.023). Notably, the supplementation of alcohol with S-AMe prohibited the alcohol induced hypermethylation. While our earlier investigation found that 5hmC was dynamically altered by prenatal alcohol, in this experimental paradigm, no alcohol or S-AMe related alterations of the 5hmC immunosignal were observed (Figure 40). While trends in the SVZ/VZ veer toward our previous observation of alcohol-induced decrease of 5hmC, this was not statistically significant (Figure 40B, P=0.079). Overall, these results provide an alternative DNA methylation landscape for tissue-wide assessments and support our earlier findings of alcohol-induced DNA methylation alterations. Additionally, they provide evidence of layer-specific methyl-related normalization of the aberrant DNA methylation signature in the upper cortex. Taken together with patterns induced by alcohol and S-AMe at the genomic level of DNA and histone-methylation conferring genes, the case for epigenetic mechanisms as regulators of alcohol teratogenesis and methyl-induced neuroprotection is strengthened.

Beyond the cellular level, which we have previously addressed as an important contextual element of epigenetic dynamics, advances in commercial technology have allowed investigators to probe the epigenetic landscape at the nucleotide level. This high-resolution strategy can be used to pinpoint precise regions of differential methylation which may be crucial for the transcription of the gene. The quest for these sites (referred hereto as functional DMRs) is a critical step toward the utilization of DNA methylation and other epigenetic landscapes as diagnostic tools. To demonstrate the capacity of this strategy in the embryonic cortex, we explored the DNA methylation landscape at various regions of the transcription factor *Fezf2*. Recall that Fezf2 is a crucial component in the specification of subcerebral fates and subcortical axon pathfinding during late embryogenesis. Additionally, Fezf2 plays an earlier role in the rostrocaudal patterning of the forebrain and *Fezf2*- deficient mice have demonstrated reduced neural progenitor differentiation, apoptosis, and reductions in forebrain size (McKenna, Betancourt et al. 2011, Zhang, Li et al. 2014).

Due to the sensitivity of the *Fezf2* transcript to both alcohol and S-AMe supplementation (Figure 37C), we set out to probe various regulatory regions for differential methylation with the aim of identifying a novel functional DMR. The *Fezf2* gene consists of a 2.7Kb promoter and four exons. Within the gene, a large portion of the promoter and a small introductory portion of exon 1 overlap with a CG rich region (CpG island). Due to the regulatory importance of the transcription start site (TSS) and areas immediately up and downstream, we investigated a 60 bp and 50 bp region of the promoter and exon 1, respectively. Additionally, based on an earlier report identifying multiple conserved regulatory regions around the *Fezf2* locus which are particularly

active during cortical formation, we selected a region ~3.5kb downstream of the fourth *Fezf2* exon, an area hereto referred as enhancer 434. This site is particularly active in cortical progenitors and bears direct binding sites for the cortico-developmental genes *Tbr1, Sox5, NFIB,* and *FOXG1* (Eckler, Larkin et al. 2014). A detailed illustration of the loci and aforementioned regulatory regions can be found in Figure 41.

Various transcription factors of relevance were predicted to bind the sequenced regions including AP-1, a transcription factor enriched during developmental plasticity in the sensory cortex (Kaminska, Mosieniak et al. 1995). Interestingly, AP-1 has demonstrated brain responsivity to environmental insults such as lead and lithium exposure (Ozaki and Chuang 1997, Pennypacker, Xiao et al. 1997). In alcohol treated cortical neurons, AP-1 binding and activity was elevated at the critical glutamate receptor subunit gene Nr2b (Qiang and Ticku 2005). The transcription factor E2F-1 has been implicated in regulation of neuronal cell death and has been identified in a previous study to be upregulated by alcohol exposure during early neurulation (Hou, Callaghan et al. 2000, Anthony, Zhou et al. 2008). Like AP-1, the transcription factor NF-kB has demonstrated redox sensitivity in response to alcohol-mediated oxidative stress. Particularly, the NF-kB neuroimmune cascade is induced in the frontal cortex by binge ethanol administration (Anton, Alen et al. 2017) and its DNA-binding properties modulated during alcohol dependence (Mittal, Nathan et al. 1999). Recently, an Ayurvedic compound (traditional Indian medicine) Ksheerabala (101) demonstrated the ability to prevent the alcohol-induced upregulation of NF-kB in the brain, concomitantly reducing measures of neurotoxicity (Rejitha, Prathibha et al. 2015).

In addition to alcohol-sensitive transcription factors, the examined regions have been predicted to bind various neurodevelopmental elements, particularly at the 434 enhancer. Beside the previously described cortical specification genes *Tbr1* and *Sox5*, the binding of HES-1 was predicted at the *Fezf2* promoter. HES-1 is involved in Notch signaling and the repression of neuronal differentiation. Its suppression has been implicated in the promotion of cortical neurogenesis (Ciarapica, Methot et al. 2014). Finally, the enhancer 434 region was enriched with POU domain transcription factor binding. POU domain TFs are a family of regulatory genes identified in the development of the mammalian brain (He, Treacy et al. 1989). Detailed investigation has previously characterized the spatiotemporal patterns of POU genes in the regional specification of the early neuroepithelium as well as laminar specification in cortical development (Alvarez-Bolado, Rosenfeld et al. 1995).

Here we observed that alcohol induced DNA hypermethylation at the *Fezf2* promoter (Figure 42A, $P < 0.0001$).While S-AMe supplementation demonstrated a normalized group average, the effect was not statistically significant. In the exon 1 region, no alcohol or S-AMe effects were detected (Figure 42B). Finally, in the enhancer 434, a regulatory region required for Fezf2 expression in the cortex (Shim, Kwan et al. 2012), alcohol once again induced hypermethylation. In the enhancer, S-AMe supplementation significantly mitigated this hypermethylation cumulatively (Figure 42C, $P=0.038$). Total methylation of the promoter region was the highest among the examined regions, ranging from 13-23% methylation depending on experimental condition. By comparison, enhancer 434 and the exonic region ranged from 8-15%, depending on experimental group. Interestingly, the promoter and enhancer share critical regulatory

roles and a degree of overlapping transcription factor binding sites and as such are proposed to work together with the enhancer 1316 to mediate the dynamic expression of *Fezf2* during cortical specification (Eckler, Larkin et al. 2014). Here, we observed the parallel hypermethylation of the crucial regulatory regions and gene suppression by alcohol. Conversely, S-AMe supplementation normalized DNA methylation levels in the enhancer region parallel to the normalization of gene expression levels, presenting evidence that important *Fezf2* regulatory sites may mediate gene regulation via DNA methylation status. An interesting thing to note was that methyl-sequencing of regulatory regions in alcohol and S-AMe unaltered transcripts (*Ascl1*, *Ngn1*, *Syt2*) revealed no differential methylation (Table B-6, Appendix B). While only complete gene coverage or site-directed epigenetic manipulation will positively resolve the functional relevance of the genomic DNA methylation landscape, our evidence here supports the thematic conclusion that indeed DNA methylation alterations play a role in permissible expression and consequent phenotypes.

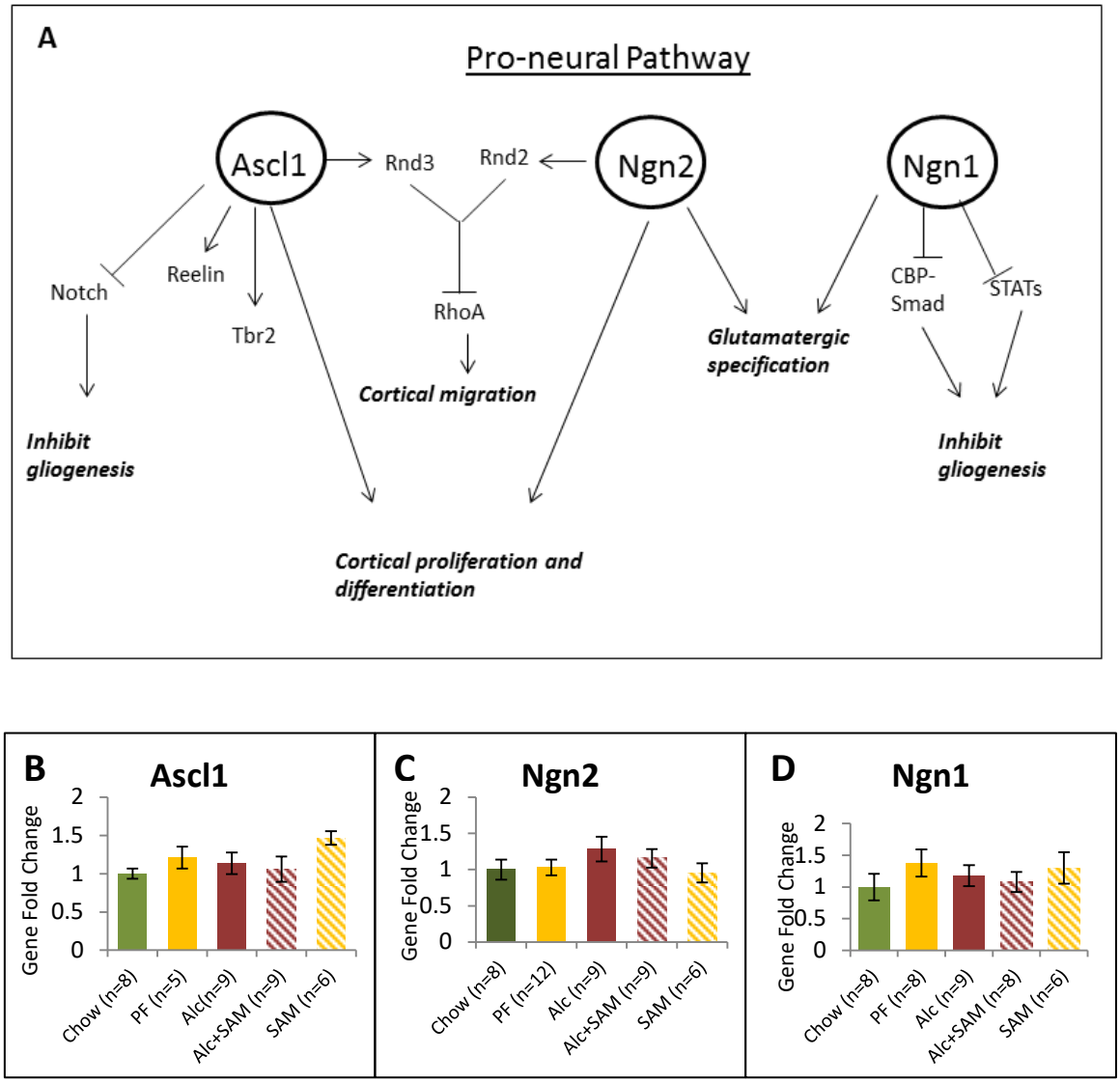

Figure 36. Alcohol does not impact early pro-neural gene expression in the E17 cortex (A)Gene networks of three pro-neural genes Ascl1, Ngn2, and Ngn1. Arrows indicate gene-associated positive regulation and T-shaped lines denote negative regulation. The networks represent a partial illustration of the known actions and gene targets of the pro-neural genes in the developing forebrain. Gene interactions ultimately manifest in contributions to broad, corticogenic processes (bold, italic font). (B) Gene expression analysis of Ascl1 (C) Ngn2 and (D) Ngn1 in the E17 embryonic cortex revealed no alcohol or methyl-sensitivity.

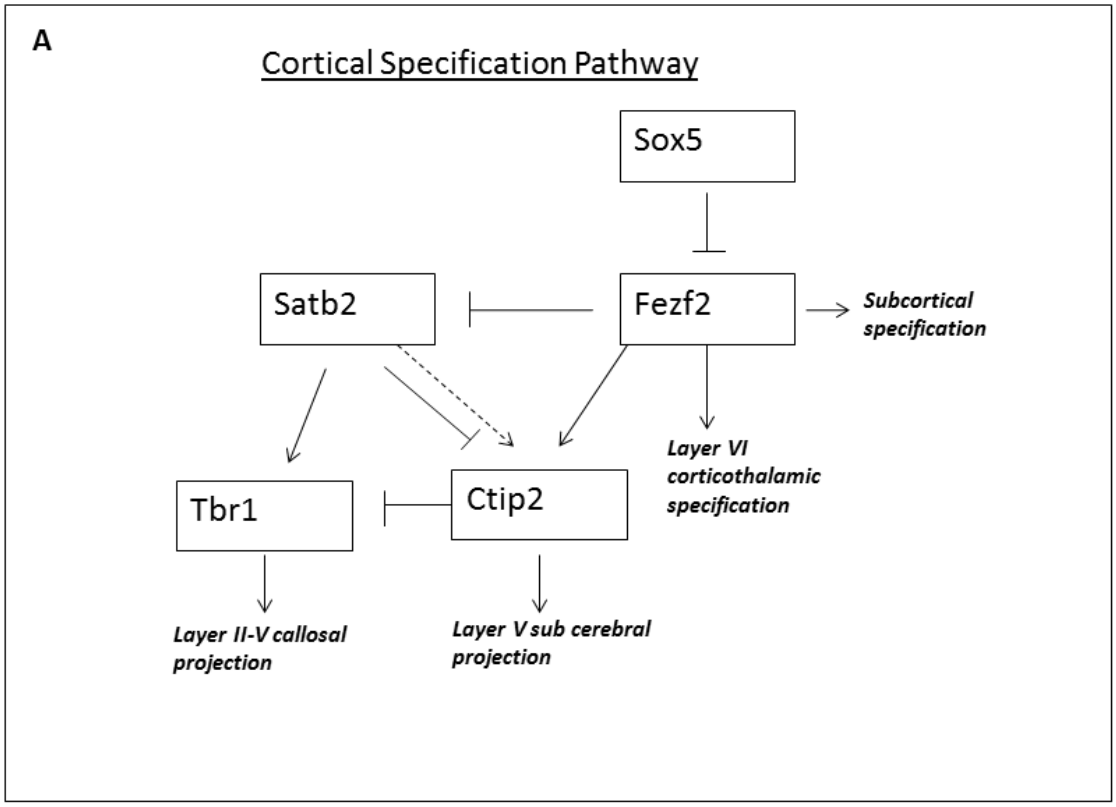
A
Cortical Specification Pathway
Sox5
Satb2
Fezf2
Subcortical specification
Layer VI corticothalamic specification
Tbr1
Ctip2
Layer II-V callosal projection
Layer V sub cerebral projection

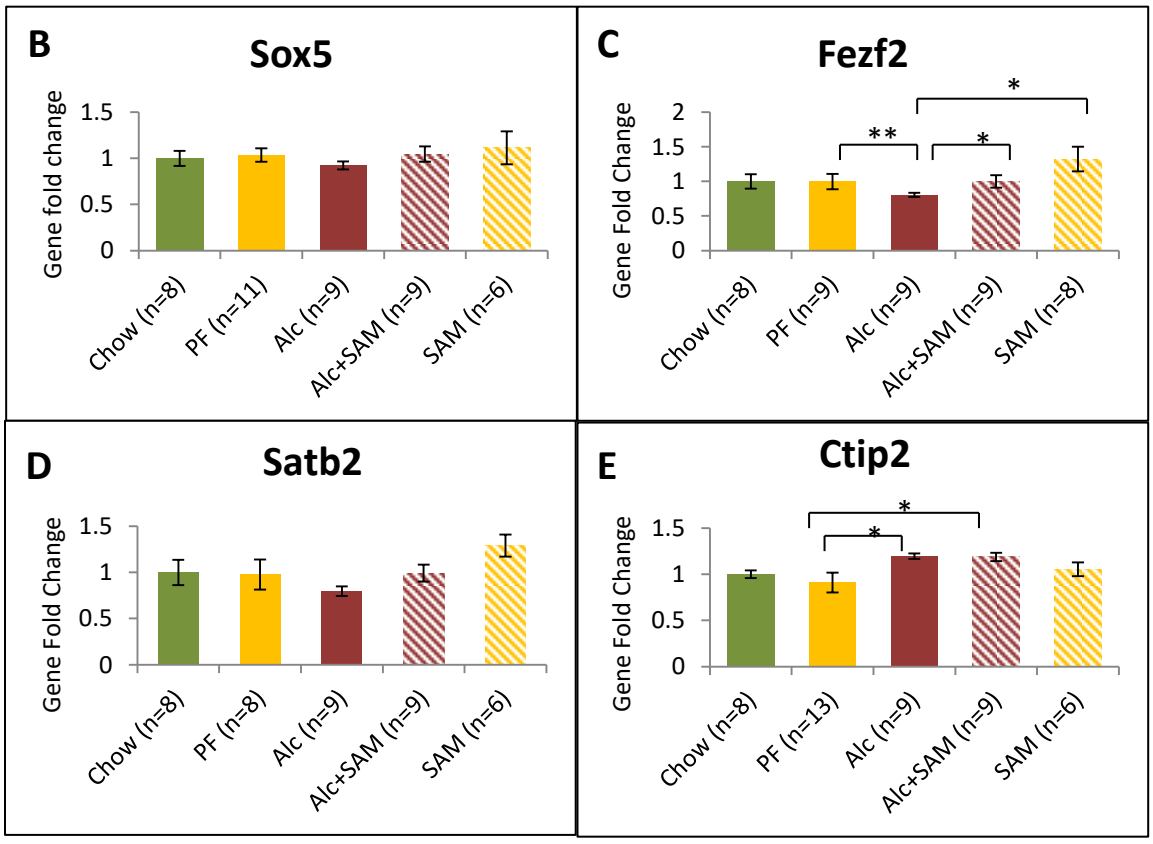
B
Sox5
Gene fold change
1.5
1
0.5
0
Chow (n=8)
PF (n=11)
Alc (n=9)
Alc+SAM (n=9)
SAM (n=6)
C
Fezf2
Gene Fold Change
2
1.5
1
0.5
0
**
*
*
Chow (n=8)
PF (n=9)
Alc (n=9)
Alc+SAM (n=9)
SAM (n=8)
D
Satb2
Gene Fold Change
1.5
1
0.5
0
Chow (n=8)
PF (n=8)
Alc (n=9)
Alc+SAM (n=9)
SAM (n=6)
E
Ctip2
Gene Fold Change
1.5
1
0.5
0
*
*
Chow (n=8)
PF (n=13)
Alc (n=9)
Alc+SAM (n=9)
SAM (n=6)

Figure 37. S-AMe supplementation partially normalizes alcohol-induced dysregulation of cortical specification genes
(A) Gene networks of the canonical cortical specification pathway including Sox5, Fezf2, Ctip2, Satb2, and Tbr1. Arrows indicate gene-associated positive regulation and T-shaped lines denote negative regulation. Dashed arrow denotes an early corticogenic relationship (relative to the remaining network).The networks represent a partial illustration of the known actions and gene targets of the cortical specification pathway as determined by multiple genetic loss and gain of function studies. Gene interactions ultimately manifest in contributions to broad, corticogenic processes (bold, italic font). (B) Gene expression analysis of Sox5 (C) Fezf2 and (D) Satb2 and (E) Ctip2 in the E17 embryonic cortex. While Sox5 and Satb2 were unchanged by experimental treatment, Fezf2 and Ctip2 were significantly affected by fetal alcohol. Only the Fezf2 gene showed normalization in the presence of S-AMe supplementation. *$p \leq 0.05$, **$p \leq 0.005$.

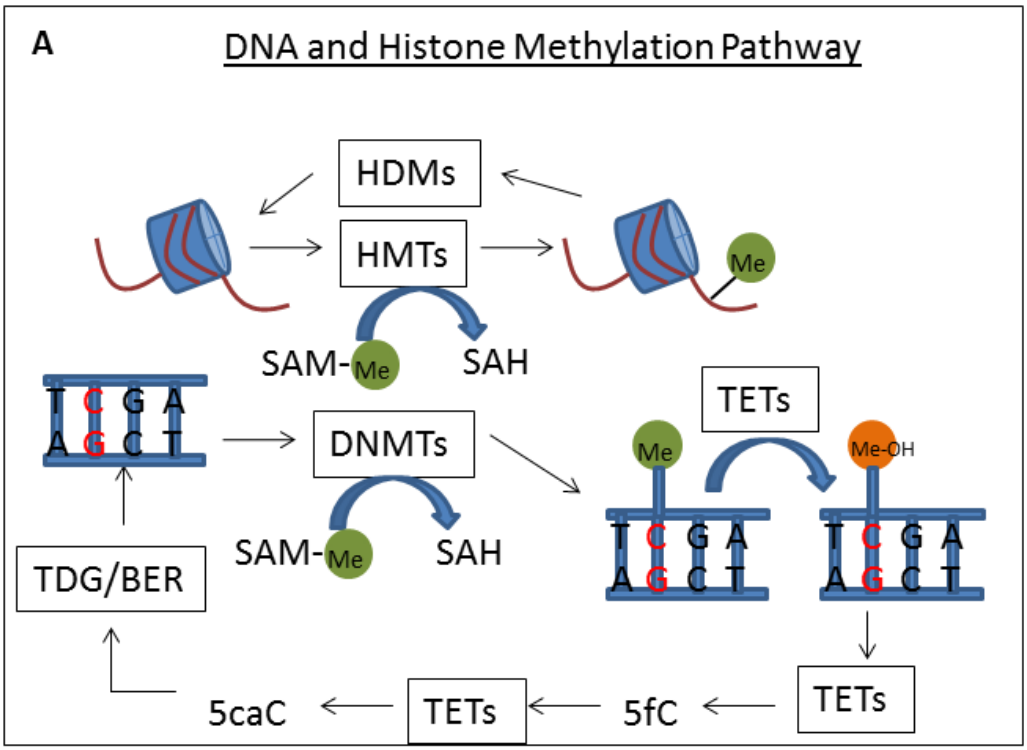

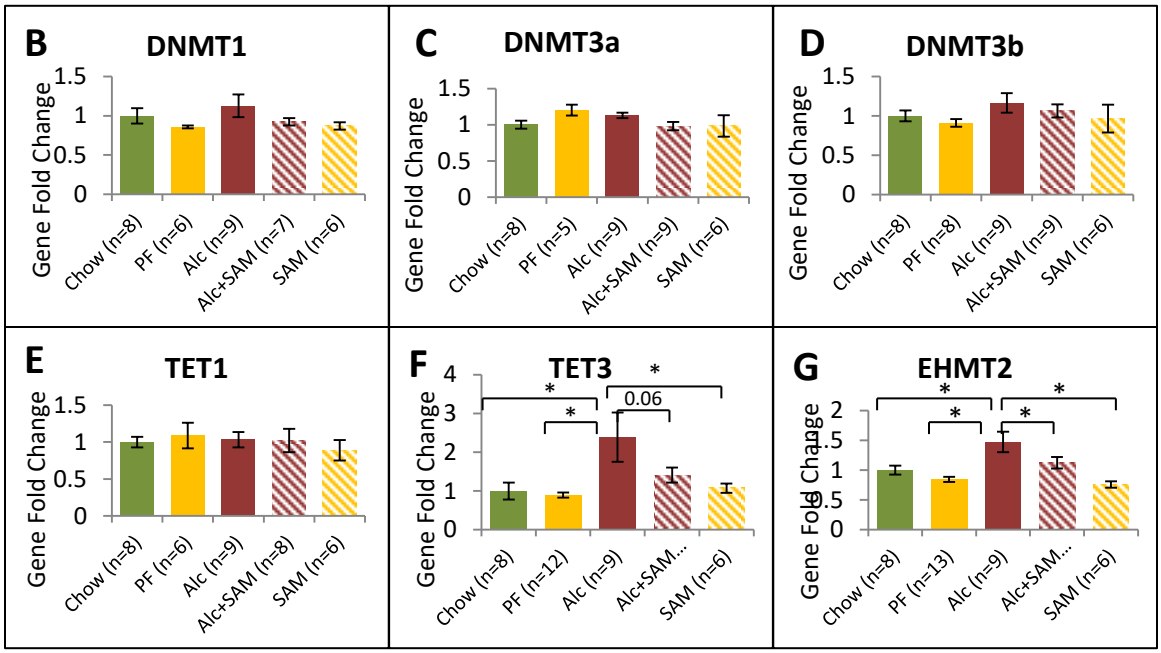

Figure 38. Alcohol- induced upregulation of the epigenetic genes Tet3 and Ehmt2 is mitigated by S-AMe supplementation

(A) The DNA and Histone Methylation Pathway consists of a series of biochemical conversions of cytosine bases (red) and histone proteins and histone tails. Using the active methyl donor (S-AMe), DNMT enzymes transfer the methyl group from S-AMe to the cytosine base, yielding 5mC and SAH in its wake. Next, TET enzymes, using 5mC as

its substrate, are responsible for the conversion of the methylated cytosine into a hydroxymethylated cytosine base (5hmC). Consequently, TET enzymes can continue the conversion of 5hmC to 5fC and 5caC, which may then go on to deamination and base excision repair processes (TDG/BER) in a demethylation path. Alternatively, S-AMe may donate its methyl group toward the methylation of histone core proteins or histone tails via the HMT enzyme families in a reversible manner. (B-D) Cortex-wide gene expression analysis showed that neither alcohol nor S-AMe produced significant transcriptional alterations of the DNMT family enzymes. On the other hand, the TET3 enzyme (F) and the histone methyltransferase Ehmt2 (G) were significantly upregulated by alcohol and markedly normalized by the alcohol+S-AMe treatment. *$p \leq 0.05$, **$p \leq 0.005$.

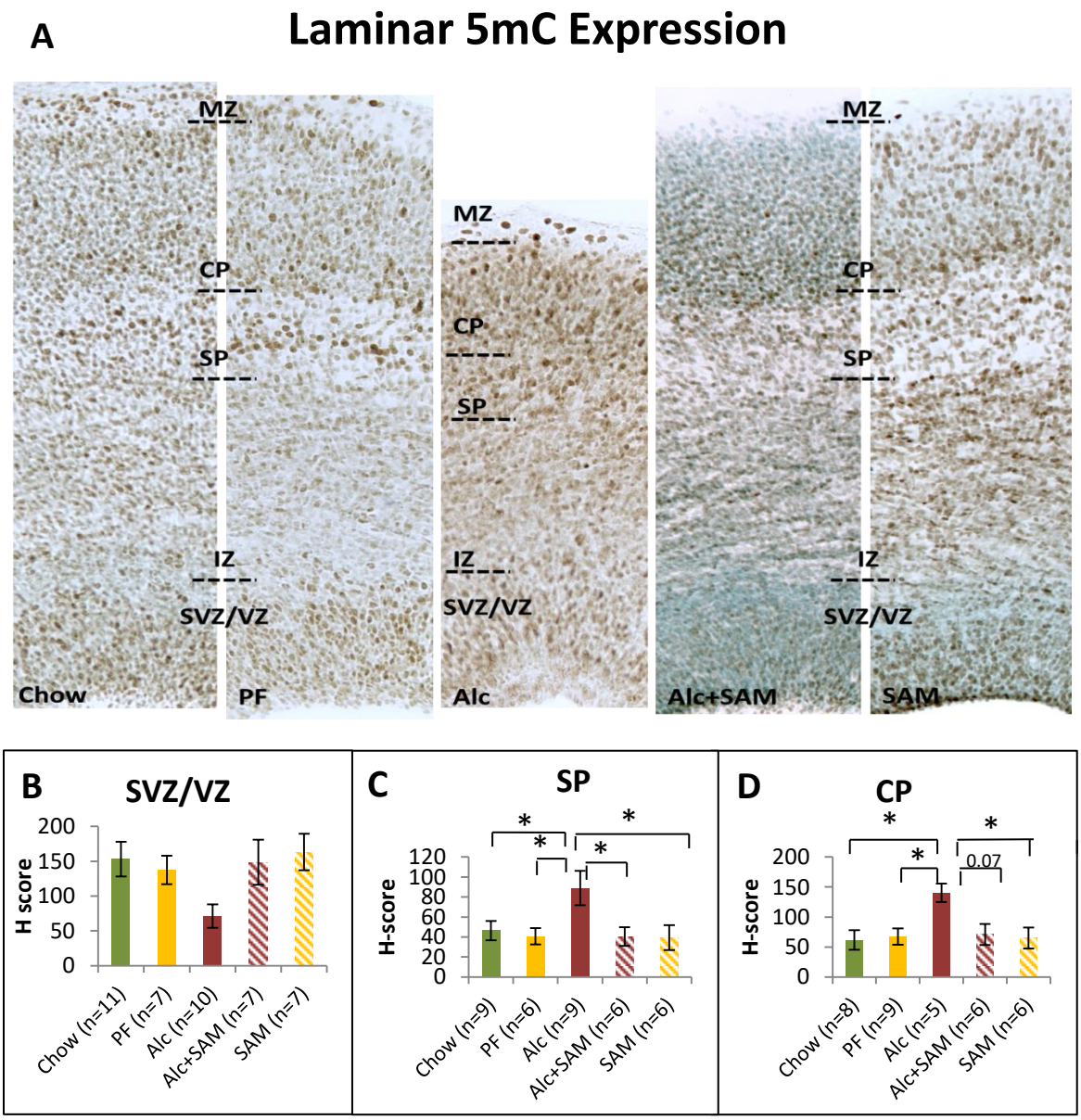

Figure 39. Alcohol-induced laminar 5mC upregulation is normalized by S-AMe supplementation

(A)Representative cortical columns immunostained for the methyl marker 5mC at E17 reveal the layer-specific distribution of 5mC. (B) Semi quantitative examination of the average intensity of the nuclear immunosignal in the SVZ/VZ identify a trend toward hypomethylation though this was not statistically significant. (C-D) In the mature layers of the cortical plate (the subplate and cortical plate), alcohol significantly increased 5mC abundance. S-AMe supplementaion of the alcohol liquid diet in all layers demonstrated a normalizing trend. *p≤0.05; SVZ/VZ: subventricular zone/ventricular zone, IZ: intermediate zone, SP: subplate, CP: cortical plate, MZ: marginal zone.

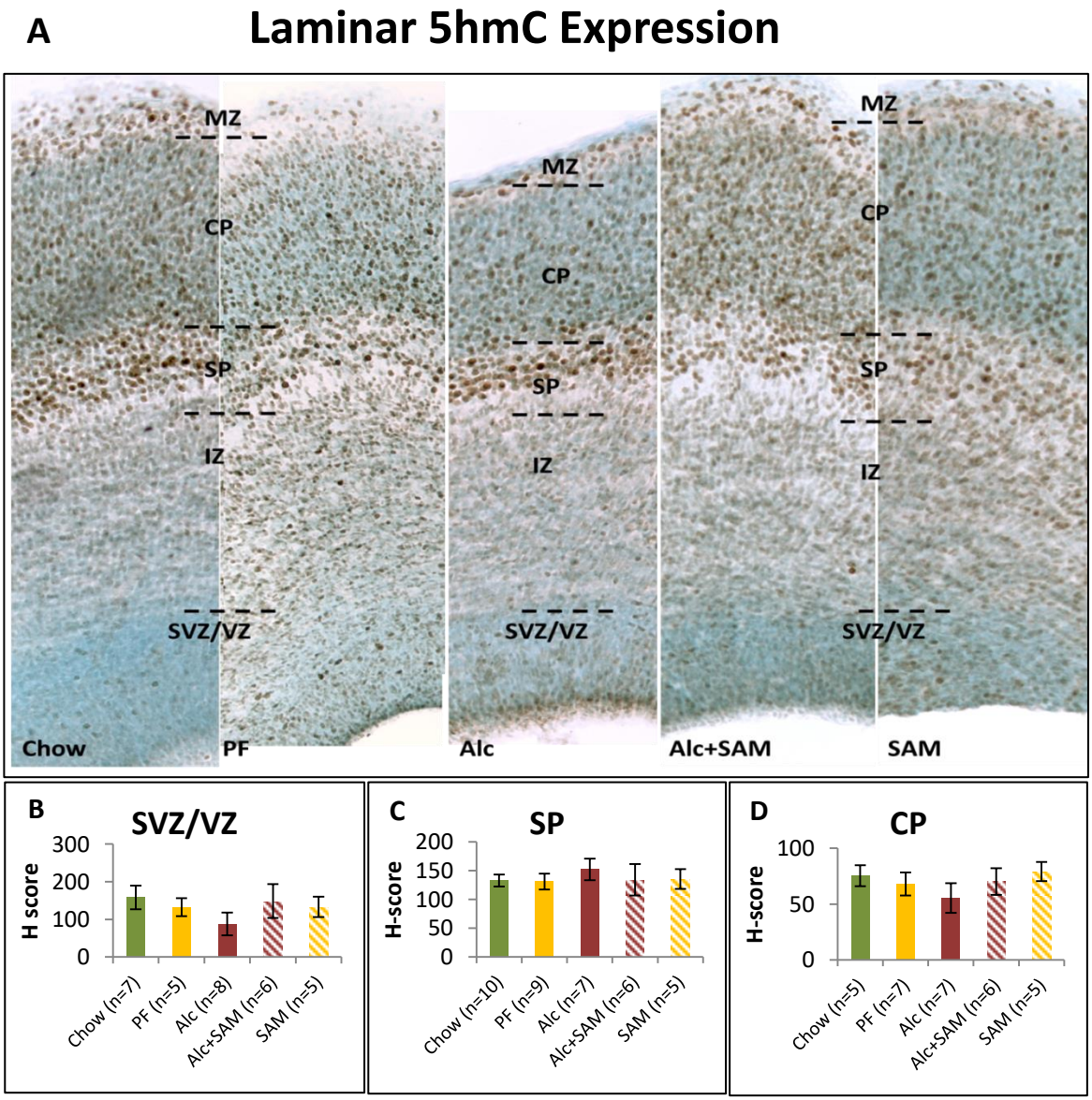

Figure 40. Laminar 5hmC is unaffected by alcohol or S-AMe in the E17 cortex
(A) Representative cortical columns immunostained for the methyl marker 5hmC at E17 reveal the layer-specific distribution of 5hmC. (B-D) Unlike 5mC, abundance of 5hmC was quantitatively unaffected by alcohol and S-AMe in both the neurogenic and mature layers of the cortical column. *$p \leq 0.05$; SVZ/VZ: subventricular zone/ventricular zone, IZ: intermediate zone, SP: subplate, CP: cortical plate, MZ: marginal zone.

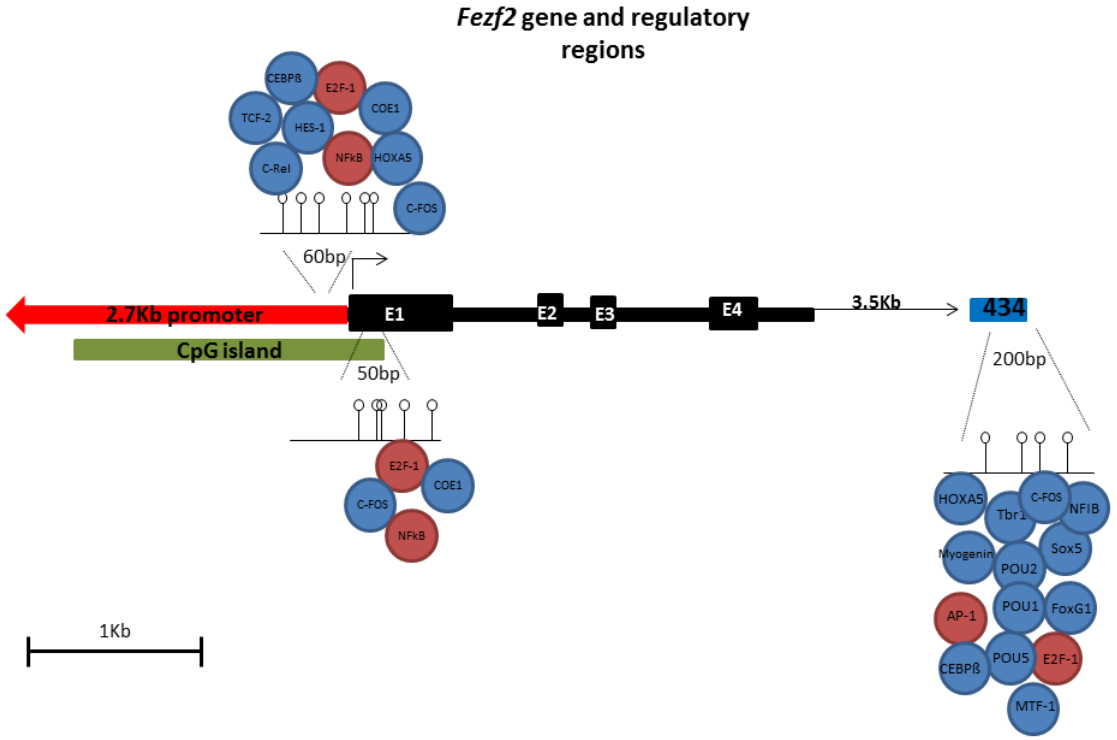

Figure 41. *Fezf2* gene, regulatory regions, and predicted transcription factor binding sites Fezf2 mouse gene contains a 2.7kb promoter, four exons, and two conserved regulatory enhancers which are enriched in cortical neurons (Enhancer 1316 not shown). A 60bp segment of the promoter directly upstream of the transcription start site (TSS), an introductory segment at exon1, and a large portion of the enhancer 434 region were chosen for DNA methyl-sequencing. Circles denote predicted transcription factor (TF) binding elements. Red circles denote TFs demonstrably modified by alcohol exposure in the brain. Blue circles indicate TFs known to be critical regulators of neural and cortical development. E: Exon; 434 denotes a conserved enhancer region of the *Fezf2* promoter; lollipops denote CpG sites within the sequenced region.

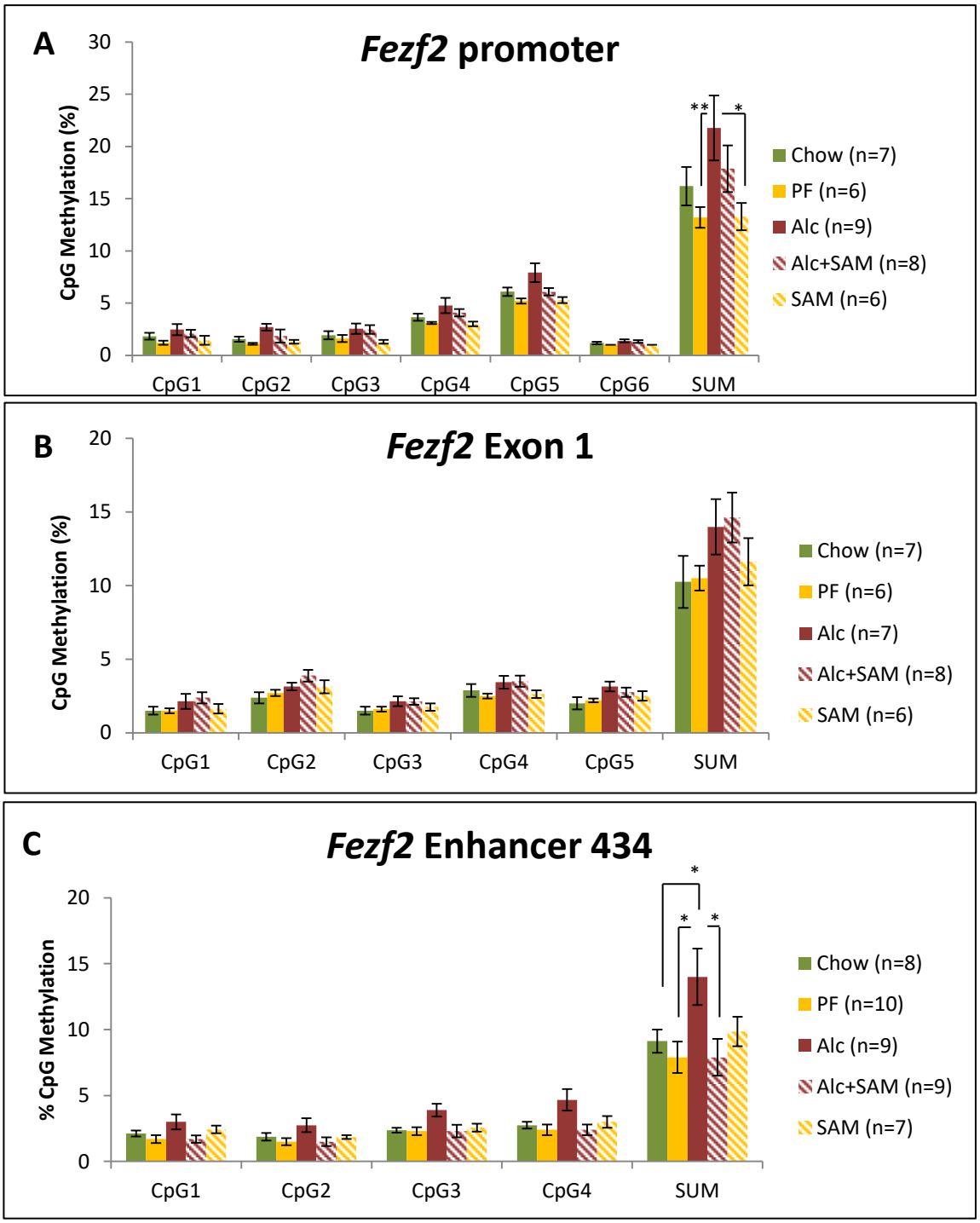

Figure 42. Fezf2 promoter and enhancer 434 are hypermethylated by alcohol treatment and partially normalized by S-AMe supplementation
(A) CpG methylation (%) distribution at each CpG within the coverage region of the Fezf2 promoter. Cumulative methylation (SUM) revealed that alcohol significantly hypermethylated the promoter region compared to PF and SAM controls. While S-AMe supplementation indicated a normalizing trend, this was not statistically significant. (B)

No group differences were detected overall in the exon 1 region (C) Alcohol treatment induced hypermethylation at the enhancer 434 region similar to the promoter. In this region, the normalizing effect of S-AMe supplementation was statistically significant. *$p \leq 0.05$;**$p \leq 0.005$.

3.4 DISCUSSION

3.4.1 Neuroprotective Role of S-AMe in Alcohol-induced Cortical Deficits

Dietary supplementation strategies have been regarded as promising therapeutic avenues in developmental disease. Due to the importance of methyl metabolism in neural development, developmental disorders with robust neuroteratogenic profiles have been particularly eyed for methyl-donor supplementation. As described earlier, methyl-supplementation across various models of developmental alcohol exposure have been previously performed (Table B-3, Appendix B). While the protective range of the strategy is expansive, its capacity in corticogenesis has not been closely scrutinized. The well-documented disruption of methyl metabolism by alcohol and the demonstrated teratogenic impact of alcohol in the embryonic cortex (Chapter 2) prompted our examination of methyl-donor supplementation in our FASD model.

As discussed previously, while the nuances of alcohol exposure likely play a role in the observed outcomes of the cortical structure, in this study our model reliably produced cortical thinning in the E17 mouse forebrain. Expanding on those findings, here we observed that this prominent alcohol-related feature was substantially ameliorated by supplementation with the active methyl donor S-AMe, as cumulative normalization of the cortical length was seen in the Alc+SAM group. While previous studies have highlighted the ability of methyl-supplements to protect against gross morphological features like reduced brain weight and microcephaly (Xu, Tang et al. 2008, Thomas, Abou et al. 2009), this is the first known report of methyl-supplemented neuroprotection of the cortical length. This was in contrast to the most similar examination to-date, performed with choline supplementation in six month old lambs (Birch, Lenox et al. 2016) and

which failed to observe improved brain volumetrics. However, the absence of regional measures (i.e. cortex) and the high-dose binge ethanol paradigm (with BECs twice that observed in this FASD model) greatly limit the comparative value of this study with our own. Another question that was uniquely addressed here was whether the neuroprotective influence of S-AMe was persistent beyond *in utero* exposure. We observed that in a distinct region of the frontal cortex (sensorimotor) at postnatal day 7 (~10 days after the final administration of experimental treatments), both alcohol and S-AMe maintained their impacts on the cortex. While FASD intervention models throughout the literature vary (methyl-donor pretreatment, simultaneous administration, and post-alcohol intervention), none to our knowledge have explored neural, molecular characteristics through the lens of lasting impact. As such, our study is the first to demonstrate that gestational intervention can produce enduring, protective effects on the most vulnerable cortical regions. Future longitudinal studies would need to be performed to resolve exactly how far into development these phenomena can detectably persist. Moreover, as human studies have linked cortical thickness of infants to long-term verbal learning and executive function (Nam, Castellanos et al. 2015), it would be interesting to investigate whether methyl-based cortical protection could translate into parallel behavioral (functional) outcomes within the same study population.

In Chapter 2, we set out to examine various potential underlying factors of alcohol-induced cortical thinning. Based upon on those findings, here we set out to answer whether S-AMe neuroprotection could be traced to each of these phenotypic parameters. This was particularly important given that FASD methyl-supplementation studies have not focused on corticogenic processes. Only one previous study was found

which examined cortical apoptosis. This study reported that prenatal alcohol increased apoptotic enzyme activity and apoptosis in the P0 rat, both of which were mitigated by folic acid (Sogut, Uysal et al. 2017). Here, we expand the neuroprotective repertoire of methyl-supplementation in the FASD cortex by presenting evidence that it mitigates alcohol-induced deficits of nuclear area, Tbr2, and NeuN expression, as well as abnormal Vglut1 upregulation. From this we can reasonably extrapolate that through the protection of multiple indicators (growth, migration, commitment, and functional maturity, respectively) S-AMe may collectively negate the deficits of alcohol on the laminar cortical structure.

Of course it should be noted that S-AMe neuroprotection was not ubiquitously observed. A survey of the protective and non-protective effects of methyl-supplementation in FASD studies (Table B-3, Appendix B) supports the idea that the capacity of methyl donor neuroprotection is often limited. Here, a prominent marker of cell proliferation (Ki67) was not normalized by S-AMe supplementation during alcohol insult. Interestingly neuroprotection of mitosis at the SVZ/VZ has also escaped methyl supplementation strategies in a model of methyl-insufficiency (Craciunescu, Johnson et al. 2010). It might be the case that pre-mitotic cells of the neocortex are less responsive to methyl-supplementation. This would be fitting with lack of neuroprotection observed in the SVZ/VZ thickness though a more detailed investigation is required. Though proliferation is one of the major phenotypic processes of the cortex, it has been highly disregarded in methyl-supplemented alcohol studies to-date. Considering cortical neuroprotection in the context of structural preservation, the absence of protected proliferation is perplexing (diminished cell number plays a major role in cortical

thickness). One may consider that the use of Ki67 as an immunohistochemical marker of cell proliferation can perhaps be improved or complimented by a more precise molecular proliferation marker such as BrdU. Alternatively, as mentioned in Chapter 2, not all cortical cells originate from the neurogenic SVZ/VZ. A large portion of inhibitory interneurons proliferate at the medial ganglionic eminence which was not evaluated here. It is possible that proliferative neuroprotection may be observed elsewhere in future studies.

3.4.2 Genomic and Epigenetic Normalization of FASD targets via S-AMe supplementation

Despite the observation of cortical normalization across various processes, the question remains how methyl supplementation (metabolism) mediates phenotypic outcomes on a molecular scale. The most logical starting point is the consideration that methyl-supplementation can normalize the aberrant methyl metabolism demonstrated by alcohol (for a review see (Resendiz 2016)). Developmentally, alcohol may also alter the dynamics of maternal-fetal methyl transport, influencing metabolic and biochemical outcomes in the fetus. Previously, in a guinea pig model of FASD, chronic folic acid supplementation was protective against reductions in fetal liver folate (Hewitt, Knuff et al. 2011). Another study observed improvements in embryonic methyl metabolism through the evaluation of hyperhomocysteinemia (homocysteine accumulation results from the diminished conversion of the substrate to methionine by betaine-homocysteine methyltransferase (BHMT) and methionine synthase (MS)) (Shi, Li et al. 2014).

Here, to evaluate the role of S-AMe supplementation on the normalization of methyl-metabolism, we investigated the enzyme conferring the active methyl donor form

S-AMe, MAT2A, in the fetal liver and brain. We found that in the fetal liver, alcohol predictably diminished MAT2A expression while S-AMe supplementation normalized the expression of the transcript. Because S-AMe metabolism is cyclical in nature (S-AMe byproducts are recycled into methionine), we can confidently extrapolate that these observations are indicative of cycle-wide trends. In the brain, MAT2A was not apparently sensitive to alcohol, though S-AMe supplementation increased MAT2A transcript levels (consistent with hepatic trends). Interestingly, this pattern was also observed in the Hewitt study, where liver folate but not brain folate was normalized in the presence of folic acid supplementation (Hewitt, Knuff et al. 2011). This increased hepatic sensitivity may be rooted in the fact that it is the predominant site of S-AMe production by MATs (Finkelstein 1990).

It should be noted that though transcriptional activity of the enzyme was altered by the experimental treatment, no enzymatic activity assay was performed. In the future, it would be more accurate to supplement gene expression analysis with molecular enzymatic assays as ultimately, enzyme activity and not simply abundance is truly reflective of metabolic activity. Due to the indirect nature of our methyl-metabolism probe, we examined liver and cortex-wide DNA methylation as a secondary function of methyl metabolism (S-AMe availability determines, among other things, DNA methylation). Consistent with alcohol-diminished methyl-metabolism, we observed liver and cortex-wide 5mC hypomethylation, but not 5hmC hypomethylation. Moreover, though S-AMe supplementation demonstrated normalizing capacity for liver Mat2a expression, the treatment did not normalize alcohol-induced liver nor cortical 5mC hypomethylation. As discussed in Chapter 2, the absence of a treatment sensitivity of

5hmC on a tissue-wide scale may be due to 1) the relatively lower abundance of the methyl mark (~1/10 of 5mC in the brain and even lower in the liver) and/or 2) the cellular specificity of 5hmC in more mature cortical cells (proportionately less than the neurogenic cells which make up the cortical column).

Regarding the normalizing capacity of S-AMe toward DNA hypomethylation in the neurogenic zones, ample evidence across non-alcohol associated hypomethylating conditions has previously substantiated the neuroprotective role of S-AMe (Cravo, Pinto et al. 1998, Tian, Zhao et al. 2012, Carlin, George et al. 2013). Here, the absence of a statistically significant difference between the Alc+S-AMe group and all controls may hint at a partially normative effect in lieu of a statistically significant differences between the Alc and Alc+S-AMe groups in some cases. This subtlety may perhaps be due the diversion of supplemented S-AMe across histone methylation, DNA methylation, and polyamine synthesis (Petrossian and Clarke 2011). Another consideration is that due to the context-specificity of DNA methylation across development, dietary methyl-supplementation may similarly exhibit site or cell specific impact. Support for this can be taken from the relatively more defined nature of methyl-supplementation in gene-specific studies versus global tissue assays. For example, in the male offspring of alcohol-treated rats, POMC gene hypermethylation was prevented by choline supplementation (Bekdash, Zhang et al. 2013). Alternatively a tissue-wide assay of alcohol-treated rat offspring revealed a more complex function, where choline supplementation alleviated hippocampal hypermethylation but not cortical hypermethylation (Otero, Thomas et al. 2012). The context specificity of DNA methylation normalization is also substantiated here. Though tissue-wide assays hint at the normalizing capacity of S-AMe,

immunohistochemical examination of the cortex (a more cell discriminatory method) distinctly demonstrates its role in the normalization of upper layer (SP and CP) DNA methylation (5mC). Clearly, the FASD methyl-supplementation literature to-date bears an emerging epigenetic view and much more investigation is required to unravel the dynamics of methyl supplementation and neuroprotective outcomes. Despite this, collective findings are building the case that like alcohol, S-AMe and other methyl donors do not unilaterally alter the epigenome. Future studies will have to address the mechanisms mediating this proposed methyl-selectivity of the genome and reconcile those with alcohol-sensitive epigenetic recruitment elements.

One crucial aspect of alcohol-related neuroteratogenicity that was not thoroughly addressed in this study and which plays a critical role in DNA and histone methylation is the direct inhibition of alcohol on the activity of epigenetic enzymes. While donor supplementation significantly mitigated cortico-developmental deficiencies and to a degree methyl metabolism and DNA methylation, it is important to keep in mind that enzyme activity ultimately dictates the rate of methylation. Though technical constraints limited our assessment of enzyme activity, a genomic screen of DNMTs, TETs, and an HMT was performed. Interestingly our expression analyses revealed that while DNMT transcripts were not impacted significantly by alcohol or S-AMe, *Tet3* and *Ehmt2* (G9a) were substantially upregulated by alcohol and normalized by S-AMe. Our observations both corroborate and deviate from previous observations made in a choline-supplementation FASD model. In that report, *Ehmt2* expression in the mediobasal hypothalamus of adult male offspring agreed with our findings in the embryonic cortex, where methyl-supplementation normalized the upregulation of the HMT. Assessing

DNMT genes, however, the authors observed upregulation of the DNMT1 transcript but erroneously conclude that choline supplementation exerted a normalizing effect. In fact, their data shows that choline supplementation actually reduced the expression of DNMT1 to levels significantly lower than all controls. Their assessment of the DNMT3a transcript further revealed that while no alcohol-effect was detected, the gene was significantly upregulated by both alc+choline and the choline control. Though significant variations in our models restrict our comparison (age, sex, brain region, methyl-donor), collectively our data suggest that perhaps HMT sensitivity to alcohol and methyl donors are more conserved across development and brain region while DNMTs may be more contextual in nature. Our report validates and extends the existing literature by presenting TET analysis and identifying Tet3 as a potential contributor to the DNA methylation landscape. Though our genomic analysis does not completely reconcile our cortex-wide DNA methylation outcomes, it certainly presents evidence that the normalizing potential of S-AMe supplementation transcends phenotypic observations, complementing molecular aspects of methyl-metabolism and DNA methylation, the complexities of which remain to be unraveled.

In continuation of our genomic assessment of S-AMe's role on alcohol-dysregulation, various critical neurodevelopmental targets were examined. While early pronerual genes did not reveal significant genomic sensitivity to either experimental treatment, an important network of cortical-specification genes was demonstrably impacted by alcohol and S-AMe. Because nearly all examined genes have previously demonstrated developmental sensitivity to alcohol across the literature, it is possible that our observational timepoint was beyond the window of transcriptional impact for the

early pro-neural genes. For example, Ascl1 and Ngn1 play a role in regionalization of the cortical neuroepithelium and early neural differentiation (Ma, Sommer et al. 1997). Though they go on to play developmental roles in post-mitotic neurons, peak expression occurs around E12 (Castro, Martynoga et al. 2011). Ascl1 and Ngn2 subsequently play a role in radial migration and deleterious effects of Ascl1 (up to E14.5) bear demonstrable phenotypic consequences (reduction of radial glial migration) in late gestation (Pacary, Heng et al. 2011). These results suggest that genomic cortico-developmental changes may precede phenotypic presentation and perhaps explain why early proneural gene networks are not seemingly responsive to the experimental treatment transcriptionally at E17.

In that vein, we assessed a network of cortical specification genes with mid-late peak embryonic expression. These included cotrico-cortico and subcerebral projection genes including *Sox5* and *Ctip2*, which, though peak in expression ~E14, continue to be genetically relevant as late as P0 (Lai, Jabaudon et al. 2008). Ablation studies also reveal that though peak expression of *Satb2* (a callosal projection gene) occurs early in corticogenesis, it maintains functional axonal guidance capacity as far as E18.5 (Alcamo, Chirivella et al. 2008). Finally, the *Fezf2* gene plays an extremely dynamic role throughout neural development. Expressed as early as E8.5, it plays an early role in rostrocaudal patterning and progenitor differentiation. In late gestation, the transcription factor maintains a prominent role in subcortical axon pathfinding and uniquely, maintains its expression into adulthood where it regulates motor cortex circuitry (Tantirigama, Oswald et al. 2014). We indeed found that the subcerebral axonal guidance factors Ctip2 and Fezf2 were significantly altered by alcohol. Of these, only Fezf2 was significantly

normalized by S-AMe supplementation. These results (in addition to the observed upregulation of Vglut1) appear to support our proposition that genomic presentation of environmental influences may rely on temporal expression, a factor that should be considered when genomic elements are investigated in the future. To further support this idea, it would be necessary to investigate the early proneural gene network at an earlier embryonic time point. *Ascl1*, for example, does demonstrate both transcriptional and epigenetic sensitivity to alcohol in cultured neural stem cells (Lo, Choudhury et al. 2017). Our genomic findings also echo an earlier theme which paints S-AMe supplementation as possessing a more potent intervention capacity in mature versus early stage cells and transcripts.

As discussed in the epigenetic gene findings, there remains a pressing need to understand what makes a gene more liable to alcohol or S-AMe sensitivity. If the answer were strictly surrounding DNA or histone methylation mechanisms, it is likely that normalization of epigenetic methylation and the conferring enzymes would be prominent and neuroprotection ubiquitous-a phenomenon that has eluded a significant portion of all methyl-supplement FASD studies, including our own. The more likely scenario is that alcohol-induced neuropathy in the fetal organism, though largely rooted in the metabolic action of alcohol and methyl donor production, diverts into other pathways beyond the reach of restorative supplementation. For example, alcohol metabolism produces harmful reaction oxygen species (ROS), the likes of which play roles as second messengers in signal transduction, potentially altering gene expression and post-translational modification of proteins (Covarrubias, Hernández-García et al. 2008). S-AMe also plays a role in the production of glutathione S-transferase, an enzyme critical for the reduction

of harmful ROS' (Tchantchou, Graves et al. 2004)). The interaction of S-AMe and ROS' is just one example of how S-AMe mediated alcohol neuroteratogenicity may utilize non-epigenetic pathways to confer phenotypic outcomes, reconciling why aberrant DNA methylation cannot fully account for the myriad of alcohol-related biological disruption.

3.4.3 Identification of a Novel, Functional DMR in the Cortical Specification Gene *Fezf2*

Ultimately, the epigenetic footprint of alcohol and S-AMe as a supplementation strategy was meaningful and far-reaching, presenting prominent structural, molecular, and to some degree transcriptional neuroprotection. Combined with the normalizing role of S-AMe supplementation on methyl metabolism, layer-specific DNA methylation and epigenetic correlates, we attempted to answer whether we could define a novel differentially methylated region (DMR) which could substantiate the hypothesis that DNA methylation plays a regulatory role in gene expression and the molecular transduction of environmental impacts at the nucleotide level. The cortical specification gene *Fezf2* was selected for proof of concept due to its dynamic roles throughout cortical development and it ties to abnormalities in cortical structure and reduction of forebrain size (Chen, Wang et al. 2008, Zhang, Li et al. 2014).

The characterization of this alcohol and S-AMe sensitive target was informed by previous literature reporting conserved regulatory regions critical for the expression of the gene in cortical progenitors and for subcerebral projection neuron identity and connectivity (Shim, Kwan et al. 2012). Additionally, we examined a region of the promoter around the TSS which shares several overlapping transcription factor elements and is essential for expression. We hypothesized that DMRs would be more likely observed in gene regulatory regions and as such, we included an exonic region

downstream of the TSS for contrast. We found that alcohol sensitivity was present at both the promoter and enhancer 434, where alcohol hypermethylated the region. This was in agreement with our observations of 5mC in the upper layers charged with production of subcerebral projection neurons. While S-AMe supplementation did not normalize DNA hypermethylation at the promoter, it did so at the critical enhancer. On the other hand, the exonic region demonstrated no statistically significant response to either alcohol or S-AMe, supporting the notion that DMRs may be confined to regulatory gene regions. As Eckler et al propose, however, the enrichment of *Fez*f2 (and similar specification genes) at the upper cortical layers suggests the existence of repressor sequences to restrict its expression to the appropriate cells (Eckler et al 2014). How and where these are presented in the DNA methylation landscape requires future investigation.

Finally, the absence of 5hmC-specific methyl sequencing prevents us from fully understanding the DNA methylation landscape of *Fezf2*. For example we cannot account for existing 5hmC within the gene body (i.e. exons) or other regions which may be differentially expressed in response to alcohol or S-AMe. Additionally, while two important regulatory regions were presented, there remains a substantial amount of uncovered loci which could reveal a more complicated relationship between the occurrence of DMRs and gene expression. Advances in epigenetic tools, including TALEN technology now allow for the site-directed manipulation of epigenetic effectors, including DNMTs and TETs. Their use in verifying the functional contributions of suspected regulatory DMRs in the future will be crucial to our understanding of that relationship.

3.4.4 Summary and Conclusions

In this study we observed that alcohol-mediated disruption of cortical development in late gestation was widespread, reaching elements of cellular maturity, migration, fate-specification, and synaptic plasticity. These observations were correlated with the alteration of important epigenetic regulators. Consequently, alcohol impacted both global and layer-specific abundance of the DNA methylation marker 5mC, which has been largely supported as a transcriptional influence in neural development. How alcohol achieves molecular outcomes was the major investigative course herein. Particularly, the role of alcohol metabolism on the methyl metabolism and DNA methylation biogenesis pathways provided rationale that the methyl-donor S-AMe could be culpable. As such, we examined whether supplementation of prenatal alcohol with S-AMe could mitigate epigenetic dysregulation and improve developmental outcomes.

We found that S-AMe was a normalizing factor across structural, cellular, and morphological aspects of development in the cortex. Moreover, the protective nature was detectable at the level of methyl metabolism and DNA methylation as evaluated in a layer-specific manner. Probing deeper into the genomic level, we found that both alcohol and S-AMe neuroprotection were detectable at nucleotide resolution. Apparently selective for regulatory regions, differential methylation patterns of the two external stimuli dually impacted gene expression, supporting the regulatory nature of the DNA methylation program in the developing cortex.

Though prominent, S-AMe neuroprotection was not as widespread as alcohol's impact. In many cases, S-AMe supplemented groups showed normalizing trends but did not achieve significance statistically, reflecting a probable muted action of S-AMe in

some respects. This limited capacity of methyl supplementation strategies (relative to alcohol) has been a feature of much of the FASD literature. Perhaps rooted in the non-exclusive nature of S-AMe as a DNA methyl donor (it is a critical donor for histone methylation and polyamine synthesis), supplemented S-AMe may be diverted toward other biological pathways. Another very likely scenario is that alcohol metabolism inflicts damage to the cell through non-epigenetic pathways. For example, the production of ROS and mitochondrial dysfunction by alcohol has been shown to induce oxidative damage in the brain. Overall, the embryonic cortex appears to be a highly responsive target of both alcohol and methyl supplementation and more importantly, demonstrates a rectifiable nature. This is substantial as a significant population is (knowingly or unknowingly) at risk for some level of gestational alcohol exposure.

A common observation throughout the evaluation of our findings was that not all cell types, phenotypes, or genes responded equally to methyl supplementation. Consistently, a pattern emerged pointing to mature cell types and late-specified genes as more susceptible to neuroprotection (versus proliferating neruogenic cells, early genes, etc.) at the examined age. The selective nature of some genomic regions versus others was similarly apparent, indicating that, perhaps, intrinsic context selectively defines the response to S-AMe. At this time however, it remains unclear if and how genome context could dictate environmental sensitivity of a gene or cell. Additionally, it is not known how this mechanism may register stimuli differentially. Another unanswered question features the reconciliation of unilateral alcohol and methyl supplementation effects at the metabolic level with bivalent outcomes at the genomic, epigenetic, and phenotypic level. For example, alcohol has consistently demonstrated an inhibitory role, and methyl

supplementation an enhancing role in the methyl metabolism cycle. Examination of DNA methylation across various contexts, however, describes the simultaneous up and downregulation of various alcohol targets. DNA methylation follows suit, displaying hyper and hypomethylation in a gene or cell-dependent manner. The unknown mechanisms at work conferring the bivalence of alcohol are apparently also at work communicating the normalizing action of S-AMe, as directionality of its effect was almost always alcohol-dependent. Importantly, here we observed that S-AMe consumption (no alcohol, *ad libitum*) in and of itself did not overstimulate the production of DNA methylation (tissue or cell wide) or negatively impact gene expression or phenotypes throughout the cortex. This is important because several lines of evidence have demonstrated that over-consumption of dietary methyl precursors can be detrimental throughout development (Pickell, Brown et al. 2011, Mikael, Deng et al. 2013). This finding hints that alcohol-driven epigenetic dysregulation may not be strictly dictated by methyl-donor insufficiency, since unrestricted methyl supplementation observed normative epigenetic, genetic, and phenotypic outcomes. A more thorough investigation in the future should reconcile enzymatic activity with the exposure patterns observed here. Regardless, our findings speak to the tolerability of S-AMe at this dosage and support its potential utility as a therapeutic in developmental disease.

COMPREHENSIVE DISCUSSION

In this Dissertation we describe that DNA methylation, as a principle epigenetic mechanism, is a dynamic and cell-unique landscape. Developmental study in the cerebellum and embryonic cortex revealed that no two cell types experience the exact presentation of DNA methylation at any given time. Rather, cells may both acquire and lose DNA methylation in unique patterns, or, "programs" that align with their developmental events. In support of this phenomenon, epigenetic correlates, including methyl-DNA binding proteins, compliment these DNA methylation programs. More importantly, developmental DNA methylation may be a crucial component regulating gene expression. For example, we demonstrated that key Purkinje cell genes reflect cell-wide DNA methylation trends at the genomic level. While simultaneous expression change was observed, it remains unclear whether DNA methylation precedes expression and developmental processes (supportive of DNA methylation as a developmental regulator) or whether DNA methylation is a by-product of cellular development. This examination also shed light on some important DNA methylation dynamics, including the mutual exclusivity of 5mC and 5hmC within the nucleus during the first postnatal week, and the gradual overlapping presentation that likely reflects genome-wide DNA methylation re-distribution. Additionally, throughout the cerebellum and in the embryonic cortex, we observe 5hmC as reliably strengthened in maturing cell types.

To build evidence for DNA methylation as a regulatory mechanism we investigated DNA methylation landscapes in an environmentally-mediated disease-state which has been transcriptionally and phenotypically linked to wide-spread brain

abnormalities for decades. A mouse model of FASD not only confirmed cortex-wide neuropathy (including reduced proliferation, migration, and maturation) but also demonstrated cumulative manifestation of the environmental insult at a structural level which could underlie a host of cognitive deficits attributed to FASD in later life. Interestingly, these events were accompanied by parallel alteration of the cortical DNA methylation program, further supporting its sensitivity to environmental exposures and relevance as a developmental device. This study importantly showed that though the impact of alcohol was identifiable from the tissue to the gene level, the DNA methylation profile of prenatal alcohol exposure was divergent across cell types. This recurring observation reiterated the cell-specificity of the developmental DNA methylation program and implies it as a mechanism that determines how a cell or loci may uniquely internalize environmental inputs.

In order to investigate how alcohol as an external signal could act upon the DNA methylation signature (and consequently, gene expression), we exploited a known methyl metabolism deficit induced by alcohol. Methyl metabolism has been reported to be crucial for early brain development and insufficiency of various metabolites producing the active methyl donor S-AMe have been linked to neuropathy and cognitive deficits similar to FASD. Because S-AMe is the sole donor for DNA and histone methylation, our previous observations of alcohol dysregulation of DNA methylation prompted us to examine whether manipulation of S-AMe in the presence of alcohol could inhibit its neuroteratogenicity. We found that indeed S-AMe was an effective (though not ubiquitous) protector against alcohol-induced structural and phenotypic deficits in the cortex. This provided support for our proposition that alcohol as an environmental insult

utilized epigenetic pathways to communicate its detrimental action at the cellular level. A missing piece of the picture, genomic analysis was subsequently undertaken to confirm the regulatory nature of DNA methylation and the environmental sensitivity of relevant genomic regions to both detrimental and neuroprotective external stimuli. Through this analysis we found that a critical gene involved in cortical fate specification and axonal guidance was hypermethylated at regulatory promoter and enhancer sites, and simultaneously exhibited transcriptional fluctuations. S-AMe's protective action was once more observed at the nucleotide and transcriptional level, indicating that the same dynamics at work in the cellular landscape of the embryonic cortex could be demonstrated at the genomic level.

While the limitations of the work are detailed throughout, much understanding was gained from these studies, individually and collectively. The major and recurrent themes included the cell-unique nature of DNA methylation patterns. Recall from Chapter 1that evolving DNA methylation landscapes have been previously characterized during neural specification. The evidence described here confirms those observations *in vivo* and proposes that the DNA methylation program, by shaping the cellular transcriptome, may underlie cell-uniqueness.

Through normal and disease states, our work also highlights the regulatory capacity that DNA methylation possesses during development. Beyond spatial, temporal, phenotypic, and genomic correlation, DNA methylation analysis at the nucleotide level provides evidence that even minute methyl signatures (at critical regions) can suffice to alter the course of gene expression. Of course, this proposition requires expansive confirmation in the form of multiple genes, gene regions, and 5mC/5hmC discriminatory

sequencing. Finally, in addition to its emerging regulatory role, DNA methylation is capable of internalizing environmental information, positioning the mechanism at the forefront of environmentally-driven disease. Interestingly, here we illuminate the dual nature of this external communication mechanism, describing that the DNA methylome can be driven bimodally by distinct stimuli. Though the particulars of the alcohol/methyl/epigenetic triad likely span beyond the limits of methyl metabolism (i.e. non-epigenetic elements, alcohol-mediated oxidative stress, enzyme activity, etc.), the epigenetic and phenotypic outcomes of alcohol and S-AMe share bilateral characteristics. Again, this diversity is likely dictated by genomic elements beyond our current understanding but nonetheless demonstrate the sensitivity and rectifiable nature of the DNA methylation program in development. The prominent role we have laid out implies that normal neural development is likely contingent upon undisrupted epigenetic progression. While not likely all-encompassing, DNA methylation may shed some light on developmental disease etiology across various environmentally-mediated states in the future.

Epigenetics as a mechanism of organismal diversity has filled a long-held void which failed to reconcile intrinsic biological factors with environmental exposures. Though the precise molecular mechanisms of environmental transduction have eluded researchers, today, epigenetic modifications like DNA methylation are offering answers. Uniquely positioned at the intersection of environmental input and epigenetic biochemistry, alcohol as an environmental pressure during development offered a window by which to view the molecular transduction of environmental inputs (Figure 43). Through this modality we probed the dynamics of epigenetic mechanisms in

response to the environment. The evidence-based concepts built here push forward a better understanding and establishment of epigenetic states or signatures which are critical to transcriptional regulation, phenotypic, and functional outcomes. Using what we learned here, the future of DNA methylation in development promises a wealth of possibilities for the landscape as a diagnostic tool. Further, epigenetic editing and epigenetic-altering compounds may become useful therapeutic tools in developmental disease.

FUTURE DIRECTIONS

The notion that DNA methylation bears capacity as a developmental regulator, though continually mounting has taken a back seat in recent years to a shifting focus of the field toward the examination of the mechanistic particulars of the feat. As such, the future of DNA methylation research will extensively feature genomic methyl profiling and targeted manipulation. Methyl profiling will be crucial toward our understanding of cell and gene-unique programs as high-throughput assays could clarify the cell-unique methylation patterns down to the level of the cellular transcriptome. Additionally, methyl-sequencing of disease experiencing patients may aid in the development of biomarkers for environmentally-driven disease (a tool already heavily employed in cancer and emerging in alcohol disease) (Wittenberger, Sleigh et al. 2014, Liu, Marioni et al. 2016). In fact, the use of methyl-profiling of the genome in disease is a crucial element toward our understanding of methylation and expression "thresholds" which trigger the onset of a disease phenotype. This will be particularly relevant in diseases driven by "Latent Early- life Associated Regulation", which proposes that epigenetic landscapes in the somatic cells can enduringly carry early life "experiences" in a cumulative fashion which may or may not eventually achieve pathological thresholds (Lahiri, Maloney et al. 2009, Maloney and Lahiri 2016). The value of such investigation in FASD is extremely relevant as many exposed offspring, through subtlety of early life phenotypes, escape diagnosis but maintain a propensity for neural and behavioral deficits in later life. Finally, DNA methylation profiles spanning larger regions of the genome will additionally clarify patterns which may underlie environmental propensity.

Ultimately, the goal is the utilization of DNA methylation signatures as quantifiable predictors of life outcomes.

On the other hand, epigenetic manipulation may be used *in vitro* to either challenge the prevailing theory of DNA methylation as a transcriptional regulator or to pinpoint obligatory elements. Further, these tools tackle the "chicken versus egg" dilemma that has plagued the field of epigenetics for years. Ongoing work in our lab has demonstrated the functionality of epigenetic editing in neural stem cells and confirmed the critical nature of DNA methylation at the regulatory promoter of the pro-neural *Ascl1* (Lo, Choudhury et al. 2017). Though the subfield of epigenetic editing has only recently taken flight, the strategy of engineering DNA-binding domains to manipulate and normalize disease-modified landscapes remains a long-term goal.

Reflecting on our current study, recurrent gaps for future consideration included the need for a better understanding of not just genomic methylation landscapes, but also the interaction of these sites with the appropriate downstream transcriptional elements (i.e. direct transcription factor binding, methyl-binding proteins, RNA polymerases, etc.). Excitingly, emerging tools including affinity assays and SILAC-based proteomic analysis and high-fidelity Fluorescence Lifetime Imaging based Forster Resonance Energy Transfer (FLIM-FRET) are beginning to unravel the mechanisms by which sequence elements like DNA methylation either recruit or prohibit binding and influence transcription (Bartke, Vermeulen et al. 2010, Chen, Damayanti et al. 2014), clarifying our understanding of the functional associations of the DNA methylome. These tools will likely prove equally useful in our understanding of inter-epigenetic frameworks. While not detailed here, cross talk between epigenetic elements (i.e. DNA methylation, histone

methylation, microRNAs) is likely prominent and will further add to the complexities of DNA methylation as a regulatory mechanism. It will be crucial in advanced epigenetic study, to consider the multitude of epigenetic mechanisms which may converge on a regulatory region to confer meaningful change.

Finally, the promising structural and molecular neuroprotection of S-AMe as a dietary intervention strategy beckons further optimization in high-risk pregnancies such as FASD. Some literature has proposed that the co-administration of methyl-supplementation and methyl metabolism co-factors (i.e. vitamin B, zinc, omega-3) may enhance the protective reach of methyl precursors, though others have found that this strategy is not consistently optimizing (Seyoum and Persaud 1997, Xu, Li et al. 2006, Kusat Ol, Kanbak et al. 2016, Sogut, Uysal et al. 2017). Future study of methyl-intervention across methyl-insufficiency associated developmental disease should further probe the differential outcomes of variable methyl supplement source (i.e. folic acid versus choline or S-AMe), dose, administration window (i.e. pretreatment versus post-exposure intervention, etc.), and/or the compound action of multiple donors and co-factors. Moreover, the identification of novel nutrient-sensitive differentially methylated regions (ns-DMRs) here should be followed by the investigation of additional ns-DMRs in nutrient-affected developmental disease, as they offer a wealth of opportunity for the safe and effective use of dietary intervention which may rival current therapeutics.

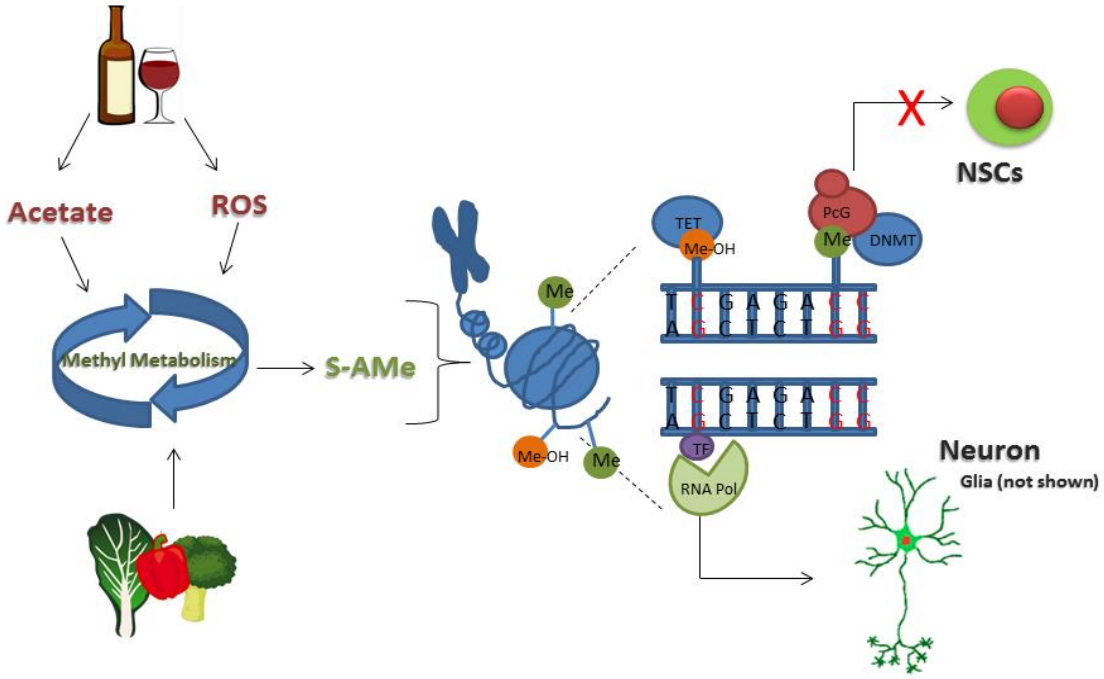

Figure 43. Environmental signal integration is mediated by methyl metabolism and epigenetic regulation of the genome

Conceptual illustration depicts the dual integrative nature of the methyl metabolism cycle toward dietary factors including alcohol and dietary folic acid. The output of the cycle, S-AMe, is the obligatory donor for DNA and histone transmethylation (middle). DNA and histone methylation (along with other epigenetic factors) influence the structure of chromatin and, ultimately, the transcription factors which dictate gene expression and confer cellular phenotypes. TF: Transcription factor, Me: Methylation, Me-OH: Hydroxymethylation, PcG: Polycomb group repressor complex, RNA Pol: RNA Polymerases, NSCs: Neural stem cells

APPENDIX A

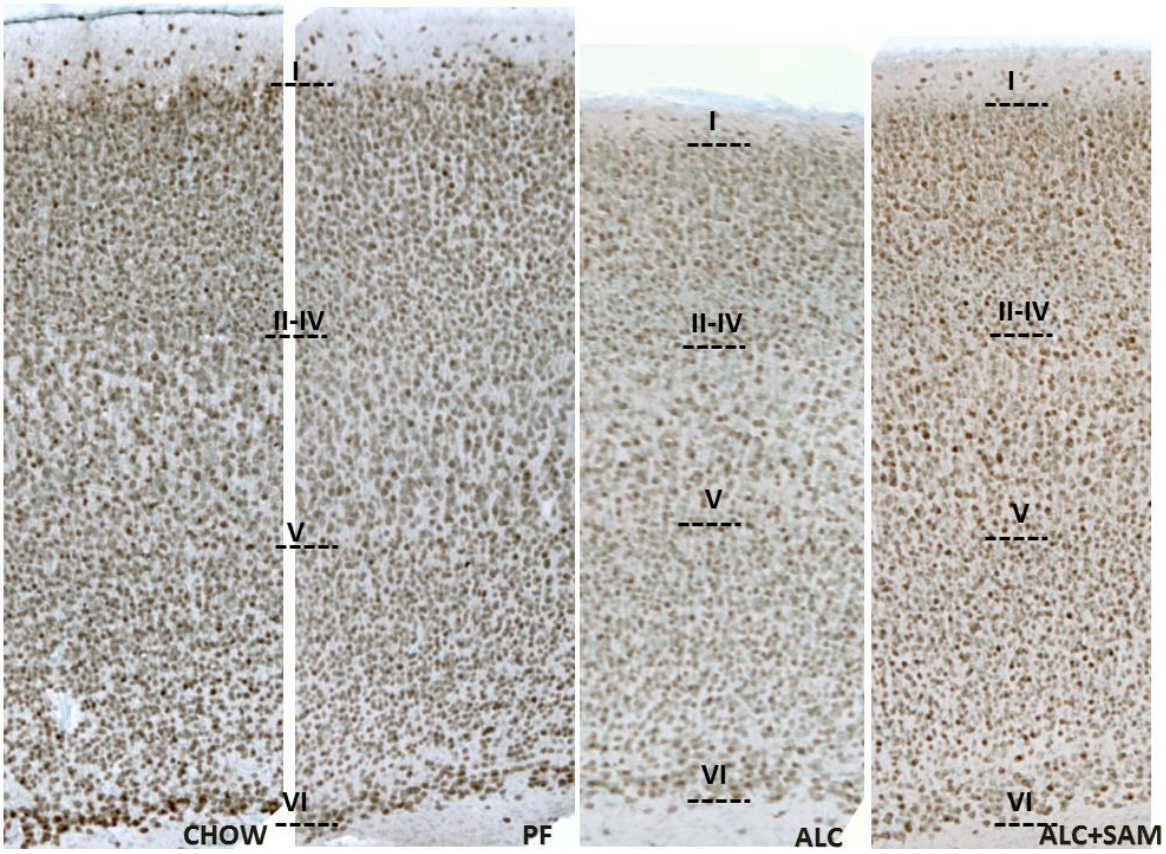

Figure A-1. Cortical Length and NeuN Distribution Across the Cortical Column at P7

Representative cortical columns of the postnatal (P) day 7 sensorimotor cortex across groups stained for the nuclear neuronal antigen NeuN. The cortical column at P7 maintains a sensitivity to alcohol at the sensorimotor region, where alcohol-induced cortical thinning persists. Offspring of groups supplemented with S-AMe are protected from cortical thinning. Numerals denote the approximate borders of the six cortical layers.

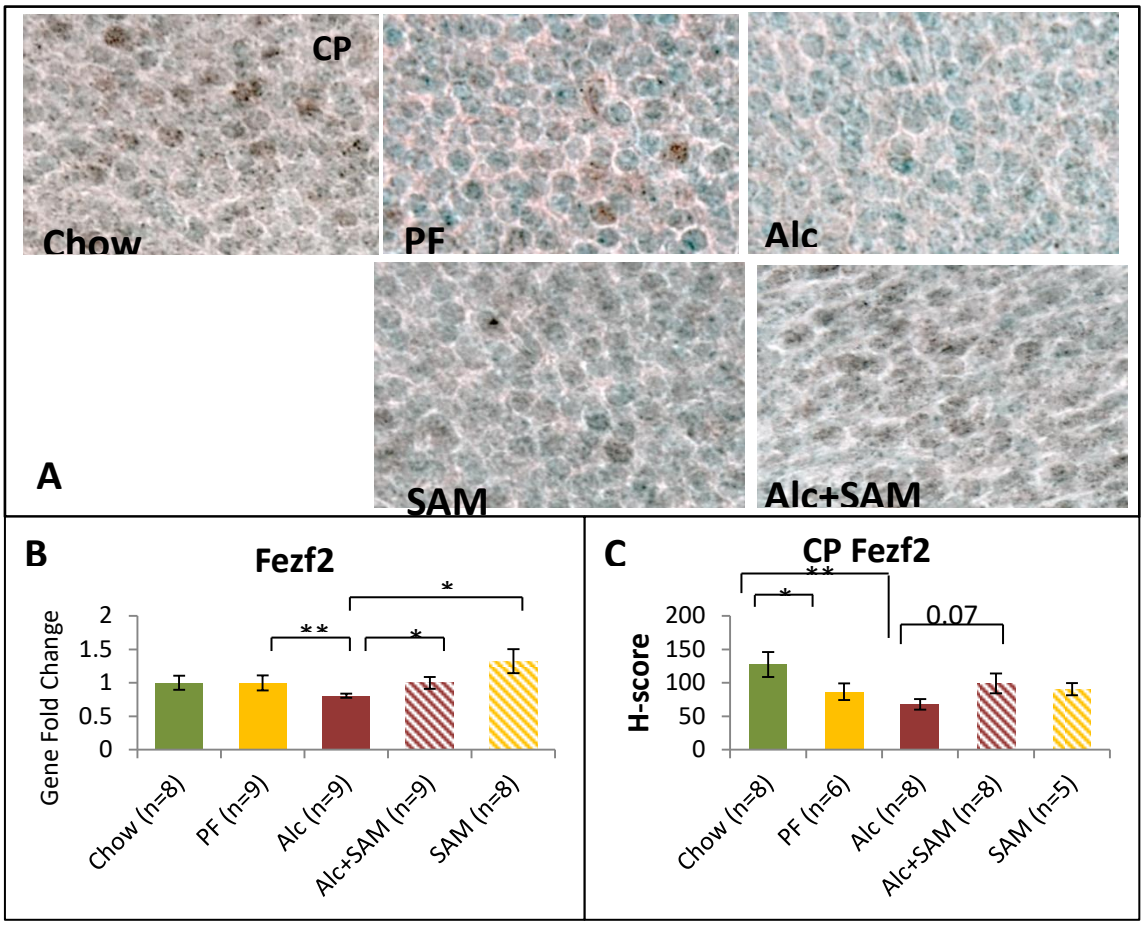

Figure A-2. The transcription factor Fezf2 is decreased by alcohol in the cortical plate and normalized by S-AMe supplementation

(A) Representative images of the cortical plate reflecting the immunoreactivity of the Fezf2 protein (B) Relative expression of Fezf2 mRNA across cortical tissue samples at E17 showed a decreased expression of the transcript in the alcohol, normalized by S-AMe supplementation (C) A similar pattern was found in the quantitation of Fezf2 immunoreactivity in the CP. All data are presented as Mean±SEM. *p≤0.05, **p≤0.005; CP: cortical plate. N reflect the number of independent litters represented in each group

APPENDIX B

Primers used for qmethyl study		
Name	Sequence	Annealing temp
Gsbs_promoter_F	ATCATTGTGGTGTCCTGCAA	62
Gsbs_promoter_R	CCAGTTGCTGGTGAGAAGGT	62
Gsbs_genebody_F	CCTGTAAGACCCGACACCAT	62
Gsbs_genebody_R	TATGAAGAGCTGGGCCTGAT	62
Itpr1_promoter_F	TCAGACACAAGTTCGCAACC	60
Itpr1_promoter_R	GCTTCAGCAGAACATCCACA	60
Itpr1_6835-7035_F	CCACCCTCCCCTGTCTATTT	62
Itpr1_6835-7035_R	GCAGAGACCAGGATGTAGGG	62
Itpr1_1481-1717_F	CGGTCCAGAATGCTCTGTTT	62
Itpr1_1481-1717_R	GCACAGTCAATAGGCGTCAA	62
Itpr1_8480-8753_F	ACCCACATCACCTTCCTGAG	62
Itpr1_8480-8753_R	TCAGCAATCGAGAGAGTCCA	62
Grid2_5625-5953_F	CATGTCTGGTGTCTGGCATC	62
Grid2_5625-5953_R	TGTTCCTTTCTGGCAGTCCT	62
Baiap2_4867-5122_F	GTTGCTGCTCTTGGTCTGGT	62
Baiap2_4867-5259_R	CTCAGACACCCCTTCCTGTC	62
Cacna1g_6602-7380_F	TCTGCTTCATGCAGGCTCTA	62
Cacna1g_6602-7380_R	CATCTCCTTCCTCCTCATCG	62
Cacna1g_0388-0643_F	AACAAGATGGGAGGGGAGAC	62
Cacna1g_0388-0643_R	TGTGGTGGAAGAACAGCAAG	62
Cacna1g_4907-5732_F	TCTTGGTGTTCAGAGGCAGA	62
Cacna1g_4907-5732_R	GCTTACCCTGCAGCCAAGT	62
Cacna1g_6856-7487_F	GGCTGTGGGTACCAGAGAAA	62
Cacna1g_6856-7487_R	ACCCCATCTTGGCAACTG	62
Atp2a3_4894-5532_F	CCTGGGAAGCTAGGAAAACC	62
Atp2a3_4894-5532_R	AGAGACAGACCTGGGGTGAA	62
Syt2_3350-4406_F	ATGTGGATTAGGGAAGATCAGCAT	62
Syt2_3350-4406_R	GAGGGACAGTGGACTTCTATTGGT	62
Nrxn2_7997-8822_F	GGATCAGGTCAGAAATGTGACAAC	62
Nrxn2_7997-8822_R	GCTCACTCATCCTTCAAGGTCTAA	62
Nrxn2_7791-8396_F	TGGATTGTTCTATAGGATGGCTCA	62
Nrxn2_7791-8396_R	AGAAAACACAGATAAAGGGCTTGG	62
Rgs8_6651-7232_F	TCTTTAGGTCCTGGTCCTCTTGTC	62
Rgs8_6651-7232_R	GCAGGAACACACACACAAGTACAG	62
Rgs8_7941-8550_F	CTCAGTCTCCTAAGAACCCATCCT	62
Rgs8_7941-8550_R	TCACCTCAAAGTCTTCACCTCTTG	62
Rims1_6189-6687_F	CACACACAATCCTGATGTGAAGAC	62
Rims1_6189-6687_R	AGAGCACCAGTGTAAGTGGAGAGA	62
Rims1_2011-2429_F	TGGCTAAGTAGGGTTATTTTACCTTC	62
Rims1_2011-2429_R	AGGACTGCTTGACAGTCAGGTTTC	62
Rims1_880-1414_F	CTAGAGCAAAGAGGATGGAACACA	62
Rims1_880-1414_R	CTGACTGCTACACCAATCTTCAGG	62
Fgf14_5025-5307_F	TAGAGCCCGTTACTTGGTTCCTAC	62
Fgf14_5025-5307_R	CCATTTACTGAAAACACCAAGTGC	62

TaqMan gene expression assay		
Gene	Assay ID	Amplicon Size (bp)
Cacna1g	Mm00486572_m1	85
Grid2	Mm00515053_m1	86
Syt2	Mm00436864_m1	64
Rgs8	Mm01290239_m1	68
Gapdh	Mm99999915_g1	107

Table B-1. List of Primers for Q-methyl Study and Taqman Probes

F: forward primer; R: reverse primer. All TaqMan gene expression assays were obtained from Applied Biosystems (Thermo Fisher Scientific) and are labeled with the appropriate catalog number.

A. Purkinje Specific Genes		Gene expression (fold change)	
Symbol	Description	P21 vs P7	P42 vs P7
Atp2a3	ATPase, Ca++ transporting, ubiquitous	4.46	3.82
Baiap2	brain-specific angiogenesis inhibitor 1-associated protein 2	1.73	1.48
Cacna1g	calcium channel, voltage-dependent, T type, alpha 1G subunit	1.93	-1.03
Calb1	calbindin 1	1.41	2.29
Car8	carbonic anhydrase VIII	2.11	2.73
Gsbs (Pp1r17)	Protein phosphatase 1, regulatory subunit 17	11.9	7.76
Gria1	glutamate receptor, ionotropic, AMPA1 a(α1)	2.21	1.43
Grid2	glutamate receptor, ionotropic, δ2	2.34	1.66
Homer3	homer homolog 3 (Drosophila)	2.94	2.12
Itpr1	inositol 1,4,5-triphosphate receptor 1	3.6	4.88
Pcp2	Purkinje cell protein 2 (L7)	1.99	3.46
Pcp4	Purkinje cell protein 4	1.62	1.57
Slc1a6	solute carrier family 1 (high affinity aspartate/glutamate transporter), member 6	1.97	1.36
Trpc3	transient receptor potential cation channel, subfamily C, member 3	4.29	1.61

B. Synaptic genes:		Gene expression (fold change)	
Symbol	Description	P21 vs P7	P42 vs P7
Fgf14	fibroblast growth factor 14	3.89	1.59
Grip1	Glutamate receptor-interacting protein 1	-5.8	-2.72
Nlgn1	Neuroligin-1	1.17	-1.51
Nrxn2	neurexin II	1.68	1.02
Plxnb2	cell adhesion and recognition-related gene; neurite growth and synapse formation-related gene	-2.19	-1.21
Rgs8	regulator of G-protein signaling 8	7.09	2.82
Rims1	Regulating synaptic membrane exocytosis 1	3.29	1.88
Syt2	SNARE synaptotagmin II	4.77	2.3
		(CDT-DB database;	(Szulwach at el 2011)

Table B-2. Developmental Gene Regulation of Purkinje Cells and Cerebellar Synaptic Targets

Developmental gene expression changes in Purkinje cell characteristic and synaptic genes. A. Table of genes predominantly expressed in Purkinje cells of the cerebellum and their expression levels at comparable stages of postnatal development. B. Table of genes playing prominent roles in synapse formation in the brain and their expression levels at comparable stages of postnatal development. Data compiled from CDT-DB database (http://www.cdtdb.neuroinf.jp/CDT/Top.jsp) and Szulwach et al 2011

Alc. Frequency	Form	Met. Frequency	Protective
Acute, Embryonic			
300mg/100mL media (E9.5-E11.5)	S-AMe	0.05-3mM (E9.5-E11.5)	embryopathic effects
2.0-8mg/mL (GD8.5-10.5)	FA	0.01mmol/L-1mg/mL (GD8.5-10.5)	head length, embryo morphology, microcephaly, neural folds; miR10a; Hoxa1 mRNA
4.0 mg/ml ethanol, (GD8.5-10.5)	FA/VB_{12}	FA (10^{-5}, 10^{-4} mol/l) or VB_{12} (10^{-6}, 10^{-5} mol/l), GD8.5-10.5	embryopathy, NTD defects
1-4%	MTHF	microinjection, N/A	neurocristopathies; hyperhomocystemia
two doses, 0.0 15 ml/g (PCD 8)	FA	5 mg/ml at 1 µl/h (PCD 6-7)	N/A
single dose 25% (E7 or E8)	Met	70 -150 mg/kg (E7 or E8)	cleft palate, limb malformation
Chronic, Embryonic			
6.4% (E6-E12 liquid diet)	Met+ Zn	Zinc (15mg/kg)+ Met (200mg/kg), E6-12	
2.4%-7.2% (E6-E22 liquid diet)	Bet+FA	Bet 1% w/v +FA 60mg/kg (E3-P0)	cortical neuroapoptosis, apoptotic proteins
3-4g/kg (GD2-68 (5x week))	FA	2mg/kg, (GD2-68 (5x week))	liver folate
5.0 g/kg (GD6-15)	FA	60.0 mg/kg (G1-16)	microcephaly, energy production, signal pathways and protein translation genes
5.8g/kg (GD9-birth)	cocktail	3SZM methyl diet (2 wks preconception-gestation)	embryonic weight, prenatal mortality, vertebral malformations
Postnatal			
2.5 g/kg (GD4-41)	C	10 mg/kg (GD4-148)	N/A
3.0 g/kg (P2-P10)	C	100mg/kg (P2-P20)	hipp hypermethylation, ameliorated by Choline supp
6.7% (G7-G21 liquid diet)	C	642mg/L liquid diet (G11-birth)	POMC and histone hypermethylation, DNMT1 and MeCP2
5.25 mg/kg (P4-P9)	C	100 mg/kg (P4-30)	hyperactivity and increased M2/4 receptor density
6.0g/kg/day (GD5-20)	C	250mg/kg (G5-20)	brain weight, behavioral outcomes
35%, liquid diet	CDP-C	100mg (P0-P21)	Pukinje cell maturity
4.8-7.2% (E6-P21 liquid diet)	Bet+ O-3	30 mg/100 g (dam wt.),E3-P21	apoptosis and neurodegeneration
Behavioral			
5.25 g/kg (P4-9)	C	100 mg/kg (PD 11-20, PD 21-30, or PD 11-30)	spatial memory, learning
6.0 g/kg (P5)	C(Cl)	10 µL of 18.8 mg/ml (P1-5 and P6-20)	balance and coordination
5.25g/kg (P4-P9)	C(Cl)	100 mg/kg (PD 40 to 60)	working memory
5.25 mg/kg (P4-P9)	C	100 mg/kg (P10-30)	trace eyelblink conditioning deficits
35% (GD 6-20)	C(Cl)	25 mg/ml (PD 2 to 21)	visuospatial discrimination
6.6 g/kg (PD4-9)	C(Cl)	18.8 mg/kg (PD4-30)	hyperactivity, spatial discrimination reversal learning
6.0 g/kg (P4-9)	C(Cl)	10, 50, or 100 mg/kg (PD 10-30)	open field hyperactivity, spatial learning
Human			
"heavy drinking"	C	750 mg, daily (Avg. 19 weeks-birth)	Bayley Mental Development Standard Score
variable	C	750 mg, daily (Avg. 19 weeks-birth)	hear rate during visual habituation
variable	C	500mg, daily (9 mo)	long-delay memory
high exposure	C	625mg/d (6 weeks)	N/A

Table B-3. Methyl-supplementation Strategies Across Developmental Alcohol Models.

A comprehensive summary of methyl-supplementation studies performed across various models of developmental alcohol exposure. Categories include acute and chronic embryonic exposure, postnatal exposure, studies focued on behavioral outcomes, and human studies. E: Embryonic Day, GD: Gestational Day, PCD: postconception day, P: Postnatal Day, C:Choline, C(Cl): Choline Chloride, SAMe: S-adenosylmethionine, FA: Folic acid, CDP-C: CDP-Choline, VB12:vitamin B12, MTHF: 5-methyltetrahydrofolate, Met: L-methionine, Bet: Betaine, O-3: omega-3 fatty acid, Zn: Zinc

Primers used for methyl pyrosequencing study		
Name	Sequence	Annealing temp
Ascl1_05_F	Qiagen, PM00219695	52
Ascl1_05_R	Qiagen, PM00219695	52
Ascl1_05_S	Qiagen, PM00219695	
Ngn1_Promoter1_F	TTTTAGGAGGGGGGTTGG	57
Ngn1_Promoter1_R	ACCCACCTCAAAACCCCTTAAATAC	57
Ngn1_Promoter1_S	CCTCCCTAACCACCT	
Ngn2_Promoter1_F	GGGAGGAGGTGGTTAGGGA	55
Ngn2_Promoter1_R	ATCAACTCCTATAAACACCAAATATAA	55
Ngn2_Promoter1_S	GAGGTGGTTAGGGAG	
Syt2_02_F	Qiagen, PM00208894	55
Syt2_02_R	Qiagen, PM00208894	55
Syt2_02_S	Qiagen, PM00208894	
Fezf2_Promoter_F	GGGTTAAGGGATATTTTGGTGATTAGA	54
Fezf2_Promoter_R	AACCCAAACCTAAACAAAATTCCT	54
Fezf2_Promoter_S	GGGGTTTTTTGAGGT	
Fezf2_Exon1_F	GGGAGTTAGTTGTTTTTTTTAAAGTTTGAG	55
Fezf2_Exon1_R	ACCATACAACCTATCTCTTCTATCACATTT	55
Fezf2_Exon1_S	GGGGGAAAGTAGGGTTT	
Fezf2_Enhancer434_F	GTTGGGAAATAAATAATTTTAAGGTAGTTG	53
Fezf2_Enhancer434_R	TCTTTTCTTCCTATCCCAAACAAT	53
Fezf2_Enhancer434_S	AGTTTGTTTTTAGAAATATGTTA	
TaqMan gene expression assay		
Gene	Assay ID	Amplicon (bp)
Ascl1	**Mm03058063_m1**	67
Ngn1	**Mm00440466_s1**	82
Syt2	**Mm00436864_m1**	64
Fezf2	**Mm01320619_m1**	76
18S	**Mm03928990_g1**	61

Table B-4. Table of Methyl-pyrosequencing Primers and Taqman probes

All proprietary primer sequences were obtained from Qiagen and are labeled with the appropriate catalog number. F: forward primer; R: reverse primer (biotinylated); S:sequencing primer. All TaqMan gene expression assays were obtained from Applied Biosystems (Thermo Fisher Scientific) and are labeled with the appropriate catalog number

Figure 27					N numbers					Mean ± SEM				
	HOV	ANOVA	F	Welchs	Chow	PF	Alc	Alc+SAM	SAM	Chow	PF	Alc	Alc+SAM	SAM
A	0.283	0.354	1.125		14	13	13	13	7	10.0214	11.3462	10.5692	9.9692	10.3943
										0.51143	0.28071	0.66152	0.548	0.74228
B	0.391	0.227	1.517			10	10	10	10		13.1269	12.3816	12.0206	13.275
											0.56273	0.50341	0.46022	0.40446
C	E7							13	12			16.3382	15.8995	
	0.181	0.685	0.169									0.52548	0.95377	
	E8							15	12			18.0108	18.0554	
	0.625	0.966	0.002									0.70357	0.73647	
	E9							15	12			17.8916	18.5409	
	0.393	0.389	0.769									0.4378	0.62219	
	E10							15	11			18.2217	17.4457	
	0.013			0.615								0.49241	1.42073	
	E11							15	13			17.0459	16.7571	
	0.038			0.823								0.46937	1.18227	
	E12							11	13			17.8325	16.5473	
	0.412	0.336	0.968									0.71462	1.03633	
	E13							13	10			16.9853	17.9381	
	0.112	0.516	0.436									1.18586	0.5536	
	E14							12	13			18.2874	16.9284	
	0.803	0.176	1.948									0.71968	0.65862	
	E15							10	12			18.5684	17.7958	
	0.509	0.556	0.359									0.7176	1.01055	
	E16							10	12			17.8721	17.2302	
	0.99	0.631	0.237									0.99009	0.87517	

Figure 28					N numbers					Mean ± SEM				
	HOV	ANOVA	F	Welchs	Chow	PF	Alc	Alc+SAM	SAM	Chow	PF	Alc	Alc+SAM	SAM
A	0.115	0.001	5.467		13	10	15	13	5	0.5658	0.5068	0.4914	0.4728	0.5724
										0.02705	0.01507	0.0107	0.01336	0.01598
B	0.223	0.31	1.268		7	6	6	5	5	0.057	0.055	0.0548	0.0531	0.0593
										0.00252	0.00181	0.00073	0.00174	0.00229
C	0.116	0.84	0.279		8	6	13	5		3.9073	3.8758	3.7375	3.9623	
										0.12674	0.27122	0.1649	0.2429	
D	0.007			0.729	5	6	5	5		0.2966	0.2728	0.2684	0.2666	
										0.0238	0.01566	0.00495	0.00722	
E	0.097	0.978	0.11		12	13	12	16	6	6.5	6.1538	6.5	6.5625	5.3333
										0.3371	0.56439	0.71244	0.35479	0.66667

Figure 29						N numbers					Mean ± SEM				
		HOV	ANOVA	F	Welchs	Chow	PF	Alc	Alc+SAM	SAM	Chow	PF	Alc	Alc+SAM	SAM
A		0.569	<0.0001	9.803		7	5	9	8	9	18.6775	18.303	19.2365	18.6855	17.881
											0.18337	0.13626	0.18782	0.1564	0.15904
B						8	5	9	7	5	18.2086	18.2222	18.2731	17.9459	17.4791
											0.07016	0.17032	0.07935	0.06715	0.17089
C	Cort	0.017			0.051	7	5	9	8	9	1.0777	1.0205	0.862	0.9336	1.0167
											0.04436	0.07404	0.04496	0.11013	0.07862
	Liver	0.0417			0.028	8	5	9	7	5	1.016	0.9779	0.691	0.8225	0.932
											0.14259	0.11516	0.03653	0.07069	0.14255
D	Cort	0.337	0.537	0.792		8	5	9	7	5	1.0084	0.9166	0.8148	0.931	0.9217
											0.05759	0.09219	0.06608	0.10351	0.07338
	Liver	0.666	0.848	0.342		10	11	8	8	8	1	1.0808	1.0121	0.9963	0.9513
											0.09344	0.08937	0.06943	0.0815	0.05607

Figure 30						N numbers					Mean ± SEM				
A		HOV	ANOVA	F	Welchs	Chow	PF	Alc	Alc+SAM	SAM	Chow	PF	Alc	Alc+SAM	SAM
	SVZ	0.729	0.05	2.546		15	11	13	12	9	236.2667	217	192.4615	216.1667	209.444
											10.18003	11.97194	10.14802	7.77996	13.18786
	IZ	0.434	0.013	3.47		15	11	13	12	9	358.6	362.0909	291.3845	345.5	335.44
											16.77209	19.66652	12.12411	13.05727	15.9104
	SP	0.047			0.001	15	11	13	12	9	144.4	148.3636	112.1538	136.5833	135.6667
											8.90361	6.83743	4.59912	6.29389	8.21922
	CP	0.805	0.028	2.963		14	11	13	12	9	321.6429	290.7273	264.3077	304.25	268
											16.70218	13.04823	13.15557	13.2757	13.71536
	MZ	0.288	0.046	2.609		14	11	13	12	9	77.2143	73.6364	65.8462	81.25	70.1111
											2.38627	4.62262	3.21424	4.06598	5.27163
	Total	0.123	0.004	4.328		14	11	13	12	9	1131.5	1091.8182	926	1085.033	1020.888
											47.73781	47.62408	24.90289	34.51333	41.50249
B	I	0.254	0.16	1.831		8	10	10	10		358.6	362.0909	291.3845	345.5	
											16.77209	19.66652	12.12411	13.05727	
	II-IV	0.61	0.002	5.846		8	10	10	10		321.3638	275.548	259.0782	273.334	
											13.35783	10.59526	9.99467	8.92807	
	V	0.452	0.218	1.555		8	10	10	10		230.7	225.529	210.7676	220.271	
											7.61334	6.82727	8.00427	3.95667	
	VI	0.615	0.018	3.82		8	10	10	10		342.6863	363.014	319.8105	340.9239	
											6.08174	8.04106	12.34289	8.25141	
	Total	0.995	0.001	6.628		9	8	9	9		919.9701	909.5708	813.9099	894.8541	
											18.88182	19.28196	20.25341	17.02551	

Figure 31						N numbers					Mean ± SEM				
		HOV	ANOVA	F	Welchs	Chow	PF	Alc	Alc+SAM	SAM	Chow	PF	Alc	Alc+SAM	SAM
A		0.677	0.898	0.266		6	8	8	7	6	192.5556	190.9167	192.8	190.444	193.3
											2.20549	2.9961	2.1746	1.9084	2.08725
B		0.034	<0.0001	8.194		5	5	5	6	5	0.2285	0.2442	0.1887	0.2525	0.2415
											0.00771	0.00778	0.01293	0.0077	0.00673

Figure 32					N numbers					Mean ± SEM				
	HOV	ANOVA	F	Welchs	Chow	PF	Alc	Alc+SAM	SAM	Chow	PF	Alc	Alc+SAM	SAM
B	0.669	0.036	2.844		11	9	9	9	7	326.1818	319.4444	255	271.6667	325.2857
										18.52017	19.84671	13.38013	17.87689	31.50337
C	0.014			0.358	8	11	9	7	6	16.475	16.3971	16.398	16.2321	15.9931
										0.13051	0.13788	0.07956	0.08616	0.24876

Figure 33						N numbers					Mean ± SEM				
B		HOV	ANOVA	F	Welchs	Chow	PF	Alc	Alc+SAM	SAM	Chow	PF	Alc	Alc+SAM	SAM
	SVZ	0.022			0.208	12	6	13	8	5	100.5	94.33	92.46	95.75	96.6
											0.427	3.98	3.601	3.89	1.469
	IZ	0.591	0.015	3.642		9	6	12	6	5	86.67	82.67	76.75	86.83	85.4
											2.357	1.58	2.35	2.257	3.44
	CP	0.144	0.016	3.485		11	6	12	8	5	93	83	78.83	85	86.2
											2.802	2.489	3.239	3.54	0.9695
C		0.385	0.977	0.113		8	9	9	9	4	16.34	16.45	16.348	16.38	16.47
											0.1935	0.1437	0.197	0.1128	0.1029

Figure 34					N numbers					Mean ± SEM				
	HOV	ANOVA	F	Welchs	Chow	PF	Alc	Alc+SAM	SAM	Chow	PF	Alc	Alc+SAM	SAM
B	0.599	0.112	2.028		8	7	9	9	6	16.2545	16.3128	16.4042	16.1855	16.1031
										0.05407	0.07311	0.07212	0.08329	0.12028
C	0.26	0.035	2.775		16	12	15	14	9	108.2193	114.2537	66.234	109.6958	145.2366
										14.93126	17.09372	8.81676	17.92579	25.09812
D	0.003			≤.0001	8	6	8	8	5	189.9061	135.5317	40.9872	116.1035	186.1549
										38.68389	28.20116	10.86077	12.70205	20.02522

Figure 35					N numbers					Mean ± SEM				
	HOV	ANOVA	F	Welchs	Chow	PF	Alc	Alc+SAM	SAM	Chow	PF	Alc	Alc+SAM	SAM
F	0.078	<0.0001	12.643		8	7	9	8	5	69.735	72.8571	102.7778	80.8333	68.3
										3.55034	3.05059	4.74748	5.08216	0.93005
G	0.26	0.035	2.775		8	6	9	9	6	16.7706	16.8613	16.3064	16.2374	16.7953
										0.16142	0.21273	0.0794	0.07286	0.3746

Figure 36					N numbers					Mean ± SEM				
	HOV	ANOVA	F	Welchs	Chow	PF	Alc	Alc+SAM	SAM	Chow	PF	Alc	Alc+SAM	SAM
B	0.67	0.055	2.61		8	5	9	9	6	16.8731	16.5978	16.6904	16.7915	16.1694
										0.09835	0.18236	0.19015	0.16397	0.11801
C	0.956	0.549	0.774		8	12	9	9	6	17.9911	17.9425	17.6296	17.781	18.0581
										0.21437	0.15887	0.20554	0.16811	0.21724
D	0.807	0.157	1.771		8	8	9	8	6	22.2637	21.4591	22.0243	22.1537	21.5282
										0.33887	0.27376	0.21806	0.22797	0.29917

Figure 37					N numbers					Mean ± SEM				
	HOV	ANOVA	F	Welchs	Chow	PF	Alc	Alc+SAM	SAM	Chow	PF	Alc	Alc+SAM	SAM
B	0.033			0.647	8	11	9	9	6	15.4469	15.3947	15.5607	15.3829	15.4451
										0.12166	0.10403	0.06954	0.11869	0.21055
C	0.183	0.004	4.785		8	9	9	9	8	16.6002	16.3064	16.839	16.5301	16.1236
										0.16697	0.08689	0.05717	0.13506	0.10759
D	0.431	0.451	0.943		8	8	9	9	6	15.4588	15.4926	15.787	15.4689	15.2794
										0.21113	0.26266	0.09489	0.1408	0.22257
E	0.038			0.01	8	13	9	9	6	16.0129	16.1466	15.7544	15.7636	15.9354
										0.06173	0.17419	0.03556	0.05608	0.06885

Figure 38					N numbers					Mean ± SEM				
	HOV	ANOVA	F	Welchs	Chow	PF	Alc	Alc+SAM	SAM	Chow	PF	Alc	Alc+SAM	SAM
B	0.046			0.256	8	6	9	7	6	15.5996	15.8202	15.4285	15.7175	15.7974
										0.14878	0.03323	0.19911	0.07473	0.08026
C	0.135	0.166	1.739		8	5	9	9	6	16.5664	16.8325	16.393	16.5924	16.5897
										0.08008	0.09333	0.04947	0.08804	0.23422
D	0.267	0.511	0.837		8	8	9	8	6	21.8189	21.9562	21.601	21.7305	21.8687
										0.10344	0.08006	0.16306	0.11781	0.29336
E	0.006			0.945	8	6	9	8	6	18.503	18.3844	18.4605	18.4742	18.6763
										0.10743	0.25197	0.15188	0.24121	0.24471
F	0.02			0.033	8	12	9	9	6	14.7215	14.8799	13.4655	14.2254	14.6163
										0.35643	0.11493	0.44562	0.21267	0.17038
G	0.575	<0.0001	8.034		8	13	9	7	6	15.5308	15.7742	14.9718	15.3653	15.927
										0.11137	0.09689	0.1782	0.12971	0.10624

Figure 39					N numbers					Mean ± SEM				
	HOV	ANOVA	F	Welchs	Chow	PF	Alc	Alc+SAM	SAM	Chow	PF	Alc	Alc+SAM	SAM
B	0.734	0.058	2.538		11	7	10	7	7	153.0897	137.4183	71.1351	148.4189	163.2351
										24.90935	20.274	16.91295	32.4203	26.07562
C	0.11	0.008	4.275		9	6	9	6	6	51.5951	40.6877	97.8914	40.4939	45.2203
										9.161	8.2889	16.67153	9.36787	13.6269
D	0.637	0.023	3.353		8	9	5	6	6	61.8255	67.2669	140.4998	70.8933	64.9849
										16.33265	13.73923	15.31996	17.48187	17.68008

Figure 40					N numbers					Mean ± SEM				
	HOV	ANOVA	F	Welchs	Chow	PF	Alc	Alc+SAM	SAM	Chow	PF	Alc	Alc+SAM	SAM
B	0.346	0.429	0.998		7	5	8	6	5	158.1197	132.1434	70.3354	148.1909	133.1606
										31.52755	23.64219	29.94231	44.9286	27.10446
C	0.658	0.975	0.118		10	9	7	6	5	132.5583	131.0069	144.9134	133.9567	135.464
										10.35864	13.75152	17.85435	27.39017	17.18245
D	0.718	0.24	1.452		5	7	7	6	5	70.829	67.2669	115.1993	70.8933	64.9849
										16.98646	13.73923	19.45655	17.48187	17.68008

Figure 42					N numbers					Mean ± SEM				
	HOV	ANOVA	F	Welchs	Chow	PF	Alc	Alc+SAM	SAM	Chow	PF	Alc	Alc+SAM	SAM
A	<0.0001			0.013	7	6	9	8	6	16.1818	13.2	20.9231	18.6923	13.2857
										1.72056	0.51208	2.83852	1.88919	0.52164
B	0.48	0.079	2.287		7	6	7	8	6	10.25	10.5	14	14.625	11.625
										1.544	0.61914	1.74574	1.52289	1.26685
C	0.031			0.038	8	10	9	9	7	9.125	7.9	14	8.7778	9.8571
										0.875	1.19675	1.40216	1.12183	0.70735

Supp Figure 2					N numbers					Mean ± SEM				
	HOV	ANOVA	F	Welchs	Chow	PF	Alc	Alc+SAM	SAM	Chow	PF	Alc	Alc+SAM	SAM
B	0.183	0.004	4.785		8	8	9	9	5	16.6002	16.3064	16.839	16.5301	16.1236
										0.16697	0.08689	0.05717	0.13506	0.10759
C	0.111	0.038	2.735		11	13	14	14	9	127.511	86.7957	67.6655	99.0575	90.478
										18.6457	12.3548	7.8335	14.7767	8.91328

Table B-5. Fetal, Phenotypic, and Genomic Summary of Statistics

Summary of statistics are presented for each indicated Figure. HOV: Homogeneity of Variance statistic, ANOVA: one-way analysis of variance, F: ANOVA F value. N numbers reflect litter number represented in each assay. All gene expression assays are presented as gene fold changes in the graph though statistical analysis was performed using delta Ct values reflected here.

***Ascl1* Promoter (4CpG coverage)**			
Sum Methylation (%)		Gene Expression (relative)	
Chow (n=5)	13.4±1.56	Chow (n=8)	1.0±0.065
PF (n=3)	15±2.0	PF (n=5)	1.21±0.143
Alc (n=5)	17.2±4.17	Alc (n=9)	1.13±0.140
Alc+SAM (n=5)	15±4.34	Alc+SAM (n=9)	1.05±0.165
SAM (n=2)	12.2±3.5	SAM (n=6)	1.07±0.068
***Ngn1* Promoter 1 (9CpG coverage)**			
Sum Methylation (%)		Gene Expression (relative)	
Chow (n=4)	74.4±12.43	Chow (n=8)	1.0±0.209
PF (n=5)	89.4±9.62	PF (n=5)	1.25±0.34
Alc (n=5)	87.2±9.3	Alc (n=9)	1.18±0.165
Alc+SAM (n=4)	73±4.01	Alc+SAM (n=8)	1.07±0.157
SAM (n=2)	72±3.0	SAM (n=6)	1.10±0.261
***Ngn1* Promoter 2 (6CpG coverage)**			
Sum Methylation (%)			
Chow (n=4)	24.25±0.83		
PF (n=4)	24.75±0.95		
Alc (n=4)	23.5±1.08		
Alc+SAM (n=4)	25±0.79		
SAM (n=2)	27±0.0		
***Syt2* Promoter (5CpG coverage)**			
Sum Methylation (%)		Gene Expression (relative)	
Chow (n=3)	22.67±3.25	Chow (n=8)	1.0±0.133
PF (n=4)	32.25±13.57	PF (n=8)	1.24±0.107
Alc (n=4)	28±5.93	Alc (n=9)	1.14±0.152
Alc+SAM (n=3)	21±6.13	Alc+SAM (n=9)	0.90±0.106
SAM (N/A)		SAM (n=6)	0.97±0.119
***Fezf2* Promoter (6CpG coverage)**			
Sum Methylation (%)		Gene Expression (relative)	
Chow (n=4)	16.2±1.84	Chow (n=8)	1.0±0.104
PF (n=5)	13.2±0.99	PF (n=9)	0.99±0.110
Alc (n=5)	21.76.2±3.11***#**	Alc (n=9)	0.80±0.031***#§**
Alc+SAM (n=8)	17.86±2.23	Alc+SAM (n=9)	0.99±0.089
SAM (n=6)	13.29±1.30	SAM (n=6)	1.32±0.177
***Fezf2* Exon 1 (4CpG coverage)**			
Sum Methylation (%)			
Chow (n=4)	10.25±1.77		
PF (n=4)	10.50±0.84		
Alc (n=4)	13.99±1.88		
Alc+SAM (n=8)	14.63±1.69		
SAM (n=6)	11.63±1.60		
***Fezf2* Enhancer 434(5CpG coverage)**			
Sum Methylation (%)			
Chow (n=4)	9.13±0.88		
PF (n=4)	7.90±1.20		
Alc (n=4)	14.0±2.14**§†#**		
Alc+SAM (n=9)	7.90±1.40		
SAM (n=7)	9.86±1.12		

Table B-6. Methyl-pyrosequencing of Multiple Neurodevelopmental Gene Targets

Cumulative methylation analysis of Ascl1, Ngn1, Syt2, and Fezf2 was performed by methyl-pyrosequencing. Results are presented parallel to relative gene expression

analysis. ł p≤0.05 vs Chow;*p≤0.05 vs SAM; #p≤0.05 vs PF; § p≤0.05 vs Alc+SAM. Neither gene expression nor promoter DNA methylation was significantly altered by alcohol or S-AMe supplementation except in the case of the Fezf2 which is detailed in Chapter 3 Figure 40.

REFERENCES

Abbott, C. W., O. O. Kozanian, J. Kanaan, K. M. Wendel and K. J. Huffman (2016). "The Impact of Prenatal Ethanol Exposure on Neuroanatomical and Behavioral Development in Mice." Alcohol Clin Exp Res **40**(1): 122-133.

Abel, E. L. (1996). "Effects of prenatal alcohol exposure on birth weight in rats: is there an inverted U-shaped function?" Alcohol **13**(1): 99-102.

Alcamo, E. A., L. Chirivella, M. Dautzenberg, G. Dobreva, I. Farinas, R. Grosschedl and S. K. McConnell (2008). "Satb2 regulates callosal projection neuron identity in the developing cerebral cortex." Neuron **57**(3): 364-377.

Altman, J. (1969). "Autoradiographic and histological studies of postnatal neurogenesis. 3. Dating the time of production and onset of differentiation of cerebellar microneurons in rats." J Comp Neurol **136**(3): 269-293.

Alvarez-Bolado, G., M. G. Rosenfeld and L. W. Swanson (1995). "Model of forebrain regionalization based on spatiotemporal patterns of POU-III homeobox gene expression, birthdates, and morphological features." J Comp Neurol **355**(2): 237-295.

Amir, R. E., I. B. Van den Veyver, M. Wan, C. Q. Tran, U. Francke and H. Y. Zoghbi (1999). "Rett syndrome is caused by mutations in X-linked MECP2, encoding methyl-CpG-binding protein 2." Nat Genet **23**(2): 185-188.

Anthony, B., S. Vinci-Booher, L. Wetherill, R. Ward, C. Goodlett and F. C. Zhou (2010). "Alcohol-induced facial dysmorphology in C57BL/6 mouse models of fetal alcohol spectrum disorder." Alcohol **44**(7-8): 659-671.

Anthony, B., F. C. Zhou, T. Ogawa, C. R. Goodlett and J. Ruiz (2008). "Alcohol exposure alters cell cycle and apoptotic events during early neurulation." Alcohol Alcohol **43**(3): 261-273.

Anton, M., F. Alen, R. Gomez de Heras, A. Serrano, F. J. Pavon, J. C. Leza, B. Garcia-Bueno, F. Rodriguez de Fonseca and L. Orio (2017). "Oleoylethanolamide prevents neuroimmune HMGB1/TLR4/NF-kB danger signaling in rat frontal cortex and depressive-like behavior induced by ethanol binge administration." Addict Biol **22**(3): 724-741.

Arancillo, M., J. J. White, T. Lin, T. L. Stay and R. V. Sillitoe (2015). "In vivo analysis of Purkinje cell firing properties during postnatal mouse development." J Neurophysiol **113**(2): 578-591.

Arlotta, P., B. J. Molyneaux, J. Chen, J. Inoue, R. Kominami and J. D. Macklis (2005). "Neuronal subtype-specific genes that control corticospinal motor neuron development in vivo." Neuron **45**(2): 207-221.

Aronne, M. P., S. G. Evrard, S. Mirochnic and A. Brusco (2008). "Prenatal ethanol exposure reduces the expression of the transcriptional factor Pax6 in the developing rat brain." Ann N Y Acad Sci **1139**: 478-498.
Aronne, M. P., T. Guadagnoli, P. Fontanet, S. G. Evrard and A. Brusco (2011). "Effects of prenatal ethanol exposure on rat brain radial glia and neuroblast migration." Exp Neurol **229**(2): 364-371.

Avila, M. A., M. V. Carretero, E. N. Rodriguez and J. M. Mato (1998). "Regulation by hypoxia of methionine adenosyltransferase activity and gene expression in rat hepatocytes." Gastroenterology **114**(2): 364-371.

Baala, L., S. Briault, H. C. Etchevers, F. Laumonnier, A. Natiq, J. Amiel, N. Boddaert, C. Picard, A. Sbiti, A. Asermouh, T. Attie-Bitach, F. Encha-Razavi, A. Munnich, A. Sefiani and S. Lyonnet (2007). "Homozygous silencing of T-box transcription factor EOMES leads to microcephaly with polymicrogyria and corpus callosum agenesis." Nat Genet **39**(4): 454-456.

Baculis, B. C., M. R. Diaz and C. F. Valenzuela (2015). "Third trimester-equivalent ethanol exposure increases anxiety-like behavior and glutamatergic transmission in the basolateral amygdala." Pharmacol Biochem Behav **137**: 78-85.

Bagga, J. S. and L. A. D'Antonio (2013). "Role of conserved cis-regulatory elements in the post-transcriptional regulation of the human MECP2 gene involved in autism." Hum Genomics **7**: 19.

Bailey, S. M., G. Robinson, A. Pinner, L. Chamlee, E. Ulasova, M. Pompilius, G. P. Page, D. Chhieng, N. Jhala, A. Landar, K. K. Kharbanda, S. Ballinger and V. Darley-Usmar (2006). "S-adenosylmethionine prevents chronic alcohol-induced mitochondrial dysfunction in the rat liver." Am J Physiol Gastrointest Liver Physiol **291**(5): G857-867.

Ball, M. P., J. B. Li, Y. Gao, J. H. Lee, E. M. LeProust, I. H. Park, B. Xie, G. Q. Daley and G. M. Church (2009). "Targeted and genome-scale strategies reveal gene-body methylation signatures in human cells." Nat Biotechnol **27**(4): 361-368.

Barak, A. J., H. C. Beckenhauer, M. E. Mailliard, K. K. Kharbanda and D. J. Tuma (2003). "Betaine lowers elevated s-adenosylhomocysteine levels in hepatocytes from ethanol-fed rats." J Nutr **133**(9): 2845-2848.

Barak, A. J., H. C. Beckenhauer and D. J. Tuma (1996). "Betaine effects on hepatic methionine metabolism elicited by short-term ethanol feeding." Alcohol **13**(5): 483-486.

Barak, A. J., H. C. Beckenhauer and D. J. Tuma (2002). "Methionine synthase. a possible prime site of the ethanolic lesion in liver." Alcohol **26**(2): 65-67.

Barbier, E., J. D. Tapocik, N. Juergens, C. Pitcairn, A. Borich, J. R. Schank, H. Sun, K. Schuebel, Z. Zhou, Q. Yuan, L. F. Vendruscolo, D. Goldman and M. Heilig (2015). "DNA methylation in the medial prefrontal cortex regulates alcohol-induced behavior and plasticity." J Neurosci **35**(15): 6153-6164.

Barrera, G. (2012). "Oxidative stress and lipid peroxidation products in cancer progression and therapy." ISRN Oncol **2012**: 137289.

Bartke, T., M. Vermeulen, B. Xhemalce, S. C. Robson, M. Mann and T. Kouzarides (2010). "Nucleosome-interacting proteins regulated by DNA and histone methylation." Cell **143**(3): 470-484.

Baydas, G., S. T. Koz, M. Tuzcu, V. S. Nedzvetsky and E. Etem (2007). "Effects of maternal hyperhomocysteinemia induced by high methionine diet on the learning and memory performance in offspring." Int J Dev Neurosci **25**(3): 133-139.

Beaudin, A. E., C. A. Perry, S. P. Stabler, R. H. Allen and P. J. Stover (2012). "Maternal Mthfd1 disruption impairs fetal growth but does not cause neural tube defects in mice." Am J Clin Nutr **95**(4): 882-891.

Bekdash, R. A., C. Zhang and D. K. Sarkar (2013). "Gestational choline supplementation normalized fetal alcohol-induced alterations in histone modifications, DNA methylation, and proopiomelanocortin (POMC) gene expression in beta-endorphin-producing POMC neurons of the hypothalamus." Alcohol Clin Exp Res **37**(7): 1133-1142.

Belinson, H., J. Nakatani, B. A. Babineau, R. Y. Birnbaum, J. Ellegood, M. Bershteyn, R. J. McEvilly, J. M. Long, K. Willert, O. D. Klein, N. Ahituv, J. P. Lerch, M. G. Rosenfeld and A. Wynshaw-Boris (2016). "Prenatal beta-catenin/Brn2/Tbr2 transcriptional cascade regulates adult social and stereotypic behaviors." Mol Psychiatry **21**(10): 1417-1433.

Bellacosa, A., L. Cicchillitti, F. Schepis, A. Riccio, A. T. Yeung, Y. Matsumoto, E. A. Golemis, M. Genuardi and G. Neri (1999). "MED1, a novel human methyl-CpG-binding endonuclease, interacts with DNA mismatch repair protein MLH1." Proc Natl Acad Sci U S A **96**(7): 3969-3974.

Bellinger, F. P., M. S. Davidson, K. S. Bedi and P. A. Wilce (2002). "Neonatal ethanol exposure reduces AMPA but not NMDA receptor levels in the rat neocortex." Brain Res Dev Brain Res **136**(1): 77-84.

Berlin, K. N., L. M. Cameron, M. Gatt and R. R. Miller, Jr. (2010). "Reduced de novo synthesis of 5-methyltetrahydrofolate and reduced taurine levels in ethanol-treated chick brains." Comp Biochem Physiol C Toxicol Pharmacol **152**(3): 353-359.

Bertrand, N., D. S. Castro and F. Guillemot (2002). "Proneural genes and the specification of neural cell types." Nat Rev Neurosci **3**(7): 517-530.

Bestor, T. H. (1992). "Activation of mammalian DNA methyltransferase by cleavage of a Zn binding regulatory domain." Embo j **11**(7): 2611-2617.

Bilinski, P., A. Wojtyla, L. Kapka-Skrzypczak, R. Chwedorowicz, M. Cyranka and T. Studzinski (2012). "Epigenetic regulation in drug addiction." Ann Agric Environ Med **19**(3): 491-496.

Birch, S. M., M. W. Lenox, J. N. Kornegay, B. Paniagua, M. A. Styner, C. R. Goodlett, T. A. Cudd and S. E. Washburn (2016). "Maternal choline supplementation in a sheep model of first trimester binge alcohol fails to protect against brain volume reductions in peripubertal lambs." Alcohol **55**: 1-8.

Boschen, K. E., S. E. McKeown, T. L. Roth and A. Y. Klintsova (2016). "Impact of exercise and a complex environment on hippocampal dendritic morphology, Bdnf gene expression, and DNA methylation in male rat pups neonatally exposed to alcohol." Dev Neurobiol.

Broadwater, M. A., W. Liu, F. T. Crews and L. P. Spear (2014). "Persistent loss of hippocampal neurogenesis and increased cell death following adolescent, but not adult, chronic ethanol exposure." Dev Neurosci **36**(3-4): 297-305.

Brooks, P. J. and S. Zakhari (2014). "Acetaldehyde and the genome: beyond nuclear DNA adducts and carcinogenesis." Environ Mol Mutagen **55**(2): 77-91.

Burd, L., M. G. Klug, J. T. Martsolf and J. Kerbeshian (2003). "Fetal alcohol syndrome: neuropsychiatric phenomics." Neurotoxicol Teratol **25**(6): 697-705.

Büttner, N., S. A. Johnsen, S. Kügler and T. Vogel (2010). "Af9/Mllt3 interferes with Tbr1 expression through epigenetic modification of histone H3K79 during development of the cerebral cortex." Proceedings of the National Academy of Sciences of the United States of America **107**(15): 7042-7047.

Cabrera, R. M., G. M. Shaw, J. L. Ballard, S. L. Carmichael, W. Yang, E. J. Lammer and R. H. Finnell (2008). "Autoantibodies to folate receptor during pregnancy and neural tube defect risk." J Reprod Immunol **79**(1): 85-92.

Canovas, J., F. A. Berndt, H. Sepulveda, R. Aguilar, F. A. Veloso, M. Montecino, C. Oliva, J. C. Maass, J. Sierralta and M. Kukuljan (2015). "The Specification of Cortical Subcerebral Projection Neurons Depends on the Direct Repression of TBR1 by CTIP1/BCL11a." J Neurosci **35**(19): 7552-7564.

Carlin, J., R. George and T. M. Reyes (2013). "Methyl donor supplementation blocks the adverse effects of maternal high fat diet on offspring physiology." PLoS One **8**(5): e63549.

Casarosa, S., C. Fode and F. Guillemot (1999). "Mash1 regulates neurogenesis in the ventral telencephalon." Development **126**(3): 525-534.

Castro, D. S., B. Martynoga, C. Parras, V. Ramesh, E. Pacary, C. Johnston, D. Drechsel, M. Lebel-Potter, L. G. Garcia, C. Hunt, D. Dolle, A. Bithell, L. Ettwiller, N. Buckley and F. Guillemot (2011). "A novel function of the proneural factor Ascl1 in progenitor proliferation identified by genome-wide characterization of its targets." Genes Dev **25**(9): 930-945.

CDC (2002). "Alcohol use among women of childbearing age---United States, 1991-1999." Morbitity and Mortality Weekly Report **51**: 273-276.

Chahrour, M., S. Y. Jung, C. Shaw, X. Zhou, S. T. Wong, J. Qin and H. Y. Zoghbi (2008). "MeCP2, a key contributor to neurological disease, activates and represses transcription." Science **320**(5880): 1224-1229.

Chawla, R. K., W. H. Watson and D. P. Jones (1996). "Effect of hypoxia on hepatic DNA methylation and tRNA methyltransferase in rat: similarities to effects of methyl-deficient diets." J Cell Biochem **61**(1): 72-80.

Chen, B., S. S. Wang, A. M. Hattox, H. Rayburn, S. B. Nelson and S. K. McConnell (2008). "The Fezf2-Ctip2 genetic pathway regulates the fate choice of subcortical projection neurons in the developing cerebral cortex." Proc Natl Acad Sci U S A **105**(32): 11382-11387.

Chen, Y., N. P. Damayanti, J. Irudayaraj, K. Dunn and F. C. Zhou (2014). "Diversity of two forms of DNA methylation in the brain." Front Genet **5**: 46.

Chen, Y., N. C. Ozturk and F. C. Zhou (2013). "DNA methylation program in developing hippocampus and its alteration by alcohol." PLoS One **8**(3): e60503.

Chen, Y. H., Z. Yu, L. Fu, M. Z. Xia, M. Zhao, H. Wang, C. Zhang, Y. F. Hu, F. B. Tao and D. X. Xu (2015). "Supplementation with vitamin D3 during pregnancy protects against lipopolysaccharide-induced neural tube defects through improving placental folate transportation." Toxicol Sci **145**(1): 90-97.

Cheung, A. F., S. Kondo, O. Abdel-Mannan, R. A. Chodroff, T. M. Sirey, L. E. Bluy, N. Webber, J. DeProto, S. J. Karlen, L. Krubitzer, H. B. Stolp, N. R. Saunders and Z. Molnar (2010). "The subventricular zone is the developmental milestone of a 6-layered neocortex: comparisons in metatherian and eutherian mammals." Cereb Cortex **20**(5): 1071-1081.

Chikhladze, R. T., N. Ramishvili, Z. G. Tsagareli and N. O. Kikalishvili (2011). "The spectrum of hemispheral cortex lesions in intrauterine alcoholic intoxication." Georgian Med News(192): 81-87.

Chittka, A., J. Nitarska, U. Grazini and W. D. Richardson (2012). "Transcription factor positive regulatory domain 4 (PRDM4) recruits protein arginine methyltransferase 5 (PRMT5) to mediate histone arginine methylation and control neural stem cell proliferation and differentiation." J Biol Chem **287**(51): 42995-43006.

Cho, B., H. J. Kim, H. Kim and W. Sun (2011). "Changes in the Histone Acetylation Patterns during the Development of the Nervous System." Exp Neurobiol **20**(2): 81-84.

Chrostek, L., W. Tomaszewski and M. Szmitkowski (2005). "The effect of green tea on the activity of aldehyde dehydrogenase (ALDH) in the liver of rats during chronic ethanol consumption." Rocz Akad Med Bialymst **50**: 220-223.

Ciarapica, R., L. Methot, Y. Tang, R. Lo, R. Dali, M. Buscarlet, F. Locatelli, G. del Sal, R. Rota and S. Stifani (2014). "Prolyl isomerase Pin1 and protein kinase HIPK2 cooperate to promote cortical neurogenesis by suppressing Groucho/TLE:Hes1-mediated inhibition of neuronal differentiation." Cell Death Differ **21**(2): 321-332.

Cimadamore, F., A. Amador-Arjona, C. Chen, C. T. Huang and A. V. Terskikh (2013). "SOX2-LIN28/let-7 pathway regulates proliferation and neurogenesis in neural precursors." Proc Natl Acad Sci U S A **110**(32): E3017-3026.

Coleman, L. G., Jr., I. Oguz, J. Lee, M. Styner and F. T. Crews (2012). "Postnatal day 7 ethanol treatment causes persistent reductions in adult mouse brain volume and cortical neurons with sex specific effects on neurogenesis." Alcohol **46**(6): 603-612.

Coles, C. D., J. A. Kable, C. L. Keen, K. L. Jones, W. Wertelecki, I. V. Granovska, A. O. Pashtepa and C. D. Chambers (2015). "Dose and Timing of Prenatal Alcohol Exposure and Maternal Nutritional Supplements: Developmental Effects on 6-Month-Old Infants." Matern Child Health J **19**(12): 2605-2614.

Cortese, R., J. Lewin, L. Backdahl, M. Krispin, R. Wasserkort, F. Eckhardt and S. Beck (2011). "Genome-wide screen for differential DNA methylation associated with neural cell differentiation in mouse." PLoS One **6**(10): e26002.

Costa, E., J. Davis, D. R. Grayson, A. Guidotti, G. D. Pappas and C. Pesold (2001). "Dendritic spine hypoplasticity and downregulation of reelin and GABAergic tone in schizophrenia vulnerability." Neurobiol Dis **8**(5): 723-742.

Covarrubias, L., D. Hernández-García, D. Schnabel, E. Salas-Vidal and S. Castro-Obregón (2008). "Function of reactive oxygen species during animal development: Passive or active?" Developmental Biology **320**(1): 1-11.

Craciunescu, C. N., A. R. Johnson and S. H. Zeisel (2010). "Dietary Choline Reverses Some, but Not All, Effects of Folate Deficiency on Neurogenesis and Apoptosis in Fetal Mouse Brain." The Journal of Nutrition **140**(6): 1162-1166.

Cravo, M. L., A. G. Pinto, P. Chaves, J. A. Cruz, P. Lage, C. Nobre Leitão and F. Costa Mira (1998). "Effect of folate supplementation on DNA methylation of rectal mucosa in patients with colonic adenomas: correlation with nutrient intake." Clinical Nutrition **17**(2): 45-49.

Cuzon, V. C., P. W. Yeh, Y. Yanagawa, K. Obata and H. H. Yeh (2008). "Ethanol consumption during early pregnancy alters the disposition of tangentially migrating GABAergic interneurons in the fetal cortex." J Neurosci **28**(8): 1854-1864.

D'Addario, C., F. F. Caputi, T. J. Ekstrom, M. Di Benedetto, M. Maccarrone, P. Romualdi and S. Candeletti (2013). "Ethanol induces epigenetic modulation of prodynorphin and pronociceptin gene expression in the rat amygdala complex." J Mol Neurosci **49**(2): 312-319.

Das, N. D., M. R. Choi, K. H. Jung, J. H. Park, H. T. Lee, A. Das, S. H. Kim and Y. G. Chai (2013). "Functional analysis of histone demethylase Jmjd2b on lipopolysaccharide-treated murine neural stem cells (NSCs)." Neurotox Res **23**(2): 154-165.

De Guio, F., J. F. Mangin, D. Riviere, M. Perrot, C. D. Molteno, S. W. Jacobson, E. M. Meintjes and J. L. Jacobson (2014). "A study of cortical morphology in children with fetal alcohol spectrum disorders." Hum Brain Mapp **35**(5): 2285-2296.

de Sanctis, L., L. Memo, S. Pichini, L. Tarani and F. Vagnarelli (2011). "Fetal alcohol syndrome: new perspectives for an ancient and underestimated problem." J Matern Fetal Neonatal Med **24 Suppl 1**: 34-37.

Detich, N., J. Theberge and M. Szyf (2002). "Promoter-specific activation and demethylation by MBD2/demethylase." J Biol Chem **277**(39): 35791-35794.

Dixit, R., C. Zimmer, R. R. Waclaw, P. Mattar, T. Shaker, C. Kovach, C. Logan, K. Campbell, F. Guillemot and C. Schuurmans (2011). "Ascl1 participates in Cajal-Retzius cell development in the neocortex." Cereb Cortex **21**(11): 2599-2611.

Downing, C., T. E. Johnson, C. Larson, T. I. Leakey, R. N. Siegfried, T. M. Rafferty and C. A. Cooney (2011). "Subtle decreases in DNA methylation and gene expression at the mouse Igf2 locus following prenatal alcohol exposure: effects of a methyl-supplemented diet." Alcohol **45**(1): 65-71.

Dunlevy, L. P., K. A. Burren, K. Mills, L. S. Chitty, A. J. Copp and N. D. Greene (2006). "Integrity of the methylation cycle is essential for mammalian neural tube closure." Birth Defects Res A Clin Mol Teratol **76**(7): 544-552.

Eckler, M. J., K. A. Larkin, W. L. McKenna, S. Katzman, C. Guo, R. Roque, A. Visel, J. L. Rubenstein and B. Chen (2014). "Multiple conserved regulatory domains promote Fezf2 expression in the developing cerebral cortex." Neural Dev **9**: 6.

Ehlers, C. L., W. Liu, D. N. Wills and F. T. Crews (2013). "Periadolescent ethanol vapor exposure persistently reduces measures of hippocampal neurogenesis that are associated with behavioral outcomes in adulthood." Neuroscience **244**: 1-15.

Eichner, E. R. and R. S. Hillman (1973). "Effect of alcohol on serum folate level." J Clin Invest **52**(3): 584-591.

El Fatimy, R., F. Miozzo, A. Le Mouel, R. Abane, L. Schwendimann, D. Saberan-Djoneidi, A. de Thonel, I. Massaoudi, L. Paslaru, K. Hashimoto-Torii, E. Christians, P. Rakic, P. Gressens and V. Mezger (2014). "Heat shock factor 2 is a stress-responsive mediator of neuronal migration defects in models of fetal alcohol syndrome." EMBO Mol Med **6**(8): 1043-1061.

El Shawa, H., C. W. Abbott, 3rd and K. J. Huffman (2013). "Prenatal ethanol exposure disrupts intraneocortical circuitry, cortical gene expression, and behavior in a mouse model of FASD." J Neurosci **33**(48): 18893-18905.

Englund, C., A. Fink, C. Lau, D. Pham, R. A. Daza, A. Bulfone, T. Kowalczyk and R. F. Hevner (2005). "Pax6, Tbr2, and Tbr1 are expressed sequentially by radial glia, intermediate progenitor cells, and postmitotic neurons in developing neocortex." J Neurosci **25**(1): 247-251.

Famy, C., A. P. Streissguth and A. S. Unis (1998). "Mental illness in adults with fetal alcohol syndrome or fetal alcohol effects." Am J Psychiatry **155**(4): 552-554.

Farber, N. B., C. E. Creeley and J. W. Olney (2010). "ALCOHOL-INDUCED NEUROAPOPTOSIS IN THE FETAL MACAQUE BRAIN." Neurobiology of disease **40**(1): 200-206.

Feltus, F. A., E. K. Lee, J. F. Costello, C. Plass and P. M. Vertino (2006). "DNA motifs associated with aberrant CpG island methylation." Genomics **87**(5): 572-579.

Finkelstein, J. D. (1990). "Methionine metabolism in mammals." J Nutr Biochem **1**(5): 228-237.
Finkelstein, J. D., J. P. Cello and W. E. Kyle (1974). "Ethanol-induced changes in methionine metabolism in rat liver." Biochem Biophys Res Commun **61**(2): 525-531.

Fisher, S. E., L. S. Inselman, L. Duffy, M. Atkinson, H. Spencer and B. Chang (1985). "Ethanol and fetal nutrition: effect of chronic ethanol exposure on rat placental growth and membrane-associated folic acid receptor binding activity." J Pediatr Gastroenterol Nutr **4**(4): 645-649.

Fode, C., Q. Ma, S. Casarosa, S. L. Ang, D. J. Anderson and F. Guillemot (2000). "A role for neural determination genes in specifying the dorsoventral identity of telencephalic neurons." Genes Dev **14**(1): 67-80.

Garro, A. J., D. L. McBeth, V. Lima and C. S. Lieber (1991). "Ethanol consumption inhibits fetal DNA methylation in mice: implications for the fetal alcohol syndrome." Alcohol Clin Exp Res **15**(3): 395-398.

Gauthier, T. W., X. D. Ping, L. Gabelaia and L. A. Brown (2010). "Delayed neonatal lung macrophage differentiation in a mouse model of in utero ethanol exposure." Am J Physiol Lung Cell Mol Physiol **299**(1): L8-16.

Geoffroy, A., R. Kerek, G. Pourie, D. Helle, J. L. Gueant, J. L. Daval and C. Bossenmeyer-Pourie (2016). "Late Maternal Folate Supplementation Rescues from Methyl Donor Deficiency-Associated Brain Defects by Restoring Let-7 and miR-34 Pathways." Mol Neurobiol.

Ghosh, A., A. Antonini, S. K. McConnell and C. J. Shatz (1990). "Requirement for subplate neurons in the formation of thalamocortical connections." Nature **347**(6289): 179-181.

Gil-Mohapel, J., A. K. Titterness, A. R. Patten, S. Taylor, A. Ratzlaff, T. Ratzlaff, J. Helfer and B. R. Christie (2014). "Prenatal ethanol exposure differentially affects hippocampal neurogenesis in the adolescent and aged brain." Neuroscience **273**: 174-188.

Golub, H. M., Q. G. Zhou, H. Zucker, M. R. McMullen, O. N. Kokiko-Cochran, E. J. Ro, L. E. Nagy and H. Suh (2015). "Chronic Alcohol Exposure is Associated with Decreased Neurogenesis, Aberrant Integration of Newborn Neurons, and Cognitive Dysfunction in Female Mice." Alcohol Clin Exp Res **39**(10): 1967-1977.

Gonseth, S., R. Roy, E. A. Houseman, A. J. de Smith, M. Zhou, S. T. Lee, S. Nussle, A. W. Singer, M. R. Wrensch, C. Metayer and J. L. Wiemels (2015). "Periconceptional folate consumption is associated with neonatal DNA methylation modifications in neural crest regulatory and cancer development genes." Epigenetics **10**(12): 1166-1176.

Goodlett, C. R., K. M. Hamre and J. R. West (1990). "Regional differences in the timing of dendritic outgrowth of Purkinje cells in the vermal cerebellum demonstrated by MAP2 immunocytochemistry." Brain Res Dev Brain Res **53**(1): 131-134.

Gordon, L., J. E. Joo, J. E. Powell, M. Ollikainen, B. Novakovic, X. Li, R. Andronikos, M. N. Cruickshank, K. N. Conneely, A. K. Smith, R. S. Alisch, R. Morley, P. M. Visscher, J. M. Craig and R. Saffery (2012). "Neonatal DNA methylation profile in human twins is specified by a complex interplay between intrauterine environmental and genetic factors, subject to tissue-specific influence." Genome Res **22**(8): 1395-1406.

Govorko, D., R. A. Bekdash, C. Zhang and D. K. Sarkar (2012). "Male germline transmits fetal alcohol adverse effect on hypothalamic proopiomelanocortin gene across generations." Biol Psychiatry **72**(5): 378-388.

Graham, J. M., Jr. and V. H. Ferm (1985). "Heat- and alcohol-induced neural tube defects: interactions with folate in a golden hamster model." Pediatr Res **19**(2): 247-251.

Green, J. H. (2007). "Fetal Alcohol Spectrum Disorders: understanding the effects of prenatal alcohol exposure and supporting students." J Sch Health **77**(3): 103-108.

Grin, I. and A. A. Ishchenko (2016). "An interplay of the base excision repair and mismatch repair pathways in active DNA demethylation." Nucleic Acids Res **44**(8): 3713-3727.

Guibert, S., Z. Zhao, M. Sjolinder, A. Gondor, A. Fernandez, V. Pant and R. Ohlsson (2012). "CTCF-binding sites within the H19 ICR differentially regulate local chromatin structures and cis-acting functions." Epigenetics **7**(4): 361-369.

Gulsuner, S., T. Walsh, Amanda C. Watts, Ming K. Lee, Anne M. Thornton, S. Casadei, C. Rippey, H. Shahin, D. Braff, Kristin S. Cadenhead, Monica E. Calkins, Dorcas J. Dobie, R. Freedman, M. Green, T. Greenwood, Raquel E. Gur, Ruben C. Gur, L. Lazzeroni, G. Light, K. Nuechterlein, A. Olincy, A. Radant, A. Ray, N. Schork, Larry J. Seidman, L. Siever, J. Silverman, William S. Stone, C. Sugar, N. Swerdlow, D. Tsuang, M. Tsuang, B. Turetsky, T. Aduroja, T. Allen, L. D. Bradford, M. E. Calkins, B. Devlin, N. B. Edwards, R. Ganguli, R. C. P. Go, R. E. Gur, R. C. Gur, J. Kwentus, A. C. Lahti, P. Lyons, K. Mathos, R. May, S. McLeod-Bryant, J. P. McEvoy, L. Montgomery-Barefield, V. L. Nimgaonkar, J. O'Jile, A. Santos, R. M. Savage, C. L. Swanson, Jr., W. Wilson, V. L. Nimgaonkar, R. C. P. Go, R. M. Savage, N. R. Swerdlow, R. E. Gur, D. L. Braff, M.-C. King and J. M. McClellan "Spatial and Temporal Mapping of De Novo Mutations in Schizophrenia to a Fetal Prefrontal Cortical Network." Cell **154**(3): 518-529.

Guo, J. U., Y. Su, C. Zhong, G. L. Ming and H. Song (2011). "Hydroxylation of 5-methylcytosine by TET1 promotes active DNA demethylation in the adult brain." Cell **145**(3): 423-434.

Guy, J., B. Hendrich, M. Holmes, J. E. Martin and A. Bird (2001). "A mouse Mecp2-null mutation causes neurological symptoms that mimic Rett syndrome." Nat Genet **27**(3): 322-326.

Gyorgy, A. B., M. Szemes, C. de Juan Romero, V. Tarabykin and D. V. Agoston (2008). "SATB2 interacts with chromatin-remodeling molecules in differentiating cortical neurons." Eur J Neurosci **27**(4): 865-873.

Hackett, J. A., R. Sengupta, J. J. Zylicz, K. Murakami, C. Lee, T. A. Down and M. A. Surani (2013). "Germline DNA demethylation dynamics and imprint erasure through 5-hydroxymethylcytosine." Science **339**(6118): 448-452.

Hahn, M. A., R. Qiu, X. Wu, A. X. Li, H. Zhang, J. Wang, J. Jui, S. G. Jin, Y. Jiang, G. P. Pfeifer and Q. Lu (2013). "Dynamics of 5-hydroxymethylcytosine and chromatin marks in Mammalian neurogenesis." Cell Rep **3**(2): 291-300.

Hajkova, P., S. Erhardt, N. Lane, T. Haaf, O. El-Maarri, W. Reik, J. Walter and M. A. Surani (2002). "Epigenetic reprogramming in mouse primordial germ cells." Mech Dev **117**(1-2): 15-23.

Han, K., V. A. Gennarino, Y. Lee, K. Pang, K. Hashimoto-Torii, S. Choufani, C. S. Raju, M. C. Oldham, R. Weksberg, P. Rakic, Z. Liu and H. Y. Zoghbi (2013). "Human-specific regulation of MeCP2 levels in fetal brains by microRNA miR-483-5p." Genes Dev **27**(5): 485-490.

Han, W., K. Y. Kwan, S. Shim, M. M. Lam, Y. Shin, X. Xu, Y. Zhu, M. Li and N. Sestan (2011). "TBR1 directly represses Fezf2 to control the laminar origin and development of the corticospinal tract." Proc Natl Acad Sci U S A **108**(7): 3041-3046.

Harper, C. C., C. H. Rocca, K. M. Thompson, J. Morfesis, S. Goodman, P. D. Darney, C. L. Westhoff and J. J. Speidel (2015). "Reductions in pregnancy rates in the USA with long-acting reversible contraception: a cluster randomised trial." Lancet **386**(9993): 562-568.

Hashimoto-Torii, K., Y. I. Kawasawa, A. Kuhn and P. Rakic (2011). "Combined transcriptome analysis of fetal human and mouse cerebral cortex exposed to alcohol." Proc Natl Acad Sci U S A **108**(10): 4212-4217.

Hatten, M. E. (1990). "Riding the glial monorail: a common mechanism for glial-guided neuronal migration in different regions of the developing mammalian brain." Trends Neurosci **13**(5): 179-184.

Hatten, M. E. (1999). "Central nervous system neuronal migration." Annu Rev Neurosci **22**: 511-539.

Haycock, P. C. and M. Ramsay (2009). "Exposure of mouse embryos to ethanol during preimplantation development: effect on DNA methylation in the h19 imprinting control region." Biol Reprod **81**(4): 618-627.

He, X., M. N. Treacy, D. M. Simmons, H. A. Ingraham, L. W. Swanson and M. G. Rosenfeld (1989). "Expression of a large family of POU-domain regulatory genes in mammalian brain development." Nature **340**(6228): 35-41.

Hegedus, A. M., A. I. Alterman and R. E. Tarter (1984). "Learning achievement in sons of alcoholics." Alcohol Clin Exp Res **8**(3): 330-333.

Heijmans, B. T., E. W. Tobi, A. D. Stein, H. Putter, G. J. Blauw, E. S. Susser, P. E. Slagboom and L. H. Lumey (2008). "Persistent epigenetic differences associated with prenatal exposure to famine in humans." Proc Natl Acad Sci U S A **105**(44): 17046-17049.

Henriksen, T. B., N. H. Hjollund, T. K. Jensen, J. P. Bonde, A. M. Andersson, H. Kolstad, E. Ernst, A. Giwercman, N. E. Skakkebaek and J. Olsen (2004). "Alcohol

consumption at the time of conception and spontaneous abortion." Am J Epidemiol **160**(7): 661-667.

Hernandez-Valero, M. A., J. Rother, I. Gorlov, M. Frazier and O. Gorlova (2013). "Interplay between polymorphisms and methylation in the H19/IGF2 gene region may contribute to obesity in Mexican-American children." J Dev Orig Health Dis **4**(6): 499-506.

Hevner, R. F., L. Shi, N. Justice, Y. Hsueh, M. Sheng, S. Smiga, A. Bulfone, A. M. Goffinet, A. T. Campagnoni and J. L. Rubenstein (2001). "Tbr1 regulates differentiation of the preplate and layer 6." Neuron **29**(2): 353-366.

Hewitt, A. J., A. L. Knuff, M. J. Jefkins, C. P. Collier, J. N. Reynolds and J. F. Brien (2011). "Chronic ethanol exposure and folic acid supplementation: fetal growth and folate status in the maternal and fetal guinea pig." Reprod Toxicol **31**(4): 500-506.

Hicks, S. D., L. Lewis, J. Ritchie, P. Burke, Y. Abdul-Malak, N. Adackapara, K. Canfield, E. Shwarts, K. Gentile, Z. S. Meszaros and F. A. Middleton (2012). "Evaluation of cell proliferation, apoptosis, and DNA-repair genes as potential biomarkers for ethanol-induced CNS alterations." BMC Neurosci **13**: 128.

Hirabayashi, K., K. Shiota and S. Yagi (2013). "DNA methylation profile dynamics of tissue-dependent and differentially methylated regions during mouse brain development." BMC Genomics **14**: 82.

Hisahara, S., S. Chiba, H. Matsumoto, M. Tanno, H. Yagi, S. Shimohama, M. Sato and Y. Horio (2008). "Histone deacetylase SIRT1 modulates neuronal differentiation by its nuclear translocation." Proc Natl Acad Sci U S A **105**(40): 15599-15604.

Hou, S. T., D. Callaghan, M. C. Fournier, I. Hill, L. Kang, B. Massie, P. Morley, C. Murray, I. Rasquinha, R. Slack and J. P. MacManus (2000). "The transcription factor E2F1 modulates apoptosis of neurons." J Neurochem **75**(1): 91-100.

Huang, H., Z. He, C. Zhu, L. Liu, H. Kou, L. Shen and H. Wang (2015). "Prenatal ethanol exposure-induced adrenal developmental abnormality of male offspring rats and its possible intrauterine programming mechanisms." Toxicol Appl Pharmacol **288**(1): 84-94.

Hutson, J. R., B. Stade, D. C. Lehotay, C. P. Collier and B. M. Kapur (2012). "Folic acid transport to the human fetus is decreased in pregnancies with chronic alcohol exposure." PLoS One **7**(5): e38057.

Idrus, N. M., K. R. Breit and J. D. Thomas (2017). "Dietary choline levels modify the effects of prenatal alcohol exposure in rats." Neurotoxicol Teratol **59**: 43-52.

Ikonomidou, C., P. Bittigau, M. J. Ishimaru, D. F. Wozniak, C. Koch, K. Genz, M. T. Price, V. Stefovska, F. Horster, T. Tenkova, K. Dikranian and J. W. Olney (2000).

"Ethanol-induced apoptotic neurodegeneration and fetal alcohol syndrome." Science **287**(5455): 1056-1060.

Inoue, A. and Y. Zhang (2011). "Replication-dependent loss of 5-hydroxymethylcytosine in mouse preimplantation embryos." Science **334**(6053): 194.

Irwin, R. E., K. Pentieva, T. Cassidy, D. J. Lees-Murdock, M. McLaughlin, G. Prasad, H. McNulty and C. P. Walsh (2016). "The interplay between DNA methylation, folate and neurocognitive development." Epigenomics **8**(6): 863-879.

Ito, S., L. Shen, Q. Dai, S. C. Wu, L. B. Collins, J. A. Swenberg, C. He and Y. Zhang (2011). "Tet proteins can convert 5-methylcytosine to 5-formylcytosine and 5-carboxylcytosine." Science **333**(6047): 1300-1303.

Iwamoto, K., M. Bundo, J. Ueda, M. C. Oldham, W. Ukai, E. Hashimoto, T. Saito, D. H. Geschwind and T. Kato (2011). "Neurons show distinctive DNA methylation profile and higher interindividual variations compared with non-neurons." Genome Res **21**(5): 688-696.

Jacobson, S. W., J. L. Jacobson, M. E. Stanton, E. M. Meintjes and C. D. Molteno (2011). "Biobehavioral markers of adverse effect in fetal alcohol spectrum disorders." Neuropsychol Rev **21**(2): 148-166.

Jayabal, S., L. Ljungberg, T. Erwes, A. Cormier, S. Quilez, S. El Jaouhari and A. J. Watt (2015). "Rapid Onset of Motor Deficits in a Mouse Model of Spinocerebellar Ataxia Type 6 Precedes Late Cerebellar Degeneration." eNeuro **2**(6).

Jobe, E. M., A. L. McQuate and X. Zhao (2012). "Crosstalk among Epigenetic Pathways Regulates Neurogenesis." Front Neurosci **6**: 59.

Jones, K. L., H. E. Hoyme, L. K. Robinson, M. Del Campo, M. A. Manning, L. M. Prewitt and C. D. Chambers (2010). "Fetal alcohol spectrum disorders: Extending the range of structural defects." Am J Med Genet A **152a**(11): 2731-2735.

Jones, P. A. and D. Takai (2001). "The role of DNA methylation in mammalian epigenetics." Science **293**(5532): 1068-1070.

Jorgensen, H. F., I. Ben-Porath and A. P. Bird (2004). "Mbd1 is recruited to both methylated and nonmethylated CpGs via distinct DNA binding domains." Mol Cell Biol **24**(8): 3387-3395.

Joubert, B. R., H. T. den Dekker, J. F. Felix, J. Bohlin, S. Ligthart, E. Beckett, H. Tiemeier, J. B. van Meurs, A. G. Uitterlinden, A. Hofman, S. E. Haberg, S. E. Reese, M. J. Peters, B. K. Andreassen, E. A. Steegers, R. M. Nilsen, S. E. Vollset, O. Midttun, P. M. Ueland, O. H. Franco, A. Dehghan, J. C. de Jongste, M. C. Wu, T. Wang, S. D. Peddada, V. W. Jaddoe, W. Nystad, L. Duijts and S. J. London (2016). "Maternal plasma folate

impacts differential DNA methylation in an epigenome-wide meta-analysis of newborns." Nat Commun **7**: 10577.

Kafri, T., M. Ariel, M. Brandeis, R. Shemer, L. Urven, J. McCarrey, H. Cedar and A. Razin (1992). "Developmental pattern of gene-specific DNA methylation in the mouse embryo and germ line." Genes Dev **6**(5): 705-714.

Kahoud, R. J., G. E. Elsen, R. F. Hevner and R. D. Hodge (2014). "Conditional ablation of Tbr2 results in abnormal development of the olfactory bulbs and subventricular zone-rostral migratory stream." Dev Dyn **243**(3): 440-450.

Kaji, K., J. Nichols and B. Hendrich (2007). "Mbd3, a component of the NuRD co-repressor complex, is required for development of pluripotent cells." Development **134**(6): 1123-1132.

Kaminen-Ahola, N., A. Ahola, M. Maga, K. A. Mallitt, P. Fahey, T. C. Cox, E. Whitelaw and S. Chong (2010). "Maternal ethanol consumption alters the epigenotype and the phenotype of offspring in a mouse model." PLoS Genet **6**(1): e1000811.

Kaminska, B., G. Mosieniak, M. Gierdalski, M. Kossut and L. Kaczmarck (1995). "Elevated AP-1 transcription factor DNA binding activity at the onset of functional plasticity during development of rat sensory cortical areas." Brain Res Mol Brain Res **33**(2): 295-304.

Kanazawa, S. and V. Herbert (1985). "Total corrinoid, cobalamin (vitamin B12), and cobalamin analogue levels may be normal in serum despite cobalamin in liver depletion in patients with alcoholism." Lab Invest **53**(1): 108-110.

Kanold, P. O., P. Kara, R. C. Reid and C. J. Shatz (2003). "Role of subplate neurons in functional maturation of visual cortical columns." Science **301**(5632): 521-525.

Kao, T. T., C. Y. Chu, G. H. Lee, T. H. Hsiao, N. W. Cheng, N. S. Chang, B. H. Chen and T. F. Fu (2014). "Folate deficiency-induced oxidative stress contributes to neuropathy in young and aged zebrafish--implication in neural tube defects and Alzheimer's diseases." Neurobiol Dis **71**: 234-244.

Kashyap, B., R. A. Frey and D. L. Stenkamp (2011). "Ethanol-induced microphthalmia is not mediated by changes in retinoic acid or sonic hedgehog signaling during retinal neurogenesis." Alcohol Clin Exp Res **35**(9): 1644-1661.

Kharbanda, K. K., D. D. Rogers, 2nd, M. E. Mailliard, G. L. Siford, A. J. Barak, H. C. Beckenhauer, M. F. Sorrell and D. J. Tuma (2005). "A comparison of the effects of betaine and S-adenosylmethionine on ethanol-induced changes in methionine metabolism and steatosis in rat hepatocytes." J Nutr **135**(3): 519-524.

Kim, K. C., H. S. Go, H. R. Bak, C. S. Choi, I. Choi, P. Kim, S. H. Han, S. M. Han, C. Y. Shin and K. H. Ko (2010). "Prenatal exposure of ethanol induces increased glutamatergic neuronal differentiation of neural progenitor cells." J Biomed Sci **17**: 85.

Kim, M., Y. K. Park, T. W. Kang, S. H. Lee, Y. H. Rhee, J. L. Park, H. J. Kim, D. Lee, D. Lee, S. Y. Kim and Y. S. Kim (2014). "Dynamic changes in DNA methylation and hydroxymethylation when hES cells undergo differentiation toward a neuronal lineage." Hum Mol Genet **23**(3): 657-667.

Kirke, P. N., A. M. Molloy, L. E. Daly, H. Burke, D. G. Weir and J. M. Scott (1993). "Maternal plasma folate and vitamin B12 are independent risk factors for neural tube defects." Q J Med **86**(11): 703-708.

Kirsch, L., N. Liscovitch and G. Chechik (2012). "Localizing genes to cerebellar layers by classifying ISH images." PLoS Comput Biol **8**(12): e1002790.

Kishi, N. and J. D. Macklis (2004). "MECP2 is progressively expressed in post-migratory neurons and is involved in neuronal maturation rather than cell fate decisions." Mol Cell Neurosci **27**(3): 306-321.

Kleiber, M. L., E. J. Diehl, B. I. Laufer, K. Mantha, A. Chokroborty-Hoque, B. Alberry and S. M. Singh (2014). "Long-term genomic and epigenomic dysregulation as a consequence of prenatal alcohol exposure: a model for fetal alcohol spectrum disorders." Front Genet **5**: 161.

Kokavec, A. (2008). "Is decreased appetite for food a physiological consequence of alcohol consumption?" Appetite **51**(2): 233-243.

Komuro, H., E. Yacubova, E. Yacubova and P. Rakic (2001). "Mode and tempo of tangential cell migration in the cerebellar external granular layer." J Neurosci **21**(2): 527-540.

Kowalczyk, T., A. Pontious, C. Englund, R. A. Daza, F. Bedogni, R. Hodge, A. Attardo, C. Bell, W. B. Huttner and R. F. Hevner (2009). "Intermediate neuronal progenitors (basal progenitors) produce pyramidal-projection neurons for all layers of cerebral cortex." Cereb Cortex **19**(10): 2439-2450.

Kozlenkov, A., M. Wang, P. Roussos, S. Rudchenko, M. Barbu, M. Bibikova, B. Klotzle, A. J. Dwork, B. Zhang, Y. L. Hurd, E. V. Koonin, M. Wegner and S. Dracheva (2016). "Substantial DNA methylation differences between two major neuronal subtypes in human brain." Nucleic Acids Res **44**(6): 2593-2612.

Kriaucionis, S. and N. Heintz (2009). "The nuclear DNA base 5-hydroxymethylcytosine is present in Purkinje neurons and the brain." Science **324**(5929): 929-930.

Kriegstein, A. R. and M. Gotz (2003). "Radial glia diversity: a matter of cell fate." Glia **43**(1): 37-43.
Kubiura, M., M. Okano, H. Kimura, F. Kawamura and M. Tada (2012). "Chromosome-wide regulation of euchromatin-specific 5mC to 5hmC conversion in mouse ES cells and female human somatic cells." Chromosome Res **20**(7): 837-848.

Kusat Ol, K., G. Kanbak, A. Oglakci Ilhan, D. Burukoglu and F. Yucel (2016). "The investigation of the prenatal and postnatal alcohol exposure-induced neurodegeneration in rat brain: protection by betaine and/or omega-3." Childs Nerv Syst **32**(3): 467-474.

Kutanzi, K., I. Koturbash and O. Kovalchuk (2010). "Reversibility of pre-malignant estrogen-induced epigenetic changes." Cell Cycle **9**(15): 3150-3156.

Kwan, K. Y., M. M. Lam, Z. Krsnik, Y. I. Kawasawa, V. Lefebvre and N. Sestan (2008). "SOX5 postmitotically regulates migration, postmigratory differentiation, and projections of subplate and deep-layer neocortical neurons." Proc Natl Acad Sci U S A **105**(41): 16021-16026.

Kyzar, E. J., H. Zhang, A. J. Sakharkar and S. C. Pandey (2016). "Adolescent alcohol exposure alters lysine demethylase 1 (LSD1) expression and histone methylation in the amygdala during adulthood." Addict Biol.

Lahiri, D. K., B. Maloney and N. H. Zawia (2009). "The LEARn model: an epigenetic explanation for idiopathic neurobiological diseases." Mol Psychiatry **14**(11): 992-1003.

Lai, T., D. Jabaudon, B. J. Molyneaux, E. Azim, P. Arlotta, J. R. L. Menezes and J. D. Macklis (2008). "SOX5 Controls the Sequential Generation of Distinct Corticofugal Neuron Subtypes." Neuron **57**(2): 232-247.

Lan, J., S. Hua, X. He and Y. Zhang (2010). "DNA methyltransferases and methyl-binding proteins of mammals." Acta Biochim Biophys Sin (Shanghai) **42**(4): 243-252.

Lane, N., W. Dean, S. Erhardt, P. Hajkova, A. Surani, J. Walter and W. Reik (2003). "Resistance of IAPs to methylation reprogramming may provide a mechanism for epigenetic inheritance in the mouse." Genesis **35**(2): 88-93.

Lange, U. C. and R. Schneider (2010). "What an epigenome remembers." Bioessays **32**(8): 659-668.

Lawrence, R. C., N. K. Otero and S. J. Kelly (2012). "Selective effects of perinatal ethanol exposure in medial prefrontal cortex and nucleus accumbens." Neurotoxicol Teratol **34**(1): 128-135.

Leasure, J. L. and K. Nixon (2010). "Exercise neuroprotection in a rat model of binge alcohol consumption." Alcohol Clin Exp Res **34**(3): 404-414.

Lebedeva, J., A. Zakharov, E. Ogievetsky, A. Minlebaeva, R. Kurbanov, E. Gerasimova, G. Sitdikova and R. Khazipov (2017). "Inhibition of Cortical Activity and Apoptosis Caused by Ethanol in Neonatal Rats In Vivo." Cereb Cortex **27**(2): 1068-1082.

Lebel, C., S. N. Mattson, E. P. Riley, K. L. Jones, C. M. Adnams, P. A. May, S. Y. Bookheimer, M. J. O'Connor, K. L. Narr, E. Kan, Z. Abaryan and E. R. Sowell (2012). "A longitudinal study of the long-term consequences of drinking during pregnancy: heavy in utero alcohol exposure disrupts the normal processes of brain development." J Neurosci **32**(44): 15243-15251.

Leichter, J. and M. Lee (1984). "Intestinal folate conjugase activity and folate absorption in the ethanol-fed pregnant rat." Drug Nutr Interact **3**(1): 53-59.

Leone, D. P., W. E. Heavner, E. A. Ferenczi, G. Dobreva, J. R. Huguenard, R. Grosschedl and S. K. McConnell (2015). "Satb2 Regulates the Differentiation of Both Callosal and Subcerebral Projection Neurons in the Developing Cerebral Cortex." Cereb Cortex **25**(10): 3406-3419.

Leto, K., A. Bartolini, Y. Yanagawa, K. Obata, L. Magrassi, K. Schilling and F. Rossi (2009). "Laminar fate and phenotype specification of cerebellar GABAergic interneurons." J Neurosci **29**(21): 7079-7091.

Levenson, J. M., T. L. Roth, F. D. Lubin, C. A. Miller, I. C. Huang, P. Desai, L. M. Malone and J. D. Sweatt (2006). "Evidence that DNA (cytosine-5) methyltransferase regulates synaptic plasticity in the hippocampus." J Biol Chem **281**(23): 15763-15773.

Li, E., T. H. Bestor and R. Jaenisch (1992). "Targeted mutation of the DNA methyltransferase gene results in embryonic lethality." Cell **69**(6): 915-926.

Li, T., D. Yang, J. Li, Y. Tang, J. Yang and W. Le (2015). "Critical role of Tet3 in neural progenitor cell maintenance and terminal differentiation." Mol Neurobiol **51**(1): 142-154.

Lin, G. W. (1991). "Maternal-fetal folate transfer: effect of ethanol and dietary folate deficiency." Alcohol **8**(3): 169-172.

Little, R. E. and C. F. Sing (1987). "Father's drinking and infant birth weight: report of an association." Teratology **36**(1): 59-65.

Liu, C., R. E. Marioni, A. K. Hedman, L. Pfeiffer, P. C. Tsai, L. M. Reynolds, A. C. Just, Q. Duan, C. G. Boer, T. Tanaka, C. E. Elks, S. Aslibekyan, J. A. Brody, B. Kuhnel, C. Herder, L. M. Almli, D. Zhi, Y. Wang, T. Huan, C. Yao, M. M. Mendelson, R. Joehanes, L. Liang, S. A. Love, W. Guan, S. Shah, A. F. McRae, A. Kretschmer, H. Prokisch, K. Strauch, A. Peters, P. M. Visscher, N. R. Wray, X. Guo, K. L. Wiggins, A. K. Smith, E. B. Binder, K. J. Ressler, M. R. Irvin, D. M. Absher, D. Hernandez, L. Ferrucci, S. Bandinelli, K. Lohman, J. Ding, L. Trevisi, S. Gustafsson, J. H. Sandling, L. Stolk, A. G. Uitterlinden, I. Yet, J. E. Castillo-Fernandez, T. D. Spector, J. D. Schwartz, P. Vokonas, L. Lind, Y. Li, M. Fornage, D. K. Arnett, N. J. Wareham, N. Sotoodehnia, K. K. Ong, J.

B. van Meurs, K. N. Conneely, A. A. Baccarelli, I. J. Deary, J. T. Bell, K. E. North, Y. Liu, M. Waldenberger, S. J. London, E. Ingelsson and D. Levy (2016). "A DNA methylation biomarker of alcohol consumption." Mol Psychiatry.

Liu, Y., Y. Balaraman, G. Wang, K. P. Nephew and F. C. Zhou (2009). "Alcohol exposure alters DNA methylation profiles in mouse embryos at early neurulation." Epigenetics **4**(7): 500-511.

Liu, Y., M. W. Mayo, A. S. Nagji, P. W. Smith, C. S. Ramsey, D. Li and D. R. Jones (2012). "Phosphorylation of RelA/p65 promotes DNMT-1 recruitment to chromatin and represses transcription of the tumor metastasis suppressor gene BRMS1." Oncogene **31**(9): 1143-1154.

Liyanage, V. R., R. M. Zachariah, J. R. Davie and M. Rastegar (2015). "Ethanol deregulates Mecp2/MeCP2 in differentiating neural stem cells via interplay between 5-methylcytosine and 5-hydroxymethylcytosine at the Mecp2 regulatory elements." Exp Neurol **265**: 102-117.

Lo, C.-L., S. R. Choudhury, J. Irudayaraj and F. C. Zhou (2017). "Epigenetic Editing of Ascl1 Gene in Neural Stem Cells by Optogenetics." Scientific Reports **7**: 42047.

Loche, E. and S. E. Ozanne (2016). "Early nutrition, epigenetics, and cardiovascular disease." Curr Opin Lipidol **27**(5): 449-458.

Lois, C. and A. Alvarez-Buylla (1993). "Proliferating subventricular zone cells in the adult mammalian forebrain can differentiate into neurons and glia." Proc Natl Acad Sci U S A **90**(5): 2074-2077.

Lu, S. C., Z. Z. Huang, H. Yang, J. M. Mato, M. A. Avila and H. Tsukamoto (2000). "Changes in methionine adenosyltransferase and S-adenosylmethionine homeostasis in alcoholic rat liver." Am J Physiol Gastrointest Liver Physiol **279**(1): G178-185.

Lumeng, L. (1978). "The role of acetaldehyde in mediating the deleterious effect of ethanol on pyridoxal 5'-phosphate metabolism." J Clin Invest **62**(2): 286-293.

Ma, Q., L. Sommer, P. Cserjesi and D. J. Anderson (1997). "Mash1 and neurogenin1 Expression Patterns Define Complementary Domains of Neuroepithelium in the Developing CNS and Are Correlated with Regions Expressing Notch Ligands." The Journal of Neuroscience **17**(10): 3644-3652.

Maatouk, D. M., L. D. Kellam, M. R. Mann, H. Lei, E. Li, M. S. Bartolomei and J. L. Resnick (2006). "DNA methylation is a primary mechanism for silencing postmigratory primordial germ cell genes in both germ cell and somatic cell lineages." Development **133**(17): 3411-3418.

Madrigano, J., A. Baccarelli, M. A. Mittleman, R. O. Wright, D. Sparrow, P. S. Vokonas, L. Tarantini and J. Schwartz (2011). "Prolonged exposure to particulate pollution, genes associated with glutathione pathways, and DNA methylation in a cohort of older men." Environ Health Perspect **119**(7): 977-982.

Maiti, A. and A. C. Drohat (2011). "Thymine DNA glycosylase can rapidly excise 5-formylcytosine and 5-carboxylcytosine: potential implications for active demethylation of CpG sites." J Biol Chem **286**(41): 35334-35338.

Maloney, B. and D. K. Lahiri (2016). "Epigenetics of dementia: understanding the disease as a transformation rather than a state." Lancet Neurol **15**(7): 760-774.

Marban, C., S. Suzanne, F. Dequiedt, S. de Walque, L. Redel, C. Van Lint, D. Aunis and O. Rohr (2007). "Recruitment of chromatin-modifying enzymes by CTIP2 promotes HIV-1 transcriptional silencing." Embo j **26**(2): 412-423.

Marjonen, H., A. Sierra, A. Nyman, V. Rogojin, O. Grohn, A. M. Linden, S. Hautaniemi and N. Kaminen-Ahola (2015). "Early maternal alcohol consumption alters hippocampal DNA methylation, gene expression and volume in a mouse model." PLoS One **10**(5): e0124931.

Marutha Ravindran, C. R. and M. K. Ticku (2004). "Changes in methylation pattern of NMDA receptor NR2B gene in cortical neurons after chronic ethanol treatment in mice." Brain Res Mol Brain Res **121**(1-2): 19-27.

Mason, S., B. Anthony, X. Lai, H. N. Ringham, M. Wang, F. A. Witzmann, J. S. You and F. C. Zhou (2012). "Ethanol exposure alters protein expression in a mouse model of fetal alcohol spectrum disorders." Int J Proteomics **2012**: 867141.

Mayer, W., A. Niveleau, J. Walter, R. Fundele and T. Haaf (2000). "Demethylation of the zygotic paternal genome." Nature **403**(6769): 501-502.

McCoy, C. R., N. L. Jackson, J. Day and S. M. Clinton (2017). "Genetic predisposition to high anxiety- and depression-like behavior coincides with diminished DNA methylation in the adult rat amygdala." Behav Brain Res **320**: 165-178.

McGuffin, R., P. Goff and R. S. Hillman (1975). "The effect of diet and alcohol on the development of folate deficiency in the rat." Br J Haematol **31**(2): 185-192.

McKay, B. E. and R. W. Turner (2005). "Physiological and morphological development of the rat cerebellar Purkinje cell." J Physiol **567**(Pt 3): 829-850.

McKenna, W. L., J. Betancourt, K. A. Larkin, B. Abrams, C. Guo, J. L. Rubenstein and B. Chen (2011). "Tbr1 and Fezf2 regulate alternate corticofugal neuronal identities during neocortical development." J Neurosci **31**(2): 549-564.

Mehedint, M. G., M. D. Niculescu, C. N. Craciunescu and S. H. Zeisel (2010). "Choline deficiency alters global histone methylation and epigenetic marking at the Re1 site of the calbindin 1 gene." Faseb j **24**(1): 184-195.

Mellen, M., P. Ayata, S. Dewell, S. Kriaucionis and N. Heintz (2012). "MeCP2 binds to 5hmC enriched within active genes and accessible chromatin in the nervous system." Cell **151**(7): 1417-1430.

Mello, T., E. Ceni, C. Surrenti and A. Galli (2008). "Alcohol induced hepatic fibrosis: role of acetaldehyde." Mol Aspects Med **29**(1-2): 17-21.

Mellott, T. J., M. T. Follettie, V. Diesl, A. A. Hill, I. Lopez-Coviella and J. K. Blusztajn (2007). "Prenatal choline availability modulates hippocampal and cerebral cortical gene expression." Faseb j **21**(7): 1311-1323.

Meza-Sosa, K. F., G. Pedraza-Alva and L. Perez-Martinez (2014). "microRNAs: key triggers of neuronal cell fate." Front Cell Neurosci **8**: 175.

Mihalas, A. B., G. E. Elsen, F. Bedogni, R. A. Daza, K. A. Ramos-Laguna, S. J. Arnold and R. F. Hevner (2016). "Intermediate Progenitor Cohorts Differentially Generate Cortical Layers and Require Tbr2 for Timely Acquisition of Neuronal Subtype Identity." Cell Rep **16**(1): 92-105.

Mikael, L. G., L. Deng, L. Paul, J. Selhub and R. Rozen (2013). "Moderately high intake of folic acid has a negative impact on mouse embryonic development." Birth Defects Res A Clin Mol Teratol **97**(1): 47-52.

Miller, C. A., S. L. Campbell and J. D. Sweatt (2008). "DNA methylation and histone acetylation work in concert to regulate memory formation and synaptic plasticity." Neurobiol Learn Mem **89**(4): 599-603.

Miller, C. A., C. F. Gavin, J. A. White, R. R. Parrish, A. Honasoge, C. R. Yancey, I. M. Rivera, M. D. Rubio, G. Rumbaugh and J. D. Sweatt (2010). "Cortical DNA methylation maintains remote memory." Nat Neurosci **13**(6): 664-666.

Miller, M. W. and S. Robertson (1993). "Prenatal exposure to ethanol alters the postnatal development and transformation of radial glia to astrocytes in the cortex." J Comp Neurol **337**(2): 253-266.

Miranda, R. C. (2012). "MicroRNAs and Fetal Brain Development: Implications for Ethanol Teratology during the Second Trimester Period of Neurogenesis." Front Genet **3**: 77.

Mittal, N., J. B. Nathan and S. C. Pandey (1999). "Neuroadaptational changes in DNA binding of stimulatory protein-1 and nuclear factor-kB gene transcription factors during ethanol dependence." Eur J Pharmacol **386**(1): 113-119.

Molloy, A. M., P. N. Kirke, L. C. Brody, J. M. Scott and J. L. Mills (2008). "Effects of folate and vitamin B12 deficiencies during pregnancy on fetal, infant, and child development." Food Nutr Bull **29**(2 Suppl): S101-111; discussion S112-105.

Monk, M., M. Boubelik and S. Lehnert (1987). "Temporal and regional changes in DNA methylation in the embryonic, extraembryonic and germ cell lineages during mouse embryo development." Development **99**(3): 371-382.

Mooney, S. M. and M. W. Miller (2011). "Role of neurotrophins on postnatal neurogenesis in the thalamus: prenatal exposure to ethanol." Neuroscience **179**: 256-266.

Morimoto-Suzki, N., Y. Hirabayashi, K. Tyssowski, J. Shinga, M. Vidal, H. Koseki and Y. Gotoh (2014). "The polycomb component Ring1B regulates the timed termination of subcerebral projection neuron production during mouse neocortical development." Development **141**(22): 4343-4353.

Morris, R. J., J. N. Beech, P. C. Barber and G. Raisman (1985). "Late emergence of Thy-1 on climbing fibres demonstrates a gradient of maturation from the fissures to the folial convexities in developing rat cerebellum." J Neurocytol **14**(3): 453-467.

Mullaney, B. C., M. V. Johnston and M. E. Blue (2004). "Developmental expression of methyl-CpG binding protein 2 is dynamically regulated in the rodent brain." Neuroscience **123**(4): 939-949.

Munzel, M., D. Globisch, C. Trindler and T. Carell (2010). "Efficient synthesis of 5-hydroxymethylcytosine containing DNA." Org Lett **12**(24): 5671-5673.

Murillo-Fuentes, M. L., M. L. Murillo and O. Carreras (2003). "Effects of maternal ethanol consumption during pregnancy or lactation on intestinal absorption of folic acid in suckling rats." Life Sci **73**(17): 2199-2209.

Nadarajah, B., P. Alifragis, R. O. Wong and J. G. Parnavelas (2003). "Neuronal migration in the developing cerebral cortex: observations based on real-time imaging." Cereb Cortex **13**(6): 607-611.

Nakatani, H., E. Martin, H. Hassani, A. Clavairoly, C. L. Maire, A. Viadieu, C. Kerninon, A. Delmasure, M. Frah, M. Weber, M. Nakafuku, B. Zalc, J. L. Thomas, F. Guillemot, B. Nait-Oumesmar and C. Parras (2013). "Ascl1/Mash1 promotes brain oligodendrogenesis during myelination and remyelination." J Neurosci **33**(23): 9752-9768.

Nam, K. W., N. Castellanos, A. Simmons, S. Froudist-Walsh, M. P. Allin, M. Walshe, R. M. Murray, A. Evans, J. S. Muehlboeck and C. Nosarti (2015). "Alterations in cortical thickness development in preterm-born individuals: Implications for high-order cognitive functions." Neuroimage **115**: 64-75.

Nardelli, A., C. Lebel, C. Rasmussen, G. Andrew and C. Beaulieu (2011). "Extensive deep gray matter volume reductions in children and adolescents with fetal alcohol spectrum disorders." Alcohol Clin Exp Res **35**(8): 1404-1417.

Ngai, Y. F., D. C. Sulistyoningrum, R. O'Neill, S. M. Innis, J. Weinberg and A. M. Devlin (2015). "Prenatal alcohol exposure alters methyl metabolism and programs serotonin transporter and glucocorticoid receptor expression in brain." Am J Physiol Regul Integr Comp Physiol **309**(5): R613-622.

Nguyen, T. T., R. D. Risbud, S. N. Mattson, C. D. Chambers and J. D. Thomas (2016). "Randomized, double-blind, placebo-controlled clinical trial of choline supplementation in school-aged children with fetal alcohol spectrum disorders." Am J Clin Nutr **104**(6): 1683-1692.

Niculescu, M. D., C. N. Craciunescu and S. H. Zeisel (2006). "Dietary choline deficiency alters global and gene-specific DNA methylation in the developing hippocampus of mouse fetal brains." Faseb j **20**(1): 43-49.

Noctor, S. C., V. Martinez-Cerdeno, L. Ivic and A. R. Kriegstein (2004). "Cortical neurons arise in symmetric and asymmetric division zones and migrate through specific phases." Nat Neurosci **7**(2): 136-144.

Nogales, F., M. L. Ojeda, M. J. Delgado, K. Jotty, J. Diaz Castro, M. L. Murillo and O. Carreras (2011). "Effects of antioxidant supplementation on duodenal Se-Met absorption in ethanol-exposed rat offspring in vivo." J Reprod Dev **57**(6): 708-714.

O'Connor, M. J., B. Shah, S. Whaley, P. Cronin, B. Gunderson and J. Graham (2002). "Psychiatric illness in a clinical sample of children with prenatal alcohol exposure." Am J Drug Alcohol Abuse **28**(4): 743-754.

O'Hare, E. D., E. Kan, J. Yoshii, S. N. Mattson, E. P. Riley, P. M. Thompson, A. W. Toga and E. R. Sowell (2005). "Mapping cerebellar vermal morphology and cognitive correlates in prenatal alcohol exposure." Neuroreport **16**(12): 1285-1290.

Okano, M., D. W. Bell, D. A. Haber and E. Li (1999). "DNA methyltransferases Dnmt3a and Dnmt3b are essential for de novo methylation and mammalian development." Cell **99**(3): 247-257.

Ollikainen, M., K. R. Smith, E. J. Joo, H. K. Ng, R. Andronikos, B. Novakovic, N. K. Abdul Aziz, J. B. Carlin, R. Morley, R. Saffery and J. M. Craig (2010). "DNA methylation analysis of multiple tissues from newborn twins reveals both genetic and intrauterine components to variation in the human neonatal epigenome." Hum Mol Genet **19**(21): 4176-4188.

Otero, N. K., J. D. Thomas, C. A. Saski, X. Xia and S. J. Kelly (2012). "Choline supplementation and DNA methylation in the hippocampus and prefrontal cortex of rats exposed to alcohol during development." Alcohol Clin Exp Res **36**(10): 1701-1709.

Othman, T., D. Legare, P. Sadri, W. W. Lautt and F. E. Parkinson (2002). "A preliminary investigation of the effects of maternal ethanol intake during gestation and lactation on brain adenosine A(1) receptor expression in rat offspring." Neurotoxicol Teratol **24**(2): 275-279.

Ouko, L. A., K. Shantikumar, J. Knezovich, P. Haycock, D. J. Schnugh and M. Ramsay (2009). "Effect of alcohol consumption on CpG methylation in the differentially methylated regions of H19 and IG-DMR in male gametes: implications for fetal alcohol spectrum disorders." Alcohol Clin Exp Res **33**(9): 1615-1627.

Ozaki, N. and D. M. Chuang (1997). "Lithium increases transcription factor binding to AP-1 and cyclic AMP-responsive element in cultured neurons and rat brain." J Neurochem **69**(6): 2336-2344.

Pacary, E., J. Heng, R. Azzarelli, P. Riou, D. Castro, M. Lebel-Potter, C. Parras, D. M. Bell, A. J. Ridley, M. Parsons and F. Guillemot (2011). "Proneural transcription factors regulate different steps of cortical neuron migration through Rnd-mediated inhibition of RhoA signaling." Neuron **69**(6): 1069-1084.

Padmanabhan, N., D. Jia, C. Geary-Joo, X. Wu, A. C. Ferguson-Smith, E. Fung, M. C. Bieda, F. F. Snyder, R. A. Gravel, J. C. Cross and E. D. Watson (2013). "Mutation in folate metabolism causes epigenetic instability and transgenerational effects on development." Cell **155**(1): 81-93.
Padmanabhan, R., A. Ibrahim and A. Bener (2002). "Effect of maternal methionine pre-treatment on alcohol-induced exencephaly and axial skeletal dysmorphogenesis in mouse fetuses." Drug Alcohol Depend **65**(3): 263-281.

Parlesak, A., C. Bode and J. C. Bode (1998). "Free methionine supplementation limits alcohol-induced liver damage in rats." Alcohol Clin Exp Res **22**(2): 352-358.

Pastor, W. A., U. J. Pape, Y. Huang, H. R. Henderson, R. Lister, M. Ko, E. M. McLoughlin, Y. Brudno, S. Mahapatra, P. Kapranov, M. Tahiliani, G. Q. Daley, X. S. Liu, J. R. Ecker, P. M. Milos, S. Agarwal and A. Rao (2011). "Genome-wide mapping of 5-hydroxymethylcytosine in embryonic stem cells." Nature **473**(7347): 394-397.

Paul, A., Y. Cai, G. S. Atwal and Z. J. Huang (2012). "Developmental Coordination of Gene Expression between Synaptic Partners During GABAergic Circuit Assembly in Cerebellar Cortex." Front Neural Circuits **6**: 37.

Pauwels, S., M. Ghosh, R. C. Duca, B. Bekaert, K. Freson, I. Huybrechts, A. S. L. S, G. Koppen, R. Devlieger and L. Godderis (2017). "Dietary and supplemental maternal methyl-group donor intake and cord blood DNA methylation." Epigenetics **12**(1): 1-10.

Pennypacker, K. R., Y. Xiao, R. H. Xu and G. J. Harry (1997). "Lead-induced developmental changes in AP-1 DNA binding in rat brain." Int J Dev Neurosci **15**(3): 321-328.

Petrossian, T. C. and S. G. Clarke (2011). "Uncovering the human methyltransferasome." Mol Cell Proteomics **10**(1): M110.000976.
Pickell, L., K. Brown, D. Li, X. L. Wang, L. Deng, Q. Wu, J. Selhub, L. Luo, L. Jerome-Majewska and R. Rozen (2011). "High intake of folic acid disrupts embryonic development in mice." Birth Defects Res A Clin Mol Teratol **91**(1): 8-19.

Polache, A., R. V. Martin-Algarra and C. Guerri (1996). "Effects of chronic alcohol consumption on enzyme activities and active methionine absorption in the small intestine of pregnant rats." Alcohol Clin Exp Res **20**(7): 1237-1242.

Popp, C., W. Dean, S. Feng, S. J. Cokus, S. Andrews, M. Pellegrini, S. E. Jacobsen and W. Reik (2010). "Genome-wide erasure of DNA methylation in mouse primordial germ cells is affected by AID deficiency." Nature **463**(7284): 1101-1105.

Powrozek, T. A. and F. C. Zhou (2005). "Effects of prenatal alcohol exposure on the development of the vibrissal somatosensory cortical barrel network." Brain Res Dev Brain Res **155**(2): 135-146.

Price, E. M., M. S. Penaherrera, E. Portales-Casamar, P. Pavlidis, M. I. Van Allen, D. E. McFadden and W. P. Robinson (2016). "Profiling placental and fetal DNA methylation in human neural tube defects." Epigenetics Chromatin **9**: 6.

Przybycien-Szymanska, M. M., Y. S. Rao, S. A. Prins and T. R. Pak (2014). "Parental binge alcohol abuse alters F1 generation hypothalamic gene expression in the absence of direct fetal alcohol exposure." PLoS One **9**(2): e89320.

Qian, Y. Y., X. L. Huang, H. Liang, Z. F. Zhang, J. H. Xu, J. P. Chen, W. Yuan, L. He, L. Wang, M. H. Miao, J. Du and D. K. Li (2016). "Effects of maternal folic acid supplementation on gene methylation and being small for gestational age." J Hum Nutr Diet **29**(5): 643-651.

Qiang, M. and M. K. Ticku (2005). "Role of AP-1 in ethanol-induced N-methyl-D-aspartate receptor 2B subunit gene up-regulation in mouse cortical neurons." J Neurochem **95**(5): 1332-1341.

Rejitha, S., P. Prathibha and I. Madambath (2015). "The Ayurvedic drug Ksheerabala (101) ameliorates alcohol-induced neurotoxicity by down-regulating the expression of transcription factor (NFkB) in rat brain." Ayu **36**(3): 323-328.

Resendiz, M., Y. Chen, N. C. Ozturk and F. C. Zhou (2013). "Epigenetic medicine and fetal alcohol spectrum disorders." Epigenomics **5**(1): 73-86.

Resendiz, M., Chiao-Ling, L., Badin, J.K., Chiu, Y., and Zhou F.C. (2016). Alcohol Metabolism and Epigenetic Methylation and Acetylation. Molecular Ascpetcs of Alcohol and Nutrition. V. B. Patel. Waltham, MA, Academic Press**:** 287-303.

Resendiz, M., S. Mason, C. L. Lo and F. C. Zhou (2014). "Epigenetic regulation of the neural transcriptome and alcohol interference during development." Front Genet **5**: 285.

Reynolds, J. D., D. H. Penning, F. Dexter, B. Atkins, J. Hrdy, D. Poduska, D. H. Chestnut and J. F. Brien (1995). "Dose-dependent effects of acute in vivo ethanol exposure on extracellular glutamate concentration in the cerebral cortex of the near-term fetal sheep." Alcohol Clin Exp Res **19**(6): 1447-1453.
Riar, A. K., M. Narasimhan, M. L. Rathinam, G. I. Henderson and L. Mahimainathan (2016). "Ethanol induces cytostasis of cortical basal progenitors." J Biomed Sci **23**: 6.

Rimm, D. L., J. M. Giltnane, C. Moeder, M. Harigopal, G. G. Chung, R. L. Camp and B. Burtness (2007). "Bimodal Population or Pathologist Artifact?" Journal of Clinical Oncology **25**(17): 2487-2488.

Robert, M.-F., S. Morin, N. Beaulieu, F. Gauthier, I. C. Chute, A. Barsalou and A. R. MacLeod (2003). "DNMT1 is required to maintain CpG methylation and aberrant gene silencing in human cancer cells." Nat Genet **33**(1): 61-65.

Robertson, F. C., K. L. Narr, C. D. Molteno, J. L. Jacobson, S. W. Jacobson and E. M. Meintjes (2016). "Prenatal Alcohol Exposure is Associated with Regionally Thinner Cortex During the Preadolescent Period." Cereb Cortex **26**(7): 3083-3095.

Rong, Y., T. Wang and J. I. Morgan (2004). "Identification of candidate Purkinje cell-specific markers by gene expression profiling in wild-type and pcd(3J) mice." Brain Res Mol Brain Res **132**(2): 128-145.

Rosenfeld, J. A., B. C. Ballif, A. Lucas, E. J. Spence, C. Powell, A. S. Aylsworth, B. A. Torchia and L. G. Shaffer (2009). "Small Deletions of SATB2 Cause Some of the Clinical Features of the 2q33.1 Microdeletion Syndrome." PLOS ONE **4**(8): e6568.

Ross, R. G., S. K. Hunter, L. McCarthy, J. Beuler, A. K. Hutchison, B. D. Wagner, S. Leonard, K. E. Stevens and R. Freedman (2013). "Perinatal choline effects on neonatal pathophysiology related to later schizophrenia risk." Am J Psychiatry **170**(3): 290-298.

Sarkar, D. K. (2016). "Male germline transmits fetal alcohol epigenetic marks for multiple generations: a review." Addict Biol **21**(1): 23-34.

Savage, D. D., C. Y. Montano, M. A. Otero and L. L. Paxton (1991). "Prenatal ethanol exposure decreases hippocampal NMDA-sensitive [3H]-glutamate binding site density in 45-day-old rats." Alcohol **8**(3): 193-201.

Schaefer, A., S. C. Sampath, A. Intrator, A. Min, T. S. Gertler, D. J. Surmeier, A. Tarakhovsky and P. Greengard (2009). "Control of cognition and adaptive behavior by the GLP/G9a epigenetic suppressor complex." Neuron **64**(5): 678-691.

Schiesser, S., B. Hackner, T. Pfaffeneder, M. Muller, C. Hagemeier, M. Truss and T. Carell (2012). "Mechanism and stem-cell activity of 5-carboxycytosine decarboxylation determined by isotope tracing." Angew Chem Int Ed Engl **51**(26): 6516-6520.

Schmitz, S. U., M. Albert, M. Malatesta, L. Morey, J. V. Johansen, M. Bak, N. Tommerup, I. Abarrategui and K. Helin (2011). "Jarid1b targets genes regulating development and is involved in neural differentiation." Embo j **30**(22): 4586-4600.

Schuurmans, C., O. Armant, M. Nieto, J. M. Stenman, O. Britz, N. Klenin, C. Brown, L. M. Langevin, J. Seibt, H. Tang, J. M. Cunningham, R. Dyck, C. Walsh, K. Campbell, F. Polleux and F. Guillemot (2004). "Sequential phases of cortical specification involve Neurogenin-dependent and -independent pathways." Embo j **23**(14): 2892-2902.
Segal, N. L., Y. S. Montoya, Y. J. Loke and J. M. Craig (2017). "Identical twins doubly exchanged at birth: a case report of genetic and environmental influences on the adult epigenome." Epigenomics **9**(1): 5-12.

Sen, A., N. Heredia, M. C. Senut, M. Hess, S. Land, W. Qu, K. Hollacher, M. O. Dereski and D. M. Ruden (2015). "Early life lead exposure causes gender-specific changes in the DNA methylation profile of DNA extracted from dried blood spots." Epigenomics **7**(3): 379-393.

Serandour, A. A., S. Avner, F. Oger, M. Bizot, F. Percevault, C. Lucchetti-Miganeh, G. Palierne, C. Gheeraert, F. Barloy-Hubler, C. L. Peron, T. Madigou, E. Durand, P. Froguel, B. Staels, P. Lefebvre, R. Metivier, J. Eeckhoute and G. Salbert (2012). "Dynamic hydroxymethylation of deoxyribonucleic acid marks differentiation-associated enhancers." Nucleic Acids Res **40**(17): 8255-8265.

Serrano, M., M. T. Garcia-Silva, E. Martin-Hernandez, M. O'Callaghan Mdel, P. Quijada, A. Martinez-Aragon, A. Ormazabal, A. Blazquez, M. A. Martin, P. Briones, E. Lopez-Gallardo, E. Ruiz-Pesini, J. Montoya, R. Artuch and M. Pineda (2010). "Kearns-Sayre syndrome: cerebral folate deficiency, MRI findings and new cerebrospinal fluid biochemical features." Mitochondrion **10**(5): 429-432.

Sessa, A., C. A. Mao, G. Colasante, A. Nini, W. H. Klein and V. Broccoli (2010). "Tbr2-positive intermediate (basal) neuronal progenitors safeguard cerebral cortex expansion by controlling amplification of pallial glutamatergic neurons and attraction of subpallial GABAergic interneurons." Genes Dev **24**(16): 1816-1826.

Seyoum, G. and T. V. Persaud (1997). "Ethanol effects on postimplantation rat embryos: influence of zinc and methionine." Exp Toxicol Pathol **49**(3-4): 267-271.

Sharma, A. (2013). "Transgenerational epigenetic inheritance: focus on soma to germline information transfer." Prog Biophys Mol Biol **113**(3): 439-446.

Shaw, G. M., D. Schaffer, E. M. Velie, K. Morland and J. A. Harris (1995). "Periconceptional vitamin use, dietary folate, and the occurrence of neural tube defects." Epidemiology **6**(3): 219-226.

Shi, Y., J. Li, C. Chen, M. Gong, Y. Chen, Y. Liu, J. Chen, T. Li and W. Song (2014). "5-Mehtyltetrahydrofolate rescues alcohol-induced neural crest cell migration abnormalities." Mol Brain **7**: 67.

Shim, S., K. Y. Kwan, M. Li, V. Lefebvre and N. Sestan (2012). "Cis-regulatory control of corticospinal system development and evolution." Nature **486**(7401): 74-79.

Siegenthaler, J. A. and M. W. Miller (2004). "Transforming growth factor beta1 modulates cell migration in rat cortex: effects of ethanol." Cereb Cortex **14**(7): 791-802.

Siler, S. Q., R. A. Neese and M. K. Hellerstein (1999). "De novo lipogenesis, lipid kinetics, and whole-body lipid balances in humans after acute alcohol consumption." Am J Clin Nutr **70**(5): 928-936.

Singh, R. P., K. Shiue, D. Schomberg and F. C. Zhou (2009). "Cellular epigenetic modifications of neural stem cell differentiation." Cell Transplant **18**(10): 1197-1211.
Skorput, A. G., V. P. Gupta, P. W. Yeh and H. H. Yeh (2015). "Persistent Interneuronopathy in the Prefrontal Cortex of Young Adult Offspring Exposed to Ethanol In Utero." J Neurosci **35**(31): 10977-10988.

Sogut, I., O. Uysal, A. Oglakci, F. Yucel, K. Kartkaya and G. Kanbak (2017). "Prenatal alcohol-induced neuroapoptosis in rat brain cerebral cortex: protective effect of folic acid and betaine." Childs Nerv Syst **33**(3): 407-417.

Soliman, M. L., M. D. Smith, H. M. Houdek and T. A. Rosenberger (2012). "Acetate supplementation modulates brain histone acetylation and decreases interleukin-1beta expression in a rat model of neuroinflammation." J Neuroinflammation **9**: 51.

Song, C. X., K. E. Szulwach, Y. Fu, Q. Dai, C. Yi, X. Li, Y. Li, C. H. Chen, W. Zhang, X. Jian, J. Wang, L. Zhang, T. J. Looney, B. Zhang, L. A. Godley, L. M. Hicks, B. T. Lahn, P. Jin and C. He (2011). "Selective chemical labeling reveals the genome-wide distribution of 5-hydroxymethylcytosine." Nat Biotechnol **29**(1): 68-72.

Sotelo, C. (2004). "Cellular and genetic regulation of the development of the cerebellar system." Prog Neurobiol **72**(5): 295-339.

Sowell, E. R., S. N. Mattson, E. Kan, P. M. Thompson, E. P. Riley and A. W. Toga (2008). "Abnormal cortical thickness and brain-behavior correlation patterns in individuals with heavy prenatal alcohol exposure." Cereb Cortex **18**(1): 136-144.

Srinivasan, K., D. P. Leone, R. K. Bateson, G. Dobreva, Y. Kohwi, T. Kohwi-Shigematsu, R. Grosschedl and S. K. McConnell (2012). "A network of genetic repression and derepression specifies projection fates in the developing neocortex." Proc Natl Acad Sci U S A **109**(47): 19071-19078.

St-Cyr, S. and P. O. McGowan (2015). "Programming of stress-related behavior and epigenetic neural gene regulation in mice offspring through maternal exposure to predator odor." Front Behav Neurosci **9**: 145.

Stroud, H., S. Feng, S. Morey Kinney, S. Pradhan and S. E. Jacobsen (2011). "5-Hydroxymethylcytosine is associated with enhancers and gene bodies in human embryonic stem cells." Genome Biol **12**(6): R54.

Subbanna, S., M. Shivakumar, D. Psychoyos, S. Xie and B. S. Basavarajappa (2013). "Anandamide-CB1 receptor signaling contributes to postnatal ethanol-induced neonatal neurodegeneration, adult synaptic, and memory deficits." J Neurosci **33**(15): 6350-6366.

Subramanian, V. S., S. B. Subramanya, A. Ghosal and H. M. Said (2013). "Chronic alcohol feeding inhibits physiological and molecular parameters of intestinal and renal riboflavin transport." Am J Physiol Cell Physiol **305**(5): C539-546.

Suderman, M., P. O. McGowan, A. Sasaki, T. C. Huang, M. T. Hallett, M. J. Meaney, G. Turecki and M. Szyf (2012). "Conserved epigenetic sensitivity to early life experience in the rat and human hippocampus." Proc Natl Acad Sci U S A **109 Suppl 2**: 17266-17272.

Sun, Y., M. Nadal-Vicens, S. Misono, M. Z. Lin, A. Zubiaga, X. Hua, G. Fan and M. E. Greenberg (2001). "Neurogenin promotes neurogenesis and inhibits glial differentiation by independent mechanisms." Cell **104**(3): 365-376.

Szulwach, K. E., X. Li, Y. Li, C. X. Song, J. W. Han, S. Kim, S. Namburi, K. Hermetz, J. J. Kim, M. K. Rudd, Y. S. Yoon, B. Ren, C. He and P. Jin (2011). "Integrating 5-hydroxymethylcytosine into the epigenomic landscape of human embryonic stem cells." PLoS Genet **7**(6): e1002154.

Szulwach, K. E., X. Li, Y. Li, C. X. Song, H. Wu, Q. Dai, H. Irier, A. K. Upadhyay, M. Gearing, A. I. Levey, A. Vasanthakumar, L. A. Godley, Q. Chang, X. Cheng, C. He and P. Jin (2011). "5-hmC-mediated epigenetic dynamics during postnatal neurodevelopment and aging." Nat Neurosci **14**(12): 1607-1616.

Tahiliani, M., K. P. Koh, Y. Shen, W. A. Pastor, H. Bandukwala, Y. Brudno, S. Agarwal, L. M. Iyer, D. R. Liu, L. Aravind and A. Rao (2009). "Conversion of 5-methylcytosine to 5-hydroxymethylcytosine in mammalian DNA by MLL partner TET1." Science **324**(5929): 930-935.

Tan, L., L. Xiong, W. Xu, F. Wu, N. Huang, Y. Xu, L. Kong, L. Zheng, L. Schwartz, Y. Shi and Y. G. Shi (2013). "Genome-wide comparison of DNA hydroxymethylation in mouse embryonic stem cells and neural progenitor cells by a new comparative hMeDIP-seq method." Nucleic Acids Res **41**(7): e84.

Tan, S. L., M. Nishi, T. Ohtsuka, T. Matsui, K. Takemoto, A. Kamio-Miura, H. Aburatani, Y. Shinkai and R. Kageyama (2012). "Essential roles of the histone methyltransferase ESET in the epigenetic control of neural progenitor cells during development." Development **139**(20): 3806-3816.

Tantirigama, M. L. S., M. J. Oswald, C. Duynstee, S. M. Hughes and R. M. Empson (2014). "Expression of the Developmental Transcription Factor Fezf2 Identifies a Distinct Subpopulation of Layer 5 Intratelencephalic-Projection Neurons in Mature Mouse Motor Cortex." The Journal of Neuroscience **34**(12): 4303-4308.

Tarabykin, V., A. Stoykova, N. Usman and P. Gruss (2001). "Cortical upper layer neurons derive from the subventricular zone as indicated by Svet1 gene expression." Development **128**(11): 1983-1993.

Tavares, E., O. Carreras, A. Gomez-Tubio, D. Murillo and M. L. Murillo (2000). "Effects of folic acid and amino acids supplementation on zinc intestinal absorption in the progeny of ethanol-treated rats." J Physiol Biochem **56**(3): 247-256.

Tavares, E., A. Gomez-Tubio, M. L. Murillo and O. Carreras (1999). "Folic acid intestinal absorption in newborn rats at 21 day postpartum: effects of maternal ethanol consumption." Life Sci **64**(22): 2001-2010.

Taverna, E., M. Gotz and W. B. Huttner (2014). "The cell biology of neurogenesis: toward an understanding of the development and evolution of the neocortex." Annu Rev Cell Dev Biol **30**: 465-502.

Tchantchou, F., M. Graves, D. Ortiz, E. Rogers and T. B. Shea (2004). "Dietary supplementation with 3-deaza adenosine, N-acetyl cysteine, and S-adenosyl methionine provide neuroprotection against multiple consequences of vitamin deficiency and oxidative challenge: relevance to age-related neurodegeneration." Neuromolecular Med **6**(2-3): 93-103.

Teixeira, F. B., L. N. Santana, F. R. Bezerra, S. De Carvalho, E. A. Fontes-Junior, R. D. Prediger, M. E. Crespo-Lopez, C. S. Maia and R. R. Lima (2014). "Chronic ethanol exposure during adolescence in rats induces motor impairments and cerebral cortex damage associated with oxidative stress." PLoS One **9**(6): e101074.

Thomas, J. D., E. J. Abou and H. D. Dominguez (2009). "Prenatal choline supplementation mitigates the adverse effects of prenatal alcohol exposure on development in rats." Neurotoxicol Teratol **31**(5): 303-311.

Thomas, J. D., M. Garrison and T. M. O'Neill (2004). "Perinatal choline supplementation attenuates behavioral alterations associated with neonatal alcohol exposure in rats." Neurotoxicol Teratol **26**(1): 35-45.

Tian, W., M. Zhao, M. Li, T. Song, M. Zhang, L. Quan, S. Li and Z. S. Sun (2012). "Reversal of cocaine-conditioned place preference through methyl supplementation in mice: altering global DNA methylation in the prefrontal cortex." PLoS One **7**(3): e33435.

Tinker, S. C., M. E. Cogswell, O. Devine and R. J. Berry (2010). "Folic acid intake among U.S. women aged 15-44 years, National Health and Nutrition Examination Survey, 2003-2006." Am J Prev Med **38**(5): 534-542.

Tobi, E. W., L. H. Lumey, R. P. Talens, D. Kremer, H. Putter, A. D. Stein, P. E. Slagboom and B. T. Heijmans (2009). "DNA methylation differences after exposure to prenatal famine are common and timing- and sex-specific." Hum Mol Genet **18**(21): 4046-4053.

Toda, T., Y. Shinmyo, T. A. Dinh Duong, K. Masuda and H. Kawasaki (2016). "An essential role of SVZ progenitors in cortical folding in gyrencephalic mammals." Sci Rep **6**: 29578.

Tompkins, J. D., C. Hall, V. C. Chen, A. X. Li, X. Wu, D. Hsu, L. A. Couture and A. D. Riggs (2012). "Epigenetic stability, adaptability, and reversibility in human embryonic stem cells." Proc Natl Acad Sci U S A **109**(31): 12544-12549.

Toso, L., S. H. Poggi, D. Abebe, R. Roberson, V. Dunlap, J. Park and C. Y. Spong (2005). "N-methyl-D-aspartate subunit expression during mouse development altered by in utero alcohol exposure." Am J Obstet Gynecol **193**(4): 1534-1539.

Tran, P. V., B. C. Kennedy, Y. C. Lien, R. A. Simmons and M. K. Georgieff (2015). "Fetal iron deficiency induces chromatin remodeling at the Bdnf locus in adult rat hippocampus." Am J Physiol Regul Integr Comp Physiol **308**(4): R276-282.

Treit, S., D. Zhou, A. E. Chudley, G. Andrew, C. Rasmussen, S. M. Nikkel, D. Samdup, A. Hanlon-Dearman, C. Loock and C. Beaulieu (2016). "Relationships between Head Circumference, Brain Volume and Cognition in Children with Prenatal Alcohol Exposure." PLoS One **11**(2): e0150370.

Tyler, C. R. and A. M. Allan (2014). "Prenatal alcohol exposure alters expression of neurogenesis-related genes in an ex vivo cell culture model." Alcohol **48**(5): 483-492.
Umulis, D. M., N. M. Gurmen, P. Singh and H. S. Fogler (2005). "A physiologically based model for ethanol and acetaldehyde metabolism in human beings." Alcohol **35**(1): 3-12.

Valenzuela, C. F., R. A. Morton, M. R. Diaz and L. Topper (2012). "Does moderate drinking harm the fetal brain? Insights from animal models." Trends Neurosci **35**(5): 284-292.

Valles, S., M. Sancho-Tello, R. Minana, E. Climent, J. Renau-Piqueras and C. Guerri (1996). "Glial fibrillary acidic protein expression in rat brain and in radial glia culture is delayed by prenatal ethanol exposure." J Neurochem **67**(6): 2425-2433.

Vasistha, N. A., F. Garcia-Moreno, S. Arora, A. F. Cheung, S. J. Arnold, E. J. Robertson and Z. Molnar (2015). "Cortical and Clonal Contribution of Tbr2 Expressing Progenitors in the Developing Mouse Brain." Cereb Cortex **25**(10): 3290-3302.

Vecsey, C. G., J. D. Hawk, K. M. Lattal, J. M. Stein, S. A. Fabian, M. A. Attner, S. M. Cabrera, C. B. McDonough, P. K. Brindle, T. Abel and M. A. Wood (2007). "Histone deacetylase inhibitors enhance memory and synaptic plasticity via CREB:CBP-dependent transcriptional activation." J Neurosci **27**(23): 6128-6140.

Veenendaal, M. V., R. C. Painter, S. R. de Rooij, P. M. Bossuyt, J. A. van der Post, P. D. Gluckman, M. A. Hanson and T. J. Roseboom (2013). "Transgenerational effects of prenatal exposure to the 1944-45 Dutch famine." Bjog **120**(5): 548-553.

Vineis, P., A. Chatziioannou, V. T. Cunliffe, J. M. Flanagan, M. Hanson, M. Kirsch-Volders and S. Kyrtopoulos (2017). "Epigenetic memory in response to environmental stressors." Faseb j.

Vinueza Veloz, M. F., K. Zhou, L. W. Bosman, J. W. Potters, M. Negrello, R. M. Seepers, C. Strydis, S. K. Koekkoek and C. I. De Zeeuw (2015). "Cerebellar control of gait and interlimb coordination." Brain Struct Funct **220**(6): 3513-3536.

Vire, E., C. Brenner, R. Deplus, L. Blanchon, M. Fraga, C. Didelot, L. Morey, A. Van Eynde, D. Bernard, J. M. Vanderwinden, M. Bollen, M. Esteller, L. Di Croce, Y. de Launoit and F. Fuks (2006). "The Polycomb group protein EZH2 directly controls DNA methylation." Nature **439**(7078): 871-874.

Viswanathan, M., K. A. Treiman, J. Kish-Doto, J. C. Middleton, E. J. Coker-Schwimmer and W. K. Nicholson (2017). "Folic Acid Supplementation for the Prevention of Neural Tube Defects: An Updated Evidence Report and Systematic Review for the US Preventive Services Task Force." Jama **317**(2): 190-203.

Volk, B., J. Maletz, M. Tiedemann, G. Mall, C. Klein and H. H. Berlet (1981). "Impaired maturation of Purkinje cells in the fetal alcohol syndrome of the rat. Light and electron microscopic investigations." Acta Neuropathol **54**(1): 19-29.

Volpe, J. J. and R. D. Adams (1972). "Cerebro-hepato-renal syndrome of Zellweger: an inherited disorder of neuronal migration." Acta Neuropathol **20**(3): 175-198.

Wang, L. L., Z. Zhang, Q. Li, R. Yang, X. Pei, Y. Xu, J. Wang, S. F. Zhou and Y. Li (2009). "Ethanol exposure induces differential microRNA and target gene expression and teratogenic effects which can be suppressed by folic acid supplementation." Hum Reprod **24**(3): 562-579.
Wang, M., Z. Yue, R. Paus and Y. Ramot (2014). "SIRT2 as a new player in epigenetic programming of keratinocyte differentiation and a candidate tumor suppressor." Exp Dermatol **23**(9): 636-638.

Wang, Y., N. Surzenko, W. B. Friday and S. H. Zeisel (2016). "Maternal dietary intake of choline in mice regulates development of the cerebral cortex in the offspring." Faseb j **30**(4): 1566-1578.

Warnault, V., E. Darcq, A. Levine, S. Barak and D. Ron (2013). "Chromatin remodeling--a novel strategy to control excessive alcohol drinking." Transl Psychiatry **3**: e231.

Watanabe, D., K. Uchiyama and K. Hanaoka (2006). "Transition of mouse de novo methyltransferases expression from Dnmt3b to Dnmt3a during neural progenitor cell development." Neuroscience **142**(3): 727-737.

White, S. A., J. N. Weber, C. D. Howard and C. B. Favero (2015). "Effects of binge ethanol exposure during first-trimester equivalent on corticothalamic neurons in Swiss Webster outbred mice." Neuroreport **26**(18): 1083-1088.

Whitney, E. R., T. L. Kemper, D. L. Rosene, M. L. Bauman and G. J. Blatt (2008). "Calbindin-D28k is a more reliable marker of human Purkinje cells than standard Nissl stains: a stereological experiment." J Neurosci Methods **168**(1): 42-47.

Wiehle, L., G. Raddatz, T. Musch, M. M. Dawlaty, R. Jaenisch, F. Lyko and A. Breiling (2015). "Tet1 and Tet2 Protect DNA Methylation Canyons against Hypermethylation." Mol Cell Biol **36**(3): 452-461.

Wittenberger, T., S. Sleigh, D. Reisel, M. Zikan, B. Wahl, M. Alunni-Fabbroni, A. Jones, I. Evans, J. Koch, T. Paprotka, H. Lempiainen, T. Rujan, B. Rack, D. Cibula and M. Widschwendter (2014). "DNA methylation markers for early detection of women's cancer: promise and challenges." Epigenomics **6**(3): 311-327.

Wozniak, J. R., A. J. Fuglestad, J. K. Eckerle, B. A. Fink, H. L. Hoecker, C. J. Boys, J. P. Radke, M. G. Kroupina, N. C. Miller, A. M. Brearley, S. H. Zeisel and M. K. Georgieff (2015). "Choline supplementation in children with fetal alcohol spectrum disorders: a randomized, double-blind, placebo-controlled trial." Am J Clin Nutr **102**(5): 1113-1125.

Wozniak, J. R., A. J. Fuglestad, J. K. Eckerle, M. G. Kroupina, N. C. Miller, C. J. Boys, A. M. Brearley, B. A. Fink, H. L. Hoecker, S. H. Zeisel and M. K. Georgieff (2013). "Choline supplementation in children with fetal alcohol spectrum disorders has high feasibility and tolerability." Nutr Res **33**(11): 897-904.

Wu, B. T., R. A. Dyer, D. J. King, K. J. Richardson and S. M. Innis (2012). "Early second trimester maternal plasma choline and betaine are related to measures of early cognitive development in term infants." PLoS One **7**(8): e43448.

Wu, H., V. Coskun, J. Tao, W. Xie, W. Ge, K. Yoshikawa, E. Li, Y. Zhang and Y. E. Sun (2010). "Dnmt3a-dependent nonpromoter DNA methylation facilitates transcription of neurogenic genes." Science **329**(5990): 444-448.

Wu, H., A. C. D'Alessio, S. Ito, Z. Wang, K. Cui, K. Zhao, Y. E. Sun and Y. Zhang (2011). "Genome-wide analysis of 5-hydroxymethylcytosine distribution reveals its dual function in transcriptional regulation in mouse embryonic stem cells." Genes Dev **25**(7): 679-684.

Wu, S. C. and Y. Zhang (2010). "Active DNA demethylation: many roads lead to Rome." Nat Rev Mol Cell Biol **11**(9): 607-620.

Xu, L., Y. Yang, L. Gao, J. Zhao, Y. Cai, J. Huang, S. Jing, X. Bao, Y. Wang, J. Gao, H. Xu and X. Fan (2015). "Protective effects of resveratrol on the inhibition of hippocampal neurogenesis induced by ethanol during early postnatal life." Biochim Biophys Acta **1852**(7): 1298-1310.

Xu, Y., L. Li, Z. Zhang and Y. Li (2006). "Effects of folinic acid and Vitamin B12 on ethanol-induced developmental toxicity in mouse." Toxicol Lett **167**(3): 167-172.

Xu, Y., Y. Tang and Y. Li (2008). "Effect of folic acid on prenatal alcohol-induced modification of brain proteome in mice." Br J Nutr **99**(3): 455-461.

Yamazaki, Y., M. R. Mann, S. S. Lee, J. Marh, J. R. McCarrey, R. Yanagimachi and M. S. Bartolomei (2003). "Reprogramming of primordial germ cells begins before migration into the genital ridge, making these cells inadequate donors for reproductive cloning." Proc Natl Acad Sci U S A **100**(21): 12207-12212.

Yang, J., T. R. Corsello and Y. Ma (2012). "Stem cell gene SALL4 suppresses transcription through recruitment of DNA methyltransferases." J Biol Chem **287**(3): 1996-2005.

Yang, Y., O. R. Phillips, E. Kan, K. K. Sulik, S. N. Mattson, E. P. Riley, K. L. Jones, C. M. Adnams, P. A. May, M. J. O'Connor, K. L. Narr and E. R. Sowell (2012). "Callosal thickness reductions relate to facial dysmorphology in fetal alcohol spectrum disorders." Alcohol Clin Exp Res **36**(5): 798-806.

Yang, Y., F. Roussotte, E. Kan, K. K. Sulik, S. N. Mattson, E. P. Riley, K. L. Jones, C. M. Adnams, P. A. May, M. J. O'Connor, K. L. Narr and E. R. Sowell (2012). "Abnormal cortical thickness alterations in fetal alcohol spectrum disorders and their relationships with facial dysmorphology." Cereb Cortex **22**(5): 1170-1179.

Yehuda, R., N. P. Daskalakis, A. Lehrner, F. Desarnaud, H. N. Bader, I. Makotkine, J. D. Flory, L. M. Bierer and M. J. Meaney (2014). "Influences of maternal and paternal PTSD on epigenetic regulation of the glucocorticoid receptor gene in Holocaust survivor offspring." Am J Psychiatry **171**(8): 872-880.

Yen, C. L., M. H. Mar, R. B. Meeker, A. Fernandes and S. H. Zeisel (2001). "Choline deficiency induces apoptosis in primary cultures of fetal neurons." Faseb j **15**(10): 1704-1710.

Yunes, R., C. R. Estrella, S. Garcia, H. E. Lara and R. Cabrera (2015). "Postnatal administration of allopregnanolone modifies glutamate release but not BDNF content in striatum samples of rats prenatally exposed to ethanol." Biomed Res Int **2015**: 734367.

Zakhari, S. (2013). "Alcohol metabolism and epigenetics changes." Alcohol Res **35**(1): 6-16.

Zeisel, S. H. (2008). "Genetic polymorphisms in methyl-group metabolism and epigenetics: lessons from humans and mouse models." Brain Res **1237**: 5-11.

Zhang, J., J. Parvin and K. Huang (2012). "Redistribution of H3K4me2 on neural tissue specific genes during mouse brain development." BMC Genomics **13 Suppl 8**: S5.

Zhang, L. and J. E. Goldman (1996). "Developmental fates and migratory pathways of dividing progenitors in the postnatal rat cerebellum." J Comp Neurol **370**(4): 536-550.

Zhang, S., J. Li, R. Lea, K. Vleminckx and E. Amaya (2014). "Fezf2 promotes neuronal differentiation through localised activation of Wnt/beta-catenin signalling during forebrain development." Development **141**(24): 4794-4805.

Zhou, D., C. Lebel, C. Lepage, C. Rasmussen, A. Evans, K. Wyper, J. Pei, G. Andrew, A. Massey, D. Massey and C. Beaulieu (2011). "Developmental cortical thinning in fetal alcohol spectrum disorders." NeuroImage **58**(1): 16-25.

Zhou, F. C. (2012). "DNA methylation program during development." Front Biol (Beijing) **7**(6): 485-494.

Zhou, F. C., Y. Chen and A. Love (2011). "Cellular DNA methylation program during neurulation and its alteration by alcohol exposure." Birth Defects Res A Clin Mol Teratol **91**(8): 703-715.

Zhou, F. C., T. D. Patel, D. Swartz, Y. Xu and M. R. Kelley (1999). "Production and characterization of an anti-serotonin 1A receptor antibody which detects functional 5-HT1A binding sites." Brain Res Mol Brain Res **69**(2): 186-201.

Zhou, F. C., Y. Sari, T. Powrozek, C. R. Goodlett and T. K. Li (2003). "Moderate alcohol exposure compromises neural tube midline development in prenatal brain." Brain Res Dev Brain Res **144**(1): 43-55.

Zhou, F. C., Y. Sari and T. A. Powrozek (2005). "Fetal alcohol exposure reduces serotonin innervation and compromises development of the forebrain along the serotonergic pathway." Alcohol Clin Exp Res **29**(1): 141-149.

Zhou, F. C., Y. Sari, T. A. Powrozek and C. Y. Spong (2004). "A neuroprotective peptide antagonizes fetal alcohol exposure-compromised brain growth." J Mol Neurosci **24**(2): 189-199.

Zhou, F. C., Q. Zhao, Y. Liu, C. R. Goodlett, T. Liang, J. N. McClintick, H. J. Edenberg and L. Li (2011). "Alteration of gene expression by alcohol exposure at early neurulation." BMC Genomics **12**: 124.

Zhu, Y., X. Liao, L. Lu, W. Li, L. Zhang, C. Ji, X. Lin, H. C. Liu, J. Odle and X. Luo (2017). "Maternal dietary zinc supplementation enhances the epigenetic-activated antioxidant ability of chick embryos from maternal normal and high temperatures." Oncotarget.

Zidan, H. E., N. A. Rezk, A. A. Alnemr and A. M. Abd El Ghany (2015). "COX-2 gene promoter DNA methylation status in eutopic and ectopic endometrium of Egyptian women with endometriosis." J Reprod Immunol **112**: 63-67.

Zucca, S. and C. F. Valenzuela (2010). "Low concentrations of alcohol inhibit BDNF-dependent GABAergic plasticity via L-type Ca2+ channel inhibition in developing CA3 hippocampal pyramidal neurons." J Neurosci **30**(19): 6776-6781.

CURRICULUM VITAE

Marisol Resendiz

EDUCATION

2010-2017	Indiana University, Indianapolis, IN
	Ph.D., Medical Neuroscience; Minor, Life Science
	Advisor: Feng C. Zhou, Ph.D.
2005-2010	New Mexico State University, Las Cruces, NM
	B.S., Biology, Pre-medical
	B.A. Psychology

HONORS/AWARDS/AFFILIATIONS

Apr 2016	IUSM Graduate Student Travel Award
2015-2017	Society for Neuroscience, student member
Jun 2013-Jun 2017	T32-NIAAA Training Fellowship Recipient
May 2013-Aug 2016	Co-founder, President, Society for the Advancement of Chicanos and Native Americans in Science (SACNAS), IUPUI Chapter
Aug 2013-May 2015	IUSM Graduate Student Representative, Medical Neuroscience
Apr 2012	RSA Student Merit Award
2012-2017	Research Society on Alcoholism, student member
Apr 2011	Ford Foundation Predoctoral Fellowship, Honorable Mention
Jun-Aug 2010	National Science Foundation Summer Scholar

RESEARCH EXPERIENCE

2011-2017	Doctoral Dissertation Research
	Stark Neuroscience Research Institute, Indiana University School of Medicine, Indianapolis, IN
	Advisor: Feng C. Zhou, Ph.D.

	Thesis: *"The Regulatory Role and Environmental Sensitivity of DNA Methylation in Neural Development"*
2008-2010	Undergraduate Research (Research Initiative for Scientific Enhancement Fellow)
	Department of Biology, New Mexico State University, Las Cruces, NM
	Advisor: Graciela Unguez, Ph.D.
2007-20010	Undergraduate Research
	Department of Psychology, New Mexico State University, Las Cruces, NM
	Advisor: James Kroger, Ph.D.
	Thesis: *"A Behavioral Study of the Cognitive Pathway of Analogical Reasoning"*

PUBLICATIONS

1. Zhou FC, Resendiz M, Lo C-L. Environmental Influence of Epigenetics. June 2017. Ed. T. Tollefsbolin in Handbook of Epigenetics, 2nd Edition. 2017 June.
2. Ozturk NC, Resendiz M, Ozturk H, Zhou FC. DNA methylation program in normal and alcohol-induced thinning cortex. Alcohol. 2017 Feb 18.
3. Resendiz M, Lo CL, Badin J, FC Zhou. Alcohol metabolism and epigenetic methylation and acetylation. Molecular Aspects of Alcohol and Nutrition. 2016 December.
4. Zhou FC, Resendiz M, Lo CL, Chen Y. Cell-wide DNA de-methylation and de-methylation of Purkinje neurons in the developing cerebellum. PLoS One. 2016 Sep 1.
5. Resendiz M, Mason S, Lo CL, Zhou FC. Epigenetic regulation of the neural transcriptome and alcohol interference during development. Frontiers in Genetics. 2014 Aug 26.
6. Resendiz M, Chen Y, Ozturk NC, Zhou FC. Epigenetic medicine and fetal alcohol spectrum disorders. Epigenomics, 2013 February.

CONFERENCE ABSTRACTS AND PRESENTATIONS

1. M Resendiz & FC Zhou. Nutritional Deficiency Contributes to the Effects of Prenatal Alcohol on the Epigeneic Program of the Developing Cerebellum. Poster presentation. Research Society on Alcoholism, Orlando, FL 2013.

2. M Resendiz & FC Zhou. Methylation of Fetal Neural Cells via Alteration of DNA Methyltransferases. Poster presentation. Research Society on Alcoholism, Bellevue, WA 2014
3. M Resendiz, J Reiter & FC Zhou. Global and Site Specific Epigenetic Impact of Alcohol on the Developing Brain and Partial Protection by S-adenosylmethionine. Poster presentation. Society for Neuroscience, Chicago, IL 2015
4. M Resendiz. D Chang & FC Zhou. Global and Gene-specific Epigenetic Dysregulation in FASD and the Normalizing Potential of S-adenosylmethionine. Poster presentation. Research Society on Alcoholism, New Orleans, LA 2016
5. M. Resendiz. “Epigenetics and Neurodevelopment: the Role of Alcohol and Methionine Metabolism”. Oral presentation at Stark Neuroscience Research Institute Seminar Series, Indiana University School of Medicine, Indianapolis, IN 2015
6. M. Resendiz. "DNA Methylation and Neural Development in a Mouse Model of Fetal Alcohol Spectrum Disorder". Oral presentation at Stark Neuroscience Research Institute Seminar Series, Indiana University School of Medicine, Indianapolis, IN 2014